THE ROLE OF PARKIN-MEDIATED MITOPHAGY DURING AGING AND EXERCISE IN SKELETAL MUSCLE

CHRIS CHIN WAH CHEN

A DISSERTATION SUBMITTED TO THE FACULTY OF GRADUATE STUDIES IN PARTIAL FULFILLMENT OF THE REQUIREMENTS FOR THE DEGREE OF

DOCTOR OF PHILOSOPHY

GRADUATE PROGRAM IN KINESIOLOGY AND HEALTH SCIENCE

YORK UNIVERSITY
TORONTO, ONTARIO

FEBRUARY 2018

ABSTRACT

Mitochondria are double membrane-bound organelles that play a significant role in producing energy for the cell, as well as mediating an array of metabolic pathways. Long-lived mitochondria that are unable to sustain the energetic requirements of the cell are targeted for lysosomal degradation through a process termed mitophagy. Parkin is a ubiquitin ligase that is involved in mitophagy and the turnover of mitochondria. Parkin is extensively studied in neuronal tissue, but its role in skeletal muscle has not been fully explored. The overall purpose of this dissertation was to examine the effects of aging and exercise on Parkin-mediated mitophagy in skeletal muscle.

We first investigated the role of Parkin in the regulation of mitophagy during exercise in young and old muscle. To do this, we subjected young and aged groups of wild-type (WT) and Parkin knockout (KO) mice to an acute bout of endurance exercise. We found a robust exercise-induced rise in mitophagy flux in young WT animals, but did not observe this in the absence of Parkin. Basal mitophagy flux was elevated in aged animals, but this did not increase additionally with exercise. We also noted a reduced transcriptional drive towards mitochondrial biogenesis in KO and aged animals. The results demonstrate that acute exercise can selectively increase mitochondrial targeting for degradation, and that this process is dependent on Parkin, as well as with age.

We next focused on the role of Parkin in mitochondrial turnover with endurance training. We found that mitophagy flux did not increase with training, but that flux lessened with a subsequent bout of acute exercise. This exercise-induced adaptation was not observed in trained KO animals. Our data indicate that exercise-induced mitochondrial biogenesis diminishes Parkin-mediated mitophagy as an adaptive response to repeated bouts of exercise.

The significance of this research is that we have indicated a role for Parkin in maintaining mitochondrial turnover, and show that Parkin can facilitate mitophagy, dependent on organelle content and quality in skeletal muscle.

DEDICATION

This PhD dissertation is dedicated to my late parents, Connie and Howard, two of the strongest people I know. And to my sister and best friend, Nikki.

ACKNOWLEDGEMENTS

"*It is our choices, Harry, that show what we truly are, far more than our abilities*." – J.K. Rowling. Harry Potter and the Chamber of Secrets

I have become a stronger and better version of myself than what I first started my PhD. I have many people to thank for this, and I will always be indebted to all of you.

This dissertation would not have been possible without my family. All of you are my heart, my soul, and my everything. Thank you to my late father for sparking my scientific curiosity during my early formative years. I will always cherish the memories of those that we spent together, on the books and activities, that helped developed my inquisitive mind. Thank you to my late mother for your encouragement and support during my PhD. You always kept me grounded, and taught me the life lesson that the present is all I really need to concern myself with. The bravery that you demonstrated during the hardest part of your life will always be a self-reminder that no life task or challenge is something to be afraid of. Thank to my sister for reminding me that I am not alone. To say that we have been through a lot is an understatement. Thank you for being there when I needed you, mentally and emotionally. Thank you for putting up with my weird antics and always offering a listening ear. I couldn't ask for a better sister! This PhD belongs to you as much as it belongs to me. Thank you for your unconditional love.

This PhD most certainly would not have been possible without my advisor, Dr. David Hood. Thank you for offering me this research opportunity and your guidance over these past six years. I will always remember my excitement when I received my letter of offer from you. I may have not fully appreciated all the data and paper presentations over the years, but now that this experience is coming to an end, I can see that it has all paid off. I am a better writer, presenter and researcher all because of you. Your commitment to student success and research excellence is unparalleled. Even through the madness of teaching and research, you still made the time and effort to support my research endeavours. More importantly, thank you for your support and patience during undoubtedly the toughest part of my life, and for that I am truly grateful.

I am also thankful for my colleagues in the Hood lab. You guys are my second family when I'm not at home. Thank you for lending a hand or ear when I needed it most. Thank you for your suggestions and advice. I am particularly indebted to my volunteers who have helped made this thesis possible. Thank you to Avigail Erlich and Matthew Crilly for being in the lab at the crack of dawn when I had early morning lab experiments. I will forever cherish the laughter and fun that we had during those times. I am also very honoured and thankful to have had the opportunity to work with an exceptional group of very dedicated undergraduate students: Kate Moffett, Lucy Samoilov, Nemanja Dovijarski, and Danielle Rangel. Each one of you brought something unique, outstanding, and positively different during my time in the lab, allowing me to become a better teacher and researcher. Thank you, everyone.

TABLE OF CONTENTS

LIST OF TABLES

LIST OF FIGURES

CHAPTER 2:

CHAPTER 4:

CHAPTER 5:

APPENDIX C:

LIST OF ABBREVIATIONS

4E-BP	eukaryotic translation initiation factor 4E binding protein
ADP	adenosine diphosphate
AICAR	AMP mimetic 5-aminoimidazole-4-carboxamide ribonucleoside
AIF	apoptosis inducing factor
Ambra1	activating molecule in Beclin1-regulated autophagy
AMP	adenosine monophosphate
AMPK	AMP-activated protein kinase
AP-1	activator protein 1
AREs	antioxidant-responsive elements
Atg	autophagy-related gene
ATP	adenosine triphosphate
Bcl-2	B-cell lymphoma 2
bp	base pair
BH3	homologous BCL2 homology 3
BNIP3	Bcl-2 interacting protein 3
CaMKs	calmodulin-dependent protein kinases
C/EBPβ	ccaat-enhancer-binding proteins
CHOP	CCAAT-enhancer-binding protein homologous protein
c-Jun	AP-1 Transcription Factor Subunit
CMA	chaperone-mediated autophagy
COX	cytochrome c oxidase
DNA	deoxyribonucleic acid
EndoG	endonuclease G
ERRα	estrogen-related receptor-α
ETC	electron transport chain
Drp	dynamin-1-like protein
FIP200	FAK family kinase-interacting protein of 200 kDa
Fis1	mitochondrial fission 1 protein
FUNDC1	FUN14 Domain Containing 1
GABARAP	γ-aminobutyric acid (GABA)A-receptor-associated protein
GATE-16	golgi-associated ATPase enhancer of 16 kDa
GCN5L1	amino acid synthesis 5-like 1
Gp78	glycoprotein 78
HECT	homologous to the E6-AP Carboxyl Terminus
HSP	heat shock protein
IAPs	inhibitors of apoptosis
IBR	in-between-RING
IGF1	insulin-like growth factor 1
IMF	intermyofibrillar
IMM	inner mitochondrial membrane
IMS	intermembrane space
IP3R	inositol trisphosphate (InsP3) receptor Ca2+ channel
JNK2	c-Jun N-terminal kinase 2
kDa	kilodalton

Keap1	kelch like ECH associated protein 1
KO	knock-out
LAMP	lysosome-associated membrane glycoprotein
LC3	microtubule-associated protein 1 light chain 3
LIR	LC3-interacting region
LKB1	liver kinase B1
MAPK	p38 mitogen-activated protein kinase
MAPL	mitochondria-associated protein ligase
MDVs	mitochondrial-derived vesicles
Mff	mitochondrial fission factor
Mfn	mitofusin
Miro1	mitochondrial Rho GTPase 1
MPP	mitochondrial processing peptidase
MPPP	1-methyl-4-phenyl-4-propionoxy-piperidine
MPTP	1-methyl-4-phenyl-1,2,3,6-tetrahydropyridine
MQC	mitochondrial quality control
mRNA	messenger RNA
MSF	mitochondrial import stimulation factor
mTOR	mammalian mechanistic target of rapamycin
MTS	mitochondrial-targeting sequence
mtDNA	mitochondrial DNA
mtPTP	mitochondrial permeability transition pore
Mul1	mitochondrial ubiquitin ligase 1
MUREs	UPR^{mt} response elements
NBR1	neighbor of BRCA1 gene 1
nDNA	nuclear DNA
NDP52	calcium binding and coiled-coil domain 2
NIX	Bcl-2 interacting protein 3 like
NRF-1/2	nuclear respiratory factor-1/2
Nrf2	nuclear factor (erythroid-derived 2)-like 2
NUGEMPs	nuclear genes encoding mitochondrial proteins
OMM	outer mitochondrial membrane
Opa	mitochondrial dynamin like GTPase
OPTN	optineurin
OXPHOS	oxidative phosphorylation
p62	sequestosome 1
PAM	associated import motor
PARL	presenilins-associated rhomboid-like protein
PI3Ks	phosphatidylinositol-4,5-bisphosphate 3-kinase
PE	phosphatidylethanolamine
PIM	protein import machinery
PINK1	PTEN-induced putative kinase 1
PolG	DNA polymerase gamma
PGC-1α	peroxisome proliferator-activated receptor gamma coactivator 1-alpha
PRC	PGC-1-related coactivator
RBR	RING-between-RING

RING	really interesting new gene
RNA	ribonucleic acid
ROS	reactive oxygen species
SDH	succinate dehydrogenase
SMAC	small mitochondria-derived activator of caspases
SR	sarcoplasmic reticulum
SS	subsarcolemmal
TAX1BP1	tax1 binding protein 1
TBK1	tank-binding kinase 1
TFAM	mitochondrial transcription factor A
TFEB	transcription factor EB
TIM	translocase of the inner mitochondrial membrane
TOM	translocase of the outer mitochondrial membrane
tRNA	transfer RNA
UbcH7	ubiquitin conjugating enzyme E2 L3
Ubl	ubiquitin-like domain
Ulk1	unc-51-like kinase
UPR^{mt}	mitochondrial unfolded protein response
UPS	ubiquitin proteasome system
VDAC	voltage-dependent anion channel
Vms1	VCP/Cdc48-associated mitochondrial stress-responsive
Vps	vacuolar protein sorting
WT	wild-type

CHAPTER 1:

INTRODUCTION

Skeletal muscle plays a significant role in locomotion and whole-body metabolism. Beyond its fundamental role in movement, muscle displays a remarkable ability to adapt to different imposed metabolic stressors. The understanding of muscle plasticity, and how it contributes to our overall well-being, is a highly relevant area of investigation. The degree to which these transformations occur is in part due to changes in mitochondrial turnover. Mitochondria are considered for their primary function as energy producers for the cell. However, it is also recognized that mitochondria are highly dynamic structures that can regulate the phenotype of muscle fibres by the induction of several signaling pathways.

Endurance training can improve the oxidative capacity of muscle. This can be achieved through the activation of mitochondrial biogenesis, which allows for greater organelle density and improved substrate fuel utilization. Conversely, a decrease in mitochondrial content can lower ATP production while enhancing muscle fatigability, and this can consequently promote muscle atrophy. These detrimental effects are observed in sarcopenia, which is the age-related loss of muscle mass and function. Aged muscle also displays mitochondria that are prone to producing greater reactive oxygen species that can yield macromolecular damage. This can create a vicious cycle that accelerates cellular damage in muscle with advancing age.

Parkin is a ubiquitin ligase responsible for the selective targeting of long-lived, damaged mitochondria. This process is termed mitophagy and can aid in mitochondrial turnover. Parkin-mediated mitophagy is well-studied in neurodegeneration. Furthermore, mitophagy has been demonstrated to be altered under different disease states, including heart failure, diabetes, and

aging. The balance between organelle biogenesis and degradation is essential to maintain mitochondrial content and energetic homeostasis.

However, a clear understanding of the molecular mechanisms that govern Parkin and mitochondrial turnover is lacking. Furthermore, the importance of Parkin and mitophagy in regulating skeletal muscle health remains undetermined. The study of this relationship under different physiological states (i.e. exercise and aging) will markedly improve our knowledge of muscle plasticity. In North America, an aging population is growing, with more people recognizing that maintaining an active lifestyle is essential for long-term health. The expansion of our knowledge on the molecular underpinnings that govern mitochondrial turnover during exercise can help older individuals achieve a longer and greater quality of life. Exercise is an effective prescription to enhance mitochondrial quality control that, in turn, can enhance skeletal muscle function and promote healthy aging.

CHAPTER 2:

LITERATURE REVIEW

2.1 Skeletal Muscle and Mitochondria

2.1.1. Skeletal muscle plasticity

Skeletal muscle is a metabolic organ involved in movement, posture and breathing. It contains an architectural array of enzymes and muscle-specific protein isoforms that control force production. The elegant coordination of these structures provide muscle with the intrinsic ability to induce different biochemical and metabolic characteristics. This malleable property is called plasticity and allows for the muscle to adapt to various stimuli such as endurance training, disuse and aging. Alterations in gene expression and protein translation arise for these adaptations to occur. To understand these molecular conundrums following contractile perturbations, physiologists require a fundamental understanding of muscle structure and function

Excitation of a muscle is coupled with a sequential number of events that evoke contraction (**Figure 1**). Depolarization at the pre-synaptic membrane of an α-motorneuron unleashes increased quantal amounts of acetylcholine at the neuromuscular junction. Acetylcholine diffuses across the synaptic cleft and binds onto nicotinic acetylcholine channel receptors on the sarcolemma membrane of the muscle fibre. Opening of the channels allows for the rapid entrance of sodium ions and depolarization at the postsynaptic membrane. The propagation of the muscle action potential transverses into tubules and activate voltage-gated dihydropyridine receptors (26, 359). These receptors directly interact with ryanodine calcium release channels located on the lateral sacs of the sarcoplasmic reticulum (SR) (95). Calcium discharge allows for increased calcium binding on myofilaments to enhance cross-linking and generate force. Sarcomeric relaxation occurs when calcium-ATPase pumps calcium into the lateral sacs of the SR. These energy

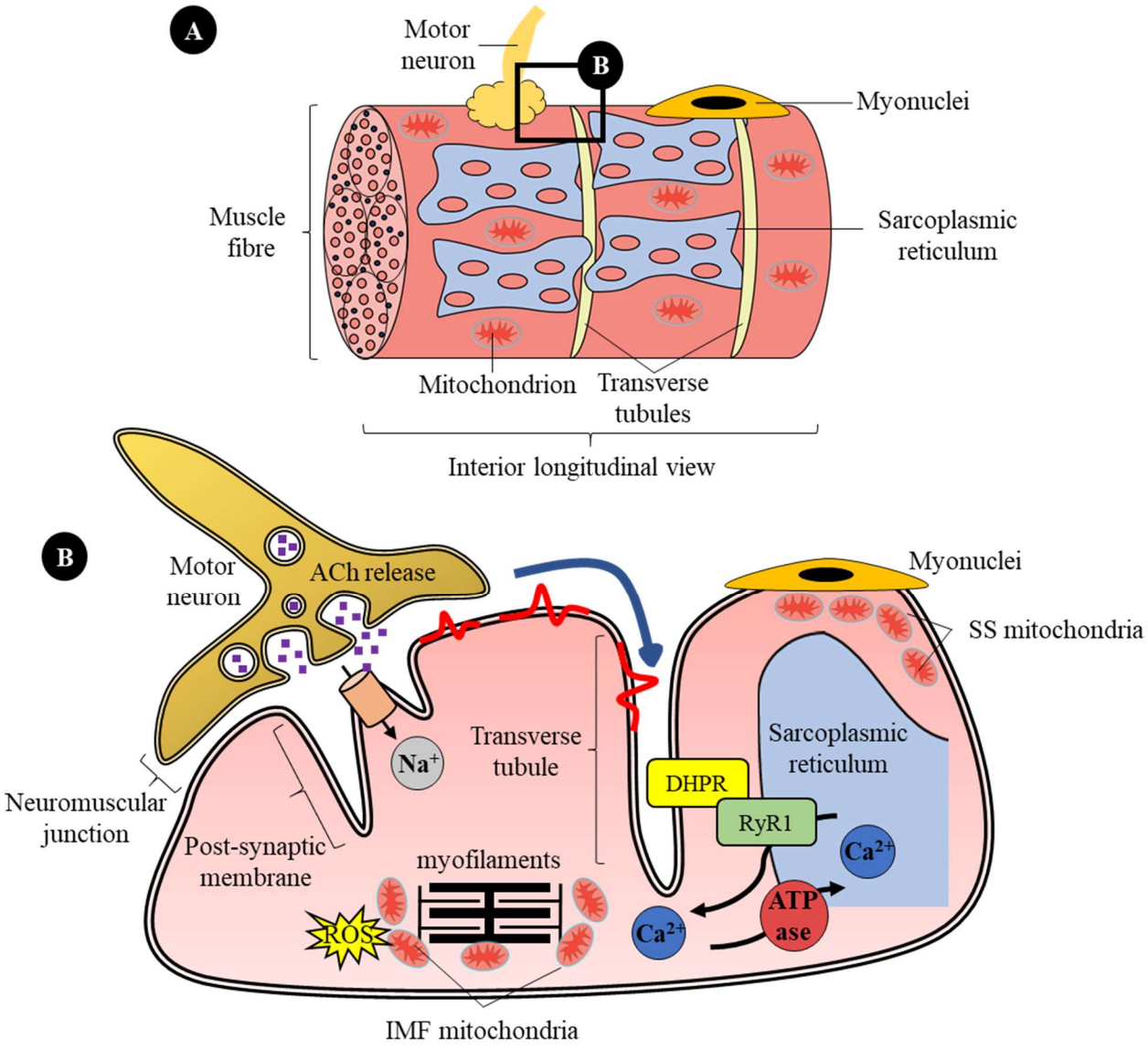

Figure 1. Muscle structure and function. A) An internal longitudinal view of a muscle fibre containing mitochondria, sarcoplasmic reticulum and transverse tubules. A motor neuron that innervates the sarcolemmal membrane forming the neuromuscular junction (NMJ) is highlighted. **B)** Magnified view of NMJ. Depolarization of the motor neuron at the pre-synaptic cleft releases acetylcholine at the NMJ. Acetycholine binds and activates receptors located on the post-synaptic membrane of the muscle fibre, which allows for the entry of sodium ions within the myofibril. The elevation in sodium elicits a muscle action potential that propagates into the transverse tubules and activates voltage-gated dihydropyridine receptors (DHPR). These receptors are tethered with ryanodine (RyR) calcium release channels located at the sarcoplasmic reticulum (SR). The release of calcium from the SR can bind onto myofilaments and evoke contractile activity. Mitochondria can store calcium and use it as a regulator of oxidative phosphorylation. In addition to producing ATP, mitochondria are considered a primary source of reactive oxygen species (ROS) emission.

demanding events are met by adjacent mitochondria to the calcium release channels. Mitochondria perform as calcium "sinks", and the transient increase in organelle calcium stimulates oxidative phosphorylation (OXPHOS) and ATP production (35). This signaling is bi-directional as local mitochondrial reactive oxygen species (ROS) emission can affect ryanodine calcium release activity (381, 474). The importance of this interplay between mitochondria and muscle function have been exemplified many times in the research. In the following section, a review on the functional properties of muscle mitochondria will be given.

2.1.2. Electron transport chain

Mitochondria are double-membrane bound organelles that have evolved to support eukaryotic cells and their energetic requirements. A majority of this energy is produced within the mitochondrial matrix, which houses the citric acid cycle. The process begins with the entry of catabolized macromolecules (i.e. carbohydrates, fatty acids and proteins) as a two-carbon atom product acetyl coenzyme A. Through a series of carefully controlled chemical reactions, the citric acid cycle manufactures two fully reduced substrates: nicotinamide adenine dinucleotide (NADH) and flavin adenine dinucleotide ($FADH_2$). Both molecules are shuttled and oxidized by the electron transport chain (ETC) to aid in OXPHOS. The ETC is positioned on the inner mitochondrial membrane (IMM) and contain five complexes (**Figure 2**). Briefly, NADH is oxidized by complex I NADH dehydrogenase and ensures the translocation of protons across the IMM into the intermembrane space (IMS), and the generation and transfer of NADH's electrons to complex III cytochrome bc_1 complex. Electrons are liberated from $FADH_2$ at complex II succinate dehydrogenase and transferred to complex III. Protons are driven across the IMM as electrons are transported through complexes III and IV. Electrons are terminally accepted at complex IV cytochrome c oxidase, where oxygen is reduced to water. The accretion of protons in the

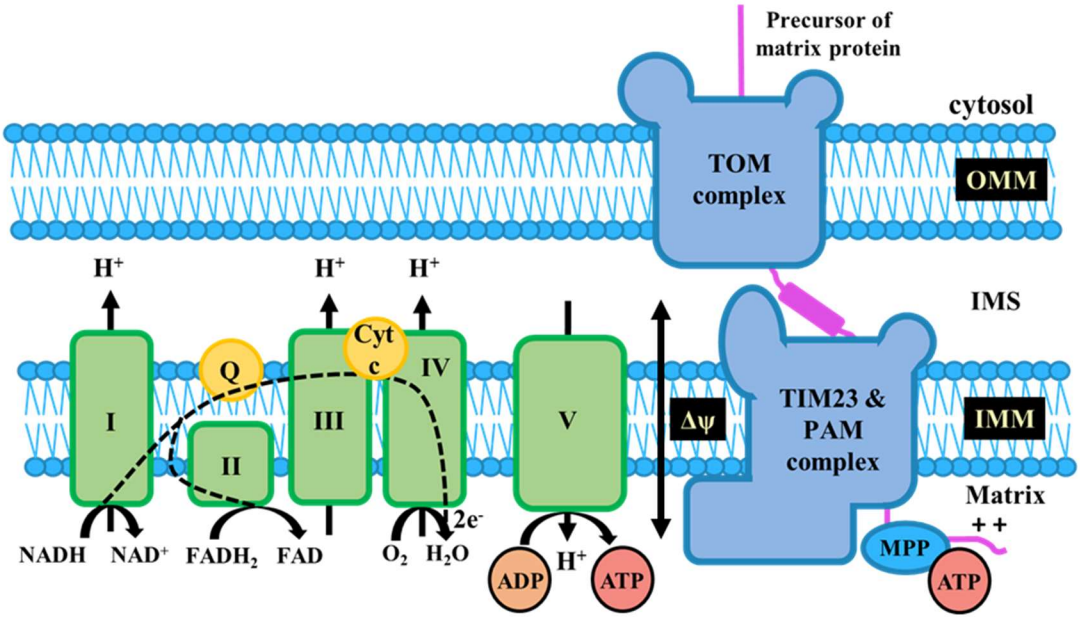

Table 1. Summary of SS and IMF mitochondrial function in skeletal muscle.

	Higher in SS	Higher in IMF
Mitochondrial Function	Membrane potential, ROS emission	Respiration, matrix ATP, protein import, protein synthesis
Function in Muscle	ATP synthesis for: myonuclei gene expression, fatty acid substrate metabolism	ATP synthesis for: Contractile activity

Figure 2. Mitochondrial function. A schematic illustrating the electron transport chain (ETC) and protein import machinery. The process of oxidative phosphorylation (OXPHOS) begins with NADH oxidation at complex I, and $FADH_2$ oxidation at complex II. The liberation of these electrons are transferred to electron carrier coenzyme Q, followed by complex III, cytochrome c (Cyt c) and complex IV. Electrons are terminally accepted at complex IV, concurrent with the reduction of oxygen into water. The transfer of matrix protons across complexes I, III and IV into the intermembrane space (IMS) generates a membrane potential ($\Delta\psi$) across the inner mitochondrial membrane (IMM). This potential energy is released through complex V in exchange for ATP generation. Precursor proteins with a mitochondrial targeting sequence are recognized by translocase of the outer membrane (TOM) complex. Matrix-destined proteins are subsequently transferred to the translocase of the inner membrane (TIM) and pre-sequence translocase-associated motors (PAM). The precursor protein is "pulled" into the matrix where its pre-sequence is cleaved by matrix mitochondrial processing peptidase (MPP). The protein import process occurs in respiring mitochondria that produce ATP, and those that exhibit a mitochondrial $\Delta\psi$.

IMS generates a membrane potential across the IMM. Release of this potential energy occurs when hydrogen atoms re-enter the matrix through complex V ATP synthase, as ADP is converted to energy-rich ATP in the matrix (292). ADP is transported from the cytosol by IMM adenine nucleotide translocator in exchange for matrix ATP, providing mitochondrial energy to the cytosol (112, 280).

2.1.3. Reactive oxygen species

Within each ETC complex is a redox site that can leak electrons to oxygen within the organelle. The one-electron reduction of oxygen can generate superoxide anions and can become a precursor for reactive oxygen species (ROS) (440). The rate of ROS production is dependent on mitochondria that are basally (state IV) or actively (state III) respiring. In a basal state, there is a lower rate of electron transport and higher backpressure of electrons. This provides a fortuitous opportunity for ROS formation. Superoxide anions generally reside in the matrix or IMS (124), or can be carried out to the cytosol by voltage-dependent anion channels (VDACs) (123). ROS-induced cellular damage is an effect of imbalanced, excessive formation of ROS and limited antioxidant defenses. Sustained oxidative stress can yield damage to DNA, lipids and proteins. Mitochondrial DNA is highly susceptible to ROS, due to its uncoiled conformation and lack of proofreading enzymes, compared to nuclear DNA (436). Superoxide dismutases (SODs) can counteract oxidative stress by converting superoxide anions into less damaging species of oxygen and hydrogen peroxide. Mitochondrial matrix SOD contains manganese at its catalytic site, whereas the cytoplasmic SOD isozyme contains copper and zinc (440). Glutathione peroxidase and catalase can further reduce hydrogen peroxide into water (270). Attenuated expression of these enzymes is believed to accelerate muscle wasting with age (414, 445), and supports the free radical theory of aging (133).

2.1.4. Mitochondrial protein import

Mitochondria exist in a dynamic reticular network (216) and assist in muscle energy distribution (105). An organelle that is unable to recover from oxidative damage can segregate from this network for targeted degradation (see next section on mitochondrial quality control) (174). Healthy mitochondria can coalesce and form a network that enhances bioenergetic function (387). The mitochondrial network is responsive to its environment and contributes to the adaptive plasticity of muscle (318). For the expansion of the reticular network to occur, the coordination of mitochondrial and nuclear genomes is required. Many of the proteins in the mitochondrial proteome are encoded within the nucleus, while approximately 1% are encoded by mitochondrial DNA. The expression of nuclear genes encoding mitochondrial proteins (NUGEMPs) is regulated by transcriptional factors (e.g. PGC-1α) and they are translated in the cytosol as precursor proteins. The majority of mitochondrial proteins carry amino-terminal pre-sequences that are recognized by receptors found on the OMM (310) (**Figure 2**). With the assistance of molecular chaperones, heat-shock protein (Hsp) 70 and mitochondrial-import stimulation factor (MSF), mitochondrial preproteins are unfolded and transferred to the translocases of the outer membrane (TOM) complex (291, 480). Once through the TOM complex, preproteins are subsequently imported into the matrix, OMM, IMM, or IMS. Matrix-destined proteins depend on specialized translocases of the inner membrane (Tim23 complex) and pre-sequence translocase-associated motors (PAM complex) for their transport across the IMM (466). A membrane potential is essential to generate an electrophoretic effect on the positively charged pre-sequence, "pulling" the preprotein into the matrix where the pre-sequence is cleaved by mitochondrial processing peptidase (MPP) (19, 336, 466). Protein refolding occurs with molecular chaperones (Hsp60 and Hsp10) soon after the protein's arrival in the matrix.

2.1.5. Subsarcolemmal (SS) and intermyofibrillar (IMF) mitochondria

Electron microscopy studies have detected two distinct populations of muscle mitochondria. SS mitochondria are located underneath the sarcolemmal membrane, often near myonuclei, and IMF mitochondria that are localized between myofibrils (216, 303, 317). The two populations differ morphologically where SS mitochondria are generally observed as spherical and lack organelle connectivity (205, 317, 337), while IMF mitochondria are elongated and exist in a reticular network near the Z-lines of sarcomeres (15, 216, 337). Mitochondrial populations can be isolated via homogenization and centrifugation (229). The characterization of SS and IMF mitochondria have yielded subtle, but divergent biochemical and functional differences. SS mitochondria exhibit a higher membrane potential, which may predispose them to ROS production (2). Free radicals produced by SS mitochondria may serve as signaling molecules, based on the proximity of SS to the myonuclei for gene expression (155) and to capillaries for transport (106). Access to blood flow can provide SS mitochondria with the ability to oxidize fatty acids (225). On the other hand, IMF mitochondria can respire in greater amounts both basally and in response to ADP (63, 229). This, in turn, can generate an elevated amount of matrix ATP that is required for IMF mitochondrial protein import (419) and protein synthesis (63). When compared to SS mitochondria, IMF mitochondria express a greater number of proteins required for OXPHOS (94). Together, these data suggest that IMF mitochondria have a greater propensity to generate the ATP required for contractile activity, based on their myofibril juxtaposition. Thus, the divergent functional properties of SS and IMF mitochondria allow for these two populations of mitochondria to adapt differently to muscle aging (52, 267), and in response to exercise (1, 417) (**Table 1**). These mitochondrial differences and their role in contributing to muscle plasticity will be elaborated in the aging and training adaptation sections of this literature review.

2.2 Mitochondria Quality Control

Mitochondria lie at the intersection of health, longevity and disease. Proper maintenance of the organelle is critical for cellular and tissue function. As such, continual mitochondrial surveillance is essential to maintain energetic homeostasis within the cell. When mitochondria become damaged, mechanisms are swiftly activated to restore mitochondrial function. Due to the post-mitotic nature of skeletal muscle, dilution of dysfunctional mitochondria through cellular division is unable to occur. Consequently, intracellular pathways have evolved to defend skeletal muscle cells from this caveat. Recent scientific advances have illuminated mitochondrial specific quality control mechanisms that are stress-dependent. Contingent on the level of organelle injury, mitochondria can undergo several cellular checkpoints before elimination from the cell (**Figure 3**).

2.2.1. Mitochondrial dynamics: Fusion and fission

A primary feature of mitochondrial dysfunction is a loss of membrane potential. When mitochondrial membrane potential is dissipated across the IMM, the ETC's ability to transfer electrons and hydrogen atoms is diminished. Ultimately, the generation of ATP is compromised. At this crossroad, a dysfunctional mitochondrion can encounter several fates. First, restoration of the membrane potential and dilution of damaged proteins can occur via organelle fusion. Cross-complementation with other mitochondria can mitigate damage through the exchange of mtDNA, lipids and proteins. This can maximize the oxidative capacity of mitochondria in response to an environmental stress, so long as the stress is below a critical threshold. Fusion arises concurrently in the IMM and OMM as two mitochondria come together. Mitofusin 1 and 2 (Mfn1/2) mediate OMM fusion (378), whereas optic atrophy 1 (Opa1) mediates IMM fusion (6, 75). Though mammals contain two different mitofusin homologs (Mfn1 and Mfn2), both proteins are generally

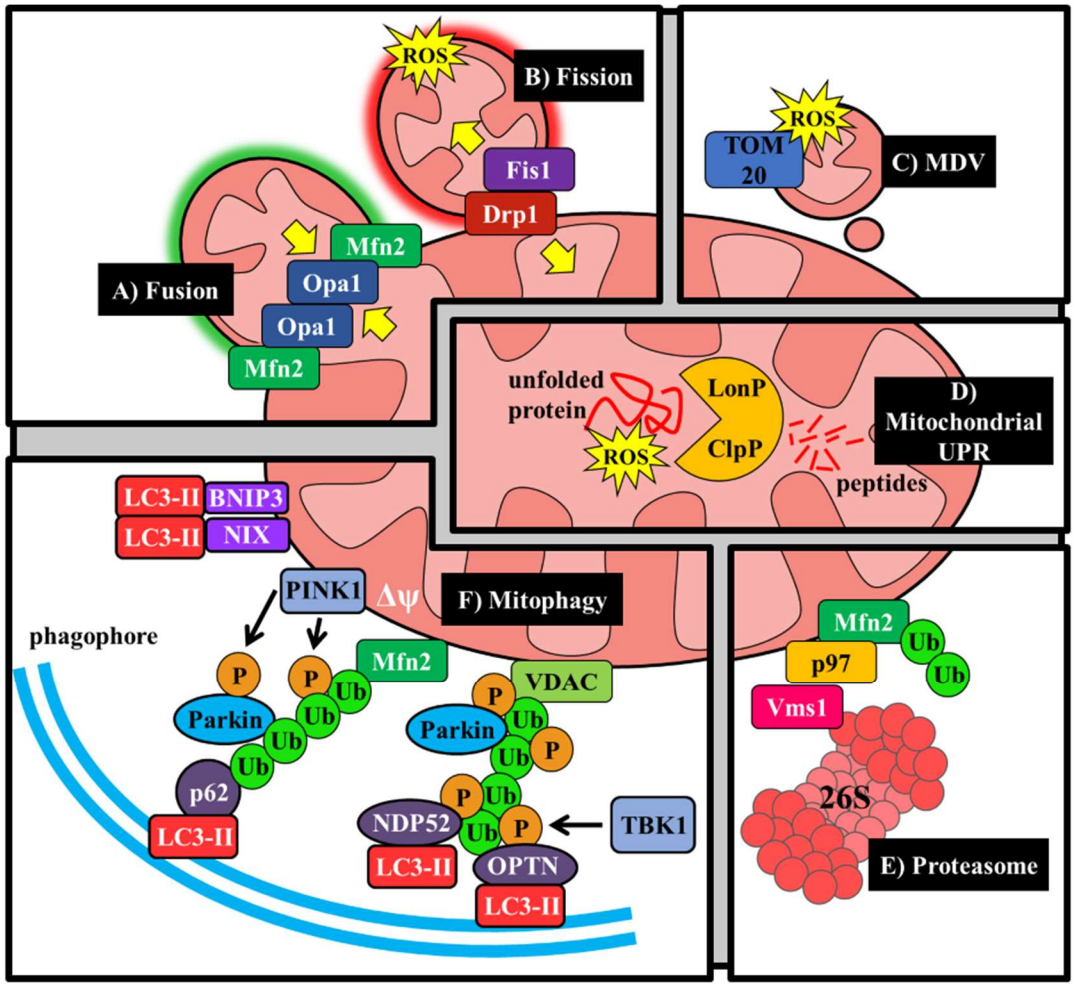

Figure 3. Mitochondrial quality control. Mitochondria are dynamic organelles that can undergo fusion and fission events. **A)** The tethering of two adjacent mitochondria is governed by fusion regulatory factors mitofusin (Mfn) and optic atrophy 1 (Opa1). **B)** Conversely, the separation of a mitochondrion from the reticular network is mainly governed by adaptor fission protein 1 (Fis1) and dynamin-like protein (Drp1). **C)** Mitochondrial-derived vesicles (MDVs) can be single or double membrane bound cavities containing oxidized proteins. This process does not depend on canonical organelle fission factors. **D)** An elevation in unfolded proteins in the mitochondrial matrix can activate Lon and Clp proteases. Dysfunctional proteins are disintegrated into peptides and can be shuttled out of the organelle as signaling molecules to activate the mitochondrial unfolded protein response (UPR). **E)** Outer mitochondrial membrane (OMM) proteins that are damaged can be targeted for degradation by the ubiquitin-proteasome system. **F)** Mitophagy is the selective removal of dysfunctional mitochondria. A loss in organelle membrane potential can stabilize PTEN-induced putative kinase 1 (PINK1) on the OMM. PINK1 can subsequently phosphorylate and activate E3 ubiquitin ligase Parkin. Polyubiquitin chains on OMM proteins associate with autophagy adaptors: sequestosome 1 (p62), nuclear domain protein 52 (NDP52) and optineurin (OPTN). The mitochondrial recruitment of TANK-binding kinase 1 (TBK1) can additionally phosphorylate these adaptor proteins to reinforce organelle ubiquitination. The phagophore membrane containing lipidated microtubule-associated protein light chain 3 (LC3II) can bind with LC3-interacting regions found on p62, NDP52 and OPTN. The elongation of the phagophore and encapsulation of the dysfunctional organelle produces the autophagosome.

expressed in the same cell, while each can independently support mitochondrial fusion (56). The importance of fusion in human disease is shown in non-proliferating neurons, where mutations in the fusion machinery can result in two human diseases, dominant optic atrophy (6) and Charcot Marie Tooth disease type 2A (493).

If mitochondrial stress levels reach beyond a critical threshold, mitochondria can segregate from the reticular network and undergo fission. Unlike fusion, organelle fission events generally begin on the OMM. Fission is initiated when adaptor fission protein 1 (Fis1) (302) and mitochondrial fission factor (Mff) (101) localize to separation sites and recruit cytosolic dynamin-like protein (Drp1) onto the OMM (400). Drp1 surrounds, constricts and severs the OMM and the IMM until the mitochondrion is partitioned from the reticular network. Once separated, the dysfunctional mitochondrion is either targeted for removal (mitophagy) (441, 442) or can return to the network if mitochondrial membrane potential is recovered (43, 479). It remains unknown whether any human diseases are related to fission protein mutations. However, recent research has revealed the importance of mitochondrial fusion and fission events, particularly in skeletal muscle health (57, 175, 362).

2.2.2. Unfolded protein response

For localized regions of mitochondrial damage, quality control mechanisms are available to prevent the complete removal of mitochondria. Most mitochondrial proteins are nuclear-encoded and require protein import for proper organelle assembly. An unbalanced contribution between nuclear and mitochondrial genomes can result in unassembled ETC complexes and increased mitochondrial stress. Cellular perturbations including mitochondrial biogenesis (290) and oxidative stress (478) can impact the protein-folding environment within mitochondria. As a result, an increase of misfolded proteins within mitochondria beyond the capacity of chaperone

proteins to handle them can activate the mitochondrial unfolded protein response (UPR^{mt}). This response can upregulate the transcriptional expression of nuclear-encoded mitochondrial proteases and chaperones (490). These chaperones, which include mtHSP70, HSP60 and HSP10, cooperate with protein import for the folding of matrix-destined proteins into a competent state (310). Proteins that fail to fold correctly are degraded by proteases to prevent protein aggregation. Lon and ClpP are ATP-dependent proteases found in the matrix. The Lon protease family provides a protective environment by degrading protein aggregates (22) and mildly-oxidized proteins (37). Lon performs a regulatory role in maintaining mtDNA copy numbers by targeting mitochondrial transcription factor A (TFAM) for degradation in the matrix (284). Furthermore, Lon protein expression is also reduced in aged skeletal muscle, and this might contribute to the proteotoxic-induced mitochondrial dysfunction seen with aging (38).

Initial work on ClpP has shown this protease to have a lower sensitivity for the detection of misfolded proteins than Lon (129). ClpP has also recently emerged as an important signaling protease in the activation of UPR^{mt}. Work done by the Haynes laboratory using *C. elegans* demonstrated that ClpP can degrade unfolded proteins into peptides, which results in their efflux from mitochondria into the cytosol (136). Accumulation of these peptides in the cytosol can affect the translocation of transcription factors into the nucleus that can upregulate the induction of mitochondrial chaperone and protease genes (137). The mechanism by which peptides affect the localization of these transcription factors remains unanswered. More importantly, the effect of UPR^{mt} activation on mitochondrial peptide release in mammals is an illuminating avenue of future research. In UPR^{mt} mammalian studies, the use of aggregate-prone matrix-destined proteins provokes phosphorylation of JNK2, leading to the activation and binding of c-Jun onto AP-1 sites found on the promoter of CHOP and C/EBPβ (160, 490). The expression and heterodimerization

of CHOP and C/EBPβ is followed by these factors binding onto CHOP promoter sites of mitochondrial chaperones and proteases (160, 490). Interestingly, these CHOP promoter sites are flanked by two conserved UPR^{mt} response elements (MUREs) that are found in several promoter regions of several human mitochondrial chaperones and proteases, including HSP60, HSP10 and ClpP (5). The discovery of MUREs provide additional insight into the integrative role of stress-responsive transcription factors and kinases in mediating the mitochondrial stress response.

2.2.3. Ubiquitin-proteasome system (UPS)

The turnover of cytosolic and OMM proteins is critical in the maintenance of mitochondrial function and morphology. The ubiquitin-proteasome system (UPS) is traditionally thought of as a degradative system responsible for the turnover of cytosolic proteins. The UPS can mark cytosolic mitochondrial-destined proteins that are misfolded or mistargeted for removal. Current studies reveal a role for the UPS in regulating the OMM proteome. In mammalian cells, oxidative stress and mitochondrial damage can induce the mitochondrial localization of AAA-ATPase p97, a component of the UPS, and cytosolic protein Vms1 (143, 144). Vms1 acts to bridge mitochondria with components of the UPS for the turnover of OMM proteins. Deletion of Vms1 in mammalian cells is deleterious, and reduces mitochondrial respiratory capacity and cell viability (143). Additionally, p97 has been shown to retro-translocate OMM proteins from the mitochondrion to the cytosolic proteasome for degradation (423, 475). Intriguingly, mitochondrial function and the UPS exhibit a mutualistic relationship. Inhibition of the 26S proteasome system prevents mitophagy from occurring, suggesting that the UPS precedes mitochondrial degradation (53, 423). Prevention of the actions of the UPS can negatively result in the accumulation of defective mitochondrial proteins and alter mitochondrial morphology (277, 350). Reciprocally, lowered

ATP production and heightened oxidative stress brought about by ETC perturbations can adversely affect proteasomal assembly and activity (165, 264)

2.2.4. Mitochondrial-derived vesicles

Aberrant proteins that accumulate on the OMM beyond the capabilities of the UPR^{mt} and the UPS can induce global mitochondrial stress. Under these circumstances, small or entire portions of mitochondria are sequestered for degradation. Pioneering microscopy work from the McBride laboratory has demonstrated that small mitochondrial-derived vesicles (MDVs) can bud from the mitochondrial membrane. The use of immuno-fluorescence and electron microscopy exposes the complexity of these vesicles. MDVs can selectively incorporate various protein cargo, depending on the nature of the mitochondrial stress induced (407). For example, the addition of complex III inhibitor (antimycin A) to mitochondria can produce MDVs enriched with IMM complex III subunit core 2 (407). However, when a general ROS inducer is used, MDVs that are generated contain only OMM protein VDAC, but not complex III subunit core 2 (407). These results reveal that MDVs can be single membrane bound vesicles containing OMM proteins, or also double membrane bound for oxidized matrix/IMM proteins (413). It is unknown how matrix proteins can trigger vesicle formation, but it appears that protein aggregation within the matrix can initiate the warping of the membrane. This process is independent of Drp1, and distinct from mitochondrial fission under basal or stimulated MDV conditions (406).

Once MDVs are formed, they can be delivered to the lysosome for protein degradation (406) or to the peroxisome for lipid degradation (311). The full function of peroxisome delivery remains unclear, but membrane-anchored protein ligase MAPL is known to assist with this trafficking (297, 311). For example, MDVs destined for peroxisomes contain MAPL but exclude mitochondrial OMM translocase protein TOM20 (311). Conversely, vesicles containing TOM20

exclude MAPL and do not fuse with peroxisomes, indicating a high level of cargo specificity in determining MDV fate (311). This selectivity is also seen with MDV delivery to the lysosome. Protein kinase PINK1 and E3 ubiquitin ligase Parkin are both required for the biogenesis and lysosomal targeting of MDVs (285). Interestingly, PINK1 and Parkin are also involved in the selective removal of entire mitochondria from the cell (see below). It is hypothesized that PINK1 and Parkin localize on small regions of failed import machinery (e.g. TOM20) as a trigger for MDV generation, rather than fully depolarized mitochondria, which would prompt mitophagy (413). Lysosomal delivery of MDVs is independent of the autophagy machinery, suggesting a complementation between MDVs and mitophagy (285, 406). Finally, the functional importance of MDV in physiological and disease states remain unknown, and is a promising avenue of future research.

2.2.5. Selective mitochondrial degradation: Autophagy and Mitophagy

Autophagy is a catabolic, evolutionary-conserved process responsible for the turnover of damaged proteins and organelles. Autophagy consists of three forms: microautophagy, macroautophagy and chaperone-mediated autophagy (CMA). Although all three processes are distinct, they all coalesce at the lysosome with the degradation and recycling of delivered cargo. CMA is the most selective process of the three, and requires assistance from heat shock cognate 70 protein (hsc70). Chaperone-mediated transport to the lysosome closely resembles the process of protein targeting to organelles within the cell. Hsc70 selectively binds soluble cytosolic proteins with an exposed amino acid KFERQ motif (77) and facilitates their transport through the lysosome-associated membrane protein type 2A (LAMP-2A) receptor (69). Microautophagy is a nonselective process in which small cytoplasmic soluble proteins are directly internalized into lysosomes via invaginations of the lysosomal membrane. Macroautophagy, herein called

autophagy, is the most prevalent and well-studied autophagic pathway. This process is characterized by the engulfment of defective proteins and organelles in their entirety, enclosed in double membrane bound vesicles called autophagosomes and terminally delivered to lysosomes (autophagolysosome) for degradation. The disintegrated substrates are then released into the cytosol as constituents for de novo synthesis of macromolecules. Insufficient or excessive autophagy can be a "double-edged sword", and regulation of this process is necessary for proper cellular function (402).

The molecular mechanisms of autophagy were first discovered in the early 1990s by Yoshinori Ohsumi's laboratory. Through a series of elegant experiments, Ohsumi and his colleagues discovered autophagy in yeast under nutrient-depleted conditions (420). His work, along with Klionsky's research group, illustrated that the autophagic process in yeast was largely similar to the lysosomal system found in mammalian cells (12, 131, 392). Taking advantage of yeast genetics, Ohsumi et. al further isolated and characterized 15 *apg* genes (autophagy-defective mutants) involved in yeast autophagy (437). *APG* yeast mutants were characterized by reduced viability and diminished protein bulk degradation, when faced with starvation (437). Since this initial finding, the autophagy field has exploded with the identification of novel autophagy proteins in yeast and other organisms. In 2003, principal autophagy researchers proposed a unified nomenclature system to reduce confusion in the scientific community by replacing all "autophagy-related" genes and proteins with *ATG* and Atg, respectively. Moving forward in this review, the new nomenclature will be used.

The formation of the autophagosome will be discussed first, as it is a common feature of autophagy and is coordinated by Atg proteins (**Figure 4**). The initial step in autophagosomal formation begins with two ubiquitination-like modifications, shown to be conserved in yeast and

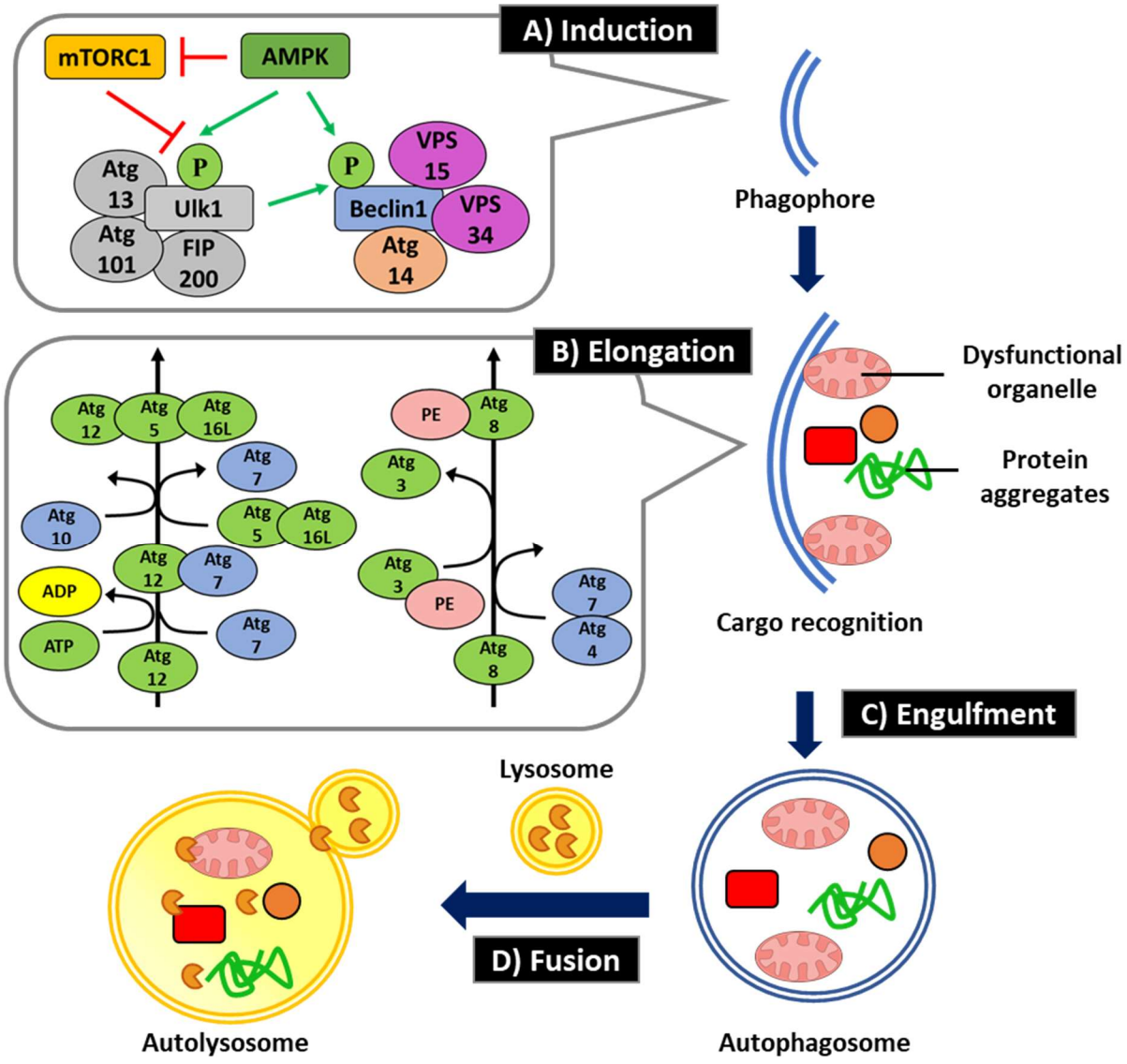

Figure 4. Autophagy regulation. A) The activation of the energy sensor AMPK is evoked during times of energetic stress. When cellular levels of AMP become elevated, AMPK can be activated and inhibit mTORC1 to supress protein synthesis and translation. In turn, AMPK can stimulate the induction of Ulk1 and the initiation of autophagy. Ulk1 can then phosphorylate and mobilize the Beclin1 complex to undertake the primary steps required for phagophore biosynthesis. **B)** The association of autophagy-like proteins Atg12-Atg5-Atg16 occur through a series of conjugating enzymes. This complex is involved in the early steps of elongating the phagophore membrane. This membrane acts as a docking platform for recognized cargo that are destined for autophagic degradation. This process is facilitated by the processing and activation of Atg8. **C)** The continual elongation of the phagophore membrane results in the encapsulation of cargo into a structure known as the autophagosome. **D)** The autophagosome is delivered to the lysosome. The fusion of these vesicles produces the autolysosome, whereby lysosomal enzymes can degrade the contents of the autophagosome. The final digested products can be recycled within the cell to maintain energetic homeostasis.

humans. Initiation begins with the activation of Atg12 with Atg7, an E1 ubiquitin-like activator requiring ATP (294). This process progresses when Atg10, an E2 conjugating-like enzyme, displaces Atg7 and facilitates the irreversible formation of Atg12-Atg5 conjugate (309). Atg16L, in conjunction with Atg12-Atg5, associates with the autophagic isolation membrane during autophagosomal formation (293). The second conjugation system involves ubiquitin-like protein Atg8 being cleaved by Atg4, and activated by Atg7 (319). Atg3 then conjugates Atg8 with phospholipid phosphatidylethanolamine (PE), a membrane component of the autophagosomal membrane (319). It has been demonstrated that Atg12-Atg5 conjugation is required for Atg8 lipidation to occur, establishing a hierarchy of the two conjugation systems (125, 295, 323).

In contrast to Atg12 and Atg5, four Atg8 homologues have been identified in mammals: microtubule-associated protein 1 light chain 3 (LC3) (274), γ-aminobutyric acid (GABA)A-receptor-associated protein (GABARAP) (459), Golgi-associated ATPase enhancer of 16 kDa (GATE-16) (371), and Atg8L (424). LC3 can exist in two forms and can be post-translationally modified. LC3-I is found in the cytosol, whereas the cleaved and lipidated form of LC3-II precipitates onto the autophagosomal membrane after processing (195). LC3-II is commonly used as an autophagosomal marker in mammals (214, 296). The remaining three Atg8 homologues are less commonly used as autophagy indicators but GABARAP and GATE-16 also partake in lipidation and localize to the autophagosomal membrane (196). GABARAP is also involved in GABA receptor clustering (58) and cytoskeleton transport (459), while GATE-16 can modulate vesicle transport within the Golgi (371). Atg8L is the least studied Atg8 homologue and its role in the cell remains elusive. However, all Atg8 homologues are similarly processed and modified by Atg4 (140), Atg7 (424, 426) and Atg3 (424, 425) homologues.

The two conjugation systems of Atg12-Atg5 and Atg8/LC3 are necessary for the elongation and closure of the autophagosome. Upstream of this autophagic process requires the activation and nucleation of two important complexes. One of these complexes is a family of phosphoinositide (PI) 3-kinases (PI3Ks) which control important cellular functions including cytoskeleton remodeling and membrane trafficking (259). There are three different PI3K classes but all three classes phosphorylate phosphatidylinositol at position 3 of the inositol ring (184). Class I and II PI3Ks are mainly involved in receptor-induced trafficking events, such as pinocytosis, phagocytosis, and exocytosis (259). In contrast, class III PI3Ks generally mediate receptor-independent trafficking events, such as endocytic membrane traffic, phagosome maturation and autophagy (259). PI3K can associate with Beclin1, a mammalian homologue of Atg6 (253), along with accessory factors Atg14, Vps15 and Vps34, to form an initiation complex required for autophagosome biosynthesis (100, 368, 427). Ulk1 is the second constitutive complex consisting of Atg13 and FIP200 (130, 289) involved in autophagy induction.

The formation of the autophagosome is a critical aspect of the removal of defective proteins and organelles. In a metabolic tissue such as muscle, the activation of autophagy is sensitive to environmental cues to maintain cellular homeostasis and growth. The energetic status of the cell is governed by ATP production and the hydrolysis of ATP's high energy pyrophosphate bonds. The ratio of the nucleotide AMP, compared to ATP levels, can mediate the activation of AMP-activated protein kinase (AMPK). AMPK is a heterotrimeric complex consisting of a catalytic α subunit, and regulatory β and γ subunits. Elevated cellular AMP can bind onto the γ subunit of AMPK and allow for its allosteric activation. Upstream AMPK kinase, LKB1, can then phosphorylate threonine residue 172 of the α subunit. The stimulation of the catalytic subunit triggers a phosphorylation cascade of downstream targets (46), including the activation of

autophagy complexes of Ulk1 and PI3K (210, 211). AMPK can also inhibit protein synthesis pathways, such as rapamycin-sensitive mTOR through the phosphorylation of suppressor complex TSC2 (173) and binding partner raptor (120). The inhibition of protein synthesis allows for protein clearance and recycling to proceed by autophagy.

Calcium is another well-established controller of numerous cellular processes including autophagy. In muscle, calcium levels are tightly regulated by the sarcoplasmic reticulum (SR) and mitochondria (268). Evidence suggests the existence of structural interactions between these two organelles via inositol trisphosphate (InsP3) receptor calcium channel (IP3R) (87). Muscle contractile events primarily rely on mitochondrial ATP production and this is necessary for the propagation of calcium release and refilling of the SR (237). With elevated SR calcium levels, Beclin1 can directly regulate IP3R activity and stimulate LC3 lipidation (74). Furthermore, mitochondrial uptake of IP3R calcium release is essential for organelle bioenergetics, and an impairment in this transfer can activate AMPK-dependent autophagy (48, 452).

Mitochondria are generally accepted as primary sites of reactive oxygen species (ROS) emission (304). These damaging species can be detoxified by superoxide dismutase (SOD), NADH and glutathione, and also by catalase in the cytosol (383). It is hypothesized that chronic impairment of mitochondrial function, and a disrupted balance between ROS production and elimination, can trigger organelle removal by mitophagy (see below). There are several mechanisms by which ROS can positively regulate autophagy. First, AMPK can be activated via the oxidation of reactive cysteines located at its α subunit (47, 492). Second, phosphorylation of autophagy adaptor protein p62 increases its affinity for Keap1, a component of the Cul3-ubiquitin E3 ligase complex responsible for degrading Nrf2 (170, 241). The inhibition of Nrf2 degradation and its cytosolic accumulation results in its translocation into the nucleus, where it can bind to

antioxidant-responsive elements (AREs) located in the promoter regions of antioxidant genes and activate their transcription (222). AMPK (121), mTOR (170), and Ulk1 (257) are several autophagy-related kinases suggested to regulate p62 phosphorylation. Moreover, a less studied group of antioxidant-like proteins called Sestrins can similarly activate Nrf2 (13) via mTORC1 inhibition and AMPK activation (248). Lastly, ROS can directly regulate autophagy proteins in a redox-dependent manner. Scherz-Shouval et al. demonstrated that the oxidation of Atg4 inactivates its delipidating activity on LC3, allowing for autophagosomal elongation to continue (384). It is hypothesized that this occurs in the proximity of dysfunctional mitochondria so that autophagosomal engulfment can occur (383). Here, the data propose mitochondria as a major source of ROS required for autophagy. In turn, autophagy can eliminate organelle oxidative stress to protect the cell from additional oxidative damage. This can also be specifically achieved by activating mitophagy.

Mitophagy is a cargo-specific process of autophagy involved in the removal of superfluous mitochondria. In the 1960s, mitophagy was first studied in mammals with the use of rat liver tissue perfused with glucagon (10). Examination by electron microscopy revealed an increased number of lysosomes containing mitochondria within the liver (10). Almost half a century later, Lemasters and colleagues coined this non-random process as mitophagy, and postulated the beneficial effects of mitophagy against oxidative stress, mitochondrial dysfunction and aging (209, 252). As discussed earlier, mitophagy is characterized as a terminal step in organelle quality control. Mitochondrial depolarization and sustained damage yields organelle fragmentation to assist in mitophagy (441, 479). In the following section, two general mitophagy pathways will be discussed: 1) ubiquitin-dependent pathways that rely on ubiquitin ligases and autophagy adaptor proteins, and 2) ubiquitin-independent pathways that depend on specific mitochondrial receptors.

Several cellular ubiquitin ligases exist, but the most well-studied ligase involved in mitophagy is Parkin, along with its associated kinase PINK1 (PTEN-induced putative kinase 1). Mutations in the Parkin gene are thought to cause autosomal recessive Parkinson's disease (72). The effect of Parkin with age will be discussed in the aging section of this literature review. Here we will discuss the mechanistic and structural basis for the activation of Parkin by PINK1. In the presence of functional mitochondria, cytosolic PINK1 protein levels are maintained at low levels through membrane potential-dependent import into the organelle (187). PINK1 arrives through the TOM complex (242), and is degraded by the IMM rhomboid protease PARL (73, 115, 187, 286). The remnants of PINK1 degradation can retro-translocate from the mitochondria, and into the cytosol where they are recognized and degraded by the proteasome (477). When the mitochondrial membrane potential dissipates, PINK1 can stabilize and accumulate on the OMM where it can selectively recruit cytosolic Parkin to impaired mitochondria (187, 224, 306, 454).

Parkin is an E3 ubiquitin ligase that performs the terminal step of ubiquitination. This process is initiated by ATP-dependent activation of E1's catalytic cysteine residue and the formation of a thioester bond with the C-terminal carboxyl group of ubiquitin. The charged ubiquitin is transferred to a second cysteine of an E2 enzyme. In the last step, E2 enzyme ubiquitin conjugates with an E3 enzyme to transfer ubiquitin to a lysine residue of a target substrate. Parkin can bind to several E2 ubiquitin conjugating enzymes, including UbcH7, UbcH8 and UbcH13 (321). In addition, Parkin can produce various ubiquitin lysine residue linkages that can mediate differing signal transduction and trafficking pathways. These include: monoubiquitination (122, 189, 281, 299), lysine 48-linked polyubiquitination (53, 258), and lysine 63-linked polyubiquitination (82, 276, 322). For example, upon mitochondrial depolarization, Parkin can target Miro1, a mitochondrial trafficking protein, for proteasomal degradation, thereby isolating

the damaged organelle from the mitochondrial reticular network (29, 461). Parkin can also target mitochondrial fusion/fission proteins to the proteasome in favour of a less reticular network in order for mitophagy to occur (59, 423, 441, 460).

Numerous studies have examined how Parkin E3 ligase activity is achieved. To date, E3 ubiquitin ligases are grouped in one of three classes: RING (really interesting new gene) ligase, HECT (homologous to the E6-AP carboxyl terminus) ligase and RING-HECT hybrid (25, 85). RING ligases function as a platform for ubiquitin transfer between E2 enzymes to target substrates, but do not directly interact with ubiquitin themselves. Conversely, HECT ligases contain an active cysteine site that can form an intermediate thioester bond with ubiquitin. Interestingly, X-ray crystallography has exposed Parkin as a RING-HECT hybrid, containing a RING domain as well as a catalytic cysteine residue (358, 465). Under basal conditions, Parkin is in an autoinhibited state due to three intraspecific interactions. First, the ubiquitin-like (Ubl) domain at the N-terminus can bind to the C-terminal RBR (ring-between-ring) domain in *cis* and consequently inhibit Parkin (55). The RBR region contains an E2-binding RING1 domain, an IBR (in-between-ring) domain and a RING2 domain that contains the catalytic cysteine residue 431 for charged ubiquitin docking (394). Second, the RING0 domain (not part of the RBR) can obstruct the ubiquitin acceptor site in RING2 (435, 463). Third, the linking of IBR and RING2 (known as the repressor element of Parkin) can bind with RING1 and block its E2 ubiquitin binding site (435, 463).

PINK1 acts upstream of Parkin and is required for Parkin recruitment to damaged mitochondria (206, 306, 454). PINK1 can directly phosphorylate Parkin's Ubl domain on residue serine 65 to activate Parkin (171, 224, 320, 322). However, early studies suggested that PINK1/Parkin do not always perform in such a linear relationship. For example, it appears that PINK1 requires autophosphorylation to recruit Parkin (320), and that PINK1 does not always

phosphorylate Parkin (454), or that PINK1 phosphorylates mitochondrial substrates for Parkin recruitment (59). These observations have led researchers to investigate additional PINK1 substrates involved in Parkin activation. In 2014, three independent laboratory groups concurrently found that PINK1 can similarly phosphorylate residue serine 65 of ubiquitin, and that phospho-ubiquitin can also activate Parkin (200, 206, 228). However, the order of events required for phospho-ubiquitin amplification remains unanswered. Does Parkin incorporate only phospho-ubiquitin directly into chains, or does ubiquitin phosphorylation precede chain formation? Furthermore, what role does phospho-ubiquitin have in other alternative ubiquitin ligases implicated in mitophagy? These questions remain unanswered. Mitochondrial ubiquitin ligase 1 (482) and Glycoprotein 78 (99) are two ubiquitin ligases also implicated in mitophagy that are Parkin-dependent and -independent, respectively. Interestingly, both ligases and Parkin act on shared targets to maintain mitochondrial integrity (59, 99, 482). This suggest that E3 ubiquitin ligases may function redundantly in organelle quality control.

Proteomic analysis on Parkin activation has yielded numerous associations with OMM proteins, autophagy receptors and the proteasome (54, 380). Parkin ubiquitination sites on the cytoplasmic surface of OMM targets include VDACs, Mfn1/2, Miro1, Fis1, TOM20 and TOM70 (380). These data reaffirm the idea that Parkin can influence the OMM proteome, and that Parkin depolarization-dependent localization to these outer surface targets can activate proteasomal (53, 423) and mitochondrial degradation (59, 103, 242, 441, 461) to occur.

Five autophagy receptors have been demonstrated to have a ubiquitin binding domain (168) and a LC3 interacting region (LIR) (28) that facilitate the connection between OMM ubiquitin targets and autophagic machinery. These five receptors are: p62/SQSTM1 (103, 223, 305, 328), NBR1 (215), TAX1BP1 (439), NDP52 (456), and OPTN (397, 468). Initial studies did not resolve

the differences between these receptors and their role in mitophagy. In 2015, Youle et. al found that NDP52 and OPTN are the primary receptors for mitophagy, and are directly recruited to phospho-ubiquitin on mitochondria in a PINK1-dependent manner (243). They also showed that NDP52 and OPTN can recruit Ulk1 downstream for autophagy induction (243). Additional studies have found that TBK1 is a secondary kinase galvanized during PINK1/Parkin-mediated mitophagy, and that it primarily phosphorylates and enhances OPTN binding to ubiquitin (145, 356). TBK1 activation can additionally phosphorylate p62, NDP52, and TAX1BP1 to reinforce mitochondrial ubiquitination and degradation (145, 356).

In mammalian cells, mitophagy can also occur in the absence of ubiquitin. The process relies on OMM integral receptors with LIR motifs. The first two receptors, BNIP3 and NIX, are part of the homologous BCL2 homology 3 (BH3) protein family, and can mediate cell death and mitophagy (487). In several studies, BNIP3 and NIX are illustrated as being required for autophagy (70, 128, 249) and for mitochondrial-mediated apoptosis to occur (172, 348, 354). However, controversy exists regarding whether these two proteins directly mediate organelle depolarization (70, 376, 486) or if their localization depends on membrane potential (399). A loss in NIX can inhibit mitochondrial membrane potential and impair mitochondrial clearance in erythroid cell development (81, 376, 390, 486). Interestingly, NIX directly binds to GABARAP but not to LC3, despite sharing the same LIR motif as BNIP3 (314, 389). The third receptor FUNDC1 is involved in hypoxia-mediated mitophagy, and it is activated by dephosphorylation to enhance its interaction with LC3 (262). BNIP3 and NIX can likewise operate mitophagy under hypoxic conditions (21, 485).

Lastly, there is a class of mitophagy receptors that are not integral OMM proteins, and that do not depend on ubiquitin. AMBRA1 is a unique protein involved in autophagy induction as well

as Parkin-mediated mitophagy. Under basal conditions, mTOR and anti-apoptotic Bcl-2 inhibit AMBRA1 (308). When autophagy is induced, Ulk1 stimulates AMBRA1 and the PI3K complex to enable autophagosome nucleation (17, 278). AMBRA1 can interact with mitochondrial Parkin to recruit activated PI3K to damaged organelles (167). Moreover, AMBRA1 can initiate perinuclear mitophagy through its LIR motif, independent of Parkin and p62 (410). Cardiolipin was recently found to contain LC3-binding sites, and the redistribution of cardiolipin from the IMM to the OMM can also serve as a mitophagic trigger (60).

2.3 Muscle Adaptations to Aerobic Exercise

2.3.1. Metabolic adaptations of muscle to exercise

Physical inactivity is a global pandemic considered as a major cause of death worldwide (219). Sedentary behaviour has been long regarded an important determinant of the occurrence of chronic metabolic syndromes including obesity and diabetes (96, 476). The beneficial effects of regular exercise and health date back to the 5th century BC, when Hippocrates said that "Eating alone will not keep a man well; he must also take exercise. For food and exercise… work together to produce health" (374). It has been demonstrated many times that regular exercise can aid in the prevention of metabolic syndromes (235), and age-related loss of muscle mass (50). However, only recently have molecular biologists uncovered the signaling pathways involved in mediating the adaptive responses to exercise. The focus of this review will be on the effect of these signaling pathways in skeletal muscle in response to exercise.

Chronic, repeated bouts of exercise can elicit alterations in muscle metabolism. Seminal work by John Holloszy in the late 1960s demonstrated that muscle can undergo biochemical adaptations following endurance training, and that an increase in muscle oxygen consumption was

an outcome of mitochondrial biogenesis (153). Long-term training can evoke mitochondrial adaptations that are fibre-type specific (159). In the case of a muscle that contains a greater composition of fast oxidative-glycolytic fibres, a dramatic alteration in enzymatic profile toward that of more slow oxidative fibres is observed with prolonged, high intensity training (114, 141). Endurance training can also induce adaptations in higher oxidative muscle fibres to a smaller degree (164). Furthermore, SS mitochondrial volume increases significantly relative to IMF mitochondria in all muscle fibre types following endurance training (164). Training-induced alterations in mitochondrial protein and enzyme expression occur at a gradual rate that outpace increases in whole body oxygen consumption (107, 142).These progressive changes reflect the activation of signaling pathways involved in mitochondrial biogenesis, and other exercise-responsive genes. A temporal sequence of transcriptional and translational events occurs prior to organelle biogenesis. For instance, transcriptional mRNA upregulation occurs after a single bout of endurance exercise (273, 340). Acute exercise can act as a stimulus towards achieving adaptation, but on its own cannot alter muscle metabolic capacity. Over time, the cumulative effects of successive exercise bouts can yield a gradual accumulation in protein content leading to improved whole muscle metabolism and exercise performance. The increased expression of metabolic enzymes can result in the enhanced sensitivity of mitochondrial respiratory control, such that a lower ADP concentration is sufficient to achieve the same level of oxygen consumption in muscle (83). Thus, following endurance training, the increase in mitochondrial content in muscle can induce a lower amount of ADP required to stimulate respiration per mitochondrion at the same absolute power output. This can consequently reduce the amount of ROS generated per oxygen consumed per gram of tissue (71). The reduced formation of ADP can attenuate glycolysis and the production of lactic acid. In addition, highly oxidative muscle fibres contain diminished expression

patterns of AMP deaminase and 5′-nucleotidase enzymes, relative to glycolytic fibres (438). Therefore, this can yield a lower rate of AMP synthesis that, in turn, can lower AMPK activation. Endurance training can lower kinase signaling (265) and GLUT-4 translocation to the plasma membrane (357). The reduction in carbohydrate handling and glycogen depletion after training is compensated by a proportional increase in lipid uptake and oxidation in muscle (421). Collectively, endurance training can improve exercise performance by increasing mitochondrial content, reducing metabolic by-products, glycogen storage sparing, and improving oxygen to ATP coupling.

2.3.2. Gene expression: PGC-1a signaling and exercise

Regular endurance exercise has an established function in stimulating mitochondrial biogenesis and function (157) (**Figure 5**). A portion of this process is mediated by PGC-1α, a transcriptional coactivator that regulates genes involved in energy metabolism (126). PGC-1α can bind and enhance the activity of several transcription factors, including nuclear respiratory factor (NRF)-1/2 and estrogen-related receptor-α (ERRα), which in turn can upregulate the transcription of NUGEMPs (169, 386, 473). PGC-1β and PGC-1-related coactivator (PRC) are two other members that belong to the PGC-1 coactivator family, with both factors being able to trans-activate nuclear respiratory factors involved in biogenesis (382). However, it is suggested that these coregulatory proteins act independent of PGC-1α, as it has been shown that PGC-1 family members, as well as NRF-1/2 and ERRα, do not exhibit compensatory responses to reduced levels of PGC-1α (126, 443). Nonetheless, PGC-1α transcription is enhanced following exercise training, implicating its role in mitochondrial biogenesis in skeletal muscle (341). This is supported in animal studies that illustrate that global or muscle-specific deletion of PGC-1α can blunt mitochondrial biogenesis during endurance training (104, 251, 483). In addition to its role in the

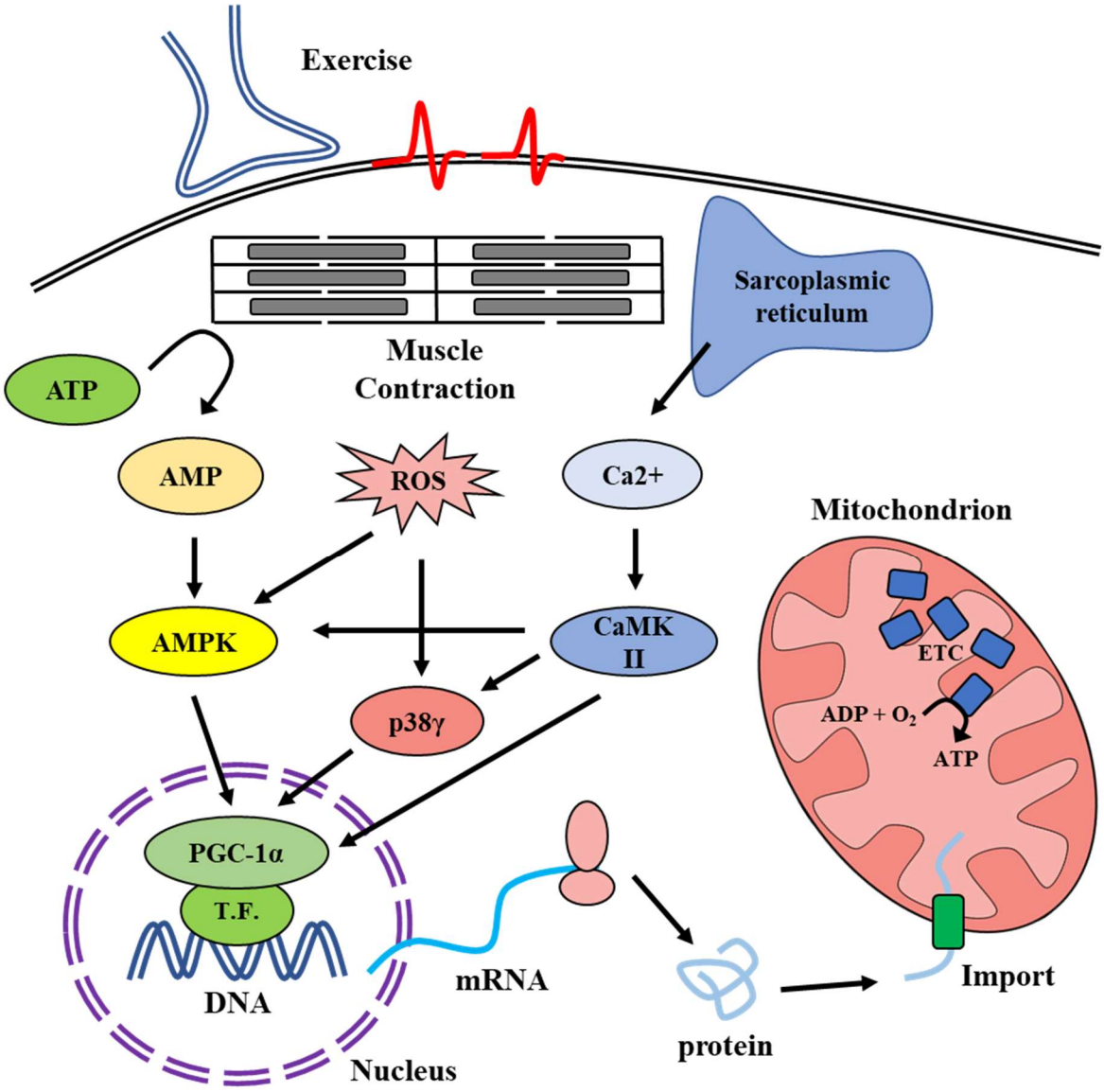

Figure 5. Exercise-induced mitochondrial biogenesis. To induce mitochondrial biogenesis during exercise, mechanical events must translate to molecular signals in order for the cell to adapt. ATP is metabolized to ADP and AMP with exercise. Elevated levels of AMP can activate AMPK. In addition, the production of reactive oxygen species (ROS) is increased during exercise and can stimulate AMPK and p38γ activity. With repeated bouts of exercise, intracellular calcium levels can rise and activate CaMKII. Cross-talk between signaling pathways can occur. For example, CaMKII can phosphorylate AMPK and p38γ. The exercise-induced activation of AMPK, CaMKII and p38γ can converge and influence PGC-1α within the nucleus. PGC-1α is a transcriptional co-activator that does not bind onto DNA directly. Rather, PGC-1α can interact with transcription factors, and promote the transcription of nuclear genes encoding mitochondrial proteins (NUGEMPs). The translation of these gene products occurs in the cytosol and they are delivered to the mitochondrion. Proteins that are destined to the mitochondrion contain mitochondrial-targeted sequences. Mitochondrial proteins undergo import which allows for their incorporation and assembly in the organelle.

nucleus, PGC-1α can translocate to the mitochondria in response to exercise, and can bind with TFAM on the D-loop of mtDNA to promote the transcription of specific mitochondrial-encoded genes (370). The ectopic expression of PGC-1α in muscle cells can induce molecular adaptations that include increased mtDNA expression, enhanced mitochondrial biogenesis and substrate utilization, as well as improved cellular respiration (464, 473). In rodents, the overexpression of PGC-1α can recapitulate the phenotype of trained muscle, illustrated by improved exercise performance, an increase in mitochondrial respiratory capacity, and greater ATP synthesis (44).

During repeated bouts of muscle contractions, energetic- and contraction-related signaling pathways are activated to regulate the expression of PGC-1α. The three primary kinases involved in regulating PGC-1α in skeletal muscle are AMPK, p38 MAPK and CAMK. AMPK is activated primarily when cellular levels of AMP are increased (199, 301). A depletion of ATP because of exercise can increase the cellular AMP/ATP ratio and activate AMPK. For example, acute exercise can phosphorylate and activate AMPK in an intensity-dependent manner (467). On the other hand, chronic endurance training can promote AMPK-mediated mitochondrial biogenesis through NRF-1 activation and expression of respiratory proteins (24). The treatment of AMP mimetic 5-aminoimidazole-4-carboxamide ribonucleoside (AICAR) in muscle cell culture can activate AMPK and its regulation on the PGC-1α promoter (178). The specific deletion of AMPK in skeletal muscle of mice can impair exercise performance and increase mitochondrial dysfunction (239). AMPK can also post-translationally modify PGC-1α by phosphorylating it at residues threonine-177 and serine-538 (179). Moreover, the translocation of PGC-1α to the nucleus and mitochondria during exercise may also be dependent on AMPK activation (405), but the mechanism by which AMPK activation can mediate PGC-1α translocation remains undetermined.

A role for p38 mitogen-activated protein kinase (MAPK) during exercise in skeletal muscle is well-established (9). It has been demonstrated numerous times that the activation of p38 MAPK promotes PGC-1α transcription during exercise-induced muscle adaptations (4, 347, 481). In vivo optical bioluminescence imaging provides direct evidence that putative regulatory factors that are typically activated by p38 MAPK, are required for PGC-1α promoter responsiveness to contractile activity (3, 489). The constitutive activation of p38 MAPK aids in mitochondrial adaptations in skeletal muscle (4), but mice with muscle-specific gene deletion of p38γ MAPK, but not those of p38α and p38β, were shown to be required for endurance exercise-induced mitochondrial biogenesis (343). An alternative mechanism of p38 MAPK activation is via the generation of free oxygen radicals brought about by exercise through the activity of respiratory chain complexes, and that of xanthine oxidase and NADPH oxidase (304). Research has shown that acute exercise can activate MAPK signaling in a ROS-dependent manner (334, 346, 488). Finally, calcium release from the SR during muscle contractions is essential for the formation of cross-bridges between myosin and actin filaments. The increase in cytosolic calcium within muscle can modulate the activity of calmodulin-dependent protein kinase (CaMKs). CaMKII is the main CaMK isoform present in skeletal muscle, and it is phosphorylated during exercise in an intensity-dependent manner (365). Due to calcium's pervasive role during muscle contractions, it may not be too surprising that CAMKII can undertake cross-talk with other pathways that influence PGC-1α transcription. It has been suggested that CAMKII can function as an upstream kinase of p38 and AMPK as a regulator of PGC-1α expression during exercise (177, 185, 365, 469, 471).

2.3.3. Regulation of autophagy and mitophagy with exercise

It is hypothesized that exercise can induce autophagy (138, 139, 233, 261, 446). During muscle contraction events, autophagy activation can function to remove dysfunctional organelles

and proteins from the cell. This can, in turn, improve cellular function. For example, it is well established that physical exercise can result in elevated oxidative stress (349). As mentioned earlier, exercise-induced ROS production is an important modulator in muscle signaling. However, chronically elevated levels of ROS can also be damaging to organelles and contractile proteins. Thus, the induction of autophagy with exercise-induced ROS emission is required to remove damaged proteins and organelles in muscle. The terminal degradation of these substrates at the lysosome provide a source of amino acids that can be recycled as a source of energy in muscle cells during energetic stress. In response to exercise, mitochondrial proteins have been observed to have a half-life of approximately 1 week (36, 142, 428). The earliest examination of the influence of exercise on autophagy was studied in the 1980s, where autophagic vacuoles were detected in the muscles of mice following prolonged strenuous exercise (375). For a period, the molecular mechanisms that regulated autophagy during exercise remained poorly understood. Within this past decade, research on this topic has rapidly accelerated. The first studies to show molecular evidence of autophagy activation with exercise occurred in the early 2010s. For instance, Collagen VI null mice display impaired autophagy induction following acute exercise and after 3 months of voluntary exercise (118). This study was the first to suggest that autophagy activation may be important in mediating muscle adaptations to exercise training. In another study, mice containing a constitutively inactive form of Bcl-2 that prevents the activation of autophagy protein Beclin1 had impaired autophagy induction in muscle with exercise (138). Furthermore, animals containing inactive Bcl-2 displayed overall reduced endurance performance and increased glucose intolerance when placed on a high-fat diet (138).

It appears that physical activity is a potent stimulus for autophagy induction in skeletal muscle, and that this is dependent on the type and duration of exercise. An acute bout of endurance

exercise can evoke a robust response in autophagy activation (118, 182, 446), where an increased expression of autophagosomal marker LC3II is observed. Interestingly, chronic exercise training elicits an increased capacity for the formation of autophagosomes, and this is required for muscle adaptation to occur (98, 194, 261). It is proposed that the alterations in energy supply brought about by exercise can activate AMPK and Ulk1 (233). This is a debated topic, as existing studies support (97, 298, 325) and refute (182, 451) AMPK's involvement in autophagy activation during exercise. AMPK can activate Ulk1 at multiple phosphorylation sites that allows for Ulk1 activation during mitophagy (86, 152, 211, 433). Several studies have shown that acute exercise can stimulate Ulk phosphorylation during mitophagy (233, 298), suggesting the importance of Ulk1 signaling in mediating mitochondrial turnover in response to exercise. The effect of Ulk1 on PINK1/Parkin-mediated mitophagy in response to exercise remains unknown. Because of the ease of genetic manipulation in mice, a limited number of studies have focused on autophagy and exercise in human subjects. In general, autophagy activation in human skeletal muscle occurs during high, intensity endurance exercise (98, 180, 181, 388), based on "classic" measurements of LC3 lipidation and p62 expression.

Autophagy is a highly dynamic process that involves the synthesis and degradation of the autophagosome, an outcome called flux. Several commercially available autophagy inhibitors can act in skeletal muscle to prevent autophagy from occurring (192). The treatment with an inhibitor and the consequent accumulation of autophagosomes within the cell can give researchers an indication of autophagy flux. For example, colchicine can destabilize the microtubule network, thereby preventing the delivery of an autophagosome to the lysosome for degradation. As a result, this will give an indication of autophagy flux up to the point of the lysosome. The description of autophagy flux without proper controls and inhibitors is incorrect. However, the utilization of

inhibitors in humans is not appropriate or feasible, and may be a limitation for measuring autophagy flux in human studies. Nonetheless, autophagy inhibitors are currently applied in many cell and animal models, allowing researchers to have a basic understanding of autophagy regulation. In one study, mice that were pre-treated with colchicine, and subjected to acute exercise, exhibited increased autophagy and mitophagy flux (446). Specifically, the study found that acute exercise was able to induce the mitochondrial localization of Parkin, ubiquitin, p62 and LC3II (446). Remarkably, these effects were abolished in the absence of PGC-1α, implicating a role for PGC-1α in mediating mitophagy in muscle during exercise. In future studies, the proper assessment of flux is essential to advancing our knowledge of autophagy activation during exercise and endurance training. There is a considerable amount of research on autophagy in muscle with physical exercise, but evidence on exercise-induced mitophagy is still lacking. A limitation in the study of mitophagy is the examination of autophagy markers in whole muscle. For example, whole muscle Parkin protein content has been shown to increase (181) and decrease (182) with endurance exercise. Therefore, researchers cannot assume that mitophagy is activated or supressed solely on whole muscle measurements. Rather, direct measurements of autophagy markers on isolated mitochondria would provide a more accurate interpretation of mitophagy in vivo. Fortunately, the recent development of mitophagy reporters (i.e. MitoTimer) can now be supplemented in the toolboxes of researchers as a method to investigate mechanisms of mitophagy signaling in vivo. MitoTimer is a mitochondria-targeted fluorescent protein that can be used to study mitochondrial turnover, dependent on its ability to irreversibly transition from green to red fluorescence over a period of 48 hours (148, 431). Newly synthesized MitoTimer is green, and its increase in mitochondria reflects greater protein import and increased mitochondrial biogenesis. As MitoTimer becomes oxidized, it irreversibly shifts to red. Following chronic voluntary wheel

running in mice, an increase in green fluorescence is observed, indicating greater biogenesis (234). In contrast, mice on a high-fat diet expressed a higher ratio of red to green MitoTimer, and this ratio was completely reduced by voluntary wheel running (234). Organelle turnover is reduced when autophagy is inhibited, and this can lead to the accumulation of red MitoTimer (93). Furthermore, co-localization of red MitoTimer and lysosomal markers can provide evidence of selective degradation of "aged" mitochondria through mitophagy. This was observed in rodents following an acute bout of endurance exercise, providing direct evidence of exercise-induced mitophagy in muscle (233). Collectively, these data establish MitoTimer as a useful tool in monitoring mitochondrial turnover, and may provide additional insight into mitochondrial biology and regulation during other metabolic challenges, such as obesity and aging.

2.3.4. Coordination of mitochondrial biogenesis and mitophagy

To maintain a healthy pool of mitochondria, cells are required to maintain a balance between the synthesis and degradation of organelles. The studies on the underlying mechanisms involved in this balance have yielded the discovery of several transcriptional factors, such as TFEB which is an important regulator of lysosomal biogenesis and autophagy (379, 396). The induction of TFEB has been found to regulate genes involved in fatty acid oxidation and mitochondrial biogenesis, that are partly mediated by PGC-1α (395). It has been proposed that TFEB and PGC-1α function in a co-regulatory loop that maintains a balance between mitochondrial biogenesis and degradation, and that this loop is in the general control of amino acid synthesis 5-like 1 (GCN5L1) (391). However, this relationship has been contested in exercise-related studies, as TFEB is required for mediating exercise-induced adaptations, and this process can be dependent (88) or independent of PGC-1α activity (275).

Parkin is well known for its role in mitophagy, but a less studied area of Parkin activity is its possible regulation on mitochondrial biogenesis. In vitro overexpression of Parkin can increase mtDNA replication as well as mitochondrial content (232, 366). More importantly, overexpressed Parkin can directly associate with TFAM on promoter sites of mtDNA to enhance transcription (232). Another mechanism linking Parkin with mitochondrial biogenesis is the recent identification of Parkin interacting substrate, PARIS (401). PARIS is a transcription factor that can bind to the promoter region of PGC-1α and repress its transcription, as well as downregulate the downstream target NRF-1 (401). Parkin is involved in the ubiquitination and UPS-dependent elimination of PARIS, and that the loss of Parkin can contribute to PARIS-dependent declines in mitochondrial content and respiration (409). Moreover, PINK1 can interact and phosphorylate serine residues 322 and 613 of PARIS to enhance its ubiquitination and clearance by Parkin (250). Whether the Parkin-PARIS-PGC-1α axis is involved in regulating mitochondrial turnover in muscle with exercise remains unknown. Future research on uncovering the mechanisms involved in fine-tuning mitochondrial content via this mechanism is of paramount importance.

2.4 Aging of Skeletal Muscle

2.4.1. Metabolic alterations with sarcopenia

Sarcopenia is an age-related process that can manifest itself as a multifactorial syndrome. Several factors that may contribute to sarcopenia have been proposed. These include a decline in endocrine function, lipid oxidation impairment, insulin resistance and chronic diseases (89). The decline in skeletal muscle quality is thought to play a critical role in muscle metabolism in the development of sarcopenia. Although the age-related decline in muscle mitochondrial content is controversial (146), a reduction in organelle content and function in aged muscle can occasionally

elicit muscle wasting, and can also promote the metabolic pathogenesis of type 2 diabetes (335), and an increase in abdominal fat deposits (51, 220, 244). An impairment in insulin signaling and incomplete fatty acid oxidation can induce mitochondrial stress (226). Inefficient substrate metabolism reduces mitochondrial bioenergetic capacity (207) and may increase superoxide formation with age (52). In addition to macromolecule damage (e.g. proteins, DNA), free radicals can induce the activation of stress pathways that inhibit insulin-stimulated glucose transport in muscle (31, 272). For example, the overexpression of mitochondrial antioxidant enzymes, such as catalase and superoxide dismutase, can prevent age-associated muscle insulin resistance (151), and mitochondrial dysfunction (247). As a result, the uncontrolled generation of free radicals can produce irreversible protein modifications that accumulate with age. Glycative and oxidative modifications are common examples of protein alterations that can negatively affect mitochondrial function and also resist proteasomal degradation, precipitating in a continual cycle of cellular damage and stress (20, 150). However, recent research has also indicated that mitochondrial ROS may not be a key regulator of muscle atrophy during aging. This is evident by studies demonstrating that the loss of muscle mass and function in old animals were not altered when supplemented with mitochondrial-targeted antioxidants (372, 373). The involvement of mitochondrial dysfunction in muscle atrophy during aging remains a contentious topic that requires further investigation.

In addition, protein synthesis and protein degradation can contribute to lower protein turnover rates in aged muscle. The decline in anabolic hormones, such as insulin-like growth factor-1 (IGF-1), can lead to reduced muscle protein synthesis rates. IGF-1 is a hormone that is analogous to insulin, but that binds to a separate receptor to stimulate cell growth and proliferation, and it is mainly mediated by the secretion of growth hormone (GH). IGF-1 and GH are shown to

both decrease with age (236, 315, 332). GH replacement strategies appear to initially reverse the phenotypic features of aging (increase lean body mass and decrease fat mass), but long term administration can also lead to the development of diabetes, glucose intolerance and increased cancer risk (18, 30, 127). On the other hand, the down-regulation of IGF-1 receptors in rodents produces extended lifespans, with reductions in fat mass (32) and improved resistance to oxidative stress (156).

With these confounding data, what exactly is the role of insulin in aging and protein metabolism? It is proposed that insulin action on protein metabolism with advancing age is reduced (34, 119), even with nutritional supplementation (455). These data suggest that muscle protein synthesis is resistant to the anabolic action of insulin (352), and may be a factor in advancing sarcopenia. A decrease in muscle protein synthesis rates can negatively impact mitochondrial function in the elderly (335) and in insulin-resistant individuals (300). In healthy individuals, insulin can promote mitochondrial protein synthesis, while individuals with type 2 diabetes may suffer a lower capacity for ATP production (207, 411). It remains undetermined if mitochondrial dysfunction with age is the result, or cause, of insulin resistance.

2.4.2. Mitochondrial DNA and age

It is well established that sarcopenia features a decline in skeletal muscle mitochondria (52). Electron micrographs from aged rodent muscle reveal that SS and IMF mitochondrial contents are both reduced, and appear more fragmented (176). In aged human muscle, these decrements are reflected by changes in maximal oxygen uptake and oxidative enzyme activities (64, 364). The diminished content of mitochondria in aged muscle is partly due to a reduced expression of the transcriptional coactivator PGC-1α (52), a protein involved in the coordinated transcription of NUGEMPs. It is therefore possible that age-related alterations arising in nuclear

genes encoding the protein import machinery (PIM) can reduce the assembly of the ETC (149). However, aged animals do not exhibit an impaired capacity for matrix-destined protein import into the organelle (67, 267). However, precursor proteins may be more rapidly degraded in the cytosol (166). Old animals also display a greater assembly rate of the outer TOM complex, which may serve as a compensatory mechanism to restore mitochondrial content or function within aged muscle (191). The restoration of the protein import pathway may aid in the import of TFAM, an important regulator of mtDNA transcription, and its absence in muscle reduces mtDNA abundance (470). Studies in humans (255) and rodents (333) demonstrate that TFAM is elevated in aged muscle, suggesting a role for TFAM in the maintenance and/or recovery of mitochondrial content and function with age.

A stoichiometric imbalance between nuclear- and mitochondrial-encoded proteins can activate the UPR^{mt}. Recent research suggests a link between UPR^{mt} and aging. A majority of UPR^{mt} investigation has been completed on lower order organisms. The link between the UPR^{mt} and lifespan was first examined in worms that were long-lived with the knockdown of nuclear-encoded cytochrome c oxidase subunit 4 (COX4) (84). Interestingly, mitochondrial mutants that lived longer required the activation of the UPR^{mt}, while long-lived mutants that did not have mitochondrial mutations relied on insulin/IGF-1 signaling, independent of UPR^{mt} activation (84). Flies with a muscle-specific knockout of a subunit of complex I exhibit lifespan extension, accompanied by UPR^{mt} and IGF-1 induction (324). It is enticing to speculate that UPR^{mt} activation can modulate the aging process though IGF-1 signaling, but the nature of the stimulus can yield varying cellular responses in different tissues (331). Furthermore, higher order organisms, such as mice, do not appear to rely on the IGF-1/insulin pathway with UPR^{mt} activation (162, 263). This divergence may be a result of IGF-1 requirement on lower order organism development (78, 329).

With advancing age, there is a greater propensity for mitochondria to generate ROS, despite no changes in antioxidant enzyme activity (52). An elevation in free radicals within aged muscle can trigger mtDNA and nDNA decay. According to the mitochondrial theory of aging, an accumulation of mtDNA mutations can lead to aging in humans and animals (132). Mammalian mtDNA encodes 13 polypeptides that are critical components of the electron transport chain (ETC). Small point mutations and large scale deletions can occur in several aged human tissues (197, 254). MtDNA mutations in skeletal muscle can negatively impact OXPHOS, decrease ATP generation, and affect general muscle performance. Mitochondria are unique as multiple copies of mtDNA can exist within an organelle. Therefore, pathological mutations are inherited via maternal inheritance and cellular segregation leading to mtDNA distribution termed heteroplasmy, which refers to the proportion of mutant to wild-type mtDNA copies within a mitochondrion. Heteroplasmy can range from 1% to 99%, with the severity of symptoms dependent on the pathological nature of the mutations. A histological phenotype can be observed in patients with age-induced mtDNA mutations, and those with mitochondrial myopathies. These mutations can lead to abnormal ETC activity at specific sites along muscle fibres (458). A cross-section of old muscle compared to a young muscle will contain an absence of cytochrome c oxidase (COX) activity, and an upregulation of nuclear-encoded succinate dehydrogenase (SDH) activity (147, 246, 269). This is the outcome of the nuclear genome compensating for mtDNA defects. This is ineffective, however, as COX activity remains required for proper ETC function.

Aged fibres from animals (147) and humans (41) are highly susceptible to atrophy and dysfunction at specific regions that have a mtDNA mutation load exceeding that of 90% total mtDNA. At these sites, mtDNA deletions can disrupt genes encoding COX, NADH dehydrogenase, ATP synthase, and a few mitochondrial transfer RNAs. The mitochondrial 4977

bp deletion, also known as the common deletion, is one of the most frequently observed mtDNA mutations associated with age and disease. This specific mtDNA mutation is highly detectable in post-mitotic tissues (i.e. muscle and brain) (65, 66, 260, 288). Common mutations in mtDNA can also occur at the displacement loop site where mtDNA transcription is initiated (90). For example, muscle biopsies taken from older individuals contain two point mutations, A189G and T408A, at the D-loop that can negatively affect the transcription of mtDNA (462). If mtDNA transcription is repressed, why do mtDNA mutations persist as an organism ages? Kowald and Kirkwood (227) hypothesized that mitochondrial transcription negatively regulates itself when there is a surplus of gene products. In young individuals, proteins are synthesized that can inhibit mtDNA transcription. The production of these inhibitory proteins is reduced with age, which can result in the propagation of mtDNA mutants. The alterations in mtDNA can be sustained in the absence of DNA polymerase gamma (PolG), an enzyme involved in mtDNA proofreading. Animals that are deficient in this proofreading enzyme present greater mtDNA damage and accelerated features of aging, and an increase in muscle caspase activation (apoptosis) (231, 436). Thus, mitochondrially mediated cell death is highly active in aged skeletal muscle, which may contribute to the progressive decline of muscle mass and function.

2.4.3. Apoptosis and age

Apoptosis, also known as programmed cell death, is an evolutionary conserved process involved in cellular development (353). While the cellular mechanisms that contribute to sarcopenia remain elusive, it has been suggested that apoptosis may be a contributing factor (52, 79, 80). ROS are primarily produced by mitochondria and can trigger the release of pro-apoptotic factors during apoptosis. To enable this discharge, a permeability transition pore (mtPTP) exists but little is known about its structure. The Bcl-2 protein family assist in governing the mtPTP,

consisting of proteins that can either be pro- (Bax, BAD, Bak) or anti-apoptotic (Bcl-2 proper, Bcl-xL, and Bcl-w). Proapoptotic homodimerization of these proteins (e.g. Bax and Bak) is crucial for the assembly of the mtPTP to induce cytochrome c release in the cytosol. Previous studies have shown a balance favouring proapoptosis in mitochondrial fractions of whole muscle from senescent animals (61, 79). Within the cytosol, cytochrome c binds with apoptotic protease activating factor-1 (Apaf-1) in the presence of ATP (256), which recruits pro-caspase-9 to generate a multiplex known as an apoptosome. In a series of proteolytic cleavages, also called the "caspase cascade", caspase-9 and its effector caspase-3 are activated. Caspase-3 translocates to the nucleus to induce genomic DNA fragmentation. In addition to cytochrome c, other mitochondrial apoptotic factors are released into the cytosol, such as SMAC (small mitochondria-derived activator of caspases), AIF (apoptosis inducing factor) and EndoG (endonuclease G). SMAC can bind to inhibitors of apoptosis (IAPs), and promote cell death through the functional inactivation of these inhibitors. AIF and EndoG are proteins that can mediate apoptosis independent of apoptosome formation, and can translocate to the nucleus to induce apoptosis without caspase activation. The release of cytochrome c and EndoG from mitochondria is shown to increase with age in skeletal muscle (52, 111, 279), suggesting increased mitochondrial apoptotic susceptibility.

2.4.4. Biochemical pathways with age

At the expense of the cell, the termination of dysfunctional mitochondria can lead to apoptosis and cell death. This is a severe outcome and under less stressful conditions alternative quality control mechanisms can be implemented to retain organelle function. The turnover of long-lived proteins and cytosolic organelles are crucial processes in the maintenance of function in an aging cell. Autophagy can aid in this removal process through the sequestration and delivery of cargo to lysosomes. Autophagy regulation is an emerging field of active research that can further

our knowledge of the aging process (16, 113, 218). Early studies primarily focused on a mechanistic view of autophagy and age on lower order organisms. These models were utilized to tease apart possible conserved genetic pathways of IGF-1 signaling and autophagy. For example, a deficiency of autophagy inhibitor mTOR in the nematode *Caenorhabditis elegans* was found to double the lifespan of the organism (450). Similarly, *C. elegans* with a loss-of-function mutation in the IGF-1 receptor are viable and live more than twice as long as wild type nematodes (208, 213). IGF-1 can activate Akt, which in turn can phosphorylate mTOR to inhibit autophagy. These data suggest that autophagy may contribute to lifespan extension. Indeed, the inactivation of autophagy activator protein Beclin-1 cancels the effect of lifespan extension in *C. elegans* (287). These results illuminate the IGF-1/Akt/mTOR pathway as an important signaling mechanism involved in aging.

With respect to muscle physiology, the IGF-1 pathway is also involved in skeletal muscle hypertrophy and atrophy (33, 363). Sarcopenia is accompanied by a reduction in circulating IGF-1 levels, along with a loss of muscle mass and reduced protein synthesis. Therefore, it is possible that the IGF-1 pathway is involved in regulating muscle mass in aging skeletal muscle. However, recent research on aged mice indicates that the IGF-1/Akt pathway is not downregulated, but that mTOR activity is elevated in sarcopenia (377). These data support the idea that caloric restriction may aid in extending longevity. Caloric-restricted aged animals display metabolic reprogramming that impedes aging by enhancing protein turnover and decreasing macromolecular damage (7, 245). When a cell encounters high energy demand and low energy supply, AMPK is activated and can inhibit mTOR activity. This can activate autophagy and re-establish the energetic status of the cell by increasing the availability of *de novo* substrates for macromolecule synthesis (23). The activation of AMPK (8, 11, 117, 434) and inhibition of mTOR (186, 198, 203, 345, 408, 450) can

extend lifespan in a variety of organisms. Evidence to support mTOR inhibition and caloric restriction is observed with the inhibition of 4E-BP, a downstream target of mTOR. 4E-BP (eukaryotic translation initiation factor 4E binding protein) is a repressor of mRNA translation and is inhibited upon mTOR activation and protein synthesis (135). Dietary restriction in flies can induce 4E-BP activity and lifespan extension by enhancing mitochondrial activity (491). These findings suggest that the attenuation of mTOR signaling and mitophagy activation might serve as a potential step by which caloric restriction can impact longevity. Alternatively, rapamycin treatment may be a possible therapeutic intervention to blunt mTOR activation and promote longevity (163, 408). Administration of rapamycin can extend the median and maximal lifespan of different mouse strains (134). AMPK regulation on mTOR provides a probable mechanism by which AMPK could influence lifespan (202). Therefore, activation of AMPK may be vital to prevent or reverse age-related physical degeneration.

2.4.5. Autophagy and mitophagy with age

AMPK activation can promote autophagy (42, 211) and mitophagy (86) by directly activating Ulk1 and inhibiting mTOR. Contraction-induced AMPK signaling is reduced in aged muscle (266, 355) and may consequently affect autophagy activation (42). Several studies hypothesize that the initiation and degradation of autophagosomes may be diminished with age (68, 367, 429). The notion of autophagy activation on decelerating the aging process is supported in studies that demonstrate AMPK overexpression (444) and mTOR knockdown (472) in different organisms produce extended lifespans. Moreover, autophagy is emerging as a critical process in the maintenance of muscle function with age. For example, autophagy impairment in aged muscle induces oxidation of contractile proteins and neuromuscular junction degeneration which can cause muscle weakness (49). In aged muscle, higher basal autophagy protein expression may

indicate diminished autophagic degradation (316). Furthermore, failure to activate autophagy in aged muscle satellite cells can impair muscle regenerative capacity (102). In post-mitotic tissue, defective mitophagy is often depicted as mitochondrial accumulation inside autophagosomes or lysosomes (102, 161, 393). Impairments in autophagosomal degradation can also be detected in aged post-mitotic tissue as lipofuscin granules (161, 316), an indication of lysosomal dysfunction (430). Lipofuscin formation can increase with sustained oxidative stress (39, 40). A possible method to mitigate lysosomal dysfunction is through the activation of recently identified transcription factor EB (TFEB) (379). Under non-stressful conditions, cytosolic TFEB is basally repressed by mTOR (330). Upon a catabolic stimulus, such as starvation or exercise (88, 275), mTOR can subsequently relieve its inhibition on TFEB and allow for its translocation into the nucleus where TFEB can express numerous genes involved in lysosomal biogenesis (327) and autophagy (396). A role for TFEB in aged muscle remains unknown and may serve as a therapeutic intervention in improving lysosomal function and autophagy.

Few studies exist on the direct examination of mitophagy regulation with age. Many of these studies have focused on aging in lower order organisms, and therefore careful interpretation and extension of the data to mammalian aging is required. In conditions of mitochondrial dysfunction and low IGF-1 signaling, mitophagy activation is required for nematode lifespan extension (326). Administration of the chemical autophagy inducer, lithium, in the nematode is beneficial for longevity and improved mitochondrial function (422). Iron is an important component of complex III and IV of the ETC, and depletion of iron in worms can also trigger mitophagy and lifespan extension (385). In yeast, Uth1p is an OMM protein that can induce mitophagy with rapamycin treatment and starvation (45). Deletion of Uth1p reduces autophagic degradation of mitochondria and decreases longevity in yeast during nutrient deprivation (217).

As noted in detail earlier in this review, Parkin is a ligase involved in mitophagy, and recent work suggests a role for Parkin in aging. As implied by its name, Parkin is involved in Parkinson's Disease (PD), an age-associated neurodegenerative disorder of the central nervous system. According to Statistics Canada in 2010, 55,000 Canadians aged 18 or older reported that they had been diagnosed with PD. PD is diagnosed by four main clinical manifestations: bradykinesia, muscular rigidity, resting tremor and postural instability (416). The impairment in motor function is attributed to a progressive loss of dopaminergic neurons in the substantia nigra, a region of the midbrain (92). The etiology of cell death in the substantia nigra remain unknown. However, the surviving neurons display cytoplasmic inclusions called Lewy bodies, which contain α-synuclein protein aggregates. Mutations in the α-synuclein gene have been identified in families with PD (344). Although the function of α-synuclein is not completely understood, studies suggest that it plays a role in regulating clustering of presynaptic vesicles (76). In the late 1990s, a Japanese research group identified *PARK2* (Parkin) as the first gene involved in early-onset PD (283, 398). A few years later, *PARK6* (PINK1) was the second gene discovered within a large Italian pedigree (447–449). The connection between PD and mitochondrial dysfunction was accidently discovered in the 1970s when drug users were exposed to 1-methyl-4-phenyl-1,2,3,6-tetrahydropyridine (MPTP), a contaminant from the synthesis of 1-methyl-4-phenyl-4-propionoxy-piperidine (MPPP) (238). MPTP is a lipophilic compound that can cross the blood brain barrier and, once metabolized by neuroglial cells, destroys primarily dopaminergic neurons. It was later found that the selective uptake of MPTP by dopaminergic neurons can cause inhibition of ETC complex I function (183, 313). The discovery of a mitochondrial targeting sequence for PINK1 ultimately strengthened the involvement of mitochondrial dysfunction in the pathophysiology of PD. Despite these advancements, there is still no cure or effective treatment options for PD as a large majority of

cases are of idiopathic origin. Although the cause(s) of PD remain unknown, great strides on research examining the genetic basis of PD have provided researchers with a better understanding of mitochondrial quality control mechanisms that might underlie PD and other neurodegenerative diseases.

Since PD is an age-related disease, a large focus has been on the role of Parkin with age. For example, overexpression of Parkin can extend lifespan in flies by reducing polyubiquitinated protein aggregates in muscle (351). Furthermore, Parkin KO mice crossed with PolG mutator mice exhibit accelerated dopaminergic neuronal cell death, indicating that endogenous Parkin preserves neuronal tissue from cellular death arising from mtDNA mutation accumulation (338). Indeed, Parkin overexpression can selectively eliminate mitochondria harboring deleterious mtDNA mutations in heteroplasmic cybrid cells (412). Unfolded proteins within the matrix can also trigger Parkin localization to the mitochondria independent of a membrane potential (188). Alternatively, PINK1 can stabilize on the OMM when Lon protease is inactivated (432). Lon is a mitochondrial matrix protease involved in the handling of misfolded and aggregated proteins (27). Increased expression of Lon can extend lifespan in a fungal model of aging (271). In aged murine skeletal muscle, increased oxidative stress can downregulate Lon protease expression, and promote the accumulation of dysfunctional proteins within mitochondria (38). Parkin can also assist in the removal of OMM proteins by mediating the selective turnover of mitochondrial ETC proteins in flies (453). *Drosophila* Parkin null mutants exhibit reduced lifespan and severe muscle generation (116). In human skeletal muscle, Parkin expression is reduced in older subjects (111). These studies collectively demonstrate Parkin's role in aging, but a large gap of knowledge exists for Parkin in a mammalian model of aging, particularly its effect on mitophagy in sarcopenic muscle. The study of mitophagy *in vivo* presents a challenge as mitochondria are constantly undergoing

turnover, and measuring this process at any one timepoint may not be representative of the entire process. Several autophagy inhibitors can prevent autophagy from occurring in skeletal muscle (192). If treatment of an inhibitor is followed by a greater accumulation of autophagosomal markers (i.e. LC3II), this can indicate greater autophagic flux. Initial evidence suggests that autophagic flux is enhanced in skeletal muscle of old animals (14). However, further research is required to clarify whether mitophagy flux is altered in aged muscle. There are several recently introduced methods that can provide information on mitochondrial turnover. Mito-Keima is a coral-derived, mitochondrial-targeted fluorescent protein that stably emits green at a neutral pH (autophagosomal induction and formation) and red at a acidic pH (autophagosomal fusion with the lysosome) (204). This fluorescent protein was recently used in a reporter mouse model. The results indicate that mitophagy was lower in the dentate gyrus brain region of aged mice (415). In future studies, the utilization of this reporter can provide novel data on mitophagy regulation in different tissues under various conditions (i.e. aging and exercise).

2.4.6. Muscle plasticity, exercise and age

Sarcopenia is characterized by a loss in muscle mass and strength. It is reported that muscle strength decreases (3 to 4% per year) more rapidly than muscle mass (1% per year), suggesting an overall decline in muscle quality (109). There is a wealth of evidence that demonstrates that physical activity and endurance exercise can help prevent some of the sarcopenia by attenuating muscle mass loss, and thereby improve the quality of life (154, 240, 307). An outcome of regular endurance exercise is an increase in mitochondrial biogenesis (50, 91, 201, 221, 403), that can improve age-related changes in mtDNA integrity and muscle oxidative capacity (369). Several pharmacological interventions exist that can activate mitochondrial biogenesis (158), and aid in aging muscle function, but do not fully recapitulate the beneficial effects of whole body exercise.

Why is it that aged muscle adapts so differently than young muscle? What are these mechanisms and how are they altered with exercise? A literature search in the aging field provides many examples in which the beneficial effects of exercise are not evident. This is mainly attributed to differing experimental age groups (404, 457), and uncontrolled activity levels that can produce varying results (158). One method to control these activity levels is the use of a chronic electrical stimulation model (418). This method is utilized mainly on rodents, but can allow for controlled workloads on the stimulated leg of the rodent, with full muscle fibre recruitment. The use of this experimental model has revealed that mitochondrial content can increase in the muscles of both young and aged animals, but that this increase is significantly attenuated in aged muscle (267). This reduced adaptive plasticity in aged muscle is mainly due to lower mitochondrial protein import and regulatory proteins involved in mitochondrial biogenesis (267). The attenuated activation of upstream signaling kinases in response to contractile activity in aged muscle may consequently reduce downstream targets that are responsible for regulating mitochondrial biogenesis (266, 355). These data indicate that aged skeletal muscle can adapt to exercise, but that initial signaling mechanisms involved in gene transcription are blunted (14). Future studies will need to examine if altering stimulus strength and duration on aged muscle can achieve similar adaptations as seen in young muscle (361).

CHAPTER 3:

PhD DISSERTATION OBJECTIVES AND HYPOTHESES

Based on the literature review, mitochondrial turnover is essential for the maintenance of proper organelle content and quality. Parkin is an important regulator of this process. Both Parkin and mitochondrial turnover appear to be altered with exercise and age. However, it is not clear whether if Parkin is involved in mediating mitophagy in skeletal muscle under different metabolic states, namely exercise and aging. Mitochondrial biogenesis can increase with endurance exercise, and decrease with aging, with evidence pointing towards Parkin being involved in both processes. Therefore, we were interested in evaluating a role for Parkin in the regulation of skeletal muscle mitochondrial turnover with age and exercise. The purpose of this dissertation was to investigate the mechanisms by which Parkin can modulate age- and endurance exercise-induced adaptations in skeletal muscle, and the degree of its activation and involvement in mitophagy and mitochondrial biogenesis. Thus, the objectives of my dissertation were three-fold:

Objective 1: To investigate the role of Parkin on mitophagic signaling, basally and during acute exercise, using a Parkin knock-out model.

Hypotheses:

1) We hypothesized that mitophagy flux would be induced with acute exercise.

2) We posited that the lack of Parkin would impair mitochondrial function and attenuate mitophagy flux, as well as reduce the expression of key transcription factors involved in mitochondrial biogenesis.

Objective 2: To assess the degree of influence that age has on Parkin-mediated mitophagy basally and following acute exercise.

Hypotheses:

1) We posited that the lack of Parkin with advancing age would result in additional decrements in mitochondrial content and function, as well as reduced muscle mass.

2) We hypothesized that the absence of Parkin would impair mitophagy flux in aged muscle, and that these pathways would remain attenuated with a subsequent bout of acute exercise.

Objective 3: To delineate the importance of Parkin-mediated mitophagy in exercise-induced mitochondrial biogenesis.

Hypotheses:

1) We expected that the absence of Parkin would reduce the degree of adaptive response to endurance training as measured by the expression of several mitochondrial content markers.

CHAPTER 4:

Parkin-mediated mitophagy with aging and exercise in skeletal muscle

Chris Chin Wah Chen[1,2], Avigail T. Erlich[1,2], Matthew J. Crilly[1,2] and David A. Hood[1,2]

[1]School of Kinesiology and Health Science,
[2]Muscle Health Research Centre，
York University, Toronto,
Ontario M3J 1P3, Canada

Running title: Parkin-mediated mitophagy in aged skeletal muscle

Keywords: Mitochondrial biogenesis, mitophagy flux, ubiquitination, reactive oxygen species, PGC-1α, PARIS

AUTHOR CONTRIBUTIONS

C.C.W.C., A.T.E. and M.J.C. performed experiments; C.C.W.C. analyzed data; C.C.W.C. and D.A.H. interpreted results of experiments; C.C.W.C. prepared figures; C.C.W.C. drafted manuscript; C.C.W.C. and D.A.H. edited and revised manuscript; C.C.W.C. and D.A.H. conception and design of research; C.C.W.C. and D.A.H. approved final version of manuscript.

This manuscript has been submitted to the American Journal of Physiology – Endocrinology and Metabolism (November 2017). Revised manuscript submitted (December 2017).

ABSTRACT

The maintenance of muscle health with advancing age is dependent on mitochondrial homeostasis. While reductions in mitochondrial biogenesis have been observed with age, less is known regarding organelle degradation. Parkin is an E3 ubiquitin ligase implicated in mitophagy, but few studies have examined Parkin's contribution to mitochondrial turnover in muscle. Wild type (WT) and Parkin knockout (KO) mice were used to delineate a role for Parkin-mediated mitochondrial degradation in aged muscle, in concurrence with exercise. Aged animals exhibited declines in muscle mass and mitochondrial content, paralleled by a nuclear environment endorsing the transcriptional repression of mitochondrial biogenesis. Mitophagic signaling was enhanced following acute endurance exercise in young WT mice, but was abolished in the absence of Parkin. Basal mitophagy flux of the autophagosomal protein LC3II was augmented in aged animals, but did not increase additionally with exercise when compared to young animals. In the absence of Parkin, exercise increased the nuclear localization of PARIS, corresponding to a decrease in nuclear PGC-1α. Remarkably, exercise enhanced mitochondrial ubiquitination in both young WT and KO animals. This suggested compensation of alternative ubiquitin ligases that were, however, unable to restore the diminished exercise-induced mitophagy in KO mice. Under basal conditions, we demonstrated that Parkin was required for mitochondrial Mfn2 ubiquitination. We also observed an abrogation of exercise-induced mitophagy in aged muscle. Our results demonstrate that acute exercise-induced mitophagy is dependent on Parkin, and attenuated with age, which likely contributes to changes in mitochondrial content and quality in aging muscle.

INTRODUCTION

Mitochondria have emerged as an important nexus of stress within the cell. Including their canonical function as energy producers, mitochondria also exhibit pleiotropic roles in regulating metabolic signaling. In a tissue such as muscle, mitochondria can respond to sustained energetic requirements by increasing organelle content via a process termed mitochondrial biogenesis. This expansion is critical for muscle adaptation to occur in response to exercise training (17). A plethora of studies have established the broad beneficial effects of exercise, but the molecular mechanisms that accompany improved muscle quality remain obscure. Recent research has suggested that autophagy is a possible mechanism for potentiating muscle plasticity in response to exercise (16, 60).

Autophagy is a catabolic, evolutionary-conserved process involved in the engulfment of dysfunctional organelles and protein aggregates. Mitophagy is a specific form of autophagy, accountable for the elimination of dysfunctional mitochondria following damage or stress. Once an entire mitochondrion becomes depolarized, organelle fragmentation permits mitophagy to eliminate the dysfunctional segment from the mitochondrial reticular network (7, 59, 63). This change in mitochondrial morphology is initiated and regulated in part by the E3 ubiquitin ligase Parkin (10, 46). Under non-stressful conditions, mitochondrial PTEN-induced putative kinase 1 (PINK1) is rapidly imported into the organelle and degraded by the inner mitochondrial membrane rhomboid protease presenilin-associated rhomboid-like protein (PARL) (23). When a mitochondrion encounters a loss in membrane potential, PINK1 stabilizes and accumulates on the outer mitochondrial membrane to selectively recruit Parkin (30, 40). The mitochondrial translocation of Parkin induces ubiquitin localization on outer mitochondrial membrane targets, and is further activated by PINK1 phosphorylation of ubiquitin (25, 26, 28). Adapter protein

sequestosome 1 (p62) interacts with mitochondrial ubiquitin and with microtubule-associated protein light chain 3 (LC3) on the autophagic phagophore membrane (2, 44). These tagged dysfunctional mitochondria are encapsulated into autophagosomes and sequestered to the lysosome for proteolytic degradation.

In muscles with disrupted autophagic signaling, pathology entailing disorganized swollen mitochondria is displayed (36). This suggests that mitophagy may have a role in the preservation of organelle content and function in muscle. While work has been done on Parkin in muscle on lower model organisms (14, 47) and in cell culture (48), the physiological function of Parkin in mammalian skeletal muscle function, and in response to physiologically relevant stressors such as exercise, remains unknown. Recent studies have investigated the influence of autophagy activation in skeletal muscle following a bout of endurance exercise (15, 16, 49, 60). We have previously demonstrated that mitochondrial Parkin localization is enhanced in response to acute exercise (60). Therefore, in this study, we sought to examine Parkin's role in skeletal muscle function, and whether Parkin is required for acute exercise-induced mitophagy flux using a Parkin KO mouse model.

Similar to the phenotype of autophagy deficiency, aged muscle displays an accumulation of dysfunctional mitochondria in lysosomal lipofuscin bodies (42). Aged animals also demonstrate an elevated amount of mitochondrial ROS emission (6), which can perpetuate organelle damage. Indeed, autophagy inhibition in muscle can elicit a reduction in muscle contractile activity due to non-autophagocytosed mitochondria (36). This notion is part of the mitochondrial-lysosomal axis theory of aging that postulates that increasing organelle dysfunction irreversibly leads to the deterioration of post-mitotic cells (4). In skeletal muscle, this process is manifested as sarcopenia, which is characterized by the age-related loss of muscle function and strength (5, 34), and a

reduced transcriptional drive for mitochondrial biogenesis (6). Yet, the selective degradation of mitochondria and its role with advancing age remains unclear. We have previously shown that the expression of autophagy proteins and their localization to mitochondria are not decreased, but rather that the induction of mitophagy remains impaired in aged muscle (42). Interestingly, the overexpression of Parkin has been shown to enhance mitophagic flux and extend lifespan in lower model organisms (47). Thus, we hypothesized that Parkin may play an increasing role in regulating skeletal muscle function and mitochondrial degradation with age. The aims of our study were to investigate: 1) the role of Parkin in acute exercise-induced mitophagy, and 2) possible age-related alterations in mitophagic flux brought about by endurance exercise.

MATERIALS AND METHODS

Mice. C57BL/6 (WT) and B6; 129S4-Park2tm1Shn/J (Parkin KO) mice (Jackson Labs, 006582) were housed in a 12 h light–dark cycle room and allowed access to food and water ad libitum. The generation of these mice has been previously described (12). Progeny were genotyped by obtaining ear clippings for DNA extraction. DNA was subsequently incubated with JumpStart REDtaq polymerase (Sigma-Aldrich, St. Louis, MO) along with forward and reverse primers for the WT or altered Parkin gene. These products were amplified using PCR and separated on a 1.5% agarose gel containing ethidium bromide for visualization the genotype. The minimum age threshold for young and aged conditions were 3 and 18 months, respectively.

Exercise Protocol and Blood Lactate. To evaluate mitophagy flux, animals were administered colchicine, or an equal amount of vehicle (water), via intraperitoneal injections every 24 hours (0.4 mg·kg−1·day−1) (24) for 2 days prior to the day of exercise and euthanization. After 2 days of habituation on the treadmill, along with the vehicle or colchicine injections, animals in the exercise (Ex) and exercise and 2 hours recovery (ExR) groups were subjected to exhaustive treadmill exercise on a 10° incline. Young WT and KO animals ran at 0 m/min for 5 minutes, 5 m/min for 5 minutes, 10 m/min for 10 minutes, 15 m/min for 15 minutes, 20 m/min for 20 minutes followed by incremental exercise at 1 m/min for every 1 minute until to failure. Aged WT and KO animals ran a similar protocol but Ex groups began incremental exercise after 10 m/min for 10 minutes. There were no ExR groups for aged WT and KO animals due to a lower sample size. The exercise bout ended when animals appeared visibly exhausted and could not continue, even in the presence of air jet stimulation. Metabolic stress was also assessed by measuring blood lactate from a small tail bleed using the Lactate Scout+ analyzer (EKF Diagnostics, Magdeburg, Germany). All animals were sacrificed by cervical dislocation immediately after exercise (Ex), or 2 hours

postexercise (ExR). All animal protocols were submitted and approved by the York University Animal Care Committee. Animals were treated in accordance with Canadian Council of Animal Care guidelines.

Muscle Extraction and Cytochrome c Oxidase (COX) Enzyme Activity. The quadriceps muscle was surgically removed and immediately freeze-clamped with metal tongs pre-cooled in liquid nitrogen and subsequently weighed and stored at –80 °C for future use. Frozen muscle samples were pulverized into powder, then dissolved in whole muscle extraction buffer, followed by sonication and centrifugation. Supernatant fractions were recovered and protein content was determined by the Bradford technique. In addition, COX activity measurements were performed on young and aged groups of Parkin KO and WT mice to measure whole muscle mitochondrial content. Briefly, whole muscle extracts were added to a test solution containing fully reduced cytochrome c. Enzyme activity was determined by the maximal oxidation rate of completely reduced cytochrome c, evaluated as the rate of change in absorbance at 550 nm using a Synergy HT microplate reader, as previously described (37). The data were gathered and calculated using KC4 software.

Mitochondrial Isolation. Mixed hindlimb muscles were immediately placed into ice-cold mitochondrial isolation buffer, followed by mincing and homogenization. Intermyofibrillar (IMF) mitochondrial subfractions were fractionated by performing differential centrifugation, as described previously (8, 37, 50, 64). Mitochondria were resuspended in 100mM KCl, 10mM MOPS, and 0.2% BSA. Freshly isolated mitochondria were used for mitochondrial respiration and reactive oxygen species (ROS) emission assays, and aliquots of mitochondrial extracts were stored at –80ºC for mitochondrial co-immunoprecipitation assay and immunoblotting analyses. The protein concentration values of the isolated mitochondria were determined using the Bradford

method.

Mitochondrial Respiration and ROS Production Assay. Basal IMF mitochondrial respiration (state 4) rates were performed in the presence of 10 mM glutamate (Sigma) followed by the addition of 0.44 mM ADP (state 3, Sigma). During state 3, NADH was added to ensure intact inner mitochondrial membrane integrity. No differences in respiration rates were observed when NADH was added to isolated mitochondria samples. All respiration rates were performed using the Mitocell S200 Micro Respirometry System (Strathkelvin Instruments, North Lanarkshire, UK). ROS emission was measured using isolated mitochondria from WT and Parkin KO mice that were incubated in a 96 well plate with VO2 buffer (in mM: 250 sucrose, 50 KCl, 25 Tris, and 10 K2HPO4, pH 7.4) at 37 °C for 30 minutes under state 4 and 3 conditions. 2',7'-dichlorodihydrofluorescein diacetate (50 μM H2DCFDA, ThermoFisher) was subsequently added and fluorescence between 480 and 520 nm was measured on a Bio-Tek Synergy HT microplate reader to directly measure ROS emission. ROS emission was expressed per nanoatom of O2 consumed, as measured during mitochondrial respiration.

Nuclear and Cytosolic Fractionation. Freshly isolated tibialis anterior muscle was removed in Con, Ex, and ExR groups and placed into ice-cold phosphate buffered saline containing protease inhibitor cocktail complete, ETDA-free (Roche Applied Science) and phosphatase inhibitor cocktail (Sigma). Nuclear and cytosolic components were obtained using a commercially available NE-PER Nuclear and Cytoplasmic Extraction Reagents kit (ThermoFisher), according to the manufacturer's instructions.

Mitochondrial Co-immunoprecipitation Assay. Isolated IMF mitochondrial fractions were solubilized with 1% Triton X-100 and supplemented with protease and phosphatase inhibitor cocktails. Mitochondria were incubated with anti-Mfn2 (M6444, Lot No. 103M4780, Sigma)

overnight at 4°C on a nutator mixer, and the supernatant was collected by centrifugation at 12,000 g for 10 minutes at 4°C. The following day protein A/G plus-agarose immunoprecipitation reagent (sc-2003, Santa Cruz) was added to the mixture and incubated for 1 hour at 4°C on a nutator mixer. The supernatant fraction was removed from the beads after centrifugation, representing unbound proteins. The collected beads were washed three times and eluted three times with 50 µl of SDS-PAGE gel loading buffer to obtain the maximum elution of purified complexes. Co-immunoprecipitates were used for immunoblot analysis for ubiquitin (SPA-203, Lot No. 1051534, Enzo Life Sciences). Anti-IgG antibody was used as a non-specific control.

Immunoblotting. Muscle extracts and isolated nuclear, cytosol and mitochondrial fractions were separated using SDS-PAGE (12-15% polyacrylamide) and later electroblotted onto nitrocellulose membranes. Membranes were blocked with 5% skim milk in TBST (Tris-buffered saline-Tween 20, 25 mM Tris HCl (pH 7.5), 1 mM NaCl, and 0.1% Tween 20) solution for 1 hour at room temperature. Next, blots were incubated with primary antibodies against LC3/microtubule-associated protein light chain 3 (4108, Lot No. 3, Cell Signaling), p62/sequestosome 1 (P0067, Lot No. 015M4877V, Sigma), ubiquitin (SPA-203, Lot No. 1051534, Enzo Life Sciences), Parkin (4211, Lot No. 4, Cell Signaling), PGC-1α/peroxisome proliferator-activated receptor-γ coactivator-1α (ab3242, Lot No. 2691399, Millipore), PARIS/parkin-interacting substrate (ab130867, Lot No. GR235090-1, abcam), H2B/histone 2B (2943S, Lot No. 4, Cell Signaling), VDAC/voltage-dependent anion channel (ab14734, Lot No. GR121056-7) and α-tubulin (CP06, Lot No. D00175772, Millipore) overnight at 4 °C. On the next day, the blots were rinsed three times in TBST, followed by a 1 hour incubation period at room temperature with appropriate horseradish peroxidase-conjugated secondary antibodies. The blots were again washed three times in TBST and visually detected using enhanced chemiluminescence (Clarity ECL Western blotting

substrates, Bio-Rad, CA) and photographic film. Of note, the top band of p62 was quantified when two bands were visible. Films were then scanned and quantified using ImageJ software (Version 1.48, NIH, USA).

Statistical Analysis. Data were analyzed with Graph Pad 6.0 software, and values are reported as means ± SEM. Data were analysed using two-way analysis of variance (ANOVA), except for Fig. 1A which was analysed using a student's t-test. For all two-way ANOVA analyses, Tukey's post hoc test was used to identify individual differences when statistical significance was observed. Statistical differences were considered significant if $P < 0.05$.

RESULTS

Aged mice exhibit reduced whole muscle mass and mitochondrial content. To determine the role of Parkin and age in skeletal muscle, we first assessed the anatomical characteristics of young and aged groups of WT and Parkin KO animals. Total body mass did not differ between WT and KO mice, but both genotypes displayed a 1.6- and 1.8-fold increase in body mass with age, respectively ($P < 0.05$; Table 1). Quadriceps muscle mass did not differ between young animals, while aged WT and KO animals exhibited 12% decreases in whole quadriceps muscle mass when corrected for tibia length, compared to young mice (Table 1). Thus, we attribute the age-related increase in body mass to an increase in body fat, as illustrated by the significant ~8-fold increase in epididymal fat mass when corrected for total body mass, irrespective of genotype ($P < 0.05$; Table 1). In addition, we measured Parkin protein expression in young and aged whole quadriceps muscle. We found a robust ~4-fold increased expression of Parkin in aged, compared to young muscle ($P < 0.05$; Fig. 1A). Whole muscle mitochondrial content was assessed by using a cytochrome c oxidase (COX) activity assay. There was no difference between young WT and KO animals, and both genotypes exhibited similar decrements of ~40% with age ($P < 0.05$; Fig. 1B).

We also examined state 4 and glutamate/pyruvate-driven state 3 mitochondrial respiration. No effect of age was observed. When young animals were compared, no differences between genotypes were noted in state 4 respiration, however a 20% decrease in state 3 mitochondrial respiration was detected in KO mice compared to WT counterparts ($P < 0.05$; Fig. 1C). In young WT and KO animals, no difference in ROS emission was observed under state 4 and 3 conditions. However, with age, Parkin KO animals displayed a ~2.7-fold increase in state 4 ROS production, when compared to WT animals ($P < 0.05$; Fig. 1D).

Aging results in reduced exercise performance and mitochondrial Parkin localization, along with increased acidosis. We next investigated the role of Parkin with aging and exercise performance. In young WT animals, we found a 1.5-fold increase in Parkin localization to mitochondria immediately following an acute bout of exercise ($P < 0.05$; Fig. 2A). Parkin localization on mitochondria was severely reduced with age, and the exercise-induced response was abolished ($P < 0.05$; Fig. 2A). To determine Parkin's requirement in endurance performance, we subjected young and aged groups of WT and KO mice to a bout of acute, prolonged exercise. No significant differences were detected for total distance run between young WT and KO animals, and both genotypes exhibited elevated blood lactate concentrations of ~8 mM immediately following exercise ($P < 0.05$; Fig. 2C). Aged mice ran only 25% of the distances of their younger counterparts ($P < 0.05$; Fig. 2B), and this response was accompanied by 1.5-2-fold higher exercise-induced increases in blood lactate levels with age ($P < 0.05$; Fig. 2C).

Mitophagy flux is induced following exercise, but this signaling is attenuated in the absence of Parkin, and with age. To evaluate a role for Parkin on mitophagy during exercise, mice were subjected to acute exercise to induce mitophagy flux. Following each condition, mitochondria were isolated from the hindlimb muscles of mice to examine the mitochondrial localization of autophagy proteins, and autophagy flux was calculated based on the difference between colchicine- and vehicle-treated animals. Our results indicate that basal mitophagy LC3II and p62 flux was not significantly different between young WT and KO animals. During exercise, mitochondrial LC3II flux was elevated by 2.7-fold in young WT animals ($P < 0.05$; Fig. 3A and 3B). This was attenuated in the absence of Parkin. We also detected a 2-fold increase in p62 flux in young mice with exercise ($P < 0.05$; Fig. 3A and 3C). These data indicate that exercise can induce mitophagic flux, and that the magnitude of this increase is Parkin-dependent.

We then directly compared the role of Parkin-mediated mitophagy between young and aged animals. Basal LC3II and p62 flux were significantly higher in aged WT animals, when compared to young WT animals ($P < 0.05$; Fig. 4A–C). With exercise, LC3II flux and p62 flux in aged WT animals did not increase additionally when compared to young WT animals (Fig. 4A–C). In the absence of Parkin, basal LC3II and p62 flux were also elevated in aged mice, compared to young mice ($P < 0.05$; Fig. 4D–F), and were not significantly different following exercise (Fig. 4D–F). In contrast to young KO animals, basal LC3II flux ($P < 0.05$; Fig. 4G) and p62 flux ($P < 0.05$; Fig. 4H) were both significantly elevated in aged KO. Furthermore, the magnitude of basal LC3II flux was significantly higher in aged KO when compared to aged WT animals ($P < 0.05$; Fig. 4G). Our data indicate that mitophagic signaling is enhanced within aged muscle, and this effect may reduce the potentiation of exercise on mitophagy flux.

Acute exercise induces mitochondrial ubiquitination in young animals, but is attenuated with age. To assess the potential role of Parkin in exercise-induced protein ubiquitination, we examined global ubiquitination on isolated mitochondrial fractions from young WT and KO animals. Basal ubiquitin flux did not differ between genotypes (Fig. 5A and 5B). Ubiquitin flux increased by ~4.1-fold in young WT, immediately following exercise ($P < 0.05$; Fig. 5A and 5B), corresponding with the increase in Parkin localization on mitochondria in young WT animals. Remarkably, mitochondrial ubiquitination was also similarly increased by exercise in young KO animals ($P < 0.05$; Fig. 5A and 5B). In aged muscle, there were also no differences in basal ubiquitin flux on isolated mitochondria between WT and KO animals (Fig. 5C and 5D). However, in contrast to young animals, ubiquitin flux was considerably higher with age (compare control conditions in Fig. 5D vs 5B), and the effect of acute exercise to increase mitochondrial ubiquitination was completely abolished (Fig. 5C and 5D).

We extended this analysis further to assess the potential function of Parkin on the ubiquitination of specific proteins during exercise. We evaluated Mitofusin-2 (Mfn2) ubiquitination, a known outer mitochondrial membrane target of Parkin, using mitochondrial co-immunoprecipitation to resolve Mfn2-ubiquitin complexes following exercise in young and aged Parkin KO and WT mice. The basal formation of Mfn2-ubiquitin complexes was significantly reduced by 52% in young KO animals, relative to young WT controls ($P < 0.05$; Fig. 5E and 5F). Consistent with the translocation of Parkin to the mitochondria with exercise, we found that exercise significantly enhanced Mfn2 ubiquitination on mitochondria of young animals by ~2-fold, relative to young WT control animals ($P < 0.05$; Fig. 5F). With age, Mfn2 ubiquitination was increased basally by ~2-fold ($P < 0.05$; Fig. 5E and 5F), in both WT and KO counterparts. This ubiquitination remained unchanged with exercise (Fig. 5E and 5F). These data indicate that Parkin is involved in maintaining basal mitochondrial protein ubiquitination in muscle, and that exercise can promote protein ubiquitination even in the absence of Parkin, in young animals.

PGC-1α and PARIS localization to the nucleus are negatively correlated in response to exercise in young animals, but this relationship is abolished with age. Parkin is not only involved in the ubiquitination of mitochondrial proteins, but has also been shown to regulate the levels of transcriptional regulators, such as Parkin interacting substrate, PARIS. It is known that PARIS transcriptionally represses PGC-1α, known as the master regulator of mitochondrial biogenesis, in the absence of Parkin. Interestingly, the basal levels of PARIS localized to the nucleus did not differ between young WT and KO animals (Fig. 6A and 6B). In aged animals, nuclear PARIS localization, when corrected for total PARIS content, was 1.3-2-fold higher in KO and WT animals, when compared to young counterparts ($P < 0.05$; Fig. 6A and 6B). Similarly, nuclear

PGC-1α abundance was not affected by the absence of Parkin, but was reduced by 35-40% in aged WT and KO mice ($P < 0.05$; Fig. 6A and 6C).

We next explored if exercise could influence the subcellular localization of these transcriptional regulators. A significant interaction between genotype and exercise on nuclear PARIS localization was found in young animals ($P < 0.05$; Fig. 7A and 7C). With acute exercise, nuclear PARIS localization diminished in WT animals, but was enhanced in the nuclear fractions of mice lacking Parkin. A similar interaction was found for PGC-1α in the nucleus of young mice following exercise ($P < 0.05$; Fig. 7A and 7E). PGC-1α increased significantly by 2.2-fold in the nucleus of WT animals, immediately after exercise ($P < 0.05$; Fig. 7A and 7E). This exercise-induced increase of nuclear PGC-1α abundance was completely negated in the absence of Parkin. In aged animals, nuclear PGC-1α and PARIS remained unchanged following exercise (Fig. 7B, 7D and 7F). These data suggest that exercise can induce the translocation of PGC-1α and PARIS but that this is qualitatively different in the absence of Parkin, and abolished with age.

DISCUSSION

Sarcopenia is defined as a loss of muscle mass and strength that occurs with age (22). It is established that sarcopenia is governed, in part, by lowered mitochondrial content (6, 34, 42) and reduced transcriptional regulation towards mitochondrial biogenesis (33). Although much is known about the synthesis of mitochondria, fewer studies have examined mitochondrial degradation (i.e. mitophagy) with age. Thus, the purpose of our research was to evaluate mitochondrial content and function, along with rates of mitophagy, in the context of sarcopenic muscle loss. Consistent with previous studies (34, 42), we observed that aged animals displayed sarcopenia, accompanied by decrements in whole muscle mitochondrial volume. This occurred concomitant with the age-related reductions in endurance performance, accompanied by elevated lactic acid levels during exercise. In contrast to these changes in mitochondrial content, we detected no differences in glutamate-stimulated mitochondrial respiration rates between young and aged animals. Mitochondrial dysfunction is a common age-related outcome (3, 9, 29, 38), but it is not always observed in aged muscle (6, 20, 34, 45), likely a result, in part, of divergent physical activity patterns among aged cohorts (18).

Parkin is an E3 ubiquitin ligase selectively recruited to dysfunctional mitochondria during mitophagy (39). Under basal conditions, endogenous Parkin is predominately found in the cytosol (39, 55). During conditions of elevated mitochondrial stress, PINK1 stabilizes on the outer mitochondrial membrane and selectively recruits Parkin from the cytosol to activate it (40). Once activated, Parkin transfers ubiquitin onto outer mitochondrial membrane targets, such as Mfn2 (7, 10) and VDAC (11), to induce the removal of superfluous mitochondria. Mitophagy is a highly dynamic process that continually degrades superfluous, dysfunctional mitochondria within the cell. The measurement of autophagy pathway proteins at any given timepoint is acknowledged to

provide only a snapshot that may not be representative of the process. As such, different inhibitors are commonly used to block certain steps of autophagy to measure flux. In our study, the microtubule-destabilizing drug colchicine was acutely injected intraperitoneally, thereby preventing autophagosomal transport to lysosomes for degradation (24). As a result, autophagy proteins did not degrade and accumulated in the cytosol, providing an indication of autophagic activity. To determine mitophagic flux, we calculated the difference between colchicine- and vehicle-treated isolated mitochondria of the same condition.

It has been shown that autophagy is required to maintain muscle mass and myofiber integrity (36), and that overexpression of Parkin can positively impact longevity (19, 47). We observed no difference in muscle mass and mitochondrial content between young WT and Parkin KO animals, and there was no apparent additional decline in muscle or mitochondria in the absence of Parkin in aged animals. These findings indicate that the basal regulation of muscle mass is Parkin-independent. Interestingly, state 3 (active) mitochondrial respiration was significantly lower in young KO animals when compared to WT animals. Given that state 3 respiration is a surrogate measure for maximal ATP production in well-coupled mitochondria, KO mice should hypothetically have a lower maximal exercise capacity than WT mice. The lack of difference in running performance between young WT and KO mice, along with similar blood lactate levels, suggest the presence of a normal excess of mitochondrial capacity within muscle. However, we did observe an elevation in mitochondrial ROS production in aged KO animals. This is likely a consequence of altered glutamate-stimulated ETC complex I function in aged KO skeletal muscle, as others have reported that the absence of Parkin sensitizes complex I to oxidative stress (43) and mitochondrial toxins (48). This is consistent with a previous study showing that oxidative stress is exacerbated with a loss of Parkin activity in neuronal cells (57).

To further explore the physiological function of Parkin on mitophagy, we assessed Parkin's ability to translocate to mitochondria with exercise and age, as previous studies have shown that mitophagy may be required for exercise-induced remodeling of muscle (60). We did observe that mitochondrial localization of Parkin increased immediately following exercise in young WT animals, consistent with our previous study (60), but that this was attenuated with age. This observation, along with an increased expression of Parkin in aged muscle, suggests an impairment of Parkin translocation to the mitochondria with age and exercise. A similar attenuation in Parkin and its association with the organelle was documented in aged cardiac mouse muscle (19).

Upon mitochondrial depolarization, a multitude of outer mitochondrial membrane proteins are targeted for Parkin ubiquitination (52). Thus, our expectation was that basal ubiquitination would be reduced in the absence of Parkin. Although we detected no differences in mitochondrial ubiquitin flux when multiple protein targets were evaluated, further scrutiny using a mitochondrial co-immunoprecipitation assay of Mfn2, a bona fide target of Parkin (7, 10, 13), revealed a basal reduction of Mfn2-ubiquitin in young KO animals. However, neither the absence of Parkin, nor the consequent reduction in target ubiquitination, were sufficient to impact mitophagic LC3II, p62 and ubiquitin flux in resting muscle. This suggests the existence of multiple mechanisms that compensate to determine basal mitophagic flux in Parkin KO animals.

During exercise, we found that Mfn2 ubiquitin flux was enhanced in young WT animals, and that this increase paralleled changes in LC3II and p62 flux, which corroborates previous studies showing that mitophagic flux is enhanced following an acute bout of exercise (60). Unexpectedly, this was also found during exercise in young KO animals, further supporting the existence of alternative unidentified E3 ubiquitin ligases that could be compensating for the lack of Parkin. However, these may not be sufficient, as exercise-induced mitophagic LC3II flux remained

impaired in young KO animals. With age, Parkin ubiquitination on general and specific OMM targets was enhanced, and remained unchanged in the absence of Parkin. Furthermore, age had an abating effect on exercise-induced ubiquitin signaling in aged animals. We speculate that this may be due to the altered activity of deubiquitinating enzymes (DUBs) contained on mitochondria and may be altered with age and/or exercise, which likely play a role in ubiquitin signaling and organelle degradation (1, 61).

The attenuated exercise-induced ubiquitin signaling that we observed in our aging animals appears to be a fundamental characteristic of aging muscle, since we have previously observed reduced signaling in response to our experimental model of endurance exercise (33). However, the requirement of Parkin and the effect of age on mitophagic flux in exercising muscle remains unknown. Under basal conditions, we did not detect a difference in mitophagic flux of LC3II, p62 and ubiquitin between young WT and KO animals. Our results did confirm an acute exercise-induced elevation of mitophagic LC3II flux in young animals, which was attenuated in the absence of Parkin. Interestingly, basal LC3II and p62 mitophagic flux were enhanced in aged WT muscle, and this was paralleled by greater generalized mitochondrial ubiquitination, as well as protein-specific (i.e. Mfn2) ubiquitination. This is in line with previous studies documenting reductions in Mfn2 protein abundance in aged muscle (21, 53). These data fortify the concept that Parkin and its association with OMM targets is altered with age. We extended these conclusions in an aged exercising mouse model, and found that the induction of LC3II and p62 mitophagic signaling with exercise was attenuated in aged muscle. This was likely due, in part, to an elevated baseline expression of these mitophagic proteins. Our data suggest that basal autophagosomal formation is not reduced with age, and that the increased expression and mitochondrial localization of ubiquitin, LC3II and p62 suggest the existence of accelerated mitophagy flux, at least up to the point of

lysosomal degradation. Although definitive data do not yet exist in skeletal muscle, our previous results suggest the idea of defective lysosomal function with age. We have previously provided evidence that aged muscle displays lipofuscin granules within lysosomes, a clear indicator of lysosomal impairment (42). This supports the mitochondrial-lysosomal axis theory of aging (4), which hypothesizes that impairments in lysosomal activity may contribute to mitochondrial accumulation and dysfunction in aged post-mitotic tissue, such as muscle (6, 34, 42). The lysosome is a vital organelle for autophagosomal degradation, and its biogenesis is regulated by transcription factor EB (TFEB) (51). Roles for TFEB in mitochondrial turnover (41, 54) and exercise (27, 35) have been recently documented. However, future studies will need to examine the possibility of lysosomal biogenesis and function by examining possible differences in TFEB activation between young and aged animals.

In recent years, there has been mounting attention on identifying regulatory factors that can control the two opposing processes of mitochondrial biogenesis and mitophagy. Recent work has documented a potential Parkin-PARIS-PGC-1α relationship. With a collapse in mitochondrial membrane potential, PARIS can localize on mitochondria where it is targeted for proteasomal degradation by PINK1 and Parkin (31). This can, in turn, diminish the repressive effect of PARIS on PGC-1α, permitting the transcription of nuclear genes encoding mitochondrial proteins (56) and improved cellular respiration (58). When Parkin is absent, it has been reported that PARIS can increase within the nucleus and transcriptionally repress PGC-1α (56, 58). This presents a potential nexus for the regulation of mitochondrial biogenesis and degradation, and remains unexplored in the context of a physiologically relevant stressor such as exercise. Thus, we expected KO animals to display an elevation in PARIS and a decrease in PGC-1α. Interestingly, our results illustrate a negative correlation between PARIS and PGC-1α localization in the nucleus that is dependent on

exercise, and on the presence of Parkin in young animals. This reciprocal relationship was not visible under resting, basal conditions. However, with exercise the nuclear abundance of PGC-1α was increased in young WT animals, as reported by other studies (32, 49, 60, 62), and the nuclear translocation of PARIS was also enhanced with exercise, but only in young KO animals. This finding recapitulates previous work showing that nuclear PARIS levels increase with Parkin knockdown, and that it translocates into the nucleus under conditions of cellular stress (31). In aged muscle, we expected that elevated Parkin expression would repress PARIS and activate PGC-1α. In contrast, nuclear PARIS abundance was increased in aged muscle of both WT and KO animals, while the levels of nuclear PGC-1α were reduced. This likely contributes to the impaired transcriptional drive for mitochondrial biogenesis in aged muscle, leading to the decrements in mitochondrial content observed with age. Furthermore, recent research has also revealed that mitochondrial Parkin activation is required for PARIS degradation (31). Since Parkin localization to the organelle is attenuated with age, this may explain the enhanced nuclear localization of PARIS in aged muscle. These findings suggest an important Parkin-PARIS-PGC-1α axis that may be involved in muscle remodeling with exercise and warrants further investigation.

In summary, our data describe a role for Parkin-mediated mitochondrial degradation during exercise in muscle. Importantly, our study demonstrates that basal mitophagic flux is not depressed but rather enhanced with age, at least up to the level of the lysosome. We show for the first time that acute exercise-induced mitophagic flux is dependent on Parkin, and that this exercise signaling is weakened with age. Additional studies are required to determine whether there is a direct connection between mitophagy flux and lysosomal activity with age, and whether exercise or contractile activity can improve mitophagic flux along with lysosomal capacity.

REFERENCES

1. **Bingol B**, **Tea JS**, **Phu L**, **Reichelt M**, **Bakalarski CE**, **Song Q**, **Foreman O**, **Kirkpatrick DS**, **Sheng M**. The mitochondrial deubiquitinase USP30 opposes parkin-mediated mitophagy. *Nature* 510: 370–5, 2014.
2. **Bjørkøy G**, **Lamark T**, **Brech A**, **Outzen H**, **Perander M**, **Øvervatn A**, **Stenmark H**, **Johansen T**. p62/SQSTM1 forms protein aggregates degraded by autophagy and has a protective effect on huntingtin-induced cell death. *J Cell Biol* 171: 603–614, 2005.
3. **Boffoli D**, **Scacco SC**, **Vergari R**, **Solarino G**, **Santacroce G**, **Papa S**. Decline with age of the respiratory chain activity in human skeletal muscle. *Biochim Biophys Acta* 1226: 73–82, 1994.
4. **Brunk UT**, **Terman A**. The mitochondrial-lysosomal axis theory of aging: accumulation of damaged mitochondria as a result of imperfect autophagocytosis. *Eur J Biochem* 269: 1996–2002, 2002.
5. **Carter HN**, **Chen CCW**, **Hood DA**. Mitochondria, Muscle Health, and Exercise with Advancing Age. *Physiology* 30: 208–223, 2015.
6. **Chabi B**, **Ljubicic V**, **Menzies KJ**, **Huang JH**, **Saleem A**, **Hood DA**, **Aldridge JE**, **Horibe T**, **Hoogenraad NJ**. Mitochondrial function and apoptotic susceptibility in aging skeletal muscle. *Aging Cell* 7: 2–12, 2008.
7. **Chen Y**, **Dorn GW**. PINK1-phosphorylated mitofusin 2 is a Parkin receptor for culling damaged mitochondria. *Science* 340: 471–5, 2013.
8. **Cogswell AM**, **Stevens RJ**, **Hood DA**. Properties of skeletal muscle mitochondria isolated from subsarcolemmal and intermyofibrillar regions. *Am J Physiol* 264: C383-9, 1993.
9. **Cooper JM**, **Mann VM**, **Schapira AH**. Analyses of mitochondrial respiratory chain

function and mitochondrial DNA deletion in human skeletal muscle: effect of ageing. *J Neurol Sci* 113: 91–8, 1992.

10. **Gegg ME**, **Cooper JM**, **Chau K-Y**, **Rojo M**, **Schapira AH V**, **Taanman J-W**. Mitofusin 1 and mitofusin 2 are ubiquitinated in a PINK1/parkin-dependent manner upon induction of mitophagy. *Hum Mol Genet* 19: 4861–70, 2010.
11. **Geisler S**, **Holmström KM**, **Skujat D**, **Fiesel FC**, **Rothfuss OC**, **Kahle PJ**, **Springer W**. PINK1/Parkin-mediated mitophagy is dependent on VDAC1 and p62/SQSTM1. *Nat Cell Biol* 12: 119–131, 2010.
12. **Goldberg MS**, **Fleming SM**, **Palacino JJ**, **Cepeda C**, **Lam HA**, **Bhatnagar A**, **Meloni EG**, **Wu N**, **Ackerson LC**, **Klapstein GJ**, **Gajendiran M**, **Roth BL**, **Chesselet M-FM-F**, **Maidment NT**, **Levine MS**, **Shen J**. Parkin-deficient mice exhibit nigrostriatal deficits but not loss of dopaminergic neurons. *J Biol Chem* 278: 43628–35, 2003.
13. **Gong G**, **Song M**, **Csordas G**, **Kelly DP**, **Matkovich SJ**, **Dorn GW**. Parkin-mediated mitophagy directs perinatal cardiac metabolic maturation in mice. *Science (80-)* 350: aad2459-aad2459, 2015.
14. **Greene JC**, **Whitworth AJ**, **Kuo I**, **Andrews LA**, **Feany MB**, **Pallanck LJ**. Mitochondrial pathology and apoptotic muscle degeneration in Drosophila parkin mutants. *Proc Natl Acad Sci U S A* 100: 4078–83, 2003.
15. **Grumati P**, **Coletto L**, **Schiavinato A**, **Castagnaro S**, **Bertaggia E**, **Sandri M**, **Bonaldo P**. *Physical exercise stimulates autophagy in normal skeletal muscles but is detrimental for collagen VI-deficient muscles*. Taylor & Francis, 2011.
16. **He C**, **Bassik MC**, **Moresi V**, **Sun K**, **Wei Y**, **Zou Z**, **An Z**, **Loh J**, **Fisher J**, **Sun Q**, **Korsmeyer S**, **Packer M**, **May HI**, **Hill JA**, **Virgin HW**, **Gilpin C**, **Xiao G**, **Bassel-Duby**

R, **Scherer PE**, **Levine B**. Exercise-induced BCL2-regulated autophagy is required for muscle glucose homeostasis. *Nature* 481: 511–5, 2012.

17. **Hood DA**. Invited Review: contractile activity-induced mitochondrial biogenesis in skeletal muscle. *J Appl Physiol* 90: 1137–57, 2001.

18. **Hood DA**, **Tryon LD**, **Carter HN**, **Kim Y**, **Chen CCW**. Unravelling the mechanisms regulating muscle mitochondrial biogenesis. *Biochem J* 473: 2295–2314, 2016.

19. **Hoshino A**, **Mita Y**, **Okawa Y**, **Ariyoshi M**, **Iwai-Kanai E**, **Ueyama T**, **Ikeda K**, **Ogata T**, **Matoba S**. Cytosolic p53 inhibits Parkin-mediated mitophagy and promotes mitochondrial dysfunction in the mouse heart. *Nat Commun* 4: 2308, 2013.

20. **Houtkooper RH**, **Argmann C**, **Houten SM**, **Cantó C**, **Jeninga EH**, **Andreux PA**, **Thomas C**, **Doenlen R**, **Schoonjans K**, **Auwerx J**. The metabolic footprint of aging in mice. *Sci Rep* 1: 134, 2011.

21. **Iqbal S**, **Ostojic O**, **Singh K**, **Joseph A-M**, **Hood DA**. Expression of mitochondrial fission and fusion regulatory proteins in skeletal muscle during chronic use and disuse. *Muscle Nerve* 48: 963–70, 2013.

22. **Janssen I**, **Heymsfield SB**, **Ross R**. Low relative skeletal muscle mass (sarcopenia) in older persons is associated with functional impairment and physical disability. *J Am Geriatr Soc* 50: 889–96, 2002.

23. **Jin SM**, **Lazarou M**, **Wang C**, **Kane LA**, **Narendra DP**, **Youle RJ**. Mitochondrial membrane potential regulates PINK1 import and proteolytic destabilization by PARL. *J Cell Biol* 191: 933–42, 2010.

24. **Ju J-S**, **Varadhachary AS**, **Miller SE**, **Weihl CC**. Quantitation of "autophagic flux" in mature skeletal muscle. *Autophagy* 6: 929–935, 2010.

25. **Kane LA**, **Lazarou M**, **Fogel AI**, **Li Y**, **Yamano K**, **Sarraf SA**, **Banerjee S**, **Youle RJ**. PINK1 phosphorylates ubiquitin to activate Parkin E3 ubiquitin ligase activity. *J Cell Biol* 205: 143–53, 2014.

26. **Kazlauskaite A**, **Kondapalli C**, **Gourlay R**, **Campbell DG**, **Ritorto MS**, **Hofmann K**, **Alessi DR**, **Knebel A**, **Trost M**, **Muqit MMK**. Parkin is activated by PINK1-dependent phosphorylation of ubiquitin at Ser 65. *Biochem J* 460: 127–139, 2014.

27. **Kim Y**, **Hood DA**. Regulation of the autophagy system during chronic contractile activity-induced muscle adaptations. *Physiol Rep* 5: e13307, 2017.

28. **Koyano F**, **Okatsu K**, **Kosako H**, **Tamura Y**, **Go E**, **Kimura M**, **Kimura Y**, **Tsuchiya H**, **Yoshihara H**, **Hirokawa T**, **Endo T**, **Fon EA**, **Trempe J-F**, **Saeki Y**, **Tanaka K**, **Matsuda N**. Ubiquitin is phosphorylated by PINK1 to activate parkin. *Nature* 510: 162–6, 2014.

29. **Kruse SE**, **Karunadharma PP**, **Basisty N**, **Johnson R**, **Beyer RP**, **MacCoss MJ**, **Rabinovitch PS**, **Marcinek DJ**. Age modifies respiratory complex I and protein homeostasis in a muscle type-specific manner. *Aging Cell* 15: 89–99, 2016.

30. **Lazarou M**, **Jin SM**, **Kane LA**, **Youle RJ**. Role of PINK1 binding to the TOM complex and alternate intracellular membranes in recruitment and activation of the E3 ligase Parkin. *Dev Cell* 22: 320–33, 2012.

31. **Lee Y**, **Stevens DA**, **Kang S-U**, **Jiang H**, **Lee Y-I**, **Ko HS**, **Scarffe LA**, **Umanah GE**, **Kang H**, **Ham S**, **Kam T-I**, **Allen K**, **Brahmachari S**, **Kim JW**, **Neifert S**, **Yun SP**, **Fiesel FC**, **Springer W**, **Dawson VL**, **Shin J-H**, **Dawson TM**. PINK1 Primes Parkin-Mediated Ubiquitination of PARIS in Dopaminergic Neuronal Survival. *Cell Rep* 18: 918–932, 2017.

32. **Little JP**, **Safdar A**, **Cermak N**, **Tarnopolsky MA**, **Gibala MJ**. Acute endurance exercise

increases the nuclear abundance of PGC-1 in trained human skeletal muscle. *AJP Regul Integr Comp Physiol* 298: R912–R917, 2010.

33. **Ljubicic V**, **Hood DA**. Diminished contraction-induced intracellular signaling towards mitochondrial biogenesis in aged skeletal muscle. *Aging Cell* 8: 394–404, 2009.

34. **Ljubicic V**, **Joseph A-M**, **Adhihetty PJ**, **Huang JH**, **Saleem A**, **Uguccioni G**, **Hood DA**. Molecular basis for an attenuated mitochondrial adaptive plasticity in aged skeletal muscle. *Aging (Albany NY)* 1: 818–30, 2009.

35. **Mansueto G**, **Armani A**, **Viscomi C**, **D'Orsi L**, **De Cegli R**, **Polishchuk E V**, **Lamperti C**, **Di Meo I**, **Romanello V**, **Marchet S**, **Saha PK**, **Zong H**, **Blaauw B**, **Solagna F**, **Tezze C**, **Grumati P**, **Bonaldo P**, **Pessin JE**, **Zeviani M**, **Sandri M**, **Ballabio A**. Transcription Factor EB Controls Metabolic Flexibility during Exercise. *Cell Metab* 25: 182–196, 2017.

36. **Masiero E**, **Agatea L**, **Mammucari C**, **Blaauw B**, **Loro E**, **Komatsu M**, **Metzger D**, **Reggiani C**, **Schiaffino S**, **Sandri M**. Autophagy is required to maintain muscle mass. *Cell Metab* 10: 507–15, 2009.

37. **Menzies KJ**, **Singh K**, **Saleem A**, **Hood DA**. Sirtuin 1-mediated effects of exercise and resveratrol on mitochondrial biogenesis. *J Biol Chem* 288: 6968–79, 2013.

38. **Nabben M**, **Hoeks J**, **Briedé JJ**, **Glatz JFC**, **Moonen-Kornips E**, **Hesselink MKC**, **Schrauwen P**. The effect of UCP3 overexpression on mitochondrial ROS production in skeletal muscle of young versus aged mice. *FEBS Lett* 582: 4147–4152, 2008.

39. **Narendra D**, **Tanaka A**, **Suen D-F**, **Youle RJ**. Parkin is recruited selectively to impaired mitochondria and promotes their autophagy. *J Cell Biol* 183: 795–803, 2008.

40. **Narendra DP**, **Jin SM**, **Tanaka A**, **Suen D-F**, **Gautier CA**, **Shen J**, **Cookson MR**, **Youle RJ**. PINK1 is selectively stabilized on impaired mitochondria to activate Parkin. *PLoS Biol*

8: e1000298, 2010.

41. **Nezich CL**, **Wang C**, **Fogel AI**, **Youle RJ**. MiT/TFE transcription factors are activated during mitophagy downstream of Parkin and Atg5. *J Cell Biol* 210: 435–450, 2015.

42. **O'Leary MF**, **Vainshtein A**, **Iqbal S**, **Ostojic O**, **Hood DA**. Adaptive plasticity of autophagic proteins to denervation in aging skeletal muscle. *Am J Physiol Cell Physiol* 304: C422-30, 2013.

43. **Palacino JJ**, **Sagi D**, **Goldberg MS**, **Krauss S**, **Motz C**, **Wacker M**, **Klose J**, **Shen J**. Mitochondrial Dysfunction and Oxidative Damage in *parkin* -deficient Mice. *J Biol Chem* 279: 18614–18622, 2004.

44. **Pankiv S**, **Clausen TH**, **Lamark T**, **Brech A**, **Bruun J-A**, **Outzen H**, **Øvervatn A**, **Bjørkøy G**, **Johansen T**. p62/SQSTM1 Binds Directly to Atg8/LC3 to Facilitate Degradation of Ubiquitinated Protein Aggregates by Autophagy. *J Biol Chem* 282: 24131–24145, 2007.

45. **Picard M**, **Ritchie D**, **Thomas MM**, **Wright KJ**, **Hepple RT**. Alterations in intrinsic mitochondrial function with aging are fiber type-specific and do not explain differential atrophy between muscles. *Aging Cell* 10, 2011.

46. **Poole AC**, **Thomas RE**, **Andrews LA**, **McBride HM**, **Whitworth AJ**, **Pallanck LJ**. The PINK1/Parkin pathway regulates mitochondrial morphology. *Proc Natl Acad Sci* 105: 1638–1643, 2008.

47. **Rana A**, **Rera M**, **Walker DW**. Parkin overexpression during aging reduces proteotoxicity, alters mitochondrial dynamics, and extends lifespan. *Proc Natl Acad Sci U S A* 110: 8638–43, 2013.

48. **Rosen KM**, **Veereshwarayya V**, **Moussa CE-H**, **Fu Q**, **Goldberg MS**, **Schlossmacher**

MG, **Shen J**, **Querfurth HW**. Parkin Protects against Mitochondrial Toxins and β-Amyloid Accumulation in Skeletal Muscle Cells. *J Biol Chem* 281: 12809–12816, 2006.

49. **Saleem A**, **Carter HN**, **Hood DA**. p53 is necessary for the adaptive changes in cellular milieu subsequent to an acute bout of endurance exercise. 306: C241-9, 2014.

50. **Saleem A**, **Iqbal S**, **Zhang Y**, **Hood DA**. Effect of p53 on mitochondrial morphology, import, and assembly in skeletal muscle. *Am J Physiol - Cell Physiol* 308, 2015.

51. **Sardiello M**, **Palmieri M**, **di Ronza A**, **Medina DL**, **Valenza M**, **Gennarino VA**, **Di Malta C**, **Donaudy F**, **Embrione V**, **Polishchuk RS**, **Banfi S**, **Parenti G**, **Cattaneo E**, **Ballabio A**. A Gene Network Regulating Lysosomal Biogenesis and Function. *Science (80-)* 325: 473–7, 2009.

52. **Sarraf SA**, **Raman M**, **Guarani-Pereira V**, **Sowa ME**, **Huttlin EL**, **Gygi SP**, **Harper JW**. Landscape of the PARKIN-dependent ubiquitylome in response to mitochondrial depolarization. *Nature* 496: 372–6, 2013.

53. **Sebastián D**, **Sorianello E**, **Segalés J**, **Irazoki A**, **Ruiz-Bonilla V**, **Sala D**, **Planet E**, **Berenguer-Llergo A**, **Muñoz JP**, **Sánchez-Feutrie M**, **Plana N**, **Hernández-Álvarez MI**, **Serrano AL**, **Palacín M**, **Zorzano A**. Mfn2 deficiency links age-related sarcopenia and impaired autophagy to activation of an adaptive mitophagy pathway. *EMBO J* 35: 1677–93, 2016.

54. **Settembre C**, **Di Malta C**, **Polito VA**, **Garcia Arencibia M**, **Vetrini F**, **Erdin SUSU**, **Erdin SUSU**, **Huynh T**, **Medina D**, **Colella P**, **Sardiello M**, **Rubinsztein DC**, **Ballabio A**, **Arencibia MG**, **Vetrini F**, **Erdin SUSU**, **Erdin SUSU**, **Huynh T**, **Medina D**, **Colella P**, **Sardiello M**, **Rubinsztein DC**, **Ballabio A**. TFEB links autophagy to lysosomal biogenesis. *Science* 332: 1429–33, 2011.

55. **Shimura H**, **Hattori N**, **Kubo S**, **Yoshikawa M**, **Kitada T**, **Matsumine H**, **Asakawa S**, **Minoshima S**, **Yamamura Y**, **Shimizu N**, **Mizuno Y**. Immunohistochemical and subcellular localization of Parkin protein: absence of protein in autosomal recessive juvenile parkinsonism patients. *Ann Neurol* 45: 668–72, 1999.

56. **Shin J-H**, **Ko HS**, **Kang H**, **Lee Y**, **Lee Y-I**, **Pletinkova O**, **Troconso JC**, **Dawson VL**, **Dawson TM**. PARIS (ZNF746) repression of PGC-1α contributes to neurodegeneration in Parkinson's disease. *Cell* 144: 689–702, 2011.

57. **Siddiqui A**, **Rane A**, **Rajagopalan S**, **Chinta SJ**, **Andersen JK**. Detrimental effects of oxidative losses in parkin activity in a model of sporadic Parkinson's disease are attenuated by restoration of PGC1alpha. *Neurobiol Dis* 93: 115–120, 2016.

58. **Stevens DA**, **Lee Y**, **Kang HC**, **Lee BD**, **Lee Y-I**, **Bower A**, **Jiang H**, **Kang S-U**, **Andrabi SA**, **Dawson VL**, **Shin J-H**, **Dawson TM**. Parkin loss leads to PARIS-dependent declines in mitochondrial mass and respiration. *Proc Natl Acad Sci U S A* 112: 11696–701, 2015.

59. **Twig G**, **Elorza A**, **Molina AJA**, **Mohamed H**, **Wikstrom JD**, **Walzer G**, **Stiles L**, **Haigh SE**, **Katz S**, **Las G**, **Alroy J**, **Wu M**, **Py BF**, **Yuan J**, **Deeney JT**, **Corkey BE**, **Shirihai OS**. Fission and selective fusion govern mitochondrial segregation and elimination by autophagy. *EMBO J* 27: 433–446, 2008.

60. **Vainshtein A**, **Tryon LD**, **Pauly M**, **Hood DA**. Role of PGC-1α during acute exercise-induced autophagy and mitophagy in skeletal muscle. *Am J Physiol Cell Physiol* 308: C710-9, 2015.

61. **Wang Y**, **Serricchio M**, **Jauregui M**, **Shanbhag R**, **Stoltz T**, **Di Paolo CT**, **Kim PK**, **McQuibban GA**. Deubiquitinating enzymes regulate PARK2-mediated mitophagy. *Autophagy* 11: 595–606, 2015.

62. **Wright DC**, **Han D-H**, **Garcia-Roves PM**, **Geiger PC**, **Jones TE**, **Holloszy JO**. Exercise-induced mitochondrial biogenesis begins before the increase in muscle PGC-1alpha expression. *J Biol Chem* 282: 194–9, 2007.

63. **Youle RJ**, **van der Bliek AM**. Mitochondrial Fission, Fusion, and Stress. *Science (80-)* 337: 1062–1065, 2012.

64. **Zhang Y**, **Iqbal S**, **O'Leary MFN**, **Menzies KJ**, **Saleem A**, **Ding S**, **Hood DA**. Altered mitochondrial morphology and defective protein import reveal novel roles for Bax and/or Bak in skeletal muscle. *Am J Physiol Cell Physiol* 305: C502-11, 2013.

FIGURE LEGENDS

Fig. 1. Effect of aging and Parkin deficiency on mitochondrial content and function. (*A)*: Representative Western blot of Parkin expression in young (*Y*) and aged (*A*) skeletal muscle of control wild-type (WT) mice above. A graphical representation is shown below (n = 4). (*B)*: Cytochrome c oxidase (COX) activity in quadriceps muscle of young and aged Parkin KO and WT animals (n = 6). *(C)*: Mitochondrial state 4 and state 3 respiration rates in KO compared with WT animals (n = 6–9, ¶$P < 0.05$, vs young WT state 3). (*D*): Mitochondrial ROS production expressed per natom of oxygen consumed in Parkin KO and WT mice (n = 6–9, #$P < 0.05$, vs remaining state 4 conditions). Values are means ± SEM. *$P < 0.05$, main effect of age. WT, wild-type; KO, Parkin knock-out; A.U., arbitrary units.

Fig. 2. Effect of Parkin and age on exercise performance. (*A*): Representative Western blot of Parkin localization on isolated mitochondria from young and aged WT muscle, prior to exercise (Con) and immediately following exercise (Ex). Quantification of mitochondrial Parkin localization is shown below, corrected for loading using mitochondrial voltage-dependent anion channel (VDAC) (n = 3). (*B*): Animal performance (i.e. total distance run) of WT and KO mice injected with water (Veh) or 0.4 mg/kg colchicine (Col) (n = 6–8). (*C*): Blood lactate levels measured prior to (Con), and immediately following exercise (Ex) (n = 6–8). Values are means ± SEM. †$P < 0.05$, interaction effect of exercise and age. *$P < 0.05$, main effect of age. ¶$P < 0.05$, vs young Con. #$P < 0.05$, significant difference from aged WT mice. WT, wild-type; KO, Parkin knock-out; A.U., arbitrary units.

Fig. 3. Mitophagy flux following an acute bout of exercise in young Parkin KO and WT mice. (*A*): Representative Western blots of LC3II and p62 localization on isolated mitochondria from WT and KO mice injected with water (Veh) or 0.4 mg/kg colchicine (Col). Quantification of mitochondrial LC3II flux (*B*) and p62 flux (*C*) is shown ($n = 8$). Mitophagy flux of LC3II and p62 were assessed prior to exercise (C), immediately following exercise (Ex), and following 2 hours of recovery (ExR). Values are means ± SEM. ¶$P < 0.05$, vs WT Con and WT ExR. Voltage-dependent anion channel (VDAC) was used as a mitochondrial loading control. WT, wild-type; KO, Parkin knock-out; LC3II, lipidated microtubule-associated protein 1A/1B-light chain 3; p62, sequestosome 1; A.U., arbitrary units.

Fig. 4. Mitophagy flux following an acute bout of exercise in young and aged Parkin KO and WT mice. (*A*): Representative Western blots of LC3II and p62 localization on isolated mitochondria from young and aged WT injected with water (Veh) or 0.4 mg/kg colchicine (Col). Quantification of mitochondrial LC3II flux (*B*) and p62 flux (*C*) is shown ($n = 6$). (*D*): Representative Western blots of LC3II and p62 localization on isolated mitochondria from young and aged KO injected with water [Veh (Vehicle)] or 0.4 mg/kg colchicine (Col). Mitochondrial LC3II flux (*E*) and p62 flux (*F*) with age and exercise are quantified ($n = 6$). Quantification of basal LC3II flux (*G*) and p62 flux (*H*) with age only. Mitophagy flux and localization of LC3II and p62 were assessed prior to exercise (C) and immediately following exercise (Ex). Values are means ± SEM. *$P < 0.05$, main effect of age. ¶$P < 0.05$, main effect of exercise. #$P < 0.05$, significant difference from aged WT mice. Voltage-dependent anion channel (VDAC) was used as a mitochondrial loading control. WT, wild-type; KO, Parkin knock-out; LC3II, lipidated microtubule-associated protein 1A/1B-light chain 3; p62, sequestosome 1; A.U., arbitrary units.

Fig. 5. Mitochondrial ubiquitination following an acute bout of exercise in young and aged Parkin KO and WT mice. (*A*): Representative Western blot of ubiquitin (Ub) on isolated mitochondria from young WT and KO mice injected with water (Veh) or 0.4 mg/kg colchicine (Col). (*B*): Quantification of mitochondrial Ub flux in young WT and KO mice (n = 8). (*C*): Representative Western blot of ubiquitin (Ub) on isolated mitochondria from aged WT and KO mice injected with water (Veh) or 0.4 mg/kg colchicine (Col). (*D*): Quantification of mitochondrial Ub flux in aged WT and KO mice (n = 6). (*E*): Mfn2 was immunoprecipitated (IP) followed by immunoblotting (IB) for ubiquitin on isolated mitochondria from young and aged groups of Parkin KO and WT animals prior to, and immediately following exercise. (*F*): Graphical representation of mitochondrial Mfn2 ubiquitination relative to young WT control values (n = 6). In young animals, mitochondrial Ub flux was assessed prior to exercise (C), immediately following exercise (Ex), and following 2 hours of recovery (ExR). There was no recovery group for the aged animals in the measurement of mitochondrial ubiquitination following exercise (*C–F*). Values are means ± SEM. ¶$P < 0.05$, main effect of exercise. #$P < 0.05$, vs young WT Con. Voltage-dependent anion channel (VDAC) was used as a mitochondrial loading control. Immunoglobulin G (IgG) was used as a negative control for co-immunoprecipitation validation. WT, wild-type; KO, Parkin knock-out; Ub, ubiquitin; Mfn2, Mitofusin-2; IgG, Immunoglobulin G; A.U., arbitrary units.

Fig. 6. Effect of Parkin and age on PARIS and PGC-1α nuclear translocation. (*A*): Representative Western blots for PARIS, PGC-1α, H2B and α-tubulin. (*B*): Graphical quantification of [nuclear (N)] PARIS represented as a percentage of total [cytosol (C) + nuclear (N)] PARIS (n = 6). (*C*): PGC-1α nuclear abundance (n = 6). Values are means ± SEM. *$P < 0.05$, main effect of age. #$P <$

0.05, significant difference from aged mice. Nuclear and cytosol protein expression were corrected for loading using nuclear histone 2B (H2B) and α-tubulin, respectively. PARIS, Parkin-Interacting Substrate; PGC-1α, peroxisome proliferator gamma coactivator-1α.

Fig. 7. Effect of Parkin and age on exercise-induced PARIS and PGC-1α subcellular localization. (*A*) and (*B*): Representative Western blots for PARIS, PGC-1α, H2B and α-tubulin are shown. Graphical representation of [nuclear (N)] PARIS represented as a percentage of total [cytosol (C) + nuclear (N)] PARIS in young (*C*) and aged (*D*) mice (n = 5–8). Graphical quantification of PGC-1α in nuclear fraction of young (*E*) and aged (*F*) animals (n = 6–7). In young animals, measurements of PARIS (*C*) and PGC-1α (*E*) were done prior to exercise (Con), immediately following exercise (Ex), and following 2 hours of recovery (ExR). There was no recovery group for aged animals in the evaluation of PARIS (*D*) and PGC-1α (*F*) subcellular localization following exercise. Values are means ± SEM. †P < 0.05, interaction effect of exercise and genotype. ¶P < 0.05, vs WT Con. Histone 2B (H2B) was used as a nuclear loading control and α-tubulin was used as a cytosol loading control. PARIS, Parkin-Interacting Substrate; PGC-1α, peroxisome proliferator gamma coactivator-1α; WT, wild-type; KO, Parkin knock-out.

Table 1. Animal characteristics of WT and Parkin KO mice

Condition	Young WT	Aged WT	Young KO	Aged KO
Body Mass, g	31.4 ± 3.4	49.7 ± 3.3*	27.2 ± 2.6	49.8 ± 1.0*
Quadriceps Mass, mg	237.8 ± 27.0	191.9 ± 11.5	187.1 ± 22.4	156.3 ± 11.7
Quadriceps Mass / Body Mass, mg/g	7.3 ± 0.3	4.0 ± 0.4*	6.7 ± 0.3	3.1 ± 0.2*
Heart Mass, mg	166.0 ± 6.4	192.9 ± 8.1	143.3 ± 16.3	184.8 ± 13.1
Heart Mass / Body Mass, mg/g	5.5 ± 0.5	4.0 ± 0.3*	5.4 ± 0.6	3.7 ± 0.3*
Epididymal Fat Mass, g	0.17 ± 0.01	2.41 ± 0.19*	0.15 ± 0.01	2.09 ± 0.17*
Epididymal Fat Mass / Body Mass, mg/g	5.9 ± 0.9	50.6 ± 6.5*	5.6 ± 0.4	42.0 ± 3.1*
Tibia length (mm)	21.7 ± 0.3	21.6 ± 0.9	21.2 ± 0.7	21.1 ± 0.6
Quadriceps Mass / Tibia Length, mg/mm	11.0 ± 1.2	8.9 ± 0.5*	8.8 ± 1.1	7.4 ± 0.6
Quadriceps Mass / Tibia Length (aged over young)	0.87 ± 0.12		0.89 ± 0.11	

Values are reported as means ± SEM, $n = 6$. * $P < 0.05$ vs. Young counterpart

Figure 1

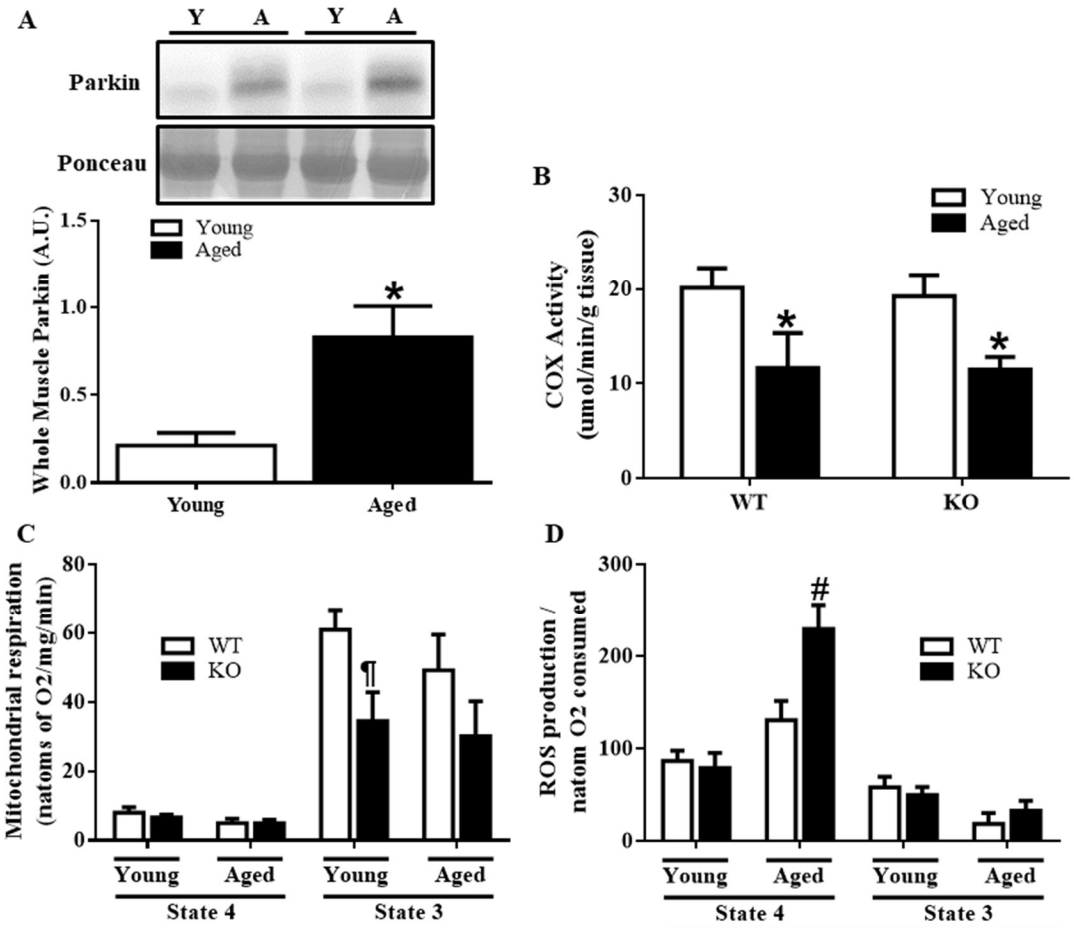
A
Y
A
Y
A
Parkin
Ponceau
Whole Muscle Parkin (A.U.)
1.5
1.0
0.5
0.0
Young
Aged
*
Young
Aged
B
COX Activity (umol/min/g tissue)
30
20
10
0
*
*
Young
Aged
WT
KO
C
Mitochondrial respiration (natoms of O2/mg/min)
80
60
40
20
0
WT
KO
¶
Young
Aged
Young
Aged
State 4
State 3
D
ROS production / natom O2 consumed
300
200
100
0
#
WT
KO
Young
Aged
Young
Aged
State 4
State 3

Figure 2

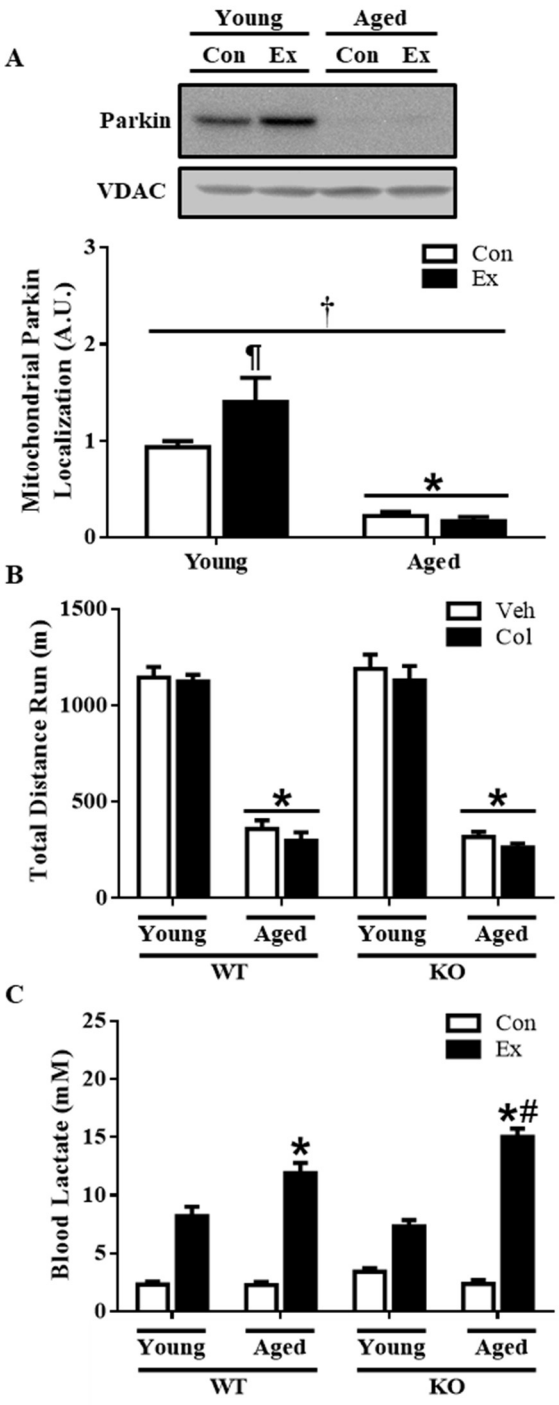
A
Young
Aged
Con
Ex
Con
Ex
Parkin
VDAC
Mitochondrial Parkin Localization (A.U.)
Con
Ex
†
¶
*
Young
Aged
B
Total Distance Run (m)
Veh
Col
*
*
Young
Aged
Young
Aged
WT
KO
C
Blood Lactate (mM)
Con
Ex
*
*#
Young
Aged
Young
Aged
WT
KO

Figure 3

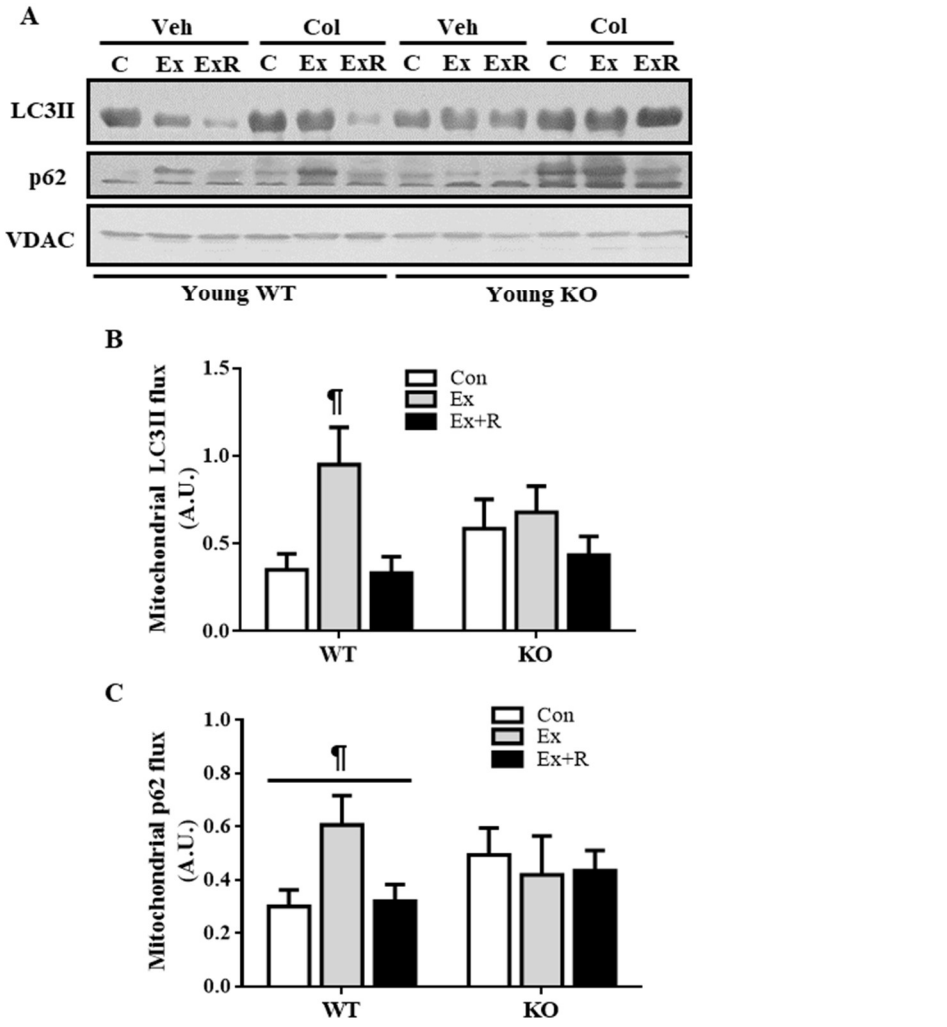
A
Veh
Col
Veh
Col
C Ex ExR C Ex ExR C Ex ExR C Ex ExR
LC3II
p62
VDAC
Young WT
Young KO
B
Mitochondrial LC3II flux (A.U.)
1.5
1.0
0.5
0.0
¶
Con
Ex
Ex+R
WT
KO
C
Mitochondrial p62 flux (A.U.)
1.0
0.8
0.6
0.4
0.2
0.0
¶
Con
Ex
Ex+R
WT
KO

Figure 4

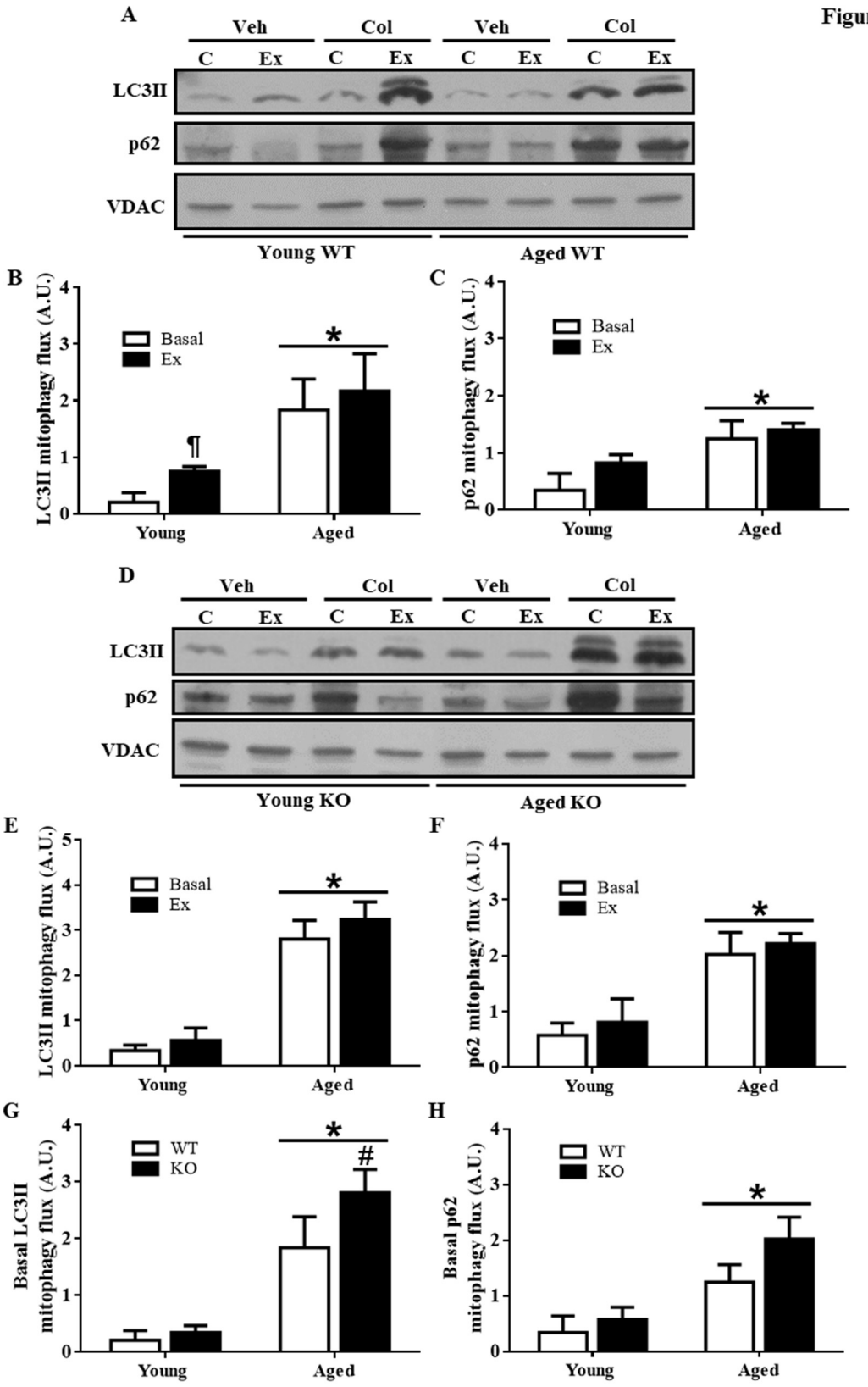
A
Veh
Col
Veh
Col
C
Ex
C
Ex
C
Ex
C
Ex
LC3II
p62
VDAC
Young WT
Aged WT
B
LC3II mitophagy flux (A.U.)
Basal
Ex
*
¶
Young
Aged
C
p62 mitophagy flux (A.U.)
Basal
Ex
*
Young
Aged
D
Veh
Col
Veh
Col
C
Ex
C
Ex
C
Ex
C
Ex
LC3II
p62
VDAC
Young KO
Aged KO
E
LC3II mitophagy flux (A.U.)
Basal
Ex
*
Young
Aged
F
p62 mitophagy flux (A.U.)
Basal
Ex
*
Young
Aged
G
Basal LC3II mitophagy flux (A.U.)
WT
KO
*
#
Young
Aged
H
Basal p62 mitophagy flux (A.U.)
WT
KO
*
Young
Aged

Figure 5

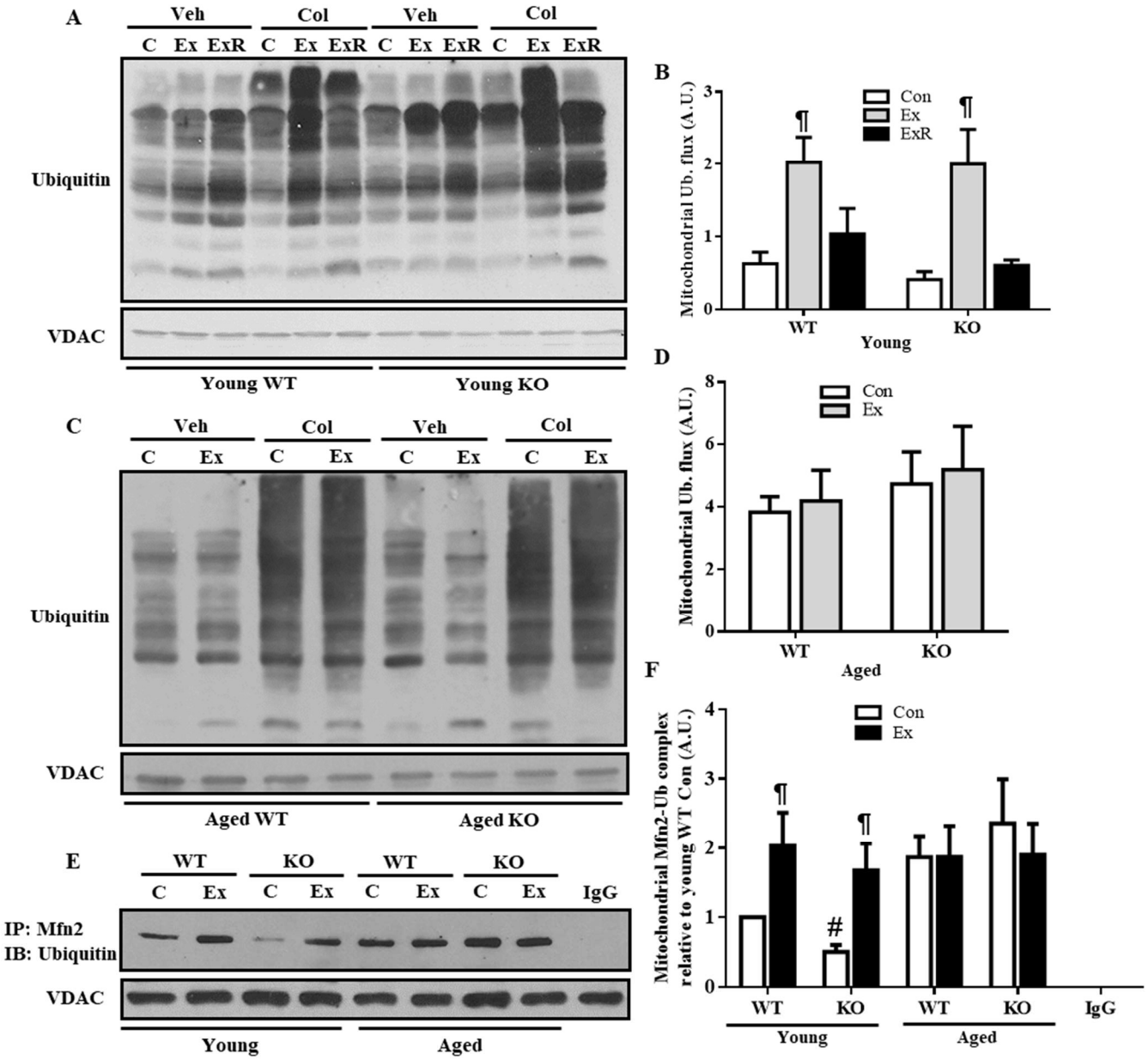
A
Veh
Col
Veh
Col
C Ex ExR C Ex ExR C Ex ExR C Ex ExR
Ubiquitin
VDAC
Young WT
Young KO
B
Con
Ex
ExR
Mitochondrial Ub. flux (A.U.)
¶
¶
WT
KO
Young
C
Veh
Col
Veh
Col
C Ex C Ex C Ex C Ex
Ubiquitin
VDAC
Aged WT
Aged KO
D
Con
Ex
Mitochondrial Ub. flux (A.U.)
WT
KO
Aged
E
WT
KO
WT
KO
C Ex C Ex C Ex C Ex IgG
IP: Mfn2
IB: Ubiquitin
VDAC
Young
Aged
F
Con
Ex
Mitochondrial Mfn2-Ub complex relative to young WT Con (A.U.)
¶
¶
#
WT
KO
WT
KO
IgG
Young
Aged

Figure 6

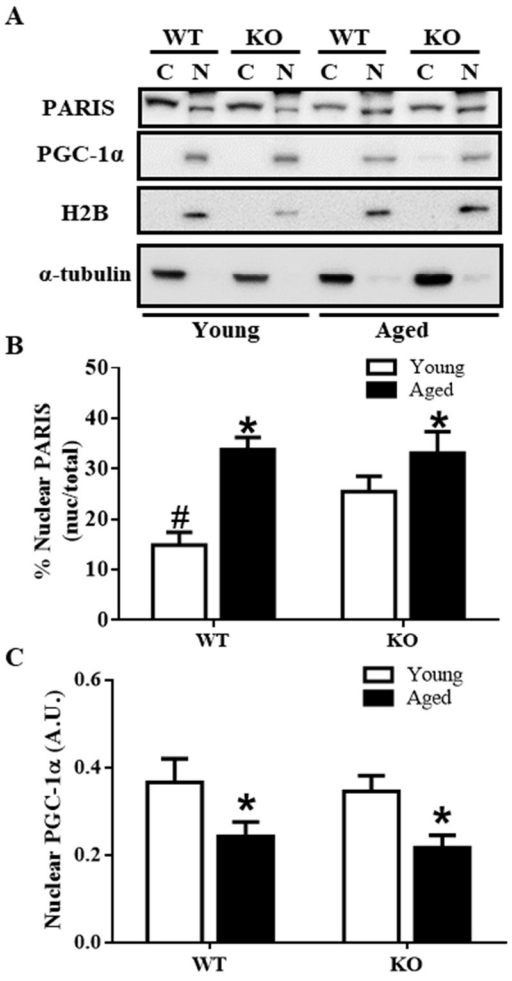
A
WT
KO
WT
KO
C N C N C N C N
PARIS
PGC-1α
H2B
α-tubulin
Young
Aged
B
Young
Aged
% Nuclear PARIS (nuc/total)
50
40
30
20
10
0
#
*
*
WT
KO
C
Young
Aged
Nuclear PGC-1α (A.U.)
0.6
0.4
0.2
0.0
*
*
WT
KO

Figure 7

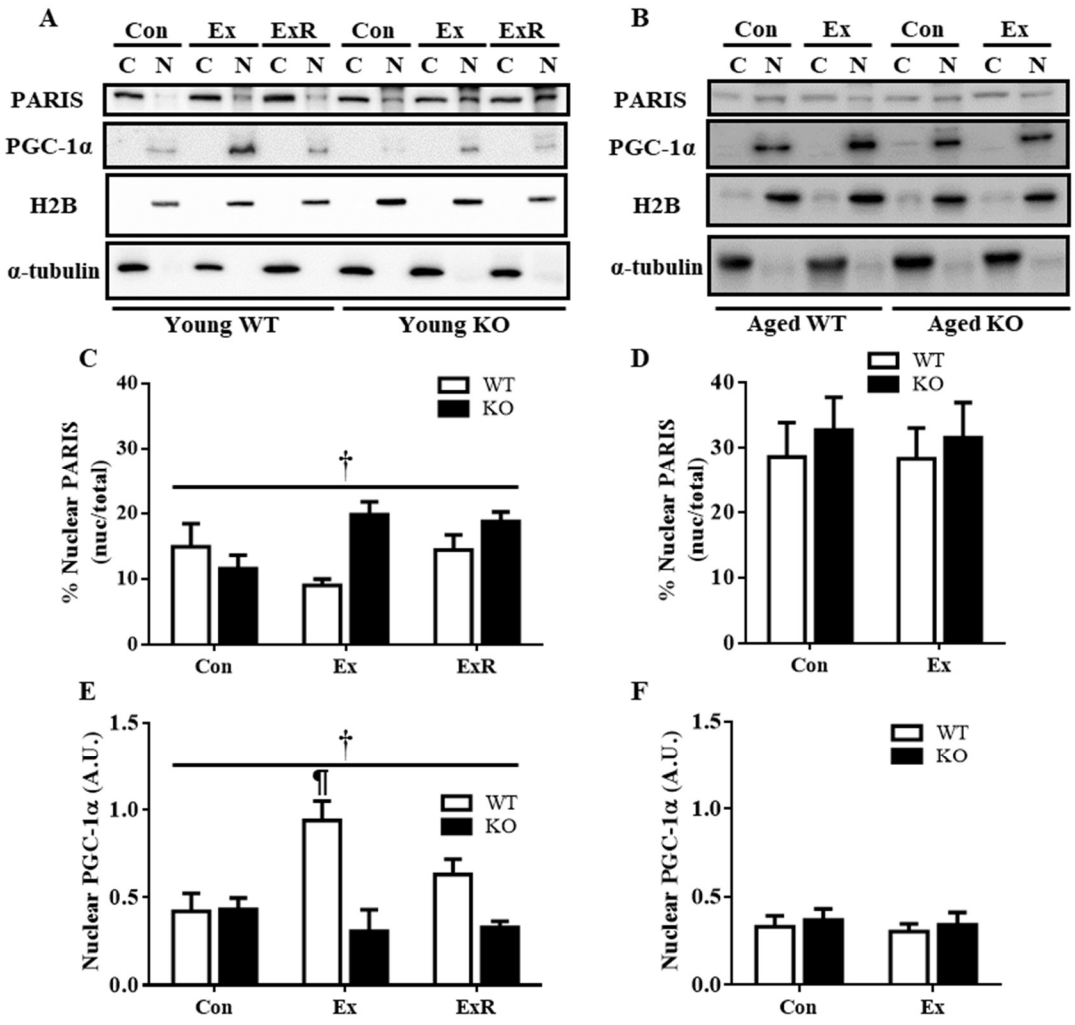
A
Con
Ex
ExR
Con
Ex
ExR
C N C N C N C N C N C N
PARIS
PGC-1α
H2B
α-tubulin
Young WT
Young KO
B
Con
Ex
Con
Ex
C N C N C N C N
PARIS
PGC-1α
H2B
α-tubulin
Aged WT
Aged KO
C
% Nuclear PARIS (nuc/total)
WT
KO
†
Con
Ex
ExR
D
% Nuclear PARIS (nuc/total)
WT
KO
Con
Ex
E
Nuclear PGC-1α (A.U.)
†
¶
WT
KO
Con
Ex
ExR
F
Nuclear PGC-1α (A.U.)
WT
KO
Con
Ex

CHAPTER 5:

Role of Parkin and endurance training on mitochondrial turnover in skeletal muscle

Chris Chin Wah Chen[1,2], Avigail T. Erlich[1,2] and David A. Hood[1,2]

[1]School of Kinesiology and Health Science,
[2]Muscle Health Research Centre，
York University, Toronto,
Ontario M3J 1P3, Canada

Running title: Parkin-mediated mitophagy in trained skeletal muscle

Keywords: Endurance training, Mitochondrial biogenesis, mitophagy flux, PGC-1α, PARIS

AUTHOR CONTRIBUTIONS

C.C.W.C. and A.T.E. performed experiments; C.C.W.C. analyzed data; C.C.W.C. and D.A.H. interpreted results of experiments; C.C.W.C. prepared figures; C.C.W.C. drafted manuscript; C.C.W.C. and D.A.H. edited and revised manuscript; C.C.W.C. and D.A.H. conception and design of research; C.C.W.C. and D.A.H. approved final version of manuscript.

This manuscript has been submitted to Skeletal Muscle Journal (December 2017).

ABSTRACT

Parkin is a ubiquitin ligase that is involved in the selective removal of dysfunctional mitochondria. This process is termed mitophagy and can assist in mitochondrial quality control. Endurance training can produce adaptations in skeletal muscle toward a more oxidative phenotype, an outcome of enhanced mitochondrial biogenesis. It remains unknown if changes in Parkin-mediated mitophagy are involved in the training-induced increases in mitochondrial content and function. Our results indicate that Parkin is required for the basal maintenance of mitochondrial function. The absence of Parkin did not alter mitophagy basally, however, acute exercise produced an elevation in mitophagy flux in a Parkin-dependent manner. Mitochondrial content was increased following training in KO animals, and this occurred without an induction of PGC-1α signaling. Interestingly, the adaptive response of increased muscle mitochondrial content to training did not influence basal mitophagy flux, despite an enhanced expression and localization of Parkin to mitochondria. Furthermore, exercise-induced mitophagy flux was attenuated with training in WT animals, suggesting a lower rate of mitochondrial degradation due to improved organelle quality with endurance training. In contrast, training did not improve mitochondrial dysfunction in KO animals, and the absence of Parkin with training may engender an accumulation of dysfunctional organelles. In KO animals, this is likely the reason for the impaired training-induced attenuation in mitophagy flux compared to WT animals. Our study demonstrates that exercise-induced mitophagy flux is Parkin-mediated, and reduced with training due to increased mitochondrial content and quality.

INTRODUCTION

Skeletal muscle is a highly malleable tissue that displays a remarkable adaptive plasticity. Chronic contractile activity of muscle can evoke molecular and biochemical adaptations that enable muscle to improve its oxidative capacity (22, 64). This enhancement is, in part, the result of greater mitochondrial enzyme gene expression (16, 24). It is well established that endurance training can increase mitochondrial biogenesis and alter muscle metabolism (9, 41, 45). In trained muscle, an elevation in mitochondrial content improves oxidative phosphorylation, while lowering the reliance on glycolysis (7, 10). The process of generating new organelles is mediated, in part, by the transcriptional regulator peroxisome proliferator-activated receptor-γ coactivator-1α, PGC-1α. During acute bouts of exercise, PGC-1α can translocate into the nucleus (40, 45, 66) and upregulate the transcription of nuclear genes encoding mitochondrial proteins (NUGEMPs) (65), as well as transcription factors (14, 55) such as mitochondrial transcription factor A (TFAM). TFAM is a nuclear-encoded protein involved in mitochondrial DNA (mtDNA) transcription, along with the expression of several protein subunits of the respiratory electron transport chain (37). Chronic contractile activity can increase TFAM protein expression, followed by accelerated mitochondrial protein import and mtDNA binding (18). TFAM abundance has been shown to increase in response to training in humans (2). Thus, the induction of mitochondrial biogenesis during exercise requires the coordination of both nuclear and mitochondrial genomes for subsequent organelle assembly and function (25, 71, 72).

Mitochondria are considered to be primary sites for free radical formation (52, 74). When this production is left unchecked, oxidative stress can impair ATP generation and induce cellular injury. To combat against sustained damage, the selective removal of dysfunctional mitochondria, known as mitophagy, is swiftly activated. Organelle turnover is the balance between mitochondrial

biogenesis and mitophagy, and the combination of these processes aids in the maintenance of energetic homeostasis. An imbalance of these two opposing pathways can lead to the development of cardiovascular diseases (17, 67), cancer (3, 69), diabetes (26, 61) and accelerate aging (5, 49, 54). The most well characterized pathway of mitophagy involves PTEN-induced putative kinase 1 (PINK1) and ubiquitin ligase Parkin (51). Under non-stressful conditions, PINK1 import into polarized mitochondria ensues, and is followed by its proteolysis (27). During cellular perturbations in which a collapse in organelle membrane potential occurs, PINK1 import into the matrix is impaired and its stabilization on the outer mitochondrial membrane (OMM) serve to recruit and activate Parkin (44, 47, 70). PINK-1 mediated phosphorylation of Parkin (33, 59) and ubiquitin (30, 31, 35) allows for the accretion of polyubiquitin chains on several protein targets of the OMM. This mobilizes the autophagy adaptor protein p62 to tagged mitochondria through its ubiquitin binding domain (13, 34). Lipidated microtubule-associated protein-light chain 3 (LC3II) is a protein bound on the phagophore membrane that can associate with p62 (4, 50), ultimately resulting in the autophagosomal enclosure of dysfunctional mitochondria as a cellular safeguard from additional oxidative damage (58). The autophagosome is then terminally degraded at the lysosome.

Recent evidence suggest that acute exercise is sufficient to activate autophagy (20, 21). However, few studies have examined the potential role of mitophagy during exercise. We have previously shown that skeletal muscle of exercised mice exhibits enhanced mitophagy flux, and that this is partially dependent on PGC-1α (66). In another study, the acute inhibition of autophagy in mice led to an accumulation of dysfunctional mitochondria in locomotor muscles during damaging eccentric exercise (68). While these studies collectively demonstrate that mitochondrial degradation occurs during acute exercise, they do not clarify the effects of prior endurance training

and how it can influence mitophagy. Current research seems to propose that autophagy may be enhanced in endurance trained muscle as an adaptation in improving exercise performance (12, 29, 32, 39). Yet, these studies do not provide a direct measurement of mitophagy using flux measurements, nor do they indicate how mitophagy may interact with the process of biogenesis that occurs with endurance training. In particular, Parkin has been shown to regulate both mitochondrial biogenesis and mitophagy, and the *in vitro* overexpression of wild-type Parkin can interact with TFAM to increase mtDNA transcription and replication, as well as increase mitochondrial mass (36, 53). Parkin can also increase PGC-1α protein expression through downregulation of Parkin-interacting substrate (PARIS) (60, 62). The activation of Parkin can target PARIS, a transcriptional repressor of PGC-1α, to the proteasome for degradation (38). Thus, Parkin may serve as a potential channel of communication between mitophagy and mitochondrial biogenesis. Thus, the purpose of our study was to investigate how Parkin is involved in mediating both biogenesis and mitophagy using, WT and Parkin KO mice that were either sedentary, or subjected to endurance training via voluntary wheel running. We also examined mitophagy flux in trained animals with a subsequent bout of acute exercise to determine the adaptive effect of prior endurance training.

MATERIALS AND METHODS

Animal Model. C57BL/6 (WT) and B6; 129S4-Park2^{tm1Shn}/J (Parkin KO; 006582) mice were obtained from Jackson Laboratories. The generation of these mice has been previously described (15). To genotype progeny, ear clippings were obtained from each animal for DNA extraction. JumpStart REDtaq polymerase (Sigma-Aldrich, St. Louis, MO) was incubated with DNA extracts, as well as forward and reverse primers specific to nucleotides of the WT or altered Parkin gene, and amplified using PCR. The reaction products were separated on a 1.5% agarose gel and visualized with the use of ethidium bromide.

Voluntary Wheel Running. Three-month-old WT and Parkin KO mice were assigned to control or trained experimental groups. During the duration of the study, all mice were housed in a 12-hour light–dark cycle room, and were allowed access to water and food *ad libitum*. Runners were placed in cages with access to a freely rotating wheel attached to an external magnetic counter (Mini-Mitter, Bend, OR). The number of revolutions were noted every 24 hours for each animal, and converted into kilometers per week. The duration of the training protocol lasted 6 weeks.

Endurance Exercise Protocol and Blood Lactate Measurement. Following the training protocol, cage wheels were taken out 2 days prior to treadmill habituation and acute exercise. During these 2 days, animals were injected intraperitoneally with colchicine (0.4 $mg \cdot kg^{-1} \cdot day^{-1}$), or an equal amount of vehicle (water) every 24 hours (28). Injections were performed in conjunction when mice were acclimatized to the treadmill. Vehicle- and colchicine treated animals in the exercise (Ex) group ran on a fixed, upward treadmill slope of 10°. Mice ran at 5 m/min for 5 minutes, 10 m/min for 10 minutes, 15 m/min for 15 minutes, and 20 m/min for 20 minutes. The speed was then incrementally increased at 1 m/min for every 1 minute until exhaustion was achieved. Exhaustion was defined as the inability of the animal to continue running on the

treadmill, even in the presence of air jet stimulation. A small tail bleed was used to measure blood lactate with a Lactate Scout+ analyzer (EKF Diagnostics, Magdeburg, Germany). All animals were sacrificed by cervical dislocation immediately after exercise (Ex). All animal protocols were submitted and approved by the York University Animal Care Committee. Animals were treated in accordance with Canadian Council of Animal Care guidelines.

Cytochrome c Oxidase (COX) Enzyme Activity. COX activity was measured as previously detailed (8), and performed on untrained and trained groups of WT and Parkin KO mice to measure whole muscle mitochondrial content. Briefly, protein extracts from mixed hindlimb muscles were added to a test solution containing fully reduced cytochrome c. Enzyme activity was determined by the maximal oxidation rate of completely reduced cytochrome c, measured by the change in absorbance at 550 nm using a Bio-Tek Synergy HT microplate reader, as previously described (45).

Mitochondrial Isolation. Mixed hindlimb muscles from both sides of the animal were immediately placed into ice-cold mitochondrial isolation buffer, and were quickly minced and homogenized. Intermyofibrillar (IMF) mitochondrial sub-fractions were subjected to differential centrifugation, as described previously (6, 45, 57). Mitochondria were resuspended in 100mM KCl, 10mM MOPS, and 0.2% BSA. Freshly isolated mitochondria were used for mitochondrial respiration and reactive oxygen species (ROS) emission assays, and aliquots of mitochondrial extracts were stored at –80ºC for immunoblotting analyses. The protein concentration values of the isolated mitochondria were quantified using the Bradford method.

Mitochondrial Respiration. Samples of isolated IMF mitochondria were incubated with VO2 buffer (in mM: 250 sucrose, 50 KCl, 25 Tris, and 10 K2HPO4, pH 7.4) with continuous stirring in a respiratory chamber. Respiration rates (nanoatom of O2/min/mg) were driven by complex I of

the mitochondrial electron transport chain in the presence of 10 mM glutamate (state 4, Sigma) accompanied by the addition of 0.44 mM ADP (state 3, Sigma). The addition of NADH during state 3 respiration did not significantly alter respiration rates, indicating intact inner mitochondrial membrane integrity. All respiration rates were evaluated using the Mitocell S200 Micro Respirometry System (Strathkelvin Instruments, North Lanarkshire, UK).

Mitochondrial ROS Production Assay. ROS emission was measured as done previously (45, 56). Briefly, isolated IMF mitochondria were incubated with VO2 buffer at 37 °C for 30 minutes in a white polystyrene 96-well plate under state 4 and 3 conditions. The addition and oxidation of 2',7'-dichlorodihydrofluorescein diacetate (50 μM H2DCFDA, ThermoFisher) emitted fluorescence between 480 and 520 nm, as measured with a Bio-Tek Synergy HT microplate reader, and is directly related to ROS emission. ROS emission was normalized per nanoatom of O2 consumed, as measured during mitochondrial respiration.

Immunoblotting. Whole quadricep muscle extracts were performed as described previously (56). Briefly, frozen muscle samples were pulverized, resuspended in buffer, sonicated and centrifuged. Muscle lysate was attained in the supernatant fraction, and the Bradford technique was used to determine protein content. Muscle homogenates and isolated mitochondrial fractions were separated using SDS-PAGE (12-15% polyacrylamide) and transferred to nitrocellulose membranes (BioRad). Blots were incubated overnight at 4 °C with primary antibodies against LC3/microtubule-associated protein light chain 3 (4108, Lot No. 3, Cell Signaling), p62/sequestosome 1 (P0067, Lot No. 015M4877V, Sigma), Parkin (4211, Lot No. 4, Cell Signaling), PGC-1α/peroxisome proliferator-activated receptor-γ coactivator-1α (ab3242, Lot No. 2691399, Millipore), PARIS/parkin-interacting substrate (ab130867, Lot No. GR235090-1, abcam), COXI/cytochrome c oxidase subunit 1 (ab14705, Lot No. GR233531-3, abcam),

COXIV/cytochrome c oxidase subunvit 4 (ab140643, Lot No. GR192963-3, abcam), TFAM/mitochondrial transcription factor A (in house), VDAC/voltage-dependent anion channel (ab14734, Lot No. GR121056-7) and α-tubulin (CP06, Lot No. D00175772, Millipore). This was followed by an hour incubation period at room temperature with appropriate horseradish peroxidase-conjugated secondary antibodies. The membranes were visually distinguished using enhanced chemiluminescence (Clarity ECL Western blotting substrates, Bio-Rad, CA) and photographic film. Films were quantified using ImageJ software (Version 1.48, NIH, USA).

Statistical Analysis. Data were analyzed with Graph Pad 6.0 software, and values are reported as means ± SEM. Data were analysed using two-way analysis of variance (ANOVA), except for Fig. 2A which was analysed using a student's t-test. For all two-way ANOVA analyses, Tukey's post hoc test was used to identify individual differences when statistical significance was observed. Statistical differences were considered significant if $P < 0.05$.

RESULTS

Physical characteristics of Parkin KO mice following endurance training. To determine the physiological importance of Parkin with training in skeletal muscle, we first assessed the physical characteristics of untrained and trained groups of WT and Parkin KO mice. During the 6 weeks of voluntary wheel running, WT and Parkin KO mice did not significantly differ in running distance, with both genotypes running up to ~70 km/week ($P < 0.05$; Fig. 1A). Total body mass, quadriceps and heart weight were measured at the end of the 6 weeks of voluntary exercise. There was no significant effect of genotype or training on body mass (Fig. 1B), or quadriceps muscle mass when corrected for body weight (Fig. 1C). In addition, no differences between WT and KO animals existed with respect to heart mass when corrected for body weight, but both genotypes exhibited ~5-7% elevations following training ($P < 0.05$; Fig. 1D).

The expression of several mitochondrial biogenesis regulatory factors is promoted following 6 weeks of voluntary exercise. We next examined the influence of endurance training on the expression of several protein markers involved in mitochondrial turnover. A large ~3-fold increase in Parkin expression was observed in trained, compared to untrained muscle ($P < 0.05$; Fig. 2A). In our study, COXIV expression did not differ between genotypes, or with training, when measured in whole muscle lysates (Fig. 2B). However, a significant interaction of genotype and training was observed for COXI ($P < 0.05$; Fig. 2B). Basal COXI expression did not differ between genotypes, but COXI expression was significantly elevated by 2.8- and 3.4-fold in both trained WT and Parkin KO animals, respectively, when compared to the untrained cohort ($P < 0.05$; Fig. 2B). Parkin can regulate mitochondrial biogenesis by targeting Parkin interacting substrate (PARIS) to the proteasome for degradation. In the absence of Parkin, PARIS can transcriptionally repress PGC-1α, a transcriptional co-activator of mitochondrial biogenesis. Surprisingly, whole

muscle PGC-1α and PARIS protein expression did not differ between untrained WT and Parkin KO animals (Fig. 2C–2E). Rather, a significant interaction of training and genotype for PGC-1α emerged ($P < 0.05$; Fig. 2C). Training induced a 1.9-fold increase in whole muscle PGC-1α expression in WT animals that was abolished in the absence of Parkin ($P < 0.05$; Fig. 2C and 2D). Similarly, a main effect of training on whole muscle PARIS levels was observed between genotypes, concomitant with a significant 75% reduction in WT animals ($P < 0.05$; Fig. 2C and 2E).

Mitochondrial adaptations in Parkin KO animals following voluntary exercise. We next evaluated the effects of Parkin deficiency and exercise training on isolated mitochondria collected from the hindlimb muscles. Interestingly, the expression of nuclear-encoded mitochondrial proteins COXIV and TFAM did not differ between genotypes, or with training (Fig. 3A). Similarly, COXI expression did not differ between genotypes, but exhibited significant 2.1- and 3.8-fold increases following 6 weeks of voluntary exercise training ($P < 0.05$; Fig. 3A and 3B). Mitochondrial yield represents the amount of mitochondrial protein extracted corrected for total muscle weight used for mitochondrial isolation. Although there was no difference between untrained WT and KO animals, both genotypes displayed significant increases with endurance training ($P < 0.05$; Fig. 3C). The biochemical assessment of cytochrome c oxidase (COX) activity confirmed the lack of difference between genotypes with respect to a marker of muscle mitochondrial content. However, voluntary wheel training significantly increased COX activity by ~1.4-fold in both WT and Parkin KO mice ($P < 0.05$; Fig. 3D). We also examined whether mitochondrial respiration and reactive oxygen species (ROS) emission differed with voluntary wheel running, and in the absence of Parkin. No significant training effect was noted on mitochondrial respiration. However, a main effect of genotype was observed on state 3

mitochondrial respiration ($P < 0.05$; Fig. 3E). When untrained animals were compared, a significant 46% decrease in state 3 mitochondrial respiration was detected in KO, compared to WT mice ($P < 0.05$; Fig. 3E). Following endurance training, the impairment in organelle respiration remained significantly depressed in KO animals ($P < 0.05$; Fig. 3E). Similarly, a significant main effect of genotype was noted on mitochondrial ROS emission ($P < 0.05$; Fig. 3E) under state 4 respiration conditions, and a significant interaction between genotype and the training response was observed. Whereas ROS emission tended to decline with training in WT animals, a significant 1.8-fold difference in ROS emission was noted between trained KO and WT animals ($P < 0.05$; Fig. 3F).

Endurance training results in improved exercise performance and attenuated mitochondrial Parkin localization following acute exercise. Following the 6 weeks of voluntary wheel training, we assessed the adaptive response of the muscle to an acute bout of exercise. In untrained WT animals, we found a 2-fold increase in Parkin localization to the mitochondria immediately following acute exercise ($P < 0.05$; Fig. 4A). In trained animals, organelle Parkin localization was already high under resting, control condition, and did not increase additionally with an acute bout of exercise ($P < 0.05$; Fig. 4A). Untrained WT and Parkin KO animals did not differ in their endurance performance when subjected to a bout of acute exercise (Fig. 4B). However, with training, both genotypes displayed ~1.8-fold increases in running distances when compared to their untrained counterparts ($P < 0.05$; Fig. 4B). Resting blood lactate levels were at ~2 mM, and significantly rose to ~7-11 mM immediately after acute exercise ($P < 0.05$; Fig. 4C). There was no genotype effect on blood lactate levels after exercise, and a trend was observed for reduced lactate concentrations following training.

Mitophagy flux is induced following exercise, but this signaling is attenuated in the absence of Parkin, and with training. To determine a role for Parkin in mediating training-induced changes in exercise-induced mitophagy flux, mice were subjected to 6 weeks of voluntary wheel training, followed by a bout of acute exercise. Autophagy protein localization was quantified on isolated mitochondria from the hindlimb muscles of mice for each condition. Immunoblots were separated by genotypes due to the number of conditions. We normalized each experimental condition to an untrained WT sample, from the same data set, to determine any differences between genotypes (Fig. 5A, 5B, 6A and 6B). Following this, we calculated autophagy flux based on the difference between colchicine- and vehicle-treated animals. When untrained and trained animals were compared, no differences in LC3II and p62 flux were detected. In WT mice only, a main effect of acute exercise on LC3II and p62 flux was observed between untrained and trained groups ($P < 0.05$; Fig. 5C and Fig. 6C). During acute exercise, a robust 2.4- and 2-fold increase in mitochondrial LC3II and p62 flux, respectively, was measured in untrained WT animals ($P < 0.05$; Fig. 5C). This response was attenuated with voluntary wheel training.

To directly determine if Parkin was required for mediating these training-induced adaptations, we then compared mitophagy flux between WT and KO animals. In untrained animals, basal LC3II and p62 flux did not differ between genotypes (Fig. 5A–C and Fig. 6A–C). With an acute bout of exercise, LC3II and p62 flux did not increase in the absence of Parkin. Similarly, LC3II and p62 flux was not altered in KO animals with 6 weeks of voluntary wheel training, or with a subsequent bout of endurance exercise.

To further analyze the adaptive potential of trained muscle, we calculated the fold change of mitophagy flux as a ratio of acute exercise-induced values over basal values. The analysis revealed a significant interaction of genotype and training on the fold change in LC3II flux ($P <$

0.05; Fig. 5D). Untrained WT animals displayed a 2.4-fold acute exercise-induced increase in LC3II flux, and this response was attenuated by 45% with training (Fig. 5D). As noted above, LC3II flux did not change with acute exercise in untrained and trained KO animals. In contrast to LC3II, a main effect of genotype was found when the fold change for p62 flux was calculated ($P < 0.05$; Fig. 6D). An increase in p62 flux was observed following a bout of endurance exercise in untrained WT animals. Following 6 weeks of voluntary wheel running, this response was attenuated by 43% (Fig. 6D). In the absence of Parkin, p62 flux remain depressed with acute exercise, and by training (Fig. 6D).

DISCUSSION

Endurance exercise training is accompanied by an adaptive increase in muscle oxidative capacity. To produce this beneficial phenotype, successive bouts of acute exercise over 6 to 8 weeks are required to elicit gradual, 50 to 100% elevations in mitochondrial protein content and enzyme activities (23). Prior to attaining an elevated mitochondrial content, a temporal sequence of transcriptional, translational and post-translational events must occur. However the precise mechanisms leading to this adaptive response are not fully established (11). Parkin is an E3 ubiquitin ligase that is known to be involved in the clearance of defective mitochondria for lysosomal degradation (46). However, recent work has also indicated a possible role for Parkin in mitochondrial biogenesis. For example, in vitro overexpression of Parkin can associate with the regulatory protein TFAM, and enhance TFAM-mediated mtDNA transcription (36, 53). Furthermore, Parkin can directly target PARIS, a transcriptional repressor of PGC-1α, to the proteasome for degradation (60, 62), thereby promoting PGC-1α action on organelle biogenesis. Whether Parkin has a role in determining muscle function and adaptation to exercise training remains currently undetermined.

To investigate this, we examined the effect of voluntary wheel running for 6 weeks in WT and Parkin KO mice. In WT animals, we found that training resulted in several expected beneficial consequences, such as improved running endurance performance, increases in markers of mitochondrial biogenesis and modest cardiac hypertrophy. Interestingly, a robust increase in Parkin expression was also measured in WT animals following 6 weeks of training. We hypothesized that this increase in Parkin would enhance PARIS degradation and thereby promote PGC-1α expression (60). As expected, we observed a significant increase in PGC-1α protein, accompanied by reduced PARIS expression following training in WT animals. These changes

likely contributed significantly to the training-induced increases in mitochondrial content and composition at the organelle level, observed as a result of training.

Our research was directed to evaluate the influence of Parkin on the regulation of muscle mitochondrial content based, in part, on recent work suggesting that Parkin can mediate both organelle biogenesis (38, 62) and degradation (46). Research in neuroblastoma cells and tissues has indicated that a deficiency in Parkin can enhance the repressive behaviour of PARIS on PGC-1α transcription (60). This could lead to a progressive impairment of mitochondrial biogenesis in a Parkin-dependent manner. However, our findings in skeletal muscle indicate that KO animals did not display a difference in mitochondrial content when compared to WT littermates. Moreover, PARIS and PGC-1α expression in muscle did not vary between genotypes. Thus, a role for Parkin in maintaining mitochondrial content via this mechanism seems unlikely, at least in muscle. Alternatively, Parkin is mainly implicated in organelle degradation as a ubiquitin ligase accountable for the removal of defective mitochondria. Thus, the absence of Parkin could lower the rate of mitophagy and increase the accumulation of dysfunctional organelles (19, 73). Consistent with this, we found that KO mice exhibited reduced glutamate-ADP-stimulated state mitochondrial respiration, a result that was consistent with previous studies (48). Thus, in contrast to the lack of change in mitochondrial content, our data provide evidence that the absence of Parkin can evoke mitochondrial dysfunction, as we have previously shown (66). This is also consistent with a previously documented role for Parkin in the elimination of mitochondria with deleterious mtDNA mutations (63). This, further suggests that Parkin is useful for the maintenance of normal, healthy mitochondrial pool in muscle.

We next sought to ascertain the role of Parkin in mediating exercise training-induced mitochondrial biogenesis in muscle. Our results clearly indicate that the absence of Parkin does

not impede the effect of exercise on mitochondrial content, as evident from increases in COX enzyme activity, as well as COXI subunit protein expression, even in KO animals. Surprisingly, these effects occurred in the absence of any induction of PGC-1α in trained KO animals, suggesting the presence of alternative signaling mechanisms in the absence of Parkin. This lack of PGC-1α induction with training was not likely accounted for by an increase in PARIS-mediated PGC-1α transcriptional repression, since training served to reduce PARIS expression. Our data illustrate that training can either reduce the synthesis of PARIS, or enhance its proteasomal degradation, even in the absence of Parkin-directed ubiquitination.

Organelle biogenesis functions in concert with degradation to maintain mitochondrial content. The molecular events that are involved in mitochondrial degradation with either acute or chronic exercise remain poorly defined. It is hypothesized that acute exercise induces mitophagy as a cellular strategy of purging superfluous mitochondria (68). A general challenge of studying autophagy is accurately measuring "flux", an outcome of autophagosomal formation and degradation. In our study, we utilized microtubule destabilization drug colchicine, which prevents autophagosome-lysosome fusion (28). We have previously provided evidence that mitophagy flux is enhanced following a single bout of endurance exercise (66), a finding that was replicated in this study. We detected significant mitochondrial Parkin localization immediately following acute exercise in WT animals, accompanied by an exercise-induced increase in the autophagosomal marker LC3II on isolated mitochondria, an effect that was abolished in the absence of Parkin. Thus, these results support a role for Parkin in mediating mitophagy during acute exercise.

Following 6 weeks of voluntary wheel training, Parkin localization to mitochondria was significantly enhanced, in concurrence with the observed increase in Parkin expression in trained muscle. However, we did not observe any downstream consequences of this translocation, such as

an increase in basal mitophagic LC3II or p62 flux in trained WT animals. Instead, we speculate that this heightened expression and localization of Parkin to mitochondria may serve to "prime" mitophagy, and increase the cellular potential for mitochondrial turnover in response to future bouts of exercise. To examine this possibility, a subgroup of trained animals was treated to an additional bout of exercise to determine the functionality of this adaptation. Our results indicate that trained animals respond to acute exercise with an attenuated mitophagy flux, compare to untrained animals. This attenuation is likely a result of reduced exercise stress signaling toward kinases that normally initiate mitophagy, in the presence of a training-induced enhancement of mitochondrial content and function (1, 45). This would include reduced activation of AMPK, p38 and ROS signaling (42, 43), accompanied by greater endurance performance and a trend for reduced lactate production in muscle with a higher oxidative capacity.

To determine if Parkin is involved in mediating these beneficial adaptations, Parkin KO animals were also subjected to 6 weeks of endurance training. As with WT animals, endurance training had no impact on basal mitophagy flux in the absence of Parkin. However, unlike WT animals, the attenuation of acute exercise-induced mitophagy flux was not observed in KO animals following training, indicating that Parkin is required to facilitate mitochondrial turnover as a result of exercise, and to confer mitophagy adaptations to endurance training.

Collectively, our study reveals several aspects of Parkin function in muscle with endurance exercise. First, Parkin is required for the maintenance of mitochondrial function as observed in KO animals that display both reduced mitochondrial respiration and enhanced ROS emission. Second, we found that KO animals do not exhibit reduced basal mitophagy flux, and this indicates that a compensatory mechanism possibly via the Nix pathway, or via an alternative ubiquitin ligase, must exist to maintain basal mitophagy flux. Additionally, acute exercise-induced mitophagy flux

did not increase in KO animals, implicating Parkin's requirement in mitochondrial turnover with exercise. This lack of response to exercise (and possibly other cellular stress) in KO animals likely contributes to the accumulation of defective organelles, as documented here, in the absence of Parkin. Finally, mitochondrial content was enhanced following training in KO mice to the same degree as in WT animals, but unlike WT animals this adaptation occurred in a PGC-1α-independent manner. This suggests that the absence of Parkin induces alternative signaling pathways that govern mitochondrial biogenesis in response to exercise. Indeed, training did not improve this mitochondrial dysfunction observed in the absence of Parkin, and this could explain why an attenuation in mitophagy by training was not observed, compared to WT animals.

REFERENCES

1. **Adhihetty PJ**, **Uguccioni G**, **Leick L**, **Hidalgo J**, **Pilegaard H**, **Hood DA**. The role of PGC-1 on mitochondrial function and apoptotic susceptibility in muscle. *AJP Cell Physiol* 297: C217–C225, 2009.
2. **Bengtsson J**, **Gustafsson T**, **Widegren U**, **Jansson E**, **Sundberg C**. Mitochondrial transcription factor A and respiratory complex IV increase in response to exercise training in humans. *Pflügers Arch* 443: 61–66, 2001.
3. **Bernardini JP**, **Lazarou M**, **Dewson G**. Parkin and mitophagy in cancer. *Oncogene* 36: 1315–1327, 2017.
4. **Bjørkøy G**, **Lamark T**, **Brech A**, **Outzen H**, **Perander M**, **Øvervatn A**, **Stenmark H**, **Johansen T**. p62/SQSTM1 forms protein aggregates degraded by autophagy and has a protective effect on huntingtin-induced cell death. *J Cell Biol* 171: 603–614, 2005.
5. **Carter HN**, **Chen CCW**, **Hood DA**. Mitochondria, Muscle Health, and Exercise with Advancing Age. *Physiology* 30: 208–223, 2015.
6. **Cogswell AM**, **Stevens RJ**, **Hood DA**. Properties of skeletal muscle mitochondria isolated from subsarcolemmal and intermyofibrillar regions. *Am J Physiol* 264: C383-9, 1993.
7. **Constable SH**, **Favier RJ**, **McLane JA**, **Fell RD**, **Chen M**, **Holloszy JO**. Energy metabolism in contracting rat skeletal muscle: adaptation to exercise training. *Am J Physiol* 253: C316-22, 1987.
8. **COOPERSTEIN SJ**, **LAZAROW A**. A microspectrophotometric method for the determination of cytochrome oxidase. *J Biol Chem* 189: 665–70, 1951.
9. **Davies KJA**, **Packer L**, **Brooks GA**. Biochemical adaptation of mitochondria, muscle, and whole-animal respiration to endurance training. *Arch Biochem Biophys* 209: 539–554,

1981.

10. **Dudley GA**, **Tullson PC**, **Terjung RL**. Influence of mitochondrial content on the sensitivity of respiratory control. *J Biol Chem* 262: 9109–14, 1987.

11. **Egan B**, **Zierath JR**. Exercise Metabolism and the Molecular Regulation of Skeletal Muscle Adaptation. *Cell Metab* 17: 162–184, 2013.

12. **Fritzen AM**, **Madsen AB**, **Kleinert M**, **Treebak JT**, **Lundsgaard A-M**, **Jensen TE**, **Richter EA**, **Wojtaszewski J**, **Kiens B**, **Frøsig C**. Regulation of autophagy in human skeletal muscle: effects of exercise, exercise training and insulin stimulation. *J Physiol* 594: 745–761, 2016.

13. **Geisler S**, **Holmström KM**, **Skujat D**, **Fiesel FC**, **Rothfuss OC**, **Kahle PJ**, **Springer W**. PINK1/Parkin-mediated mitophagy is dependent on VDAC1 and p62/SQSTM1. *Nat Cell Biol* 12: 119–131, 2010.

14. **Gleyzer N**, **Vercauteren K**, **Scarpulla RC**. Control of Mitochondrial Transcription Specificity Factors (TFB1M and TFB2M) by Nuclear Respiratory Factors (NRF-1 and NRF-2) and PGC-1 Family Coactivators. *Mol Cell Biol* 25: 1354–1366, 2005.

15. **Goldberg MS**, **Fleming SM**, **Palacino JJ**, **Cepeda C**, **Lam HA**, **Bhatnagar A**, **Meloni EG**, **Wu N**, **Ackerson LC**, **Klapstein GJ**, **Gajendiran M**, **Roth BL**, **Chesselet M-FM-F**, **Maidment NT**, **Levine MS**, **Shen J**. Parkin-deficient mice exhibit nigrostriatal deficits but not loss of dopaminergic neurons. *J Biol Chem* 278: 43628–35, 2003.

16. **Gollnick PD**, **Armstrong RB**, **Saltin B**, **Saubert CW**, **Sembrowich WL**, **Shepherd RE**. Effect of training on enzyme activity and fiber composition of human skeletal muscle. *J Appl Physiol* 34: 107–11, 1973.

17. **Gong G**, **Song M**, **Csordas G**, **Kelly DP**, **Matkovich SJ**, **Dorn GW**. Parkin-mediated

mitophagy directs perinatal cardiac metabolic maturation in mice. *Science (80-)* 350: aad2459-aad2459, 2015.

18. **Gordon JW**, **Rungi AA**, **Inagaki H**, **Hood DA**. Effects of contractile activity on mitochondrial transcription factor A expression in skeletal muscle. *J Appl Physiol* 90: 389–96, 2001.

19. **Greene JC**, **Whitworth AJ**, **Kuo I**, **Andrews LA**, **Feany MB**, **Pallanck LJ**. Mitochondrial pathology and apoptotic muscle degeneration in Drosophila parkin mutants. *Proc Natl Acad Sci U S A* 100: 4078–83, 2003.

20. **Grumati P**, **Coletto L**, **Schiavinato A**, **Castagnaro S**, **Bertaggia E**, **Sandri M**, **Bonaldo P**. Physical exercise stimulates autophagy in normal skeletal muscles but is detrimental for collagen VI-deficient muscles Taylor & Francis.

21. **He C**, **Bassik MC**, **Moresi V**, **Sun K**, **Wei Y**, **Zou Z**, **An Z**, **Loh J**, **Fisher J**, **Sun Q**, **Korsmeyer S**, **Packer M**, **May HI**, **Hill JA**, **Virgin HW**, **Gilpin C**, **Xiao G**, **Bassel-Duby R**, **Scherer PE**, **Levine B**. Exercise-induced BCL2-regulated autophagy is required for muscle glucose homeostasis. *Nature* 481: 511–5, 2012.

22. **Holloszy JO**. Biochemical adaptations in muscle. Effects of exercise on mitochondrial oxygen uptake and respiratory enzyme activity in skeletal muscle. *J Biol Chem* 242: 2278–82, 1967.

23. **Hood DA**. Invited Review: contractile activity-induced mitochondrial biogenesis in skeletal muscle. *J Appl Physiol* 90: 1137–57, 2001.

24. **Hood DA**, **Pette D**. Chronic long-term electrostimulation creates a unique metabolic enzyme profile in rabbit fast-twitch muscle. *FEBS Lett* 247: 471–4, 1989.

25. **Hood DA**, **Zak R**, **Pette D**. Chronic stimulation of rat skeletal muscle induces coordinate

increases in mitochondrial and nuclear mRNAs of cytochrome-c-oxidase subunits. *Eur J Biochem* 179: 275–80, 1989.

26. **Hoshino A**, **Ariyoshi M**, **Okawa Y**, **Kaimoto S**, **Uchihashi M**, **Fukai K**, **Iwai-Kanai E**, **Ikeda K**, **Ueyama T**, **Ogata T**, **Matoba S**. Inhibition of p53 preserves Parkin-mediated mitophagy and pancreatic β-cell function in diabetes. *Proc Natl Acad Sci U S A* 111: 3116–21, 2014.

27. **Jin SM**, **Lazarou M**, **Wang C**, **Kane LA**, **Narendra DP**, **Youle RJ**. Mitochondrial membrane potential regulates PINK1 import and proteolytic destabilization by PARL. *J Cell Biol* 191: 933–42, 2010.

28. **Ju J-S**, **Varadhachary AS**, **Miller SE**, **Weihl CC**. Quantitation of "autophagic flux" in mature skeletal muscle. *Autophagy* 6: 929–935, 2010.

29. **Ju J**, **Jeon S**, **Park J**, **Lee J**, **Lee S**, **Cho K**, **Jeong J**. Autophagy plays a role in skeletal muscle mitochondrial biogenesis in an endurance exercise-trained condition. *J Physiol Sci* 66: 417–430, 2016.

30. **Kane LA**, **Lazarou M**, **Fogel AI**, **Li Y**, **Yamano K**, **Sarraf SA**, **Banerjee S**, **Youle RJ**. PINK1 phosphorylates ubiquitin to activate Parkin E3 ubiquitin ligase activity. *J Cell Biol* 205: 143–53, 2014.

31. **Kazlauskaite A**, **Kondapalli C**, **Gourlay R**, **Campbell DG**, **Ritorto MS**, **Hofmann K**, **Alessi DR**, **Knebel A**, **Trost M**, **Muqit MMK**. Parkin is activated by PINK1-dependent phosphorylation of ubiquitin at Ser 65. *Biochem J* 460: 127–139, 2014.

32. **Kim YA**, **Kim YS**, **Oh SL**, **Kim H-J**, **Song W**. Autophagic response to exercise training in skeletal muscle with age. *J Physiol Biochem* 69: 697–705, 2013.

33. **Kim Y**, **Park J**, **Kim S**, **Song S**, **Kwon S-K**, **Lee S-H**, **Kitada T**, **Kim J-M**, **Chung J**.

PINK1 controls mitochondrial localization of Parkin through direct phosphorylation. *Biochem Biophys Res Commun* 377: 975–980, 2008.

34. **Komatsu M**, **Waguri S**, **Koike M**, **Sou Y**, **Ueno T**, **Hara T**, **Mizushima N**, **Iwata J**, **Ezaki J**, **Murata S**, **Hamazaki J**, **Nishito Y**, **Iemura S**, **Natsume T**, **Yanagawa T**, **Uwayama J**, **Warabi E**, **Yoshida H**, **Ishii T**, **Kobayashi A**, **Yamamoto M**, **Yue Z**, **Uchiyama Y**, **Kominami E**, **Tanaka K**. Homeostatic Levels of p62 Control Cytoplasmic Inclusion Body Formation in Autophagy-Deficient Mice. *Cell* 131: 1149–1163, 2007.

35. **Koyano F**, **Okatsu K**, **Kosako H**, **Tamura Y**, **Go E**, **Kimura M**, **Kimura Y**, **Tsuchiya H**, **Yoshihara H**, **Hirokawa T**, **Endo T**, **Fon EA**, **Trempe J-F**, **Saeki Y**, **Tanaka K**, **Matsuda N**. Ubiquitin is phosphorylated by PINK1 to activate parkin. *Nature* 510: 162–6, 2014.

36. **Kuroda Y**, **Mitsui T**, **Kunishige M**, **Shono M**, **Akaike M**, **Azuma H**, **Matsumoto T**. Parkin enhances mitochondrial biogenesis in proliferating cells. *Hum Mol Genet* 15: 883–895, 2006.

37. **Larsson NG**, **Barsh GS**, **Clayton DA**. Structure and chromosomal localization of the mouse mitochondrial transcription factor A gene (Tfam). *Mamm Genome* 8: 139–40, 1997.

38. **Lee Y**, **Stevens DA**, **Kang S-U**, **Jiang H**, **Lee Y-I**, **Ko HS**, **Scarffe LA**, **Umanah GE**, **Kang H**, **Ham S**, **Kam T-I**, **Allen K**, **Brahmachari S**, **Kim JW**, **Neifert S**, **Yun SP**, **Fiesel FC**, **Springer W**, **Dawson VL**, **Shin J-H**, **Dawson TM**. PINK1 Primes Parkin-Mediated Ubiquitination of PARIS in Dopaminergic Neuronal Survival. *Cell Rep* 18: 918–932, 2017.

39. **Lira VA**, **Okutsu M**, **Zhang M**, **Greene NP**, **Laker RC**, **Breen DS**, **Hoehn KL**, **Yan Z**. Autophagy is required for exercise training-induced skeletal muscle adaptation and improvement of physical performance. *FASEB J* 27: 4184–93, 2013.

40. **j**Acute endurance exercise increases the nuclear abundance of PGC-1 in trained human skeletal muscle. *AJP Regul Integr Comp Physiol* 298: R912–R917, 2010.

41. **Little JP**, **Safdar A**, **Wilkin GP**, **Tarnopolsky MA**, **Gibala MJ**. A practical model of low-volume high-intensity interval training induces mitochondrial biogenesis in human skeletal muscle: potential mechanisms. *J Physiol* 588: 1011–1022, 2010.

42. **Ljubicic V**, **Hood DA**. Kinase-specific responsiveness to incremental contractile activity in skeletal muscle with low and high mitochondrial content. *Am J Physiol Endocrinol Metab* 295: E195-204, 2008.

43. **Ljubicic V**, **Hood DA**. Specific attenuation of protein kinase phosphorylation in muscle with a high mitochondrial content. *Am J Physiol Endocrinol Metab* 297: E749-58, 2009.

44. **Matsuda N**, **Sato S**, **Shiba K**, **Okatsu K**, **Saisho K**, **Gautier CA**, **Sou Y-S**, **Saiki S**, **Kawajiri S**, **Sato F**, **Kimura M**, **Komatsu M**, **Hattori N**, **Tanaka K**. PINK1 stabilized by mitochondrial depolarization recruits Parkin to damaged mitochondria and activates latent Parkin for mitophagy. *J Cell Biol* 189: 211–21, 2010.

45. **Menzies KJ**, **Singh K**, **Saleem A**, **Hood DA**. Sirtuin 1-mediated effects of exercise and resveratrol on mitochondrial biogenesis. *J Biol Chem* 288: 6968–79, 2013.

46. **Narendra D**, **Tanaka A**, **Suen D-F**, **Youle RJ**. Parkin is recruited selectively to impaired mitochondria and promotes their autophagy. *J Cell Biol* 183: 795–803, 2008.

47. **Narendra DP**, **Jin SM**, **Tanaka A**, **Suen D-F**, **Gautier CA**, **Shen J**, **Cookson MR**, **Youle RJ**. PINK1 is selectively stabilized on impaired mitochondria to activate Parkin. *PLoS Biol* 8: e1000298, 2010.

48. **Palacino JJ**, **Sagi D**, **Goldberg MS**, **Krauss S**, **Motz C**, **Wacker M**, **Klose J**, **Shen J**. Mitochondrial Dysfunction and Oxidative Damage in *parkin* -deficient Mice. *J Biol Chem*

279: 18614–18622, 2004.

49. **Palikaras K**, **Lionaki E**, **Tavernarakis N**. Coordination of mitophagy and mitochondrial biogenesis during ageing in C. elegans. *Nature* 521: 525–528, 2015.

50. **Pankiv S**, **Clausen TH**, **Lamark T**, **Brech A**, **Bruun J-A**, **Outzen H**, **Øvervatn A**, **Bjørkøy G**, **Johansen T**. p62/SQSTM1 Binds Directly to Atg8/LC3 to Facilitate Degradation of Ubiquitinated Protein Aggregates by Autophagy. *J Biol Chem* 282: 24131–24145, 2007.

51. **Pickrell AM**, **Youle RJ**. The roles of PINK1, parkin, and mitochondrial fidelity in Parkinson's disease. *Neuron* 85: 257–73, 2015.

52. **Quinlan CL**, **Perevoshchikova I V.**, **Hey-Mogensen M**, **Orr AL**, **Brand MD**. Sites of reactive oxygen species generation by mitochondria oxidizing different substrates. *Redox Biol* 1: 304–312, 2013.

53. **Rothfuss O**, **Fischer H**, **Hasegawa T**, **Maisel M**, **Leitner P**, **Miesel F**, **Sharma M**, **Bornemann A**, **Berg D**, **Gasser T**, **Patenge N**. Parkin protects mitochondrial genome integrity and supports mitochondrial DNA repair. *Hum Mol Genet* 18: 3832–3850, 2009.

54. **Rubinsztein DC**, **Mariño G**, **Kroemer G**. Autophagy and aging. *Cell* 146: 682–95, 2011.

55. **Safdar A**, **Little JP**, **Stokl AJ**, **Hettinga BP**, **Akhtar M**, **Tarnopolsky MA**. Exercise increases mitochondrial PGC-1alpha content and promotes nuclear-mitochondrial cross-talk to coordinate mitochondrial biogenesis. *J Biol Chem* 286: 10605–17, 2011.

56. **Saleem A**, **Adhihetty PJ**, **Hood DA**. Role of p53 in mitochondrial biogenesis and apoptosis in skeletal muscle. *Physiol Genomics* 37: 58–66, 2009.

57. **Saleem A**, **Iqbal S**, **Zhang Y**, **Hood DA**. Effect of p53 on mitochondrial morphology, import, and assembly in skeletal muscle. *Am J Physiol - Cell Physiol* 308, 2015.

58. **Scherz-Shouval R**, **Shvets E**, **Fass E**, **Shorer H**, **Gil L**, **Elazar Z**. Reactive oxygen species are essential for autophagy and specifically regulate the activity of Atg4. *EMBO J* 26: 1749–1760, 2007.

59. **Shiba-Fukushima K**, **Imai Y**, **Yoshida S**, **Ishihama Y**, **Kanao T**, **Sato S**, **Hattori N**. PINK1-mediated phosphorylation of the Parkin ubiquitin-like domain primes mitochondrial translocation of Parkin and regulates mitophagy. *Sci Rep* 2: 1002, 2012.

60. **Shin J-H**, **Ko HS**, **Kang H**, **Lee Y**, **Lee Y-I**, **Pletinkova O**, **Troconso JC**, **Dawson VL**, **Dawson TM**. PARIS (ZNF746) repression of PGC-1α contributes to neurodegeneration in Parkinson's disease. *Cell* 144: 689–702, 2011.

61. **Soleimanpour SA**, **Gupta A**, **Bakay M**, **Ferrari AM**, **Groff DN**, **Fadista J**, **Spruce LA**, **Kushner JA**, **Groop L**, **Seeholzer SH**, **Kaufman BA**, **Hakonarson H**, **Stoffers DA**. The diabetes susceptibility gene Clec16a regulates mitophagy. *Cell* 157: 1577–90, 2014.

62. **Stevens DA**, **Lee Y**, **Kang HC**, **Lee BD**, **Lee Y-I**, **Bower A**, **Jiang H**, **Kang S-U**, **Andrabi SA**, **Dawson VL**, **Shin J-H**, **Dawson TM**. Parkin loss leads to PARIS-dependent declines in mitochondrial mass and respiration. *Proc Natl Acad Sci U S A* 112: 11696–701, 2015.

63. **Suen D-F**, **Narendra DP**, **Tanaka A**, **Manfredi G**, **Youle RJ**. Parkin overexpression selects against a deleterious mtDNA mutation in heteroplasmic cybrid cells. *Proc Natl Acad Sci U S A* 107: 11835–40, 2010.

64. **Takahashi M**, **Hood DA**. Chronic stimulation-induced changes in mitochondria and performance in rat skeletal muscle. *J Appl Physiol* 74: 934–41, 1993.

65. **Uguccioni G**, **Hood DA**. The importance of PGC-1 in contractile activity-induced mitochondrial adaptations. *AJP Endocrinol Metab* 300: E361–E371, 2011.

66. **Vainshtein A**, **Tryon LD**, **Pauly M**, **Hood DA**. Role of PGC-1α during acute exercise-

induced autophagy and mitophagy in skeletal muscle. *Am J Physiol Cell Physiol* 308: C710-9, 2015.

67. **Vásquez-Trincado C**, **García-Carvajal I**, **Pennanen C**, **Parra V**, **Hill JA**, **Rothermel BA**, **Lavandero S**. Mitochondrial dynamics, mitophagy and cardiovascular disease. *J Physiol* 594: 509–525, 2016.

68. **Lo Verso F**, **Carnio S**, **Vainshtein A**, **Sandri M**. Autophagy is not required to sustain exercise and PRKAA1/AMPK activity but is important to prevent mitochondrial damage during physical activity. *Autophagy* 10: 1883–94, 2014.

69. **Villa E**, **Proïcs E**, **Rubio-Patiño C**, **Obba S**, **Zunino B**, **Bossowski JP**, **Rozier RM**, **Chiche J**, **Mondragón L**, **Riley JS**, **Marchetti S**, **Verhoeyen E**, **Tait SWG**, **Ricci J-E**. Parkin-Independent Mitophagy Controls Chemotherapeutic Response in Cancer Cells. *Cell Rep* 20: 2846–2859, 2017.

70. **Vives-Bauza C**, **Zhou C**, **Huang Y**, **Cui M**, **de Vries RLA**, **Kim J**, **May J**, **Tocilescu MA**, **Liu W**, **Ko HS**, **Magrané J**, **Moore DJ**, **Dawson VL**, **Grailhe R**, **Dawson TM**, **Li C**, **Tieu K**, **Przedborski S**. PINK1-dependent recruitment of Parkin to mitochondria in mitophagy. *Proc Natl Acad Sci U S A* 107: 378–83, 2010.

71. **Williams RS**, **Salmons S**, **Newsholme EA**, **Kaufman RE**, **Mellor J**. Regulation of nuclear and mitochondrial gene expression by contractile activity in skeletal muscle. *J Biol Chem* 261: 376–80, 1986.

72. **Woodson JD**, **Chory J**. Coordination of gene expression between organellar and nuclear genomes. *Nat Rev Genet* 9: 383–95, 2008.

73. **Yang Y**, **Gehrke S**, **Imai Y**, **Huang Z**, **Ouyang Y**, **Wang J-W**, **Yang L**, **Beal MF**, **Vogel H**, **Lu B**. Mitochondrial pathology and muscle and dopaminergic neuron degeneration

caused by inactivation of Drosophila Pink1 is rescued by Parkin. *Proc Natl Acad Sci U S A* 103: 10793–8, 2006.

74. **Zorov DB**, **Juhaszova M**, **Sollott SJ**. Mitochondrial reactive oxygen species (ROS) and ROS-induced ROS release. *Physiol Rev* 94: 909–50, 2014.

FIGURE LEGENDS

Fig. 1. Effect of Parkin deficiency and training on muscle mass. (*A)*: Graphical representation of voluntary running distance (kilometers per week) between WT and KO mice ($n = 8$). Wheels were provided in animal cages for a duration of 6 weeks. (*B)*: Total body weight of untrained and trained Parkin KO and WT animals ($n = 8$). (*C)*: Quadriceps muscle mass corrected for total body weight ($n = 8$). (*D)*: Heart mass corrected for total body weight ($n = 8$). Values are means ± SEM. ¶$P < 0.05$, main effect of time. *$P < 0.05$, main effect of training. WT, wild-type; KO, Parkin knock-out; UT, untrained; T, trained.

Fig. 2. Effect of training and Parkin on whole muscle protein markers. (*A)*: Representative Western blot of Parkin expression in untrained and trained skeletal muscle of control wild-type (WT) mice above. A graphical representation is shown below ($n = 5$, *$P < 0.05$, vs UT). (*B)*: Representative immunoblots of COXI and COXIV expression in untrained and trained skeletal muscle of Parkin KO and WT animals. A graphical representation of whole muscle COXI shown below ($n = 4$, *$P < 0.05$, main effect of training; #$P < 0.05$, vs trained WT). (*C)*: Representative Western blots of PGC-1α and PARIS expression in untrained and trained skeletal muscle of Parkin KO and WT animals. (*D)*: A graphical representation of whole muscle PGC-1α ($n = 4$, *$P < 0.05$, vs untrained WT). (*E)*: Quantification of whole muscle PARIS ($n = 6$, *$P < 0.05$, main effect of training; #$P < 0.05$, vs untrained WT). Values are means ± SEM. †$P < 0.05$, interaction effect of training and genotype. α-tubulin was used for muscle loading control. WT, wild-type; KO, Parkin knock-out; UT, untrained; T, trained; COX1, cytochrome c oxidase subunit 1; COX4, cytochrome c oxidase subunit 4; PARIS, Parkin-Interacting Substrate; PGC-1α, peroxisome proliferator gamma coactivator-1α; A.U., arbitrary units.

Fig. 3. Mitochondrial adaptations following 6 weeks of voluntary wheel running. (*A)*: Representative Western blots of COXI, COXIV and TFAM expression on isolated mitochondria from untrained and trained skeletal muscle of Parkin KO and WT animals. (*B)*: Graphical representation of mitochondrial COXI expression (n = 8). (*C)*: Mitochondrial yield of mixed hindlimb muscles of Parkin KO and WT animals (n = 4). (*D)*: Skeletal muscle cytochrome c oxidase (COX) activity following training in quadriceps muscle of Parkin KO and WT animals (n = 5). (*E)*: Mitochondrial state 4 and state 3 respiration rates in KO compared with WT animals (n = 8). (*F*): Mitochondrial ROS emission expressed per natom of oxygen consumed in Parkin KO and WT mice (n = 8; ¶$P < 0.05$, vs state 4 trained WT). Values are means ± SEM. *$P < 0.05$, main effect of training; #$P < 0.05$, main effect of genotype; †$P < 0.05$, interaction effect of genotype and training. Voltage-dependent anion channel (VDAC) was used as a mitochondrial loading control. WT, wild-type; KO, Parkin knock-out; UT, untrained; T, trained; COX1, cytochrome c oxidase subunit 1; COX4, cytochrome c oxidase subunit 4; TFAM, mitochondrial transcription factor A; ROS, reactive oxygen species; A.U., arbitrary units.

Fig. 4. Effect of Parkin and training on exercise performance. (*A*): Representative Western blot of Parkin localization on isolated mitochondria from untrained and trained WT muscle, prior to exercise (Con) and immediately following exercise (Ex). Quantification of mitochondrial Parkin localization is shown below, corrected for loading using mitochondrial voltage-dependent anion channel (VDAC) (n = 6, ¶$P < 0.05$, vs untrained Con). (*B*): Animal endurance performance (i.e. total distance run) of WT and KO animals (n = 8, *$P < 0.05$, main effect of training). (*C*): Blood lactate levels measured prior to (Con), and immediately following exercise (Ex) (n = 8, #$P < 0.05$,

main effect of exercise). Values are means ± SEM. WT, wild-type; KO, Parkin knock-out; UT, untrained; T, trained; A.U., arbitrary units.

Fig. 5. Mitophagic LC3II flux following acute exercise, training, and combined treatments in WT and KO animals. Representative Western blots of mitochondrial LC3II localization of WT (*A*) and Parkin KO (*B*) mice injected with water (Veh) or 0.4 mg/kg colchicine (Col). Quantification of mitochondrial LC3II flux (*C*) is shown (n = 8). Mitophagic LC3II flux was assessed under basal conditions, and immediately following acute exercise, in untrained and trained groups of WT and KO animals. The fold change in LC3II flux (*D*) was calculated with acute exercise-induced values over basal values (n = 8). Values are means ± SEM. ¶$P < 0.05$, vs untrained WT; #$P < 0.05$, main effect of exercise; *P < 0.05, vs all other experimental conditions; †$P < 0.05$, interaction effect of genotype and training. Voltage-dependent anion channel (VDAC) was used as a mitochondrial loading control. WT, wild-type; KO, Parkin knock-out; UT, untrained; T, trained; LC3II, lipidated microtubule-associated protein 1A/1B-light chain 3; A.U., arbitrary units.

Fig. 6. Mitophagic p62 flux following acute exercise, training, and combined treatments in WT and KO animals. Representative Western blots of mitochondrial p62 localization of WT (*A*) and Parkin KO (*B*) mice injected with water (Veh) or 0.4 mg/kg colchicine (Col). Quantification of mitochondrial p62 flux (*C*) is shown (n = 5). Mitophagic p62 flux was assessed under basal conditions, and immediately following acute exercise, in untrained and trained groups of WT and KO animals. The fold change in p62 flux (*D*) was calculated with acute exercise-induced values over basal values (n = 5). Values are means ± SEM. *P < 0.05, a main effect of genotype; #$P <$ 0.05, main effect of exercise. Voltage-dependent anion channel (VDAC) was used as a

mitochondrial loading control. WT, wild-type; KO, Parkin knock-out; UT, untrained; T, trained; p62, sequestosome 1; A.U., arbitrary units.

Figure 1

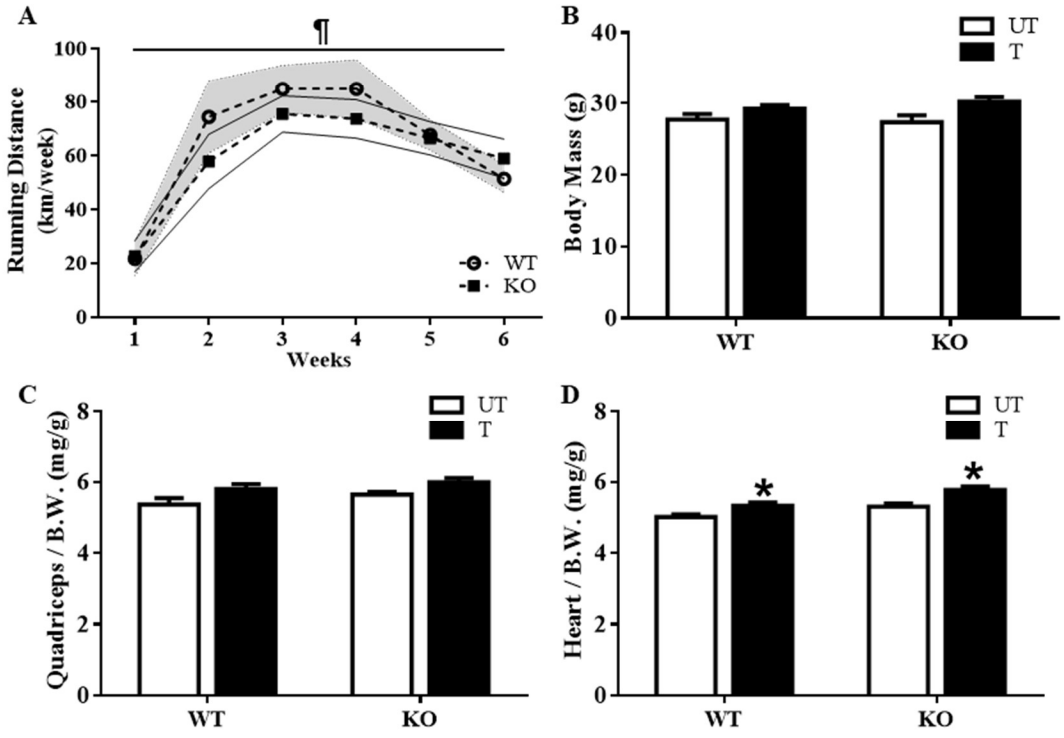
A
¶
Running Distance (km/week)
100
80
60
40
20
0
1
2
3
4
5
6
Weeks
WT
KO
B
Body Mass (g)
40
30
20
10
0
UT
T
WT
KO
C
Quadriceps / B.W. (mg/g)
8
6
4
2
0
UT
T
WT
KO
D
Heart / B.W. (mg/g)
8
6
4
2
0
*
*
UT
T
WT
KO

Figure 2

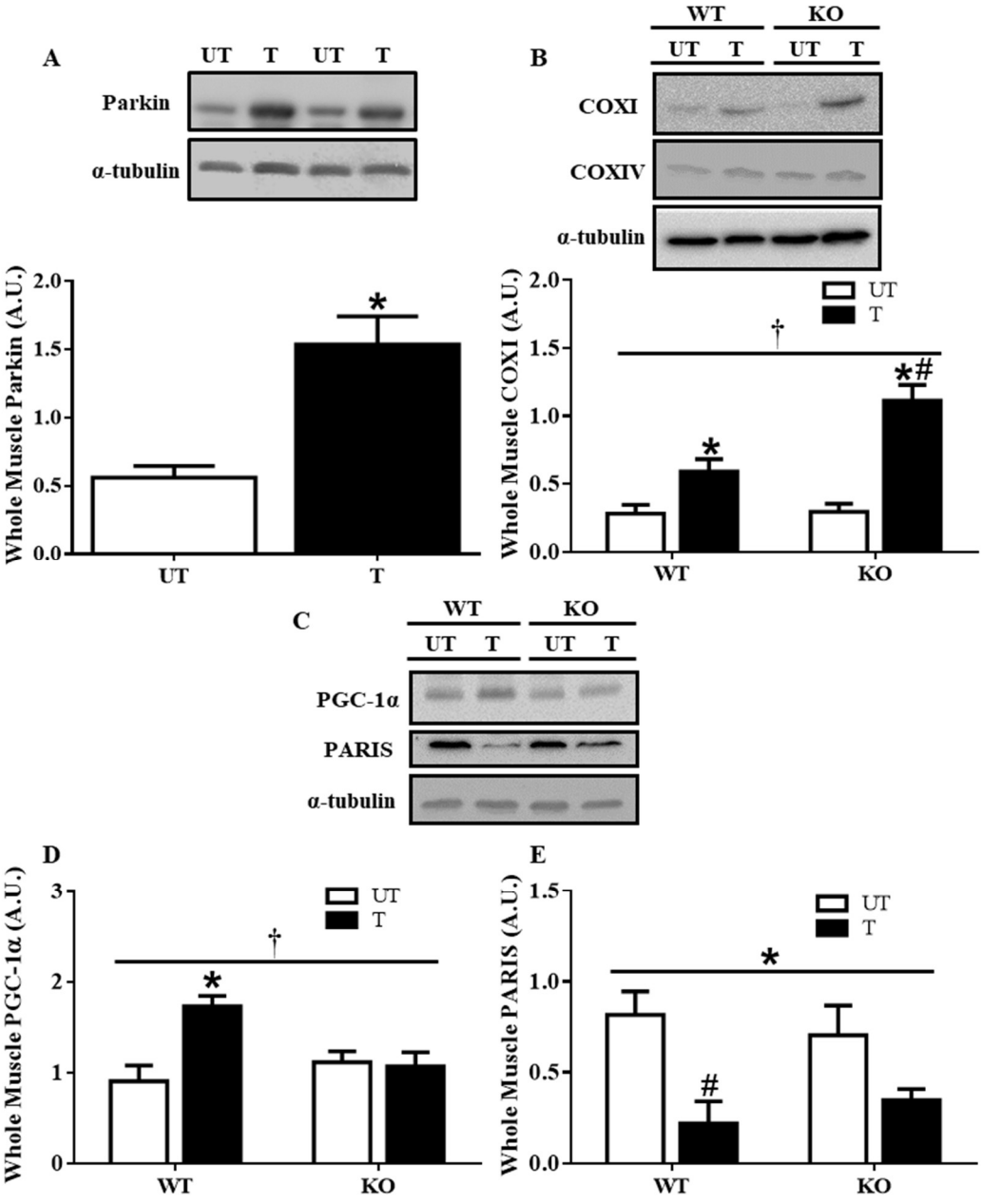
A
UT T UT T
Parkin
α-tubulin
Whole Muscle Parkin (A.U.)
2.0
1.5
1.0
0.5
0.0
*
UT
T
B
WT KO
UT T UT T
COXI
COXIV
α-tubulin
Whole Muscle COXI (A.U.)
UT
T
†
*#
*
WT
KO
C
WT KO
UT T UT T
PGC-1α
PARIS
α-tubulin
D
Whole Muscle PGC-1α (A.U.)
3
2
1
0
UT
T
†
*
WT
KO
E
Whole Muscle PARIS (A.U.)
1.5
1.0
0.5
0.0
UT
T
*
#
WT
KO

Figure 3

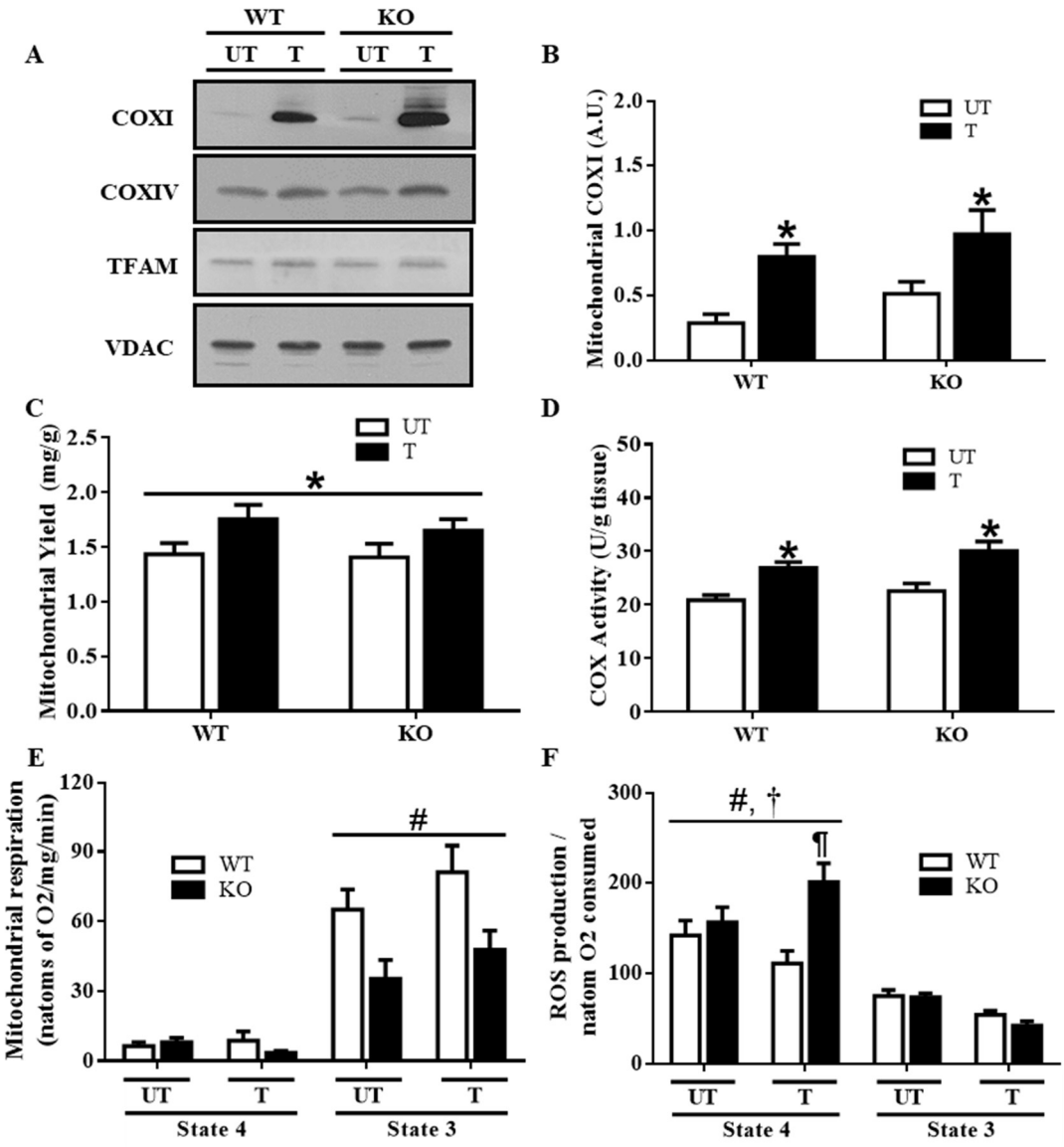
A
WT
KO
UT
T
UT
T
COXI
COXIV
TFAM
VDAC
B
Mitochondrial COXI (A.U.)
2.0
1.5
1.0
0.5
0.0
UT
T
*
*
WT
KO
C
Mitochondrial Yield (mg/g)
2.5
2.0
1.5
1.0
0.5
0.0
UT
T
*
WT
KO
D
COX Activity (U/g tissue)
50
40
30
20
10
0
UT
T
*
*
WT
KO
E
Mitochondrial respiration (natoms of O2/mg/min)
120
90
60
30
0
WT
KO
#
UT
T
UT
T
State 4
State 3
F
ROS production / natom O2 consumed
300
200
100
0
#, †
¶
WT
KO
UT
T
UT
T
State 4
State 3

Figure 4

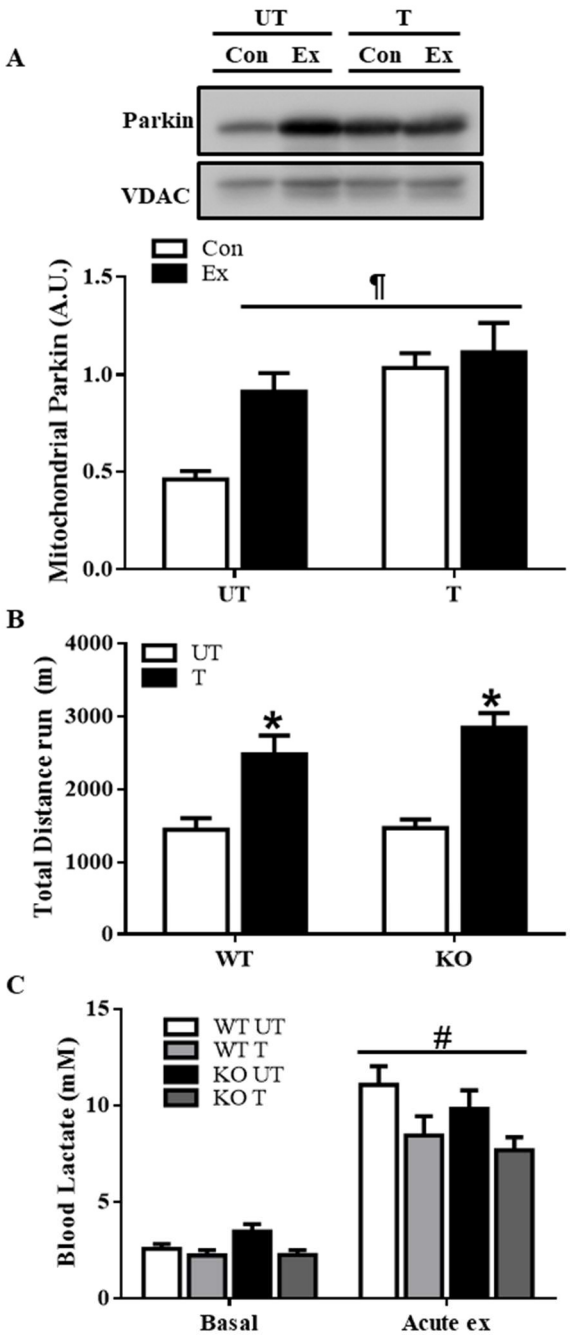
A
UT
T
Con Ex Con Ex
Parkin
VDAC
Con
Ex
Mitochondrial Parkin (A.U.)
1.5
1.0
0.5
0.0
¶
UT
T
B
Total Distance run (m)
4000
3000
2000
1000
0
UT
T
*
*
WT
KO
C
Blood Lactate (mM)
15
10
5
0
WT UT
WT T
KO UT
KO T
#
Basal
Acute ex

Figure 5

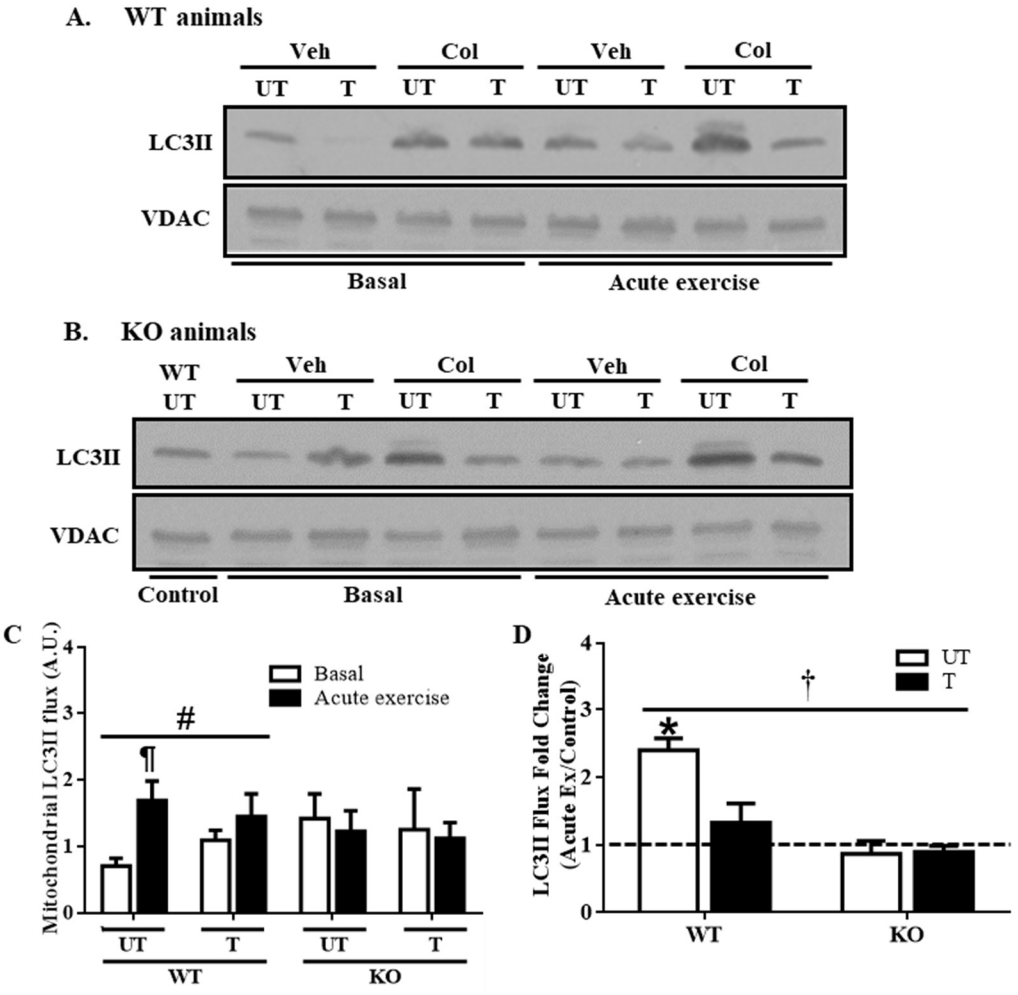
A. WT animals
Veh
Col
Veh
Col
UT
T
UT
T
UT
T
UT
T
LC3II
VDAC
Basal
Acute exercise
B. KO animals
WT
UT
Veh
Col
Veh
Col
UT
T
UT
T
UT
T
UT
T
LC3II
VDAC
Control
Basal
Acute exercise
C
Mitochondrial LC3II flux (A.U.)
Basal
Acute exercise
#
¶
UT
T
UT
T
WT
KO
D
LC3II Flux Fold Change (Acute Ex/Control)
UT
T
†
*
WT
KO

Figure 6

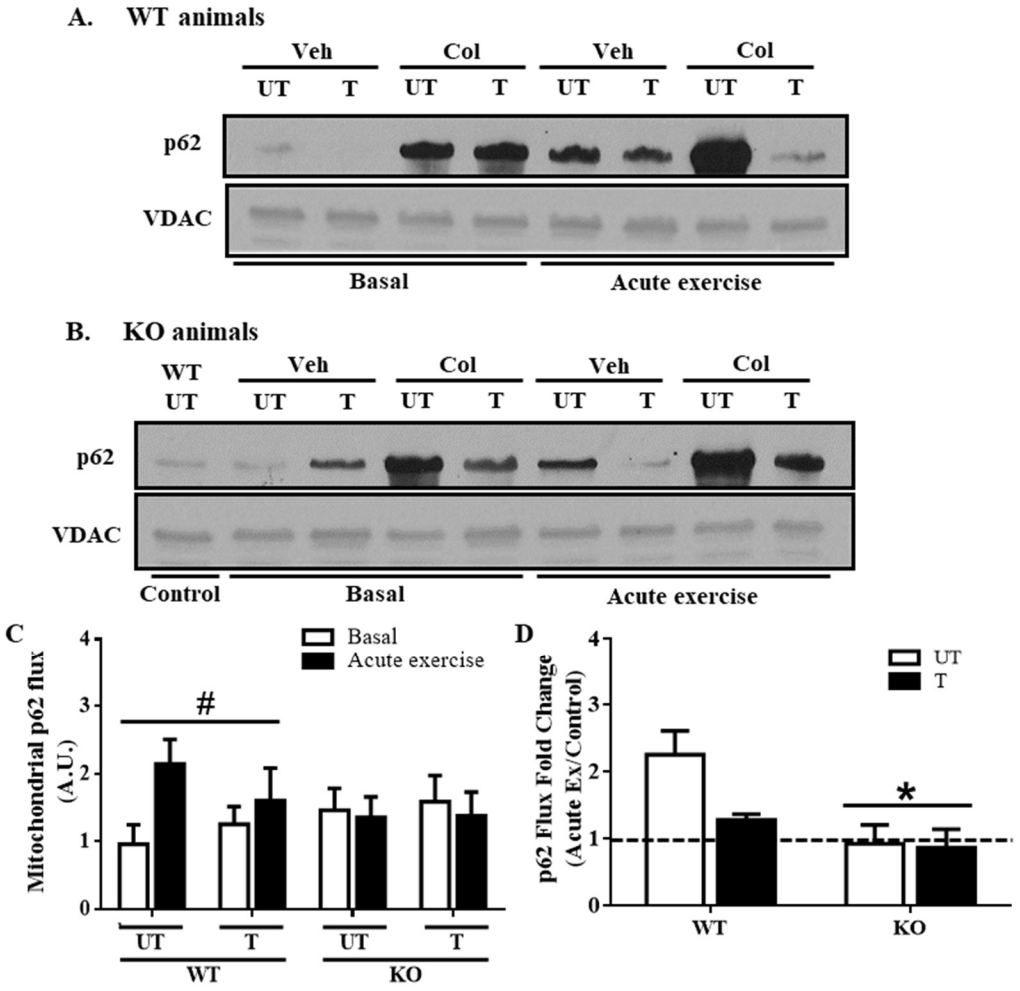
A. WT animals
Veh
Col
Veh
Col
UT
T
UT
T
UT
T
UT
T
p62
VDAC
Basal
Acute exercise
B. KO animals
WT
UT
Veh
Col
Veh
Col
UT
T
UT
T
UT
T
UT
T
p62
VDAC
Control
Basal
Acute exercise
C
Mitochondrial p62 flux (A.U.)
Basal
Acute exercise
#
UT
T
UT
T
WT
KO
D
p62 Flux Fold Change (Acute Ex/Control)
UT
T
*
WT
KO

CHAPTER 6:

SUMMARY AND CONCLUSIONS

Parkin is a ubiquitin ligase well-known for its ability to selectively target damaged mitochondria for degradation (306). Parkin is translocated to mitochondria that can no longer generate a membrane potential across the inner mitochondrial membrane (282). It can regulate the formation of ubiquitin linkages on target proteins found on the outer surface of the organelle (103, 305). This process is required for amplifying the signal that is needed to remove a damaged mitochondrion by autophagy (200, 206, 228). An impairment of this process in neural tissue is thought to contribute to neurodegeneration, a well-studied role for Parkin in Parkinson's Disease (339). As studies emerged on the relationship between mitochondrial perturbations and Parkin, research began to expeditiously investigate the mechanisms by which Parkin can regulate mitochondrial function in other metabolic tissues. The examination of Parkin function in skeletal muscle remains poorly defined, with a handful of studies on lower order organisms (62, 116). Muscle is one of the largest organs in the body, and its importance in human health is exemplified in several pathological conditions, including type II diabetes (190, 207), obesity (360), heart failure (484), as well as in aging (52). Mitochondrial dysfunction is a hallmark feature of many of these metabolic conditions, that depend on mitophagy for cell maintenance. My doctoral work has focused on investigating the function of Parkin in muscle mitochondrial turnover, and its necessity for exercise- and age-induced mitochondrial adaptations.

Objective 1: We first investigated the role of Parkin-mediated mitophagy under basal conditions and during acute exercise. We have previously shown that mitophagy flux is enhanced following an acute bout of endurance exercise (446). To determine if Parkin is required for

exercise-induced mitophagy flux, we utilized a Parkin KO animal model, and pre-treated the animals with colchicine (193) via intraperitoneal injection for 2 days prior to endurance exercise testing. Isolated mitochondria were obtained from the hindlimb muscles of control and exercised animals. We hypothesized that the lack of Parkin would yield an accumulation of dysfunctional mitochondria, and reduce the quality of muscle. We did not detect a significant difference in mitochondrial content between genotypes when assessed by COX activity. However, KO animals displayed a reduction in complex I driven mitochondrial respiration. Furthermore, basal mitophagy flux did not differ between genotypes. During acute exercise, Parkin KO mice performed to a similar degree to that of WT animals. We also demonstrated that Parkin-mediated mitophagy is required during acute exercise, as Parkin KO animals displayed attenuated exercise-induced mitophagy flux. Interestingly, mitochondrial ubiquitination increased in KO animals following acute exercise. This suggests the existence of alternative ubiquitin ligase(s) (99, 482) that may be involved during exercise, but that are unable to compensate for the lack of mitophagic signaling that occurs in the absence of Parkin. To specifically examine the role of Parkin in targeting specific outer mitochondrial surface proteins, we performed a mitochondrial co-immunoprecipitation of mitofusin-2 and its association with ubiquitin. We found that Parkin was required for basal Mfn2 ubiquitination and that acute exercise enhanced the formation of Mfn2-ubiquitin complexes. To elucidate a mechanism for Parkin during exercise-induced mitochondrial biogenesis, we measured the expression of transcriptional regulators PGC-1α and PARIS. It was previously shown that Parkin can regulate biogenesis by targeting PARIS, a transcriptional repressor of PGC-1α, to the proteasome for degradation. Interestingly, the basal expression of PARIS and PGC-1α did not differ between WT and Parkin KO animals. However, during acute exercise we detected a statistical relevant interaction for each of these regulators that varied according to genotype and

exercise. We found that PGC-1α nuclear localization was enhanced immediately following exercise in WT animals, but that this effect was abolished in the absence of Parkin. In contrast, nuclear PARIS abundance increased in the absence of Parkin during acute exercise. This study provided evidence that Parkin is required for maintaining mitochondrial function and exercise-induced mitophagy flux. We also provided mechanistic insight on how Parkin may regulate mitochondrial biogenesis in skeletal muscle.

Objective 2: We next examined the effect of age on Parkin-mediated mitophagy during basal and acute exercise conditions. For this study, we compared mitophagy flux between young (3 months) and aged (minimum 18 months) animals. We first assessed the expression of Parkin with age, and we were surprised to find a robust increase in Parkin expression in aged animals. Sarcopenia is characterized by the progressive age-related loss of muscle mass and function (50). Thus, we hypothesized that the lack of Parkin with age would evoke additional decrements in mitochondrial content and function, as well as reduced muscle mass. We observed significant decreases in muscle mass and mitochondrial content of aged animals, but these changes occurred independently of Parkin. We did not detect any alterations in mitochondrial respiration with age, however, reactive oxygen emission was enhanced in KO animals. In our study, we observed that Parkin residence on the mitochondrion was abolished with age and did not increase with acute exercise. Aged animals ran significantly less than their young counterparts, and this was reflected by their enhanced blood lactate levels. We hypothesized that the lack of Parkin would impair mitophagy in aged muscle. To our surprise, basal mitophagy flux was enhanced in aged animals compared to young, and did not increase further following acute exercise. A similar trend was detected with the association of Mfn2 and ubiquitin with age and exercise. Furthermore, we

observed enhanced nuclear PARIS abundance in aged muscle of WT and Parkin KO animals, while the levels of nuclear PGC-1α were reduced. This study provides an understanding of the molecular underpinnings of age and its influence on exercise-induced mitophagy and organelle biogenesis.

Objective 3: Based on our observations that acute exercise can activate mitophagy, we subsequently explored the requirement of Parkin for exercise-induced mitochondrial adaptations. Specifically, we wanted to determine whether Parkin is involved in mediating the adaptive response of muscle to endurance training. We subjected WT and Parkin KO animals to 6 weeks of voluntary wheel exercise, and a subset of animals were treated to a similar acute exercise paradigm as in objective 1 and 2. We first examined the importance of Parkin on mitochondrial biogenesis following exercise training, and noted an increase in COXI protein and COX activity in animals deficient in Parkin. However, the expression of the main regulator of mitochondrial biogenesis, PGC-1α, in whole muscle was repressed in KO animals following training. Concomitantly, an improvement in mitochondrial function commonly associated with mitochondrial biogenesis was absent in Parkin null animals. As shown in objective 1, we demonstrated that a bout of acute exercise was sufficient to induce mitophagy, and that this activation was dependent on Parkin. Moreover, we observed that the expression and localization of Parkin to mitochondria was enhanced following training. Despite this, Parkin downstream mitophagic signaling of LC3II and p62 flux was not altered with training. This suggested that repeated bouts of exercise can attenuate the activation of Parkin-mediated mitophagy to contribute to the attainment of a greater mitochondrial content. Indeed, WT trained animals that underwent a subsequent bout of acute exercise displayed attenuated mitophagy flux. This adaptive response to training was not observed

in the absence of Parkin. These data suggest that the diminishment of Parkin-mediated mitophagy is necessary to facilitate endurance exercise-induced mitochondrial biogenesis.

Taken together, our data confirm the fundamental role of Parkin as a regulator of mitochondrial biogenesis and degradation. In vivo animal studies were mainly used to address this topic. Specifically, these manuscripts will 1) further our understanding of Parkin-mediated mitophagy during exercise, 2) provide insight into aging-induced regulation of mitochondrial turnover in skeletal muscle, and 3) elucidate the regulatory role of Parkin in maintaining mitochondrial content and function, ultimately achieving energetic homeostasis.

CHAPTER 7:

EXPERIMENTAL LIMITATIONS

Autophagy is a dynamic intracellular mechanism that is involved in the turnover of long-lived organelles and proteins. In many situations it is necessary to measure if an experimental treatment has an inhibitory or stimulatory effect on autophagy. This measurement is termed autophagy flux and is poorly understood in vivo. To examine autophagy flux, one must select an appropriate inhibitor to "block" or prevent autophagosomal degradation. The role of the autophagosome is to transport damaged cellular components to the lysosome for degradation via microtubule filaments. Thus, measuring static changes in autophagy protein markers on an immunoblot is not adequate to indicate whether autophagy flux is altered. To directly measure autophagy flux in vivo, lysosomal degradation must be prevented. Specifically, autophagy flux is the difference between a condition treated with an autophagy blocker and the same condition treated with a vehicle. The utilization of a lysosomal inhibitor, whether bafilomycin A1, chloroquine or microtubule depolarizing agent such as colchicine, must be sufficient to significantly increase basal autophagy markers. For example, the use of an autophagy blocking agent should always increase basal LC3II levels. A major challenge of measuring autophagy flux in vivo is the variability between animals. One should expect that different animals do not always activate autophagy at the same time, or to the same degree. Thus, to improve the statistical rigor of one's findings, experiments should be repeated more than once with each experiment involving more than a few animals.

Another limitation in our studies was the amalgamation of results from both male and female mice. It is important that future work on autophagy be completed on both genders, and that data on each sex be reported separately. In a recent review by Gottlieb et al., sex differences in

autophagy in various tissues have been reported by several laboratories (110). There is little controversy on the fact that gender can influence health and disease. However, research limitations on animals can exist. For example, female mice are occasionally excluded to prevent hormonal-related confounding variables. Male mice can also be excluded when they become aggressive and must be caged separately, and this can increase the operating costs in low-budget laboratories. To combat against gender bias, more research funding agencies are calling on scientists to be mindful of considering both genders in research.

CHAPTER 8:

FUTURE DIRECTIONS

Based on our observations from the three studies summarized in this dissertation, it is evident that Parkin is involved in regulating mitophagy and mitochondrial biogenesis during endurance exercise. However, several questions arise from our studies on Parkin and its function in muscle. These are outlined below:

1. How do exercise and age affect Parkin-mediated mitophagy in the heart?

In our study, we demonstrate that exercise can induce mitophagy in skeletal muscle. However, a role for Parkin in cardiac muscle during exercise remains unknown. Cardiac muscle contains a greater mitochondrial density than skeletal muscle, and this likely indicates a greater propensity for mitophagy activation. Current data suggest that Parkin is not required for basal mitochondrial turnover, but instead functions in a greater capacity during cardiac stress in adult murine hearts (230, 249, 342). Recent findings also illustrate the importance of Parkin-mediated mitophagy during perinatal cardiomyocyte development in mice (108). Indeed, we have some preliminary data to indicate that mitophagy is inducible in the heart during exercise. The role of Parkin on cardiac mitophagy flux during exercise and with aging has never been documented. As such, the enrichment of Parkin on damaged cardiac mitochondria during exercise may be a viable means to treat metabolic defects in heart disease. According to the Government of Canada, heart disease is the second leading cause of death in Canada. The results from this future study could hold therapeutic potential in reducing the risk of cardiovascular disease. For example, upregulation of Parkin following myocardial infarction appears to rescue cardiomyocytes from cell death by enhancing mitophagy (230). Thus, Parkin may play a vital role in cardiac adaptation to stress.

2. Does Parkin impact the rate of PINK1 protein import into mitochondria?

The increased localization of Parkin to mitochondria during exercise could be the result of increased PINK1 activation. Assessing whether PINK1 is stimulated during mitophagy is a challenge. Like mitophagy flux, PINK1 is highly dynamic and can undergo rapid mitochondrial protein import (187, 188, 242, 477). Static PINK1 protein measurements are not sufficient to conclude an impairment or activation of mitophagy. This can be conducted by mitochondrial protein import experiments using a radiolabelled PINK1 precursor protein. The mechanism by which PINK1 mitochondrial import operates under exercise and with age remain unclear. We have previously shown that the mitochondrial protein import pathway is highly adaptable during chronic contractile activity-induced mitochondrial biogenesis. An examination of PINK1 kinetics can provide further mechanistic insight on mitochondrial turnover under the influence of different stimuli: muscle disuse such as denervation, and increased contractility such as exercise.

3. How does the absence of Parkin impair mitophagic signaling in response to exercise?

The role of exercise training and the mechanisms controlling the synthesis of new mitochondria are well-studied (443). However, our understanding of how exercise can promote the removal of damaged and dysfunctional mitochondria remain largely unknown (194, 212, 261). A comprehensive examination of downstream exercise-responsive kinases and their activation between WT and Parkin KO animals would help. To elucidate this, the measurement of autophagy inducers, Ulk1 and TFEB, during acute exercise may provide added evidence of Parkin-mitophagy activation on downstream regulators. In vitro studies have revealed that PINK1/Parkin can recruit autophagy factor Ulk1 to initiate autophagosomal biogenesis on damaged mitochondria (298). Furthermore, it was recently demonstrated that TFEB activation occurs downstream of Parkin

(312). Recent evidence indicates that Atg5 activity is required for Parkin-mediated TFEB nuclear accumulation (312). Atg5 facilitates the formation of the autophagosomal membrane. The effect of Parkin on TFEB subcellular localization could provide evidence of cross-talk between mitophagy activation and lysosomal biogenesis. Our study on aging and mitophagy revealed a possible dysfunction in lysosomes. Thus, the role of TFEB in regulating lysosomal biogenesis during age and exercise remains a potential avenue of future research.

Furthermore, we examined an overall increase of LC3II localization to the mitochondria in KO animals. LC3 is part of the Atg8 family that contains three other mammalian homologues including: GABARAP, GATE-16 and Atg8L. There is very little evidence of these proteins contributing to autophagosomal biogenesis in mammals. Whether these proteins are regulated in a Parkin-dependent manner remains elusive. To further inspect this, we could measure the localization of the Atg8 family proteins on mitochondrial fractions in the presence and absence of Parkin. Alternatively, we can use CRISPR/Cas9 gene editing technology to generate knockouts of each Atg8 subfamily to determine the contribution and necessity for selective mitochondrial degradation. In a recent study, it was shown that autophagy adaptor proteins OPTN and NDP52 are directly recruited to damaged mitochondria (243). To further inspect the process of autophagosomal biogenesis, we can subject WT and Parkin KO mice to an acute bout of exercise, and immunoprecipitate autophagy adaptor proteins from mitochondrial sub-fractions. The precipitates can thereafter be probed for Atg8 family members to directly assess the requirement of Parkin on the recruitment of each Atg8 family member to initiate mitophagy.

In summary, our research has led to a few research questions and directions which can improve our understanding on how mitophagy is regulated in muscle. An impairment in mitophagy can contribute to age-associated declines in muscle mass and function. Exercise is a very potent stimulus to promote mitochondrial turnover. The answers to these questions can help uncover new ways to promote healthy aging.

CHAPTER 9:

REFERENCES

1. **Adhihetty PJ**, **Ljubicic V**, **Hood DA**. Effect of chronic contractile activity on SS and IMF mitochondrial apoptotic susceptibility in skeletal muscle. *Am J Physiol Endocrinol Metab* 292: E748-55, 2007.
2. **Adhihetty PJ**, **Ljubicic V**, **Menzies KJ**, **Hood DA**. Differential susceptibility of subsarcolemmal and intermyofibrillar mitochondria to apoptotic stimuli. *AJP Cell Physiol* 289: C994–C1001, 2005.
3. **Akimoto T**, **Li P**, **Yan Z**. Functional interaction of regulatory factors with the Pgc-1alpha promoter in response to exercise by in vivo imaging. *Am J Physiol Cell Physiol* 295: C288-92, 2008.
4. **Akimoto T**, **Pohnert SC**, **Li P**, **Zhang M**, **Gumbs C**, **Rosenberg PB**, **Williams RS**, **Yan Z**. Exercise Stimulates *Pgc-1α* Transcription in Skeletal Muscle through Activation of the p38 MAPK Pathway. *J Biol Chem* 280: 19587–19593, 2005.
5. **Aldridge JE**, **Horibe T**, **Hoogenraad NJ**. Discovery of Genes Activated by the Mitochondrial Unfolded Protein Response (mtUPR) and Cognate Promoter Elements. *PLoS One* 2: e874, 2007.
6. **Alexander C**, **Votruba M**, **Pesch UEA**, **Thiselton DL**, **Mayer S**, **Moore A**, **Rodriguez M**, **Kellner U**, **Leo-Kottler B**, **Auburger G**, **Bhattacharya SS**, **Wissinger B**. OPA1, encoding a dynamin-related GTPase, is mutated in autosomal dominant optic atrophy linked to chromosome 3q28. *Nat Genet* 26: 211–215, 2000.
7. **Anderson RM**, **Weindruch R**. Metabolic reprogramming, caloric restriction and aging. *Trends Endocrinol Metab* 21: 134–141, 2010.
8. **Apfeld J**, **O'Connor G**, **McDonagh T**, **DiStefano PS**, **Curtis R**. The AMP-activated protein kinase AAK-2 links energy levels and insulin-like signals to lifespan in C. elegans. *Genes Dev* 18: 3004–3009, 2004.
9. **Aronson D**, **Violan MA**, **Dufresne SD**, **Zangen D**, **Fielding RA**, **Goodyear LJ**. Exercise stimulates the mitogen-activated protein kinase pathway in human skeletal muscle. *J Clin Invest* 99: 1251–1257, 1997.
10. **ASHFORD TP**, **PORTER KR**. Cytoplasmic components in hepatic cell lysosomes. *J Cell Biol* 12: 198–202, 1962.
11. **Ashrafi K**, **Lin SS**, **Manchester JK**, **Gordon JI**. Sip2p and its partner snf1p kinase affect aging in S. cerevisiae. *Genes Dev* 14: 1872–85, 2000.
12. **Baba M**, **Takeshige K**, **Baba N**, **Ohsumi Y**. Ultrastructural analysis of the autophagic process in yeast: detection of autophagosomes and their characterization. *J Cell Biol* 124: 903–13, 1994.
13. **Bae SH**, **Sung SH**, **Oh SY**, **Lim JM**, **Lee SK**, **Park YN**, **Lee HE**, **Kang D**, **Rhee SG**. Sestrins Activate Nrf2 by Promoting p62-Dependent Autophagic Degradation of Keap1 and Prevent Oxidative Liver Damage. *Cell Metab* 17: 73–84, 2013.
14. **Baehr LM**, **West DWD**, **Marcotte G**, **Marshall AG**, **De Sousa LG**, **Baar K**, **Bodine SC**. Age-related deficits in skeletal muscle recovery following disuse are associated with neuromuscular junction instability and ER stress, not impaired protein synthesis. *Aging (Albany NY)* 8: 127–46, 2016.
15. **Bakeeva LE**, **Chentsov YuS**, **Skulachev VP**. Mitochondrial framework (reticulum mitochondriale) in rat diaphragm muscle. *Biochim Biophys Acta* 501: 349–69, 1978.
16. **Baker BM**, **Haynes CM**. Mitochondrial protein quality control during biogenesis and aging. *Trends Biochem Sci* 36: 254–261, 2011.
17. **Di Bartolomeo S**, **Corazzari M**, **Nazio F**, **Oliverio S**, **Lisi G**, **Antonioli M**, **Pagliarini V**, **Matteoni S**, **Fuoco C**, **Giunta L**, **D'Amelio M**, **Nardacci R**, **Romagnoli A**, **Piacentini M**, **Cecconi F**, **Fimia GM**. The dynamic interaction of AMBRA1 with the dynein motor complex regulates mammalian autophagy. *J Cell Biol* 191: 155–168, 2010.
18. **Barzilai N**, **Huffman DM**, **Muzumdar RH**, **Bartke A**. The critical role of metabolic pathways in aging. *Diabetes* 61: 1315–22, 2012.
19. **Bauer MF**, **Sirrenberg C**, **Neupert W**, **Brunner M**. Role of Tim23 as voltage sensor and presequence receptor in protein import into mitochondria. *Cell* 87: 33–41, 1996.
20. **Baynes JW**. The role of AGEs in aging: causation or correlation. *Exp Gerontol* 36: 1527–37, 2001.
21. **Bellot G**, **Garcia-Medina R**, **Gounon P**, **Chiche J**, **Roux D**, **Pouysségur J**, **Mazure NM**. Hypoxia-induced autophagy is mediated through hypoxia-inducible factor induction of BNIP3 and BNIP3L via their BH3 domains. *Mol Cell Biol* 29: 2570–81, 2009.
22. **Bender T**, **Lewrenz I**, **Franken S**, **Baitzel C**, **Voos W**. Mitochondrial enzymes are protected from stress-induced aggregation by mitochondrial chaperones and the Pim1/LON protease. *Mol Biol Cell* 22: 541–554, 2011.

23. **Bergamini E**, **Cavallini G**, **Donati A**, **Gori Z**. The anti-ageing effects of caloric restriction may involve stimulation of macroautophagy and lysosomal degradation, and can be intensified pharmacologically. *Biomed Pharmacother* 57: 203–8, [date unknown].
24. **Bergeron R**, **Ren JM**, **Cadman KS**, **Moore IK**, **Perret P**, **Pypaert M**, **Young LH**, **Semenkovich CF**, **Shulman GI**. Chronic activation of AMP kinase results in NRF-1 activation and mitochondrial biogenesis. *Am J Physiol Endocrinol Metab* 281: E1340-6, 2001.
25. **Berndsen CE**, **Wolberger C**. New insights into ubiquitin E3 ligase mechanism. *Nat Struct Mol Biol* 21: 301–307, 2014.
26. **Bers DM**, **Stiffel VM**. Ratio of ryanodine to dihydropyridine receptors in cardiac and skeletal muscle and implications for E-C coupling. *Am J Physiol* 264: C1587-93, 1993.
27. **Bezawork-Geleta A**, **Brodie EJ**, **Dougan DA**, **Truscott KN**. LON is the master protease that protects against protein aggregation in human mitochondria through direct degradation of misfolded proteins. *Sci Rep* 5: 17397, 2015.
28. **Birgisdottir ÅB**, **Lamark T**, **Johansen T**. The LIR motif - crucial for selective autophagy. *J Cell Sci* 126: 3237–47, 2013.
29. **Birsa N**, **Norkett R**, **Wauer T**, **Mevissen TET**, **Wu H-C**, **Foltynie T**, **Bhatia K**, **Hirst WD**, **Komander D**, **Plun-Favreau H**, **Kittler JT**. Lysine 27 ubiquitination of the mitochondrial transport protein Miro is dependent on serine 65 of the Parkin ubiquitin ligase. *J Biol Chem* 289: 14569–82, 2014.
30. **Blackman MR**, **Sorkin JD**, **Münzer T**, **Bellantoni MF**, **Busby-Whitehead J**, **Stevens TE**, **Jayme J**, **O'Connor KG**, **Christmas C**, **Tobin JD**, **Stewart KJ**, **Cottrell E**, **St Clair C**, **Pabst KM**, **Harman SM**. Growth hormone and sex steroid administration in healthy aged women and men: a randomized controlled trial. *JAMA* 288: 2282–92, 2002.
31. **Blair AS**, **Hajduch E**, **Litherland GJ**, **Hundal HS**. Regulation of glucose transport and glycogen synthesis in L6 muscle cells during oxidative stress. Evidence for cross-talk between the insulin and SAPK2/p38 mitogen-activated protein kinase signaling pathways. *J Biol Chem* 274: 36293–9, 1999.
32. **Blüher M**, **Kahn BB**, **Kahn CR**. Extended longevity in mice lacking the insulin receptor in adipose tissue. *Science* 299: 572–4, 2003.
33. **Bodine SC**, **Stitt TN**, **Gonzalez M**, **Kline WO**, **Stover GL**, **Bauerlein R**, **Zlotchenko E**, **Scrimgeour A**, **Lawrence JC**, **Glass DJ**, **Yancopoulos GD**. Akt/mTOR pathway is a crucial regulator of skeletal muscle hypertrophy and can prevent muscle atrophy in vivo. *Nat Cell Biol* 3: 1014–1019, 2001.
34. **Boirie Y**, **Gachon P**, **Cordat N**, **Ritz P**, **Beaufrère B**. Differential insulin sensitivities of glucose, amino acid, and albumin metabolism in elderly men and women. *J Clin Endocrinol Metab* 86: 638–44, 2001.
35. **Boncompagni S**, **Rossi AE**, **Micaroni M**, **Beznoussenko G V**, **Polishchuk RS**, **Dirksen RT**, **Protasi F**. Mitochondria are linked to calcium stores in striated muscle by developmentally regulated tethering structures. *Mol Biol Cell* 20: 1058–67, 2009.
36. **Booth F**. Effects of endurance exercise on cytochrome C turnover in skeletal muscle. *Ann N Y Acad Sci* 301: 431–9, 1977.
37. **Bota DA**, **Davies KJA**. Lon protease preferentially degrades oxidized mitochondrial aconitase by an ATP-stimulated mechanism. *Nat Cell Biol* 4: 674–680, 2002.
38. **Bota DA**, **Van Remmen H**, **Davies KJA**. Modulation of Lon protease activity and aconitase turnover during aging and oxidative stress. *FEBS Lett* 532: 103–6, 2002.
39. **Brunk UT**, **Terman A**. The mitochondrial-lysosomal axis theory of aging: accumulation of damaged mitochondria as a result of imperfect autophagocytosis. *Eur J Biochem* 269: 1996–2002, 2002.
40. **Brunk UT**, **Terman A**. Lipofuscin: mechanisms of age-related accumulation and influence on cell function. *Free Radic Biol Med* 33: 611–9, 2002.
41. **Bua E**, **Johnson J**, **Herbst A**, **Delong B**, **McKenzie D**, **Salamat S**, **Aiken JM**. Mitochondrial DNA-deletion mutations accumulate intracellularly to detrimental levels in aged human skeletal muscle fibers. *Am J Hum Genet* 79: 469–80, 2006.
42. **Bujak AL**, **Crane JD**, **Lally JS**, **Ford RJ**, **Kang SJ**, **Rebalka IA**, **Green AE**, **Kemp BE**, **Hawke TJ**, **Schertzer JD**, **Steinberg GR**. AMPK Activation of Muscle Autophagy Prevents Fasting-Induced Hypoglycemia and Myopathy during Aging. *Cell Metab* 21: 883–890, 2015.
43. **Busch KB**, **Kowald A**, **Spelbrink JN**. Quality matters: how does mitochondrial network dynamics and quality control impact on mtDNA integrity? *Philos Trans R Soc Lond B Biol Sci* 369: 20130442, 2014.
44. **Calvo JA**, **Daniels TG**, **Wang X**, **Paul A**, **Lin J**, **Spiegelman BM**, **Stevenson SC**, **Rangwala SM**. Muscle-specific expression of PPAR coactivator-1 improves exercise performance and increases peak oxygen uptake. *J Appl Physiol* 104: 1304–1312, 2008.

45. **CAMOUGRAND N**, **KISSOVA I**, **VELOURS G**, **MANON S**. Uth1p: a yeast mitochondrial protein at the crossroads of stress, degradation and cell death. *FEMS Yeast Res* 5: 133–140, 2004.
46. **Cantó C**, **Auwerx J**. AMP-activated protein kinase and its downstream transcriptional pathways. *Cell Mol Life Sci* 67: 3407–3423, 2010.
47. **Cardaci S**, **Filomeni G**, **Ciriolo MR**. Redox implications of AMPK-mediated signal transduction beyond energetic clues. *J Cell Sci* 125: 2115–2125, 2012.
48. **Cárdenas C**, **Miller RA**, **Smith I**, **Bui T**, **Molgó J**, **Müller M**, **Vais H**, **Cheung K-H**, **Yang J**, **Parker I**, **Thompson CB**, **Birnbaum MJ**, **Hallows KR**, **Foskett JK**. Essential Regulation of Cell Bioenergetics by Constitutive InsP3 Receptor Ca2+ Transfer to Mitochondria. *Cell* 142: 270–283, 2010.
49. **Carnio S**, **LoVerso F**, **Baraibar MA**, **Longa E**, **Khan MM**, **Maffei M**, **Reischl M**, **Canepari M**, **Loefler S**, **Kern H**, **Blaauw B**, **Friguet B**, **Bottinelli R**, **Rudolf R**, **Sandri M**. Autophagy Impairment in Muscle Induces Neuromuscular Junction Degeneration and Precocious Aging. *Cell Rep* 8: 1509–1521, 2014.
50. **Carter HN**, **Chen CCW**, **Hood DA**. Mitochondria, Muscle Health, and Exercise with Advancing Age. *Physiology* 30: 208–223, 2015.
51. **Cefalu WT**, **Wang ZQ**, **Werbel S**, **Bell-Farrow A**, **Crouse JR**, **Hinson WH**, **Terry JG**, **Anderson R**. Contribution of visceral fat mass to the insulin resistance of aging. *Metabolism* 44: 954–959, 1995.
52. **Chabi B**, **Ljubicic V**, **Menzies KJ**, **Huang JH**, **Saleem A**, **Hood DA**, **Aldridge JE**, **Horibe T**, **Hoogenraad NJ**. Mitochondrial function and apoptotic susceptibility in aging skeletal muscle. *Aging Cell* 7: 2–12, 2008.
53. **Chan NC**, **Salazar AM**, **Pham AH**, **Sweredoski MJ**, **Kolawa NJ**, **Graham RLJ**, **Hess S**, **Chan DC**. Broad activation of the ubiquitin?proteasome system by Parkin is critical for mitophagy. *Hum Mol Genet* 20: 1726–1737, 2011.
54. **Chan NC**, **Salazar AM**, **Pham AH**, **Sweredoski MJ**, **Kolawa NJ**, **Graham RLJ**, **Hess S**, **Chan DC**. Broad activation of the ubiquitin–proteasome system by Parkin is critical for mitophagy. *Hum Mol Genet* 20: 1726–1737, 2011.
55. **Chaugule VK**, **Burchell L**, **Barber KR**, **Sidhu A**, **Leslie SJ**, **Shaw GS**, **Walden H**. Autoregulation of Parkin activity through its ubiquitin-like domain. *EMBO J* 30: 2853–67, 2011.
56. **Chen H**, **Detmer SA**, **Ewald AJ**, **Griffin EE**, **Fraser SE**, **Chan DC**. Mitofusins Mfn1 and Mfn2 coordinately regulate mitochondrial fusion and are essential for embryonic development. *J Cell Biol* 160: 189–200, 2003.
57. **Chen H**, **Vermulst M**, **Wang YE**, **Chomyn A**, **Prolla TA**, **McCaffery JM**, **Chan DC**. Mitochondrial Fusion Is Required for mtDNA Stability in Skeletal Muscle and Tolerance of mtDNA Mutations. *Cell* 141: 280–289, 2010.
58. **Chen L**, **Wang H**, **Vicini S**, **Olsen RW**. The gamma -aminobutyric acid type A (GABAA) receptor-associated protein (GABARAP) promotes GABAA receptor clustering and modulates the channel kinetics. *Proc Natl Acad Sci* 97: 11557–11562, 2000.
59. **Chen Y**, **Dorn GW**. PINK1-phosphorylated mitofusin 2 is a Parkin receptor for culling damaged mitochondria. *Science* 340: 471–5, 2013.
60. **Chu CT**, **Ji J**, **Dagda RK**, **Jiang JF**, **Tyurina YY**, **Kapralov AA**, **Tyurin VA**, **Yanamala N**, **Shrivastava IH**, **Mohammadyani D**, **Qiang Wang KZ**, **Zhu J**, **Klein-Seetharaman J**, **Balasubramanian K**, **Amoscato AA**, **Borisenko G**, **Huang Z**, **Gusdon AM**, **Cheikhi A**, **Steer EK**, **Wang R**, **Baty C**, **Watkins S**, **Bahar I**, **Bayır H**, **Kagan VE**. Cardiolipin externalization to the outer mitochondrial membrane acts as an elimination signal for mitophagy in neuronal cells. *Nat Cell Biol* 15: 1197–1205, 2013.
61. **Chung L**, **Ng Y-C**. Age-related alterations in expression of apoptosis regulatory proteins and heat shock proteins in rat skeletal muscle. *Biochim Biophys Acta - Mol Basis Dis* 1762: 103–109, 2006.
62. **Clark IE**, **Dodson MW**, **Jiang C**, **Cao JH**, **Huh JR**, **Seol JH**, **Yoo SJ**, **Hay BA**, **Guo M**. Drosophila pink1 is required for mitochondrial function and interacts genetically with parkin. *Nature* 441: 1162–6, 2006.
63. **Cogswell AM**, **Stevens RJ**, **Hood DA**. Properties of skeletal muscle mitochondria isolated from subsarcolemmal and intermyofibrillar regions. *Am J Physiol* 264: C383-9, 1993.
64. **Conley KE**, **Jubrias SA**, **Esselman PC**. Oxidative capacity and ageing in human muscle. *J Physiol* 526 Pt 1: 203–10, 2000.
65. **Cortopassi GA**, **Arnheim N**. Detection of a specific mitochondrial DNA deletion in tissues of older humans. *Nucleic Acids Res* 18: 6927–33, 1990.
66. **Cortopassi GA**, **Shibata D**, **Soong NW**, **Arnheim N**. A pattern of accumulation of a somatic deletion of mitochondrial DNA in aging human tissues. *Proc Natl Acad Sci U S A* 89: 7370–4, 1992.
67. **Craig EE**, **Hood DA**. Influence of aging on protein import into cardiac mitochondria. *Am J Physiol* 272:

H2983-8, 1997.
68. **Cuervo AM**. Autophagy and aging: keeping that old broom working. *Trends Genet* 24: 604–12, 2008.
69. **Cuervo AM**, **Dice JF**. A receptor for the selective uptake and degradation of proteins by lysosomes. *Science* 273: 501–3, 1996.
70. **Daido S**, **Kanzawa T**, **Yamamoto A**, **Takeuchi H**, **Kondo Y**, **Kondo S**. Pivotal Role of the Cell Death Factor BNIP3 in Ceramide-Induced Autophagic Cell Death in Malignant Glioma Cells. *Cancer Res* 64: 4286–4293, 2004.
71. **Davies KJA**, **Packer L**, **Brooks GA**. Biochemical adaptation of mitochondria, muscle, and whole-animal respiration to endurance training. *Arch Biochem Biophys* 209: 539–554, 1981.
72. **Dawson TM**, **Dawson VL**. The role of parkin in familial and sporadic Parkinson's disease. *Mov Disord* 25: S32–S39, 2010.
73. **Deas E**, **Plun-Favreau H**, **Gandhi S**, **Desmond H**, **Kjaer S**, **Loh SHY**, **Renton AEM**, **Harvey RJ**, **Whitworth AJ**, **Martins LM**, **Abramov AY**, **Wood NW**. PINK1 cleavage at position A103 by the mitochondrial protease PARL. *Hum Mol Genet* 20: 867–879, 2011.
74. **Decuypere J-P**, **Welkenhuyzen K**, **Luyten T**, **Ponsaerts R**, **Dewaele M**, **Molgó J**, **Agostinis P**, **Missiaen L**, **De Smedt H**, **Parys JB**, **Bultynck G**. Ins(1,4,5)P3 receptor-mediated Ca2+ signaling and autophagy induction are interrelated. *Autophagy* 7: 1472–89, 2011.
75. **Delettre C**, **Lenaers G**, **Griffoin J-M**, **Gigarel N**, **Lorenzo C**, **Belenguer P**, **Pelloquin L**, **Grosgeorge J**, **Turc-Carel C**, **Perret E**, **Astarie-Dequeker C**, **Lasquellec L**, **Arnaud B**, **Ducommun B**, **Kaplan J**, **Hamel CP**. Nuclear gene OPA1, encoding a mitochondrial dynamin-related protein, is mutated in dominant optic atrophy. *Nat Genet* 26: 207–210, 2000.
76. **Diao J**, **Burré J**, **Vivona S**, **Cipriano DJ**, **Sharma M**, **Kyoung M**, **Südhof TC**, **Brunger AT**. Native α-synuclein induces clustering of synaptic-vesicle mimics via binding to phospholipids and synaptobrevin-2/VAMP2. *Elife* 2: e00592, 2013.
77. **Dice JF**. Peptide sequences that target cytosolic proteins for lysosomal proteolysis. *Trends Biochem Sci* 15: 305–9, 1990.
78. **Dillin A**, **Crawford DK**, **Kenyon C**. Timing requirements for insulin/IGF-1 signaling in C. elegans. *Science* 298: 830–4, 2002.
79. **Dirks A**, **Leeuwenburgh C**. Apoptosis in skeletal muscle with aging. *Am J Physiol Regul Integr Comp Physiol* 282: R519-27, 2002.
80. **Dirks AJ**, **Leeuwenburgh C**. The role of apoptosis in age-related skeletal muscle atrophy. *Sports Med* 35: 473–83, 2005.
81. **Diwan A**, **Koesters AG**, **Odley AM**, **Pushkaran S**, **Baines CP**, **Spike BT**, **Daria D**, **Jegga AG**, **Geiger H**, **Aronow BJ**, **Molkentin JD**, **Macleod KF**, **Kalfa TA**, **Dorn GW**. Unrestrained erythroblast development in Nix-/- mice reveals a mechanism for apoptotic modulation of erythropoiesis. *Proc Natl Acad Sci* 104: 6794–6799, 2007.
82. **Doss-Pepe EW**, **Chen L**, **Madura K**. α-Synuclein and Parkin Contribute to the Assembly of Ubiquitin Lysine 63-linked Multiubiquitin Chains. *J Biol Chem* 280: 16619–16624, 2005.
83. **Dudley GA**, **Tullson PC**, **Terjung RL**. Influence of mitochondrial content on the sensitivity of respiratory control. *J Biol Chem* 262: 9109–14, 1987.
84. **Durieux J**, **Wolff S**, **Dillin A**. The cell-non-autonomous nature of electron transport chain-mediated longevity. *Cell* 144: 79–91, 2011.
85. **Dye BT**, **Schulman BA**. Structural Mechanisms Underlying Posttranslational Modification by Ubiquitin-Like Proteins. *Annu Rev Biophys Biomol Struct* 36: 131–150, 2007.
86. **Egan DF**, **Shackelford DB**, **Mihaylova MM**, **Gelino S**, **Kohnz RA**, **Mair W**, **Vasquez DS**, **Joshi A**, **Gwinn DM**, **Taylor R**, **Asara JM**, **Fitzpatrick J**, **Dillin A**, **Viollet B**, **Kundu M**, **Hansen M**, **Shaw RJ**. Phosphorylation of ULK1 (hATG1) by AMP-Activated Protein Kinase Connects Energy Sensing to Mitophagy. *Science (80-)* 331: 456–461, 2011.
87. **Eisner V**, **Csordás G**, **Hajnóczky G**. Interactions between sarco-endoplasmic reticulum and mitochondria in cardiac and skeletal muscle - pivotal roles in Ca^{2+} and reactive oxygen species signaling. *J Cell Sci* 126: 2965–78, 2013.
88. **Erlich AT**, **Brownlee DM**, **Beyfuss K**, **Hood DA**. Exercise induces TFEB expression and activity in skeletal muscle in a PGC-1α-dependent manner. *Am. J. Physiol. Cell Physiol.* (October 18, 2017). doi: 10.1152/ajpcell.00162.2017.
89. **Evans WJ**, **Paolisso G**, **Abbatecola AM**, **Corsonello A**, **Bustacchini S**, **Strollo F**, **Lattanzio F**. Frailty and muscle metabolism dysregulation in the elderly. *Biogerontology* 11: 527–36, 2010.

90. **Falkenberg M**, **Larsson N-G**, **Gustafsson CM**. DNA replication and transcription in mammalian mitochondria. *Annu Rev Biochem* 76: 679–99, 2007.
91. **Farrar RP**, **Martin TP**, **Ardies CM**. The interaction of aging and endurance exercise upon the mitochondrial function of skeletal muscle. *J Gerontol* 36: 642–7, 1981.
92. **Fearnley JM**, **Lees AJ**. Ageing and Parkinson's disease: substantia nigra regional selectivity. *Brain* 114 (Pt 5): 2283–301, 1991.
93. **Ferree AW**, **Trudeau K**, **Zik E**, **Benador IY**, **Twig G**, **Gottlieb RA**, **Shirihai OS**. MitoTimer probe reveals the impact of autophagy, fusion, and motility on subcellular distribution of young and old mitochondrial protein and on relative mitochondrial protein age. *Autophagy* 9: 1887–1896, 2013.
94. **Ferreira R**, **Vitorino R**, **Alves RMP**, **Appell HJ**, **Powers SK**, **Duarte JA**, **Amado F**. Subsarcolemmal and intermyofibrillar mitochondria proteome differences disclose functional specializations in skeletal muscle. *Proteomics* 10: 3142–3154, 2010.
95. **Fill M**, **Copello JA**. Ryanodine receptor calcium release channels. *Physiol Rev* 82: 893–922, 2002.
96. **Ford ES**, **Kohl HW**, **Mokdad AH**, **Ajani UA**. Sedentary Behavior, Physical Activity, and the Metabolic Syndrome among U.S. Adults. *Obes Res* 13: 608–614, 2005.
97. **Fritzen AM**, **Frøsig C**, **Jeppesen J**, **Jensen TE**, **Lundsgaard AM**, **Serup AK**, **Schjerling P**, **Proud CG**, **Richter EA**, **Kiens B**. Role of AMPK in regulation of LC3 lipidation as a marker of autophagy in skeletal muscle. *Cell Signal* 28: 663–674, 2016.
98. **Fritzen AM**, **Madsen AB**, **Kleinert M**, **Treebak JT**, **Lundsgaard A-M**, **Jensen TE**, **Richter EA**, **Wojtaszewski J**, **Kiens B**, **Frøsig C**. Regulation of autophagy in human skeletal muscle: effects of exercise, exercise training and insulin stimulation. *J Physiol* 594: 745–761, 2016.
99. **Fu M**, **St-Pierre P**, **Shankar J**, **Wang PTC**, **Joshi B**, **Nabi IR**. Regulation of mitophagy by the Gp78 E3 ubiquitin ligase. *Mol Biol Cell* 24: 1153–62, 2013.
100. **Funderburk SF**, **Wang QJ**, **Yue Z**. The Beclin 1-VPS34 complex--at the crossroads of autophagy and beyond. *Trends Cell Biol* 20: 355–62, 2010.
101. **Gandre-Babbe S**, **van der Bliek AM**. The Novel Tail-anchored Membrane Protein Mff Controls Mitochondrial and Peroxisomal Fission in Mammalian Cells. *Mol Biol Cell* 19: 2402–2412, 2008.
102. **García-Prat L**, **Martínez-Vicente M**, **Perdiguero E**, **Ortet L**, **Rodríguez-Ubreva J**, **Rebollo E**, **Ruiz-Bonilla V**, **Gutarra S**, **Ballestar E**, **Serrano AL**, **Sandri M**, **Muñoz-Cánoves P**. Autophagy maintains stemness by preventing senescence. *Nature* 529: 37–42, 2016.
103. **Geisler S**, **Holmström KM**, **Skujat D**, **Fiesel FC**, **Rothfuss OC**, **Kahle PJ**, **Springer W**. PINK1/Parkin-mediated mitophagy is dependent on VDAC1 and p62/SQSTM1. *Nat Cell Biol* 12: 119–131, 2010.
104. **Geng T**, **Li P**, **Okutsu M**, **Yin X**, **Kwek J**, **Zhang M**, **Yan Z**. PGC-1 plays a functional role in exercise-induced mitochondrial biogenesis and angiogenesis but not fiber-type transformation in mouse skeletal muscle. *AJP Cell Physiol* 298: C572–C579, 2010.
105. **Glancy B**, **Hartnell LM**, **Malide D**, **Yu Z-X**, **Combs CA**, **Connelly PS**, **Subramaniam S**, **Balaban RS**. Mitochondrial reticulum for cellular energy distribution in muscle. *Nature* 523: 617–20, 2015.
106. **Glancy B**, **Hsu L-Y**, **Dao L**, **Bakalar M**, **French S**, **Chess DJ**, **Taylor JL**, **Picard M**, **Aponte A**, **Daniels MP**, **Esfahani S**, **Cushman S**, **Balaban RS**. *In Vivo* Microscopy Reveals Extensive Embedding of Capillaries within the Sarcolemma of Skeletal Muscle Fibers. *Microcirculation* 21: 131–147, 2014.
107. **Gollnick PD**, **Armstrong RB**, **Saltin B**, **Saubert CW**, **Sembrowich WL**, **Shepherd RE**. Effect of training on enzyme activity and fiber composition of human skeletal muscle. *J Appl Physiol* 34: 107–11, 1973.
108. **Gong G**, **Song M**, **Csordas G**, **Kelly DP**, **Matkovich SJ**, **Dorn GW**. Parkin-mediated mitophagy directs perinatal cardiac metabolic maturation in mice. *Science (80-)* 350: aad2459-aad2459, 2015.
109. **Goodpaster BH**, **Park SW**, **Harris TB**, **Kritchevsky SB**, **Nevitt M**, **Schwartz A V**, **Simonsick EM**, **Tylavsky FA**, **Visser M**, **Newman AB**. The loss of skeletal muscle strength, mass, and quality in older adults: the health, aging and body composition study. *J Gerontol A Biol Sci Med Sci* 61: 1059–64, 2006.
110. **Gottlieb RA**, **Andres AM**, **Sin J**, **Taylor DPJ**. Untangling Autophagy Measurements: All Fluxed Up. *Circ Res* 116: 504–514, 2015.
111. **Gouspillou G**, **Sgarioto N**, **Kapchinsky S**, **Purves-Smith F**, **Norris B**, **Pion CH**, **Barbat-Artigas S**, **Lemieux F**, **Taivassalo T**, **Morais JA**, **Aubertin-Leheudre M**, **Hepple RT**. Increased sensitivity to mitochondrial permeability transition and myonuclear translocation of endonuclease G in atrophied muscle of physically active older humans. *FASEB J* 28: 1621–33, 2014.
112. **Graham BH**, **Waymire KG**, **Cottrell B**, **Trounce IA**, **MacGregor GR**, **Wallace DC**. A mouse model for mitochondrial myopathy and cardiomyopathy resulting from a deficiency in the heart/muscle isoform of the adenine nucleotide translocator. *Nat Genet* 16: 226–234, 1997.

113. **Green DR**, **Galluzzi L**, **Kroemer G**. Mitochondria and the Autophagy-Inflammation-Cell Death Axis in Organismal Aging. *Science (80-)* 333: 1109–1112, 2011.
114. **Green HJ**, **Reichmann H**, **Pette D**. Fibre type specific transformations in the enzyme activity pattern of rat vastus lateralis muscle by prolonged endurance training. *Pflugers Arch* 399: 216–22, 1983.
115. **Greene AW**, **Grenier K**, **Aguileta MA**, **Muise S**, **Farazifard R**, **Haque ME**, **McBride HM**, **Park DS**, **Fon EA**. Mitochondrial processing peptidase regulates PINK1 processing, import and Parkin recruitment. *EMBO Rep* 13: 378–385, 2012.
116. **Greene JC**, **Whitworth AJ**, **Kuo I**, **Andrews LA**, **Feany MB**, **Pallanck LJ**. Mitochondrial pathology and apoptotic muscle degeneration in Drosophila parkin mutants. *Proc Natl Acad Sci U S A* 100: 4078–83, 2003.
117. **Greer EL**, **Dowlatshahi D**, **Banko MR**, **Villen J**, **Hoang K**, **Blanchard D**, **Gygi SP**, **Brunet A**. An AMPK-FOXO Pathway Mediates Longevity Induced by a Novel Method of Dietary Restriction in C. elegans. *Curr Biol* 17: 1646–1656, 2007.
118. **Grumati P**, **Coletto L**, **Schiavinato A**, **Castagnaro S**, **Bertaggia E**, **Sandri M**, **Bonaldo P**. *Physical exercise stimulates autophagy in normal skeletal muscles but is detrimental for collagen VI-deficient muscles*. Taylor & Francis, 2011.
119. **Guillet C**, **Zangarelli A**, **Gachon P**, **Morio B**, **Giraudet C**, **Rousset P**, **Boirie Y**. Whole body protein breakdown is less inhibited by insulin, but still responsive to amino acid, in nondiabetic elderly subjects. *J Clin Endocrinol Metab* 89: 6017–24, 2004.
120. **Gwinn DM**, **Shackelford DB**, **Egan DF**, **Mihaylova MM**, **Mery A**, **Vasquez DS**, **Turk BE**, **Shaw RJ**. AMPK Phosphorylation of Raptor Mediates a Metabolic Checkpoint. *Mol Cell* 30: 214–226, 2008.
121. **Ha S**, **Jeong S-H**, **Yi K**, **Chung KM**, **Hong CJ**, **Kim SW**, **Kim E-K**, **Yu S-W**. Phosphorylation of p62 by AMP-activated protein kinase mediates autophagic cell death in adult hippocampal neural stem cells. *J Biol Chem* 292: 13795–13808, 2017.
122. **Hampe C**, **Ardila-Osorio H**, **Fournier M**, **Brice A**, **Corti O**. Biochemical analysis of Parkinson's disease-causing variants of Parkin, an E3 ubiquitin-protein ligase with monoubiquitylation capacity. *Hum Mol Genet* 15: 2059–2075, 2006.
123. **Han D**, **Antunes F**, **Canali R**, **Rettori D**, **Cadenas E**. Voltage-dependent Anion Channels Control the Release of the Superoxide Anion from Mitochondria to Cytosol. *J Biol Chem* 278: 5557–5563, 2003.
124. **Han D**, **Williams E**, **Cadenas E**. Mitochondrial respiratory chain-dependent generation of superoxide anion and its release into the intermembrane space. *Biochem J* 353: 411–6, 2001.
125. **Hanada T**, **Noda NN**, **Satomi Y**, **Ichimura Y**, **Fujioka Y**, **Takao T**, **Inagaki F**, **Ohsumi Y**. The Atg12-Atg5 conjugate has a novel E3-like activity for protein lipidation in autophagy. *J Biol Chem* 282: 37298–302, 2007.
126. **Handschin C**, **Chin S**, **Li P**, **Liu F**, **Maratos-Flier E**, **LeBrasseur NK**, **Yan Z**, **Spiegelman BM**. Skeletal Muscle Fiber-type Switching, Exercise Intolerance, and Myopathy in PGC-1α Muscle-specific Knock-out Animals. *J Biol Chem* 282: 30014–30021, 2007.
127. **Hankinson SE**, **Willett WC**, **Colditz GA**, **Hunter DJ**, **Michaud DS**, **Deroo B**, **Rosner B**, **Speizer FE**, **Pollak M**. Circulating concentrations of insulin-like growth factor-I and risk of breast cancer. *Lancet* 351: 1393–6, 1998.
128. **Hanna RA**, **Quinsay MN**, **Orogo AM**, **Giang K**, **Rikka S**, **Gustafsson ÅB**. Microtubule-associated protein 1 light chain 3 (LC3) interacts with Bnip3 protein to selectively remove endoplasmic reticulum and mitochondria via autophagy. *J Biol Chem* 287: 19094–104, 2012.
129. **Hansen J**, **Gregersen N**, **Bross P**. Differential degradation of variant medium-chain acyl-CoA dehydrogenase by the protein quality control proteases Lon and ClpXP. *Biochem Biophys Res Commun* 333: 1160–1170, 2005.
130. **Hara T**, **Takamura A**, **Kishi C**, **Iemura S-I**, **Natsume T**, **Guan J-L**, **Mizushima N**. FIP200, a ULK-interacting protein, is required for autophagosome formation in mammalian cells. *J Cell Biol* 181: 497–510, 2008.
131. **Harding TM**, **Hefner-Gravink A**, **Thumm M**, **Klionsky DJ**. Genetic and phenotypic overlap between autophagy and the cytoplasm to vacuole protein targeting pathway. *J Biol Chem* 271: 17621–4, 1996.
132. **HARMAN D**. Aging: a theory based on free radical and radiation chemistry. *J Gerontol* 11: 298–300, 1956.
133. **HARMAN D**. Free Radical Theory of Aging: An Update: Increasing the Functional Life Span. *Ann N Y Acad Sci* 1067: 10–21, 2006.
134. **Harrison DE**, **Strong R**, **Sharp ZD**, **Nelson JF**, **Astle CM**, **Flurkey K**, **Nadon NL**, **Wilkinson JE**, **Frenkel K**, **Carter CS**, **Pahor M**, **Javors MA**, **Fernandez E**, **Miller RA**. Rapamycin fed late in life extends lifespan in genetically heterogeneous mice. *Nature* 460: 392–5, 2009.

135. **Hay N**, **Sonenberg N**. Upstream and downstream of mTOR. *Genes Dev* 18: 1926–45, 2004.
136. **Haynes CM**, **Petrova K**, **Benedetti C**, **Yang Y**, **Ron D**. ClpP Mediates Activation of a Mitochondrial Unfolded Protein Response in C. elegans. *Dev Cell* 13: 467–480, 2007.
137. **Haynes CM**, **Yang Y**, **Blais SP**, **Neubert TA**, **Ron D**. The Matrix Peptide Exporter HAF-1 Signals a Mitochondrial UPR by Activating the Transcription Factor ZC376.7 in C. elegans. *Mol Cell* 37: 529–540, 2010.
138. **He C**, **Bassik MC**, **Moresi V**, **Sun K**, **Wei Y**, **Zou Z**, **An Z**, **Loh J**, **Fisher J**, **Sun Q**, **Korsmeyer S**, **Packer M**, **May HI**, **Hill JA**, **Virgin HW**, **Gilpin C**, **Xiao G**, **Bassel-Duby R**, **Scherer PE**, **Levine B**. Exercise-induced BCL2-regulated autophagy is required for muscle glucose homeostasis. *Nature* 481: 511–5, 2012.
139. **He C**, **Sumpter R**, **Levine B**. Exercise induces autophagy in peripheral tissues and in the brain. *Autophagy* 8: 1548–51, 2012.
140. **Hemelaar J**, **Lelyveld VS**, **Kessler BM**, **Ploegh HL**. A Single Protease, Apg4B, Is Specific for the Autophagy-related Ubiquitin-like Proteins GATE-16, MAP1-LC3, GABARAP, and Apg8L. *J Biol Chem* 278: 51841–51850, 2003.
141. **Henriksson J**, **Reitman JS**. Quantitative Measures of Enzyme Activities in Type I and Type II Muscle Fibres of Man after Training. *Acta Physiol Scand* 97: 392–397, 1976.
142. **Henriksson J**, **Reitman JS**. Time Course of Changes in Human Skeletal Muscle Succinate Dehydrogenase and Cytochrome Oxidase Activities and Maximal Oxygen Uptake with Physical Activity and Inactivity. *Acta Physiol Scand* 99: 91–97, 1977.
143. **Heo J-M**, **Livnat-Levanon N**, **Taylor EB**, **Jones KT**, **Dephoure N**, **Ring J**, **Xie J**, **Brodsky JL**, **Madeo F**, **Gygi SP**, **Ashrafi K**, **Glickman MH**, **Rutter J**. A Stress-Responsive System for Mitochondrial Protein Degradation. *Mol Cell* 40: 465–480, 2010.
144. **Heo J-M**, **Nielson JR**, **Dephoure N**, **Gygi SP**, **Rutter J**. Intramolecular interactions control Vms1 translocation to damaged mitochondria. *Mol Biol Cell* 24: 1263–1273, 2013.
145. **Heo J-M**, **Ordureau A**, **Paulo JA**, **Rinehart J**, **Harper JW**. The PINK1-PARKIN Mitochondrial Ubiquitylation Pathway Drives a Program of OPTN/NDP52 Recruitment and TBK1 Activation to Promote Mitophagy. *Mol Cell* 60: 7–20, 2015.
146. **Hepple RT**. Mitochondrial Involvement and Impact in Aging Skeletal Muscle. *Front Aging Neurosci* 6: 211, 2014.
147. **Herbst A**, **Pak JW**, **McKenzie D**, **Bua E**, **Bassiouni M**, **Aiken JM**. Accumulation of mitochondrial DNA deletion mutations in aged muscle fibers: evidence for a causal role in muscle fiber loss. *J Gerontol A Biol Sci Med Sci* 62: 235–45, 2007.
148. **Hernandez G**, **Thornton C**, **Stotland A**, **Lui D**, **Sin J**, **Ramil J**, **Magee N**, **Andres A**, **Quarato G**, **Carreira RS**, **Sayen MR**, **Wolkowicz R**, **Gottlieb RA**. MitoTimer: A novel tool for monitoring mitochondrial turnover. *Autophagy* 9: 1852–1861, 2013.
149. **Hiona A**, **Sanz A**, **Kujoth GC**, **Pamplona R**, **Seo AY**, **Hofer T**, **Someya S**, **Miyakawa T**, **Nakayama C**, **Samhan-Arias AK**, **Servais S**, **Barger JL**, **Portero-Otín M**, **Tanokura M**, **Prolla TA**, **Leeuwenburgh C**. Mitochondrial DNA Mutations Induce Mitochondrial Dysfunction, Apoptosis and Sarcopenia in Skeletal Muscle of Mitochondrial DNA Mutator Mice. *PLoS One* 5: e11468, 2010.
150. **Hipkiss AR**. Accumulation of altered proteins and ageing: causes and effects. *Exp Gerontol* 41: 464–73, 2006.
151. **Hoehn KL**, **Salmon AB**, **Hohnen-Behrens C**, **Turner N**, **Hoy AJ**, **Maghzal GJ**, **Stocker R**, **Van Remmen H**, **Kraegen EW**, **Cooney GJ**, **Richardson AR**, **James DE**. Insulin resistance is a cellular antioxidant defense mechanism. *Proc Natl Acad Sci U S A* 106: 17787–92, 2009.
152. **Hoffman NJ**, **Parker BL**, **Chaudhuri R**, **Wojtaszewski JFP**, **Richter EA**, **Correspondence DEJ**. Global Phosphoproteomic Analysis of Human Skeletal Muscle Reveals a Network of Exercise- Regulated Kinases and AMPK Substrates. *Cell Metab* 22: 1–14, 2015.
153. **Holloszy JO**. Biochemical adaptations in muscle. Effects of exercise on mitochondrial oxygen uptake and respiratory enzyme activity in skeletal muscle. *J Biol Chem* 242: 2278–82, 1967.
154. **Holloszy JO**, **Smith EK**, **Vining M**, **Adams S**. Effect of voluntary exercise on longevity of rats. *J Appl Physiol* 59: 826–31, 1985.
155. **Holloway GP**, **Gurd BJ**, **Snook LA**, **Lally J**, **Bonen A**. Compensatory increases in nuclear PGC1alpha protein are primarily associated with subsarcolemmal mitochondrial adaptations in ZDF rats. *Diabetes* 59: 819–28, 2010.
156. **Holzenberger M**, **Dupont J**, **Ducos B**, **Leneuve P**, **Géloën A**, **Even PC**, **Cervera P**, **Le Bouc Y**. IGF-1

receptor regulates lifespan and resistance to oxidative stress in mice. *Nature* 421: 182–7, 2003.
157. **Hood DA**. Invited Review: contractile activity-induced mitochondrial biogenesis in skeletal muscle. *J Appl Physiol* 90: 1137–57, 2001.
158. **Hood DA**, **Tryon LD**, **Carter HN**, **Kim Y**, **Chen CCW**. Unravelling the mechanisms regulating muscle mitochondrial biogenesis. *Biochem J* 473: 2295–2314, 2016.
159. **Hoppeler H**. Exercise-Induced Ultrastructural Changes in Skeletal Muscle*. *Int J Sports Med* 7: 187–204, 1986.
160. **Horibe T**, **Hoogenraad NJ**. The chop gene contains an element for the positive regulation of the mitochondrial unfolded protein response. *PLoS One* 2: e835, 2007.
161. **Hoshino A**, **Mita Y**, **Okawa Y**, **Ariyoshi M**, **Iwai-Kanai E**, **Ueyama T**, **Ikeda K**, **Ogata T**, **Matoba S**. Cytosolic p53 inhibits Parkin-mediated mitophagy and promotes mitochondrial dysfunction in the mouse heart. *Nat Commun* 4: 2308, 2013.
162. **Houtkooper RH**, **Mouchiroud L**, **Ryu D**, **Moullan N**, **Katsyuba E**, **Knott G**, **Williams RW**, **Auwerx J**. Mitonuclear protein imbalance as a conserved longevity mechanism. *Nature* 497: 451–7, 2013.
163. **Houtkooper RH**, **Williams RW**, **Auwerx J**. Metabolic Networks of Longevity. *Cell* 142: 9–14, 2010.
164. **Howald H**, **Hoppeler H**, **Claassen H**, **Mathieu O**, **Straub R**. Influences of endurance training on the ultrastructural composition of the different muscle fiber types in humans. *Pflugers Arch* 403: 369–76, 1985.
165. **Huang H**, **Zhang X**, **Li S**, **Liu N**, **Lian W**, **McDowell E**, **Zhou P**, **Zhao C**, **Guo H**, **Zhang C**, **Yang C**, **Wen G**, **Dong X**, **Lu L**, **Ma N**, **Dong W**, **Dou QP**, **Wang X**, **Liu J**. Physiological levels of ATP negatively regulate proteasome function. *Cell Res* 20: 1372–1385, 2010.
166. **Huang JH**, **Joseph A-M**, **Ljubicic V**, **Iqbal S**, **Hood DA**. Effect of age on the processing and import of matrix-destined mitochondrial proteins in skeletal muscle. *J Gerontol A Biol Sci Med Sci* 65: 138–46, 2010.
167. **Van Humbeeck C**, **Cornelissen T**, **Hofkens H**, **Mandemakers W**, **Gevaert K**, **De Strooper B**, **Vandenberghe W**. Parkin Interacts with Ambra1 to Induce Mitophagy. *J Neurosci* 31: 10249–10261, 2011.
168. **Hurley JH**, **Lee S**, **Prag G**. Ubiquitin-binding domains. *Biochem J* 399: 361–72, 2006.
169. **Ichida M**, **Nemoto S**, **Finkel T**. Identification of a Specific Molecular Repressor of the Peroxisome Proliferator-activated Receptor γ Coactivator-1 α (PGC-1α). *J Biol Chem* 277: 50991–50995, 2002.
170. **Ichimura Y**, **Waguri S**, **Sou Y**, **Kageyama S**, **Hasegawa J**, **Ishimura R**, **Saito T**, **Yang Y**, **Kouno T**, **Fukutomi T**, **Hoshii T**, **Hirao A**, **Takagi K**, **Mizushima T**, **Motohashi H**, **Lee M-S**, **Yoshimori T**, **Tanaka K**, **Yamamoto M**, **Komatsu M**. Phosphorylation of p62 Activates the Keap1-Nrf2 Pathway during Selective Autophagy. *Mol Cell* 51: 618–631, 2013.
171. **Iguchi M**, **Kujuro Y**, **Okatsu K**, **Koyano F**, **Kosako H**, **Kimura M**, **Suzuki N**, **Uchiyama S**, **Tanaka K**, **Matsuda N**. Parkin-catalyzed Ubiquitin-Ester Transfer Is Triggered by PINK1-dependent Phosphorylation. *J Biol Chem* 288: 22019–22032, 2013.
172. **Imazu T**, **Shimizu S**, **Tagami S**, **Matsushima M**, **Nakamura Y**, **Miki T**, **Okuyama A**, **Tsujimoto Y**. Bcl-2/E1B 19 kDa-interacting protein 3-like protein (Bnip3L) interacts with Bcl-2/Bcl-xL and induces apoptosis by altering mitochondrial membrane permeability. *Oncogene* 18: 4523–4529, 1999.
173. **Inoki K**, **Zhu T**, **Guan K-L**. TSC2 mediates cellular energy response to control cell growth and survival. *Cell* 115: 577–90, 2003.
174. **Iqbal S**, **Hood DA**. Oxidative stress-induced mitochondrial fragmentation and movement in skeletal muscle myoblasts. *AJP Cell Physiol* 306: C1176–C1183, 2014.
175. **Iqbal S**, **Hood DA**. The role of mitochondrial fusion and fission in skeletal muscle function and dysfunction. *Front Biosci (Landmark Ed* 20: 157–72, 2015.
176. **Iqbal S**, **Ostojic O**, **Singh K**, **Joseph A-M**, **Hood DA**. Expression of mitochondrial fission and fusion regulatory proteins in skeletal muscle during chronic use and disuse. *Muscle Nerve* 48: 963–70, 2013.
177. **Irrcher I**, **Adhihetty PJ**, **Sheehan T**, **Joseph A-M**, **Hood DA**. PPARgamma coactivator-1alpha expression during thyroid hormone- and contractile activity-induced mitochondrial adaptations. *AJP Cell Physiol* 284: C1669–C1677, 2003.
178. **Irrcher I**, **Ljubicic V**, **Kirwan AF**, **Hood DA**. AMP-Activated Protein Kinase-Regulated Activation of the PGC-1α Promoter in Skeletal Muscle Cells. *PLoS One* 3: e3614, 2008.
179. **Jager S**, **Handschin C**, **St.-Pierre J**, **Spiegelman BM**. AMP-activated protein kinase (AMPK) action in skeletal muscle via direct phosphorylation of PGC-1. *Proc Natl Acad Sci* 104: 12017–12022, 2007.
180. **Jamart C**, **Benoit N**, **Raymackers JM**, **Kim HJ**, **Kim CK**, **Francaux M**. Autophagy-related and autophagy-regulatory genes are induced in human muscle after ultraendurance exercise. *Eur J Appl Physiol* 112: 3173–3177, 2012.
181. **Jamart C**, **Francaux M**, **Millet GY**, **Deldicque L**, **Frère D**, **Féasson L**. Modulation of autophagy and

ubiquitin-proteasome pathways during ultra-endurance running. *J Appl Physiol* 112: 1529–1537, 2012.
182. **Jamart C**, **Naslain D**, **Gilson H**, **Francaux M**. Higher activation of autophagy in skeletal muscle of mice during endurance exercise in the fasted state. *AJP Endocrinol Metab* 305: E964–E974, 2013.
183. **Javitch JA**, **D'Amato RJ**, **Strittmatter SM**, **Snyder SH**. Parkinsonism-inducing neurotoxin, N-methyl-4-phenyl-1,2,3,6 -tetrahydropyridine: uptake of the metabolite N-methyl-4-phenylpyridine by dopamine neurons explains selective toxicity. *Proc Natl Acad Sci U S A* 82: 2173–7, 1985.
184. **Jean S**, **Kiger AA**. Classes of phosphoinositide 3-kinases at a glance. *J Cell Sci* 127: 923–8, 2014.
185. **Jensen TE**, **Rose AJ**, **Jorgensen SB**, **Brandt N**, **Schjerling P**, **Wojtaszewski JFP**, **Richter EA**. Possible CaMKK-dependent regulation of AMPK phosphorylation and glucose uptake at the onset of mild tetanic skeletal muscle contraction. *AJP Endocrinol Metab* 292: E1308–E1317, 2007.
186. **Jia K**, **Chen D**, **Riddle DL**. The TOR pathway interacts with the insulin signaling pathway to regulate C. elegans larval development, metabolism and life span. *Development* 131: 3897–3906, 2004.
187. **Jin SM**, **Lazarou M**, **Wang C**, **Kane LA**, **Narendra DP**, **Youle RJ**. Mitochondrial membrane potential regulates PINK1 import and proteolytic destabilization by PARL. *J Cell Biol* 191: 933–42, 2010.
188. **Jin SM**, **Youle RJ**. The accumulation of misfolded proteins in the mitochondrial matrix is sensed by PINK1 to induce PARK2/Parkin-mediated mitophagy of polarized mitochondria. *Autophagy* 9: 1750–7, 2013.
189. **Joch M**, **Ase AR**, **Chen CX-Q**, **MacDonald PA**, **Kontogiannea M**, **Corera AT**, **Brice A**, **Séguéla P**, **Fon EA**. Parkin-mediated monoubiquitination of the PDZ protein PICK1 regulates the activity of acid-sensing ion channels. *Mol Biol Cell* 18: 3105–18, 2007.
190. **Joseph A-M**, **Hood DA**. Diabetes and Physical Activity. Basel: S. KARGER AG, 2014.
191. **Joseph A-M**, **Ljubicic V**, **Adhihetty PJ**, **Hood DA**. Biogenesis of the mitochondrial Tom40 channel in skeletal muscle from aged animals and its adaptability to chronic contractile activity. *Am J Physiol Cell Physiol* 298: C1308-14, 2010.
192. **Ju J-S**, **Varadhachary AS**, **Miller SE**, **Weihl CC**. Quantitation of "autophagic flux" in mature skeletal muscle. *Autophagy* 6: 929–35, 2010.
193. **Ju J-S**, **Varadhachary AS**, **Miller SE**, **Weihl CC**. Quantitation of "autophagic flux" in mature skeletal muscle. *Autophagy* 6: 929–935, 2010.
194. **Ju J**, **Jeon S**, **Park J**, **Lee J**, **Lee S**, **Cho K**, **Jeong J**. Autophagy plays a role in skeletal muscle mitochondrial biogenesis in an endurance exercise-trained condition. *J Physiol Sci* 66: 417–430, 2016.
195. **Kabeya Y**, **Mizushima N**, **Ueno T**, **Yamamoto A**, **Kirisako T**, **Noda T**, **Kominami E**, **Ohsumi Y**, **Yoshimori T**. LC3, a mammalian homologue of yeast Apg8p, is localized in autophagosome membranes after processing. *EMBO J* 19: 5720–8, 2000.
196. **Kabeya Y**, **Mizushima N**, **Yamamoto A**, **Oshitani-Okamoto S**, **Ohsumi Y**, **Yoshimori T**. LC3, GABARAP and GATE16 localize to autophagosomal membrane depending on form-II formation. *J Cell Sci* 117: 2805–2812, 2004.
197. **Kadenbach B**, **Münscher C**, **Frank V**, **Müller-Höcker J**, **Napiwotzki J**. Human aging is associated with stochastic somatic mutations of mitochondrial DNA. *Mutat Res* 338: 161–72, 1995.
198. **Kaeberlein M**, **Powers RW**, **Steffen KK**, **Westman EA**, **Hu D**, **Dang N**, **Kerr EO**, **Kirkland KT**, **Fields S**, **Kennedy BK**. Regulation of Yeast Replicative Life Span by TOR and Sch9 in Response to Nutrients. *Science (80-)* 310: 1193–1196, 2005.
199. **Kahn BB**, **Alquier T**, **Carling D**, **Hardie DG**. AMP-activated protein kinase: Ancient energy gauge provides clues to modern understanding of metabolism. *Cell Metab* 1: 15–25, 2005.
200. **Kane LA**, **Lazarou M**, **Fogel AI**, **Li Y**, **Yamano K**, **Sarraf SA**, **Banerjee S**, **Youle RJ**. PINK1 phosphorylates ubiquitin to activate Parkin E3 ubiquitin ligase activity. *J Cell Biol* 205: 143–53, 2014.
201. **Kang C**, **Chung E**, **Diffee G**, **Ji LL**. Exercise training attenuates aging-associated mitochondrial dysfunction in rat skeletal muscle: Role of PGC-1α. *Exp Gerontol* 48: 1343–1350, 2013.
202. **Kapahi P**, **Chen D**, **Rogers AN**, **Katewa SD**, **Li PW-L**, **Thomas EL**, **Kockel L**. With TOR, Less Is More: A Key Role for the Conserved Nutrient-Sensing TOR Pathway in Aging. *Cell Metab* 11: 453–465, 2010.
203. **Kapahi P**, **Zid BM**, **Harper T**, **Koslover D**, **Sapin V**, **Benzer S**. Regulation of Lifespan in Drosophila by Modulation of Genes in the TOR Signaling Pathway. *Curr Biol* 14: 885–890, 2004.
204. **Katayama H**, **Kogure T**, **Mizushima N**, **Yoshimori T**, **Miyawaki A**. A sensitive and quantitative technique for detecting autophagic events based on lysosomal delivery. *Chem Biol* 18: 1042–52, 2011.
205. **Kayar SR**, **Hoppeler H**, **Mermod L**, **Weibel ER**. Mitochondrial size and shape in equine skeletal muscle: A three-dimensional reconstruction study. *Anat Rec* 222: 333–339, 1988.
206. **Kazlauskaite A**, **Kondapalli C**, **Gourlay R**, **Campbell DG**, **Ritorto MS**, **Hofmann K**, **Alessi DR**, **Knebel A**, **Trost M**, **Muqit MMK**. Parkin is activated by PINK1-dependent phosphorylation of ubiquitin at Ser 65.

Biochem J 460: 127–139, 2014.
207. **Kelley DE**, **He J**, **Menshikova E V**, **Ritov VB**. Dysfunction of mitochondria in human skeletal muscle in type 2 diabetes. *Diabetes* 51: 2944–50, 2002.
208. **Kenyon C**, **Chang J**, **Gensch E**, **Rudner A**, **Tabtiang R**. A C. elegans mutant that lives twice as long as wild type. *Nature* 366: 461–464, 1993.
209. **Kim I**, **Rodriguez-Enriquez S**, **Lemasters JJ**. Selective degradation of mitochondria by mitophagy. *Arch Biochem Biophys* 462: 245–253, 2007.
210. **Kim J**, **Kim YC**, **Fang C**, **Russell RC**, **Kim JH**, **Fan W**, **Liu R**, **Zhong Q**, **Guan K-L**. Differential Regulation of Distinct Vps34 Complexes by AMPK in Nutrient Stress and Autophagy. *Cell* 152: 290–303, 2013.
211. **Kim J**, **Kundu M**, **Viollet B**, **Guan K-L**. AMPK and mTOR regulate autophagy through direct phosphorylation of Ulk1. *Nat Cell Biol* 13: 132–41, 2011.
212. **Kim Y**, **Hood DA**. Regulation of the autophagy system during chronic contractile activity-induced muscle adaptations. *Physiol Rep* 5: e13307, 2017.
213. **Kimura KD**, **Tissenbaum HA**, **Liu Y**, **Ruvkun G**, **Hall DH**, **Levine B**. daf-2, an Insulin Receptor-Like Gene That Regulates Longevity and Diapause in Caenorhabditis elegans. *Science (80-)* 277: 942–946, 1997.
214. **Kimura S**, **Noda T**, **Yoshimori T**. Dissection of the autophagosome maturation process by a novel reporter protein, tandem fluorescent-tagged LC3. *Autophagy* 3: 452–60, [date unknown].
215. **Kirkin V**, **Lamark T**, **Sou Y-S**, **Bjørkøy G**, **Nunn JL**, **Bruun J-A**, **Shvets E**, **McEwan DG**, **Clausen TH**, **Wild P**, **Bilusic I**, **Theurillat J-P**, **Øvervatn A**, **Ishii T**, **Elazar Z**, **Komatsu M**, **Dikic I**, **Johansen T**. A role for NBR1 in autophagosomal degradation of ubiquitinated substrates. *Mol Cell* 33: 505–16, 2009.
216. **Kirkwood SP**, **Munn EA**, **Brooks GA**. Mitochondrial reticulum in limb skeletal muscle. *Am J Physiol* 251: C395-402, 1986.
217. **Kissová I**, **Deffieu M**, **Manon S**, **Camougrand N**. Uth1p Is Involved in the Autophagic Degradation of Mitochondria. *J Biol Chem* 279: 39068–39074, 2004.
218. **Koga H**, **Kaushik S**, **Cuervo AM**. Protein homeostasis and aging: The importance of exquisite quality control. *Ageing Res Rev* 10: 205–215, 2011.
219. **Kohl HW**, **Craig CL**, **Lambert EV**, **Inoue S**, **Alkandari JR**, **Leetongin G**, **Kahlmeier S**, **Lancet Physical Activity Series Working Group**. The pandemic of physical inactivity: global action for public health. *Lancet* 380: 294–305, 2012.
220. **Kohrt WM**, **Kirwan JP**, **Staten MA**, **Bourey RE**, **King DS**, **Holloszy JO**. Insulin Resistance in Aging Is Related to Abdominal Obesity. *Diabetes* 42: 273–281, 1993.
221. **Koltai E**, **Hart N**, **Taylor AW**, **Goto S**, **Ngo JK**, **Davies KJA**, **Radak Z**. Age-associated declines in mitochondrial biogenesis and protein quality control factors are minimized by exercise training. *Am J Physiol Regul Integr Comp Physiol* 303: R127-34, 2012.
222. **Komatsu M**, **Kurokawa H**, **Waguri S**, **Taguchi K**, **Kobayashi A**, **Ichimura Y**, **Sou Y-S**, **Ueno I**, **Sakamoto A**, **Tong KI**, **Kim M**, **Nishito Y**, **Iemura S**, **Natsume T**, **Ueno T**, **Kominami E**, **Motohashi H**, **Tanaka K**, **Yamamoto M**. The selective autophagy substrate p62 activates the stress responsive transcription factor Nrf2 through inactivation of Keap1. *Nat Cell Biol* 12: 213–23, 2010.
223. **Komatsu M**, **Waguri S**, **Koike M**, **Sou Y**, **Ueno T**, **Hara T**, **Mizushima N**, **Iwata J**, **Ezaki J**, **Murata S**, **Hamazaki J**, **Nishito Y**, **Iemura S**, **Natsume T**, **Yanagawa T**, **Uwayama J**, **Warabi E**, **Yoshida H**, **Ishii T**, **Kobayashi A**, **Yamamoto M**, **Yue Z**, **Uchiyama Y**, **Kominami E**, **Tanaka K**. Homeostatic Levels of p62 Control Cytoplasmic Inclusion Body Formation in Autophagy-Deficient Mice. *Cell* 131: 1149–1163, 2007.
224. **Kondapalli C**, **Kazlauskaite A**, **Zhang N**, **Woodroof HI**, **Campbell DG**, **Gourlay R**, **Burchell L**, **Walden H**, **Macartney TJ**, **Deak M**, **Knebel A**, **Alessi DR**, **Muqit MMK**. PINK1 is activated by mitochondrial membrane potential depolarization and stimulates Parkin E3 ligase activity by phosphorylating Serine 65. *Open Biol* 2: 120080–120080, 2012.
225. **Koves TR**, **Noland RC**, **Bates AL**, **Henes ST**, **Muoio DM**, **Cortright RN**. Subsarcolemmal and intermyofibrillar mitochondria play distinct roles in regulating skeletal muscle fatty acid metabolism. *AJP Cell Physiol* 288: C1074–C1082, 2005.
226. **Koves TR**, **Ussher JR**, **Noland RC**, **Slentz D**, **Mosedale M**, **Ilkayeva O**, **Bain J**, **Stevens R**, **Dyck JRB**, **Newgard CB**, **Lopaschuk GD**, **Muoio DM**. Mitochondrial overload and incomplete fatty acid oxidation contribute to skeletal muscle insulin resistance. *Cell Metab* 7: 45–56, 2008.
227. **Kowald A**, **Kirkwood TBL**. Transcription could be the key to the selection advantage of mitochondrial deletion mutants in aging. *Proc Natl Acad Sci U S A* 111: 2972–7, 2014.

228. **Koyano F**, **Okatsu K**, **Kosako H**, **Tamura Y**, **Go E**, **Kimura M**, **Kimura Y**, **Tsuchiya H**, **Yoshihara H**, **Hirokawa T**, **Endo T**, **Fon EA**, **Trempe J-F**, **Saeki Y**, **Tanaka K**, **Matsuda N**. Ubiquitin is phosphorylated by PINK1 to activate parkin. *Nature* 510: 162–6, 2014.
229. **Krieger DA**, **Tate CA**, **McMillin-Wood J**, **Booth FW**. Populations of rat skeletal muscle mitochondria after exercise and immobilization. *J Appl Physiol* 48: 23–8, 1980.
230. **Kubli DA**, **Zhang X**, **Lee Y**, **Hanna RA**, **Quinsay MN**, **Nguyen CK**, **Jimenez R**, **Petrosyan S**, **Murphy AN**, **Gustafsson AB**. Parkin protein deficiency exacerbates cardiac injury and reduces survival following myocardial infarction. *J Biol Chem* 288: 915–26, 2013.
231. **Kujoth GC**, **Hiona A**, **Pugh TD**, **Someya S**, **Panzer K**, **Wohlgemuth SE**, **Hofer T**, **Seo AY**, **Sullivan R**, **Jobling WA**, **Morrow JD**, **Van Remmen H**, **Sedivy JM**, **Yamasoba T**, **Tanokura M**, **Weindruch R**, **Leeuwenburgh C**, **Prolla TA**. Mitochondrial DNA mutations, oxidative stress, and apoptosis in mammalian aging. *Science* 309: 481–4, 2005.
232. **Kuroda Y**, **Mitsui T**, **Kunishige M**, **Shono M**, **Akaike M**, **Azuma H**, **Matsumoto T**. Parkin enhances mitochondrial biogenesis in proliferating cells. *Hum Mol Genet* 15: 883–895, 2006.
233. **Laker RC**, **Drake JC**, **Wilson RJ**, **Lira VA**, **Lewellen BM**, **Ryall KA**, **Fisher CC**, **Zhang M**, **Saucerman JJ**, **Goodyear LJ**, **Kundu M**, **Yan Z**. Ampk phosphorylation of Ulk1 is required for targeting of mitochondria to lysosomes in exercise-induced mitophagy. *Nat Commun* 8: 548, 2017.
234. **Laker RC**, **Xu P**, **Ryall KA**, **Sujkowski A**, **Kenwood BM**, **Chain KH**, **Zhang M**, **Royal MA**, **Hoehn KL**, **Driscoll M**, **Adler PN**, **Wessells RJ**, **Saucerman JJ**, **Yan Z**. A Novel *MitoTimer* Reporter Gene for Mitochondrial Content, Structure, Stress, and Damage *in Vivo*. *J Biol Chem* 289: 12005–12015, 2014.
235. **Lakka TA**, **Laaksonen DE**. Physical activity in prevention and treatment of the metabolic syndrome. *Appl Physiol Nutr Metab* 32: 76–88, 2007.
236. **Landin-Wilhelmsen K**, **Wilhelmsen L**, **Lappas G**, **Rosén T**, **Lindstedt G**, **Lundberg PA**, **Bengtsson BA**. Serum insulin-like growth factor I in a random population sample of men and women: relation to age, sex, smoking habits, coffee consumption and physical activity, blood pressure and concentrations of plasma lipids, fibrinogen, parathyroid hormone and oste. *Clin Endocrinol (Oxf)* 41: 351–7, 1994.
237. **Landolfi B**, **Curci S**, **Debellis L**, **Pozzan T**, **Hofer AM**. Ca2+ homeostasis in the agonist-sensitive internal store: functional interactions between mitochondria and the ER measured In situ in intact cells. *J Cell Biol* 142: 1235–43, 1998.
238. **Langston JW**, **Ballard P**, **Tetrud JW**, **Irwin I**. Chronic Parkinsonism in humans due to a product of meperidine-analog synthesis. *Science* 219: 979–80, 1983.
239. **Lantier L**, **Fentz J**, **Mounier R**, **Leclerc J**, **Treebak JT**, **Pehmoller C**, **Sanz N**, **Sakakibara I**, **Saint-Amand E**, **Rimbaud S**, **Maire P**, **Marette A**, **Ventura-Clapier R**, **Ferry A**, **Wojtaszewski JFP**, **Foretz M**, **Viollet B**. AMPK controls exercise endurance, mitochondrial oxidative capacity, and skeletal muscle integrity. *FASEB J* 28: 3211–3224, 2014.
240. **Lanza IR**, **Short DK**, **Short KR**, **Raghavakaimal S**, **Basu R**, **Joyner MJ**, **McConnell JP**, **Nair KS**. Endurance Exercise as a Countermeasure for Aging. *Diabetes* 57: 2933–2942, 2008.
241. **Lau A**, **Wang X-J**, **Zhao F**, **Villeneuve NF**, **Wu T**, **Jiang T**, **Sun Z**, **White E**, **Zhang DD**. A Noncanonical Mechanism of Nrf2 Activation by Autophagy Deficiency: Direct Interaction between Keap1 and p62. *Mol Cell Biol* 30: 3275–3285, 2010.
242. **Lazarou M**, **Jin SM**, **Kane LA**, **Youle RJ**. Role of PINK1 binding to the TOM complex and alternate intracellular membranes in recruitment and activation of the E3 ligase Parkin. *Dev Cell* 22: 320–33, 2012.
243. **Lazarou M**, **Sliter DA**, **Kane LA**, **Sarraf SA**, **Wang C**, **Burman JL**, **Sideris DP**, **Fogel AI**, **Youle RJ**. The ubiquitin kinase PINK1 recruits autophagy receptors to induce mitophagy. *Nature* 524: 309–314, 2015.
244. **Lee CG**, **Boyko EJ**, **Strotmeyer ES**, **Lewis CE**, **Cawthon PM**, **Hoffman AR**, **Everson-Rose SA**, **Barrett-Connor E**, **Orwoll ES**. Association between insulin resistance and lean mass loss and fat mass gain in older men without diabetes mellitus. *J Am Geriatr Soc* 59: 1217–24, 2011.
245. **Lee CK**, **Klopp RG**, **Weindruch R**, **Prolla TA**. Gene expression profile of aging and its retardation by caloric restriction. *Science* 285: 1390–3, 1999.
246. **Lee CM**, **Lopez ME**, **Weindruch R**, **Aiken JM**. Association of age-related mitochondrial abnormalities with skeletal muscle fiber atrophy. *Free Radic Biol Med* 25: 964–72, 1998.
247. **Lee H-Y**, **Choi CS**, **Birkenfeld AL**, **Alves TC**, **Jornayvaz FR**, **Jurczak MJ**, **Zhang D**, **Woo DK**, **Shadel GS**, **Ladiges W**, **Rabinovitch PS**, **Santos JH**, **Petersen KF**, **Samuel VT**, **Shulman GI**. Targeted expression of catalase to mitochondria prevents age-associated reductions in mitochondrial function and insulin resistance. *Cell Metab* 12: 668–74, 2010.
248. **Lee JH**, **Budanov A V.**, **Park EJ**, **Birse R**, **Kim TE**, **Perkins GA**, **Ocorr K**, **Ellisman MH**, **Bodmer R**,

Bier E, **Karin M**. Sestrin as a Feedback Inhibitor of TOR That Prevents Age-Related Pathologies. *Science (80-)* 327: 1223–1228, 2010.
249. **Lee Y** et al. Mitochondrial autophagy by Bnip3 involves Drp1-mediated mitochondrial fission and recruitment of Parkin in cardiac myocytes. *Am J Physiol Heart Circ Physiol* 301: H1924-31, 2011.
250. **Lee Y**, **Stevens DA**, **Kang S-U**, **Jiang H**, **Lee Y-I**, **Ko HS**, **Scarffe LA**, **Umanah GE**, **Kang H**, **Ham S**, **Kam T-I**, **Allen K**, **Brahmachari S**, **Kim JW**, **Neifert S**, **Yun SP**, **Fiesel FC**, **Springer W**, **Dawson VL**, **Shin J-H**, **Dawson TM**. PINK1 Primes Parkin-Mediated Ubiquitination of PARIS in Dopaminergic Neuronal Survival. *Cell Rep* 18: 918–932, 2017.
251. **Leick L**, **Lyngby SS**, **Wojtasewski JF**, **Pilegaard H**, **Pilegaard H**. PGC-1α is required for training-induced prevention of age-associated decline in mitochondrial enzymes in mouse skeletal muscle. *Exp Gerontol* 45: 336–342, 2010.
252. **Lemasters JJ**. Selective Mitochondrial Autophagy, or Mitophagy, as a Targeted Defense Against Oxidative Stress, Mitochondrial Dysfunction, and Aging. *Rejuvenation Res* 8: 3–5, 2005.
253. **Levine B**, **Liang XH**, **Jackson S**, **Seaman M**, **Brown K**, **Kempkes B**, **Hibshoosh H**. Induction of autophagy and inhibition of tumorigenesis by beclin 1. *Nature* 402: 672–676, 1999.
254. **Lezza AM**, **Boffoli D**, **Scacco S**, **Cantatore P**, **Gadaleta MN**. Correlation between mitochondrial DNA 4977-bp deletion and respiratory chain enzyme activities in aging human skeletal muscles. *Biochem Biophys Res Commun* 205: 772–9, 1994.
255. **Lezza AM**, **Pesce V**, **Cormio A**, **Fracasso F**, **Vecchiet J**, **Felzani G**, **Cantatore P**, **Gadaleta MN**. Increased expression of mitochondrial transcription factor A and nuclear respiratory factor-1 in skeletal muscle from aged human subjects. *FEBS Lett* 501: 74–8, 2001.
256. **Li P**, **Nijhawan D**, **Budihardjo I**, **Srinivasula SM**, **Ahmad M**, **Alnemri ES**, **Wang X**. Cytochrome c and dATP-dependent formation of Apaf-1/caspase-9 complex initiates an apoptotic protease cascade. *Cell* 91: 479–89, 1997.
257. **Lim J**, **Lachenmayer ML**, **Wu S**, **Liu W**, **Kundu M**, **Wang R**, **Komatsu M**, **Oh YJ**, **Zhao Y**, **Yue Z**. Proteotoxic Stress Induces Phosphorylation of p62/SQSTM1 by ULK1 to Regulate Selective Autophagic Clearance of Protein Aggregates. *PLOS Genet* 11: e1004987, 2015.
258. **Lim KL**, **Chew KCM**, **Tan JMM**, **Wang C**, **Chung KKK**, **Zhang Y**, **Tanaka Y**, **Smith W**, **Engelender S**, **Ross CA**, **Dawson VL**, **Dawson TM**. Parkin Mediates Nonclassical, Proteasomal-Independent Ubiquitination of Synphilin-1: Implications for Lewy Body Formation. *J Neurosci* 25: 2002–2009, 2005.
259. **Lindmo K**, **Stenmark H**. Regulation of membrane traffic by phosphoinositide 3-kinases. *J Cell Sci* 119: 605–14, 2006.
260. **Linnane AW**, **Baumer A**, **Maxwell RJ**, **Preston H**, **Zhang CF**, **Marzuki S**. Mitochondrial gene mutation: the ageing process and degenerative diseases. *Biochem Int* 22: 1067–76, 1990.
261. **Lira VA**, **Okutsu M**, **Zhang M**, **Greene NP**, **Laker RC**, **Breen DS**, **Hoehn KL**, **Yan Z**. Autophagy is required for exercise training-induced skeletal muscle adaptation and improvement of physical performance. *FASEB J* 27: 4184–93, 2013.
262. **Liu L**, **Feng D**, **Chen G**, **Chen M**, **Zheng Q**, **Song P**, **Ma Q**, **Zhu C**, **Wang R**, **Qi W**, **Huang L**, **Xue P**, **Li B**, **Wang X**, **Jin H**, **Wang J**, **Yang F**, **Liu P**, **Zhu Y**, **Sui S**, **Chen Q**. Mitochondrial outer-membrane protein FUNDC1 mediates hypoxia-induced mitophagy in mammalian cells. *Nat Cell Biol* 14: 177–185, 2012.
263. **Liu X**, **Jiang N**, **Hughes B**, **Bigras E**, **Shoubridge E**, **Hekimi S**. Evolutionary conservation of the clk-1-dependent mechanism of longevity: loss of mclk1 increases cellular fitness and lifespan in mice. *Genes Dev* 19: 2424–34, 2005.
264. **Livnat-Levanon N**, **Kevei É**, **Kleifeld O**, **Krutauz D**, **Segref A**, **Rinaldi T**, **Erpapazoglou Z**, **Cohen M**, **Reis N**, **Hoppe T**, **Glickman MH**. Reversible 26S proteasome disassembly upon mitochondrial stress. *Cell Rep* 7: 1371–80, 2014.
265. **Ljubicic V**, **Hood DA**. Kinase-specific responsiveness to incremental contractile activity in skeletal muscle with low and high mitochondrial content. *Am J Physiol Endocrinol Metab* 295: E195-204, 2008.
266. **Ljubicic V**, **Hood DA**. Diminished contraction-induced intracellular signaling towards mitochondrial biogenesis in aged skeletal muscle. *Aging Cell* 8: 394–404, 2009.
267. **Ljubicic V**, **Joseph A-M**, **Adhihetty PJ**, **Huang JH**, **Saleem A**, **Uguccioni G**, **Hood DA**. Molecular basis for an attenuated mitochondrial adaptive plasticity in aged skeletal muscle. *Aging (Albany NY)* 1: 818–30, 2009.
268. **Lopez-Crisosto C**, **Pennanen C**, **Vasquez-Trincado C**, **Morales PE**, **Bravo-Sagua R**, **Quest AFG**, **Chiong M**, **Lavandero S**. Sarcoplasmic reticulum–mitochondria communication in cardiovascular

pathophysiology. *Nat Rev Cardiol* 14: 342–360, 2017.
269. **Lopez ME**, **Van Zeeland NL**, **Dahl DB**, **Weindruch R**, **Aiken JM**. Cellular phenotypes of age-associated skeletal muscle mitochondrial abnormalities in rhesus monkeys. *Mutat Res* 452: 123–38, 2000.
270. **Lubos E**, **Loscalzo J**, **Handy DE**. Glutathione peroxidase-1 in health and disease: from molecular mechanisms to therapeutic opportunities. *Antioxid Redox Signal* 15: 1957–97, 2011.
271. **Luce K**, **Osiewacz HD**. Increasing organismal healthspan by enhancing mitochondrial protein quality control. *Nat Cell Biol* 11: 852–858, 2009.
272. **Maddux BA**, **See W**, **Lawrence JC**, **Goldfine AL**, **Goldfine ID**, **Evans JL**. Protection against oxidative stress-induced insulin resistance in rat L6 muscle cells by mircomolar concentrations of alpha-lipoic acid. *Diabetes* 50: 404–10, 2001.
273. **Mahoney DJ**, **Parise G**, **Melov S**, **Safdar A**, **Tarnopolsky MA**. Analysis of global mRNA expression in human skeletal muscle during recovery from endurance exercise. *FASEB J* 19: 1498–500, 2005.
274. **Mann SS**, **Hammarback JA**. Molecular characterization of light chain 3. A microtubule binding subunit of MAP1A and MAP1B. *J Biol Chem* 269: 11492–7, 1994.
275. **Mansueto G**, **Armani A**, **Viscomi C**, **D'Orsi L**, **De Cegli R**, **Polishchuk E V**, **Lamperti C**, **Di Meo I**, **Romanello V**, **Marchet S**, **Saha PK**, **Zong H**, **Blaauw B**, **Solagna F**, **Tezze C**, **Grumati P**, **Bonaldo P**, **Pessin JE**, **Zeviani M**, **Sandri M**, **Ballabio A**. Transcription Factor EB Controls Metabolic Flexibility during Exercise. *Cell Metab* 25: 182–196, 2017.
276. **Manzanillo PS**, **Ayres JS**, **Watson RO**, **Collins AC**, **Souza G**, **Rae CS**, **Schneider DS**, **Nakamura K**, **Shiloh MU**, **Cox JS**. The ubiquitin ligase parkin mediates resistance to intracellular pathogens. *Nature* 501: 512–6, 2013.
277. **Margineantu DH**, **Emerson CB**, **Diaz D**, **Hockenbery DM**. Hsp90 Inhibition Decreases Mitochondrial Protein Turnover. *PLoS One* 2: e1066, 2007.
278. **Maria Fimia G**, **Stoykova A**, **Romagnoli A**, **Giunta L**, **Di Bartolomeo S**, **Nardacci R**, **Corazzari M**, **Fuoco C**, **Ucar A**, **Schwartz P**, **Gruss P**, **Piacentini M**, **Chowdhury K**, **Cecconi F**. Ambra1 regulates autophagy and development of the nervous system. *Nature* 447: 1121–5, 2007.
279. **Marzetti E**, **Wohlgemuth SE**, **Lees HA**, **Chung H-Y**, **Giovannini S**, **Leeuwenburgh C**. Age-related activation of mitochondrial caspase-independent apoptotic signaling in rat gastrocnemius muscle. *Mech Ageing Dev* 129: 542–549, 2008.
280. **Marzo I**, **Brenner C**, **Zamzami N**, **Jürgensmeier JM**, **Susin SA**, **Vieira HL**, **Prévost MC**, **Xie Z**, **Matsuyama S**, **Reed JC**, **Kroemer G**. Bax and adenine nucleotide translocator cooperate in the mitochondrial control of apoptosis. *Science* 281: 2027–31, 1998.
281. **Matsuda N**, **Kitami T**, **Suzuki T**, **Mizuno Y**, **Hattori N**, **Tanaka K**. Diverse Effects of Pathogenic Mutations of Parkin That Catalyze Multiple Monoubiquitylation *in Vitro*. *J Biol Chem* 281: 3204–3209, 2006.
282. **Matsuda N**, **Sato S**, **Shiba K**, **Okatsu K**, **Saisho K**, **Gautier CA**, **Sou Y-S**, **Saiki S**, **Kawajiri S**, **Sato F**, **Kimura M**, **Komatsu M**, **Hattori N**, **Tanaka K**. PINK1 stabilized by mitochondrial depolarization recruits Parkin to damaged mitochondria and activates latent Parkin for mitophagy. *J Cell Biol* 189: 211–21, 2010.
283. **Matsumine H**, **Saito M**, **Shimoda-Matsubayashi S**, **Tanaka H**, **Ishikawa A**, **Nakagawa-Hattori Y**, **Yokochi M**, **Kobayashi T**, **Igarashi S**, **Takano H**, **Sanpei K**, **Koike R**, **Mori H**, **Kondo T**, **Mizutani Y**, **Schäffer AA**, **Yamamura Y**, **Nakamura S**, **Kuzuhara S**, **Tsuji S**, **Mizuno Y**. Localization of a gene for an autosomal recessive form of juvenile Parkinsonism to chromosome 6q25.2-27. *Am J Hum Genet* 60: 588–96, 1997.
284. **Matsushima Y**, **Goto Y -i.**, **Kaguni LS**. Mitochondrial Lon protease regulates mitochondrial DNA copy number and transcription by selective degradation of mitochondrial transcription factor A (TFAM). *Proc Natl Acad Sci* 107: 18410–18415, 2010.
285. **McLelland G-L**, **Soubannier V**, **Chen CX**, **McBride HM**, **Fon EA**. Parkin and PINK1 function in a vesicular trafficking pathway regulating mitochondrial quality control. *EMBO J* 33: 282–95, 2014.
286. **Meissner C**, **Lorenz H**, **Hehn B**, **Lemberg MK**. Intramembrane protease PARL defines a negative regulator of PINK1- and PARK2/Parkin-dependent mitophagy. *Autophagy* 11: 1484–1498, 2015.
287. **Melendez A**, **Tallóczy Z**, **Seaman M**, **Eskelinen E-L**, **Hall DH**, **Levine B**. Autophagy Genes Are Essential for Dauer Development and Life-Span Extension in C. elegans. *Science (80-)* 301: 1387–1391, 2003.
288. **Melov S**, **Shoffner JM**, **Kaufman A**, **Wallace DC**. Marked increase in the number and variety of mitochondrial DNA rearrangements in aging human skeletal muscle. *Nucleic Acids Res* 23: 4122–6, 1995.
289. **Mercer CA**, **Kaliappan A**, **Dennis PB**. A novel, human Atg13 binding protein, Atg101, interacts with ULK1 and is essential for macroautophagy. *Autophagy* 5: 649–62, 2009.

290. **Mesbah Moosavi ZS**, **Hood DA**. The unfolded protein response in relation to mitochondrial biogenesis in skeletal muscle cells. *Am J Physiol - Cell Physiol* 312: C583–C594, 2017.
291. **Mihara K**, **Omura T**. Cytoplasmic chaperones in precursor targeting to mitochondria: the role of MSF and hsp 70. *Trends Cell Biol* 6: 104–8, 1996.
292. **MITCHELL P**. Coupling of phosphorylation to electron and hydrogen transfer by a chemi-osmotic type of mechanism. *Nature* 191: 144–8, 1961.
293. **Mizushima N**, **Kuma A**, **Kobayashi Y**, **Yamamoto A**, **Matsubae M**, **Takao T**, **Natsume T**, **Ohsumi Y**, **Yoshimori T**. Mouse Apg16L, a novel WD-repeat protein, targets to the autophagic isolation membrane with the Apg12-Apg5 conjugate. *J Cell Sci* 116: 1679–88, 2003.
294. **Mizushima N**, **Sugita H**, **Yoshimori T**, **Ohsumi Y**. A new protein conjugation system in human. The counterpart of the yeast Apg12p conjugation system essential for autophagy. *J Biol Chem* 273: 33889–92, 1998.
295. **Mizushima N**, **Yamamoto A**, **Hatano M**, **Kobayashi Y**, **Kabeya Y**, **Suzuki K**, **Tokuhisa T**, **Ohsumi Y**, **Yoshimori T**. Dissection of autophagosome formation using Apg5-deficient mouse embryonic stem cells. *J Cell Biol* 152: 657–68, 2001.
296. **Mizushima N**, **Yamamoto A**, **Matsui M**, **Yoshimori T**, **Ohsumi Y**. In vivo analysis of autophagy in response to nutrient starvation using transgenic mice expressing a fluorescent autophagosome marker. *Mol Biol Cell* 15: 1101–11, 2004.
297. **Mohanty A**, **McBride HM**. Emerging roles of mitochondria in the evolution, biogenesis, and function of peroxisomes. *Front Physiol* 4: 268, 2013.
298. **Møller AB**, **Vendelbo MH**, **Christensen B**, **Clasen BF**, **Bak AM**, **Jørgensen JOL**, **Møller N**, **Jessen N**. Physical exercise increases autophagic signaling through ULK1 in human skeletal muscle. *J Appl Physiol* 118: 971–979, 2015.
299. **Moore DJ**, **West AB**, **Dikeman DA**, **Dawson VL**, **Dawson TM**. Parkin mediates the degradation-independent ubiquitination of Hsp70. *J Neurochem* 105: 1806–1819, 2008.
300. **Mootha VK**, **Lindgren CM**, **Eriksson K-F**, **Subramanian A**, **Sihag S**, **Lehar J**, **Puigserver P**, **Carlsson E**, **Ridderstråle M**, **Laurila E**, **Houstis N**, **Daly MJ**, **Patterson N**, **Mesirov JP**, **Golub TR**, **Tamayo P**, **Spiegelman B**, **Lander ES**, **Hirschhorn JN**, **Altshuler D**, **Groop LC**. PGC-1α-responsive genes involved in oxidative phosphorylation are coordinately downregulated in human diabetes. *Nat Genet* 34: 267–273, 2003.
301. **Mounier R**, **Théret M**, **Lantier L**, **Foretz M**, **Viollet B**. Expanding roles for AMPK in skeletal muscle plasticity. *Trends Endocrinol Metab* 26: 275–86, 2015.
302. **Mozdy AD**, **McCaffery JM**, **Shaw JM**. Dnm1p GTPase-mediated mitochondrial fission is a multi-step process requiring the novel integral membrane component Fis1p. *J Cell Biol* 151: 367–80, 2000.
303. **Müller W**. Subsarcolemmal mitochondria and capillarization of soleus muscle fibers in young rats subjected to an endurance training. A morphometric study of semithin sections. *Cell Tissue Res* 174: 367–89, 1976.
304. **Murphy MP**. How mitochondria produce reactive oxygen species. *Biochem J* 417: 1–13, 2009.
305. **Narendra D**, **Kane LA**, **Hauser DN**, **Fearnley IM**, **Youle RJ**. p62/SQSTM1 is required for Parkin-induced mitochondrial clustering but not mitophagy; VDAC1 is dispensable for both. *Autophagy* 6: 1090–106, 2010.
306. **Narendra D**, **Tanaka A**, **Suen D-F**, **Youle RJ**. Parkin is recruited selectively to impaired mitochondria and promotes their autophagy. *J Cell Biol* 183: 795–803, 2008.
307. **Navarro A**, **Gomez C**, **López-Cepero JM**, **Boveris A**. Beneficial effects of moderate exercise on mice aging: survival, behavior, oxidative stress, and mitochondrial electron transfer. *AJP Regul Integr Comp Physiol* 286: 505R–511, 2004.
308. **Nazio F**, **Strappazzon F**, **Antonioli M**, **Bielli P**, **Cianfanelli V**, **Bordi M**, **Gretzmeier C**, **Dengjel J**, **Piacentini M**, **Fimia GM**, **Cecconi F**. mTOR inhibits autophagy by controlling ULK1 ubiquitylation, self-association and function through AMBRA1 and TRAF6. *Nat Cell Biol* 15: 406–416, 2013.
309. **Nemoto T**, **Tanida I**, **Tanida-Miyake E**, **Minematsu-Ikeguchi N**, **Yokota M**, **Ohsumi M**, **Ueno T**, **Kominami E**. The mouse APG10 homologue, an E2-like enzyme for Apg12p conjugation, facilitates MAP-LC3 modification. *J Biol Chem* 278: 39517–26, 2003.
310. **Neupert W**, **Herrmann JM**. Translocation of proteins into mitochondria. *Annu Rev Biochem* 76: 723–49, 2007.
311. **Neuspiel M**, **Schauss AC**, **Braschi E**, **Zunino R**, **Rippstein P**, **Rachubinski RA**, **Andrade-Navarro MA**, **McBride HM**. Cargo-Selected Transport from the Mitochondria to Peroxisomes Is Mediated by Vesicular Carriers. *Curr Biol* 18: 102–108, 2008.
312. **Nezich CL**, **Wang C**, **Fogel AI**, **Youle RJ**. MiT/TFE transcription factors are activated during mitophagy

downstream of Parkin and Atg5. *J Cell Biol* 210: 435–450, 2015.
313. **Nicklas WJ**, **Vyas I**, **Heikkila RE**. Inhibition of NADH-linked oxidation in brain mitochondria by 1-methyl-4-phenyl-pyridine, a metabolite of the neurotoxin, 1-methyl-4-phenyl-1,2,5,6-tetrahydropyridine. *Life Sci* 36: 2503–8, 1985.
314. **Novak I**, **Kirkin V**, **McEwan DG**, **Zhang J**, **Wild P**, **Rozenknop A**, **Rogov V**, **Löhr F**, **Popovic D**, **Occhipinti A**, **Reichert AS**, **Terzic J**, **Dötsch V**, **Ney PA**, **Dikic I**. Nix is a selective autophagy receptor for mitochondrial clearance. *EMBO Rep* 11: 45–51, 2010.
315. **O'Connor KG**, **Tobin JD**, **Harman SM**, **Plato CC**, **Roy TA**, **Sherman SS**, **Blackman MR**. Serum levels of insulin-like growth factor-I are related to age and not to body composition in healthy women and men. *J Gerontol A Biol Sci Med Sci* 53: M176-82, 1998.
316. **O'Leary MF**, **Vainshtein A**, **Iqbal S**, **Ostojic O**, **Hood DA**. Adaptive plasticity of autophagic proteins to denervation in aging skeletal muscle. *Am J Physiol Cell Physiol* 304: C422-30, 2013.
317. **Ogata T**, **Yamasaki Y**. Scanning electron-microscopic studies on the three-dimensional structure of sarcoplasmic reticulum in the mammalian red, white and intermediate muscle fibers. *Cell Tissue Res* 242: 461–7, 1985.
318. **Ogata T**, **Yamasaki Y**. High-resolution scanning electron-microscopic studies on the three-dimensional structure of mitochondria and sarcoplasmic reticulum in the different twitch muscle fibers of the frog. *Cell Tissue Res* 250: 489–97, 1987.
319. **Ohsumi Y**, **Ichimura Y**, **Kirisako T**, **Takao T**, **Satomi Y**, **Shimonishi Y**, **Ishihara N**, **Mizushima N**, **Tanida I**, **Kominami E**, **Ohsumi M**, **Noda T**. A ubiquitin-like system mediates protein lipidation. *Nature* 408: 488–492, 2000.
320. **Okatsu K**, **Oka T**, **Iguchi M**, **Imamura K**, **Kosako H**, **Tani N**, **Kimura M**, **Go E**, **Koyano F**, **Funayama M**, **Shiba-Fukushima K**, **Sato S**, **Shimizu H**, **Fukunaga Y**, **Taniguchi H**, **Komatsu M**, **Hattori N**, **Mihara K**, **Tanaka K**, **Matsuda N**. PINK1 autophosphorylation upon membrane potential dissipation is essential for Parkin recruitment to damaged mitochondria. *Nat Commun* 3: 1016, 2012.
321. **Olzmann JA**, **Li L**, **Chudaev M V.**, **Chen J**, **Perez FA**, **Palmiter RD**, **Chin L-S**. Parkin-mediated K63-linked polyubiquitination targets misfolded DJ-1 to aggresomes via binding to HDAC6. *J Cell Biol* 178: 1025–1038, 2007.
322. **Ordureau A**, **Sarraf SA**, **Duda DM**, **Heo J-M**, **Jedrychowski MP**, **Sviderskiy VO**, **Olszewski JL**, **Koerber JT**, **Xie T**, **Beausoleil SA**, **Wells JA**, **Gygi SP**, **Schulman BA**, **Harper JW**. Quantitative Proteomics Reveal a Feedforward Mechanism for Mitochondrial PARKIN Translocation and Ubiquitin Chain Synthesis. *Mol Cell* 56: 360–375, 2014.
323. **Otomo C**, **Metlagel Z**, **Takaesu G**, **Otomo T**. Structure of the human ATG12~ATG5 conjugate required for LC3 lipidation in autophagy. *Nat Struct Mol Biol* 20: 59–66, 2012.
324. **Owusu-Ansah E**, **Song W**, **Perrimon N**. Muscle mitohormesis promotes longevity via systemic repression of insulin signaling. *Cell* 155: 699–712, 2013.
325. **Pagano AF**, **Py G**, **Bernardi H**, **Candau RB**, **Sanchez AMJ**. Autophagy and protein turnover signaling in slow-twitch muscle during exercise. *Med Sci Sports Exerc* 46: 1314–1325, 2014.
326. **Palikaras K**, **Lionaki E**, **Tavernarakis N**. Coordination of mitophagy and mitochondrial biogenesis during ageing in C. elegans. *Nature* 521: 525–528, 2015.
327. **Palmieri M**, **Impey S**, **Kang H**, **di Ronza A**, **Pelz C**, **Sardiello M**, **Ballabio A**. Characterization of the CLEAR network reveals an integrated control of cellular clearance pathways. *Hum Mol Genet* 20: 3852–66, 2011.
328. **Pankiv S**, **Clausen TH**, **Lamark T**, **Brech A**, **Bruun J-A**, **Outzen H**, **Øvervatn A**, **Bjørkøy G**, **Johansen T**. p62/SQSTM1 Binds Directly to Atg8/LC3 to Facilitate Degradation of Ubiquitinated Protein Aggregates by Autophagy. *J Biol Chem* 282: 24131–24145, 2007.
329. **Partridge L**, **Alic N**, **Bjedov I**, **Piper MDW**. Ageing in Drosophila: The role of the insulin/Igf and TOR signalling network. *Exp Gerontol* 46: 376–381, 2011.
330. **Peña-Llopis S**, **Vega-Rubin-de-Celis S**, **Schwartz JC**, **Wolff NC**, **Tran TAT**, **Zou L**, **Xie X-J**, **Corey DR**, **Brugarolas J**. Regulation of TFEB and V-ATPases by mTORC1. *EMBO J* 30: 3242–58, 2011.
331. **Peña S**, **Sherman T**, **Brookes PS**, **Nehrke K**. The Mitochondrial Unfolded Protein Response Protects against Anoxia in Caenorhabditis elegans. *PLoS One* 11: e0159989, 2016.
332. **Perrini S**, **Laviola L**, **Carreira MC**, **Cignarelli A**, **Natalicchio A**, **Giorgino F**. The GH/IGF1 axis and signaling pathways in the muscle and bone: mechanisms underlying age-related skeletal muscle wasting and osteoporosis. *J Endocrinol* 205: 201–10, 2010.
333. **Pesce V**, **Cormio A**, **Fracasso F**, **Lezza AMS**, **Cantatore P**, **Gadaleta MN**. Age-related changes of

mitochondrial DNA content and mitochondrial genotypic and phenotypic alterations in rat hind-limb skeletal muscles. *J Gerontol A Biol Sci Med Sci* 60: 715–23, 2005.
334. **Petersen AC**, **McKenna MJ**, **Medved I**, **Murphy KT**, **Brown MJ**, **Della Gatta P**, **Cameron-Smith D**. Infusion with the antioxidant N-acetylcysteine attenuates early adaptive responses to exercise in human skeletal muscle. *Acta Physiol* 204: 382–392, 2012.
335. **Petersen KF**, **Befroy D**, **Dufour S**, **Dziura J**, **Ariyan C**, **Rothman DL**, **DiPietro L**, **Cline GW**, **Shulman GI**. Mitochondrial dysfunction in the elderly: possible role in insulin resistance. *Science* 300: 1140–2, 2003.
336. **Pfanner N**, **Truscott KN**. Powering mitochondrial protein import. *Nat Struct Biol* 9: 234–6, 2002.
337. **Picard M**, **White K**, **Turnbull DM**. Mitochondrial morphology, topology, and membrane interactions in skeletal muscle: a quantitative three-dimensional electron microscopy study. *J Appl Physiol* 114: 161–71, 2013.
338. **Pickrell AM**, **Huang C-H**, **Kennedy SR**, **Ordureau A**, **Sideris DP**, **Hoekstra JG**, **Harper JW**, **Youle RJ**. Endogenous Parkin Preserves Dopaminergic Substantia Nigral Neurons following Mitochondrial DNA Mutagenic Stress. *Neuron* 87: 371–381, 2015.
339. **Pickrell AM**, **Youle RJ**. The roles of PINK1, parkin, and mitochondrial fidelity in Parkinson's disease. *Neuron* 85: 257–73, 2015.
340. **Pilegaard H**, **Ordway GA**, **Saltin B**, **Neufer PD**. Transcriptional regulation of gene expression in human skeletal muscle during recovery from exercise. *Am J Physiol Endocrinol Metab* 279: E806-14, 2000.
341. **Pilegaard H**, **Saltin B**, **Neufer PD**. Exercise induces transient transcriptional activation of the PGC-1alpha gene in human skeletal muscle. *J Physiol* 546: 851–8, 2003.
342. **Piquereau J**, **Godin R**, **Deschênes S**, **Bessi VL**, **Mofarrahi M**, **Hussain SN**, **Burelle Y**. Protective role of PARK2/Parkin in sepsis-induced cardiac contractile and mitochondrial dysfunction. *Autophagy* 9: 1837–51, 2013.
343. **Pogozelski AR**, **Geng T**, **Li P**, **Yin X**, **Lira VA**, **Zhang M**, **Chi J-T**, **Yan Z**. p38gamma mitogen-activated protein kinase is a key regulator in skeletal muscle metabolic adaptation in mice. *PLoS One* 4: e7934, 2009.
344. **Polymeropoulos MH**, **Lavedan C**, **Leroy E**, **Ide SE**, **Dehejia A**, **Dutra A**, **Pike B**, **Root H**, **Rubenstein J**, **Boyer R**, **Stenroos ES**, **Chandrasekharappa S**, **Athanassiadou A**, **Papapetropoulos T**, **Johnson WG**, **Lazzarini AM**, **Duvoisin RC**, **Di Iorio G**, **Golbe LI**, **Nussbaum RL**. Mutation in the alpha-synuclein gene identified in families with Parkinson's disease. *Science* 276: 2045–7, 1997.
345. **Powers RW**, **Kaeberlein M**, **Caldwell SD**, **Kennedy BK**, **Fields S**. Extension of chronological life span in yeast by decreased TOR pathway signaling. *Genes Dev* 20: 174–184, 2006.
346. **Powers SK**, **Duarte J**, **Kavazis AN**, **Talbert EE**. Reactive oxygen species are signalling molecules for skeletal muscle adaptation. *Exp Physiol* 95: 1–9, 2010.
347. **Puigserver P**, **Rhee J**, **Lin J**, **Wu Z**, **Yoon JC**, **Zhang CY**, **Krauss S**, **Mootha VK**, **Lowell BB**, **Spiegelman BM**. Cytokine stimulation of energy expenditure through p38 MAP kinase activation of PPARgamma coactivator-1. *Mol Cell* 8: 971–82, 2001.
348. **Quinsay MN**, **Thomas RL**, **Lee Y**, **Gustafsson AB**. Bnip3-mediated mitochondrial autophagy is independent of the mitochondrial permeability transition pore. *Autophagy* 6: 855–62, 2010.
349. **Radak Z**, **Zhao Z**, **Koltai E**, **Ohno H**, **Atalay M**. Oxygen Consumption and Usage During Physical Exercise: The Balance Between Oxidative Stress and ROS-Dependent Adaptive Signaling. *Antioxid Redox Signal* 18: 1208–1246, 2013.
350. **Radke S**, **Chander H**, **Schafer P**, **Meiss G**, **Kruger R**, **Schulz JB**, **Germain D**. Mitochondrial Protein Quality Control by the Proteasome Involves Ubiquitination and the Protease Omi. *J Biol Chem* 283: 12681–12685, 2008.
351. **Rana A**, **Rera M**, **Walker DW**. Parkin overexpression during aging reduces proteotoxicity, alters mitochondrial dynamics, and extends lifespan. *Proc Natl Acad Sci U S A* 110: 8638–43, 2013.
352. **Rasmussen BB**, **Fujita S**, **Wolfe RR**, **Mittendorfer B**, **Roy M**, **Rowe VL**, **Volpi E**. Insulin resistance of muscle protein metabolism in aging. *FASEB J* 20: 768–9, 2006.
353. **Rasola A**, **Bernardi P**. The mitochondrial permeability transition pore and its involvement in cell death and in disease pathogenesis. *Apoptosis* 12: 815–833, 2007.
354. **Regula KM**, **Ens K**, **Kirshenbaum LA**. Inducible expression of BNIP3 provokes mitochondrial defects and hypoxia-mediated cell death of ventricular myocytes. *Circ Res* 91: 226–31, 2002.
355. **Reznick RM**, **Zong H**, **Li J**, **Morino K**, **Moore IK**, **Yu HJ**, **Liu Z-X**, **Dong J**, **Mustard KJ**, **Hawley SA**, **Befroy D**, **Pypaert M**, **Hardie DG**, **Young LH**, **Shulman GI**. Aging-Associated Reductions in AMP-Activated Protein Kinase Activity and Mitochondrial Biogenesis. *Cell Metab* 5: 151–156, 2007.
356. **Richter B**, **Sliter DA**, **Herhaus L**, **Stolz A**, **Wang C**, **Beli P**, **Zaffagnini G**, **Wild P**, **Martens S**, **Wagner**

SA, **Youle RJ**, **Dikic I**. Phosphorylation of OPTN by TBK1 enhances its binding to Ub chains and promotes selective autophagy of damaged mitochondria. *Proc Natl Acad Sci* 113: 4039–4044, 2016.
357. **Richter EA**, **Jensen P**, **Kiens B**, **Kristiansen S**. during exercise are diminished by endurance training Sarcolemmal glucose transport and GLUT-4 translocation Sarcolemmal glucose transport and GLUT-4 translocation during exercise are diminished by endurance training. *Am J Physiol Endocrinol Metab Am J Physiol -Endocrinology Metab Doshisha Univ* 274: 89–95, 1998.
358. **Riley BE**, **Lougheed JC**, **Callaway K**, **Velasquez M**, **Brecht E**, **Nguyen L**, **Shaler T**, **Walker D**, **Yang Y**, **Regnstrom K**, **Diep L**, **Zhang Z**, **Chiou S**, **Bova M**, **Artis DR**, **Yao N**, **Baker J**, **Yednock T**, **Johnston JA**. Structure and function of Parkin E3 ubiquitin ligase reveals aspects of RING and HECT ligases. *Nat Commun* 4: ncomms2982, 2013.
359. **Rios E**, **Brum G**. Involvement of dihydropyridine receptors in excitation–contraction coupling in skeletal muscle. *Nature* 325: 717–720, 1987.
360. **Ritov VB**, **Menshikova E V**, **He J**, **Ferrell RE**, **Goodpaster BH**, **Kelley DE**. Deficiency of subsarcolemmal mitochondria in obesity and type 2 diabetes. *Diabetes* 54: 8–14, 2005.
361. **Rogers MA**, **Evans WJ**. Changes in skeletal muscle with aging: effects of exercise training. *Exerc Sport Sci Rev* 21: 65–102, 1993.
362. **Romanello V**, **Guadagnin E**, **Gomes L**, **Roder I**, **Sandri C**, **Petersen Y**, **Milan G**, **Masiero E**, **Del Piccolo P**, **Foretz M**, **Scorrano L**, **Rudolf R**, **Sandri M**. Mitochondrial fission and remodelling contributes to muscle atrophy. *EMBO J* 29: 1774–1785, 2010.
363. **Rommel C**, **Bodine SC**, **Clarke BA**, **Rossman R**, **Nunez L**, **Stitt TN**, **Yancopoulos GD**, **Glass DJ**. Mediation of IGF-1-induced skeletal myotube hypertrophy by PI(3)K/Akt/mTOR and PI(3)K/Akt/GSK3 pathways. *Nat Cell Biol* 3: 1009–1013, 2001.
364. **Rooyackers OE**, **Adey DB**, **Ades PA**, **Nair KS**. Effect of age on in vivo rates of mitochondrial protein synthesis in human skeletal muscle. *Proc Natl Acad Sci U S A* 93: 15364–9, 1996.
365. **Rose AJ**, **Kiens B**, **Richter EA**. Ca $^{2+}$ -calmodulin-dependent protein kinase expression and signalling in skeletal muscle during exercise. *J Physiol* 574: 889–903, 2006.
366. **Rothfuss O**, **Fischer H**, **Hasegawa T**, **Maisel M**, **Leitner P**, **Miesel F**, **Sharma M**, **Bornemann A**, **Berg D**, **Gasser T**, **Patenge N**. Parkin protects mitochondrial genome integrity and supports mitochondrial DNA repair. *Hum Mol Genet* 18: 3832–3850, 2009.
367. **Rubinsztein DC**, **Mariño G**, **Kroemer G**. Autophagy and aging. *Cell* 146: 682–95, 2011.
368. **Russell RC**, **Tian Y**, **Yuan H**, **Park HW**, **Chang Y-Y**, **Kim J**, **Kim H**, **Neufeld TP**, **Dillin A**, **Guan K-L**. ULK1 induces autophagy by phosphorylating Beclin-1 and activating VPS34 lipid kinase. *Nat Cell Biol* 15: 741–750, 2013.
369. **Safdar A**, **Bourgeois JM**, **Ogborn DI**, **Little JP**, **Hettinga BP**, **Akhtar M**, **Thompson JE**, **Melov S**, **Mocellin NJ**, **Kujoth GC**, **Prolla TA**, **Tarnopolsky MA**. Endurance exercise rescues progeroid aging and induces systemic mitochondrial rejuvenation in mtDNA mutator mice. *Proc Natl Acad Sci U S A* 108: 4135–40, 2011.
370. **Safdar A**, **Little JP**, **Stokl AJ**, **Hettinga BP**, **Akhtar M**, **Tarnopolsky MA**. Exercise increases mitochondrial PGC-1alpha content and promotes nuclear-mitochondrial cross-talk to coordinate mitochondrial biogenesis. *J Biol Chem* 286: 10605–17, 2011.
371. **Sagiv Y**, **Legesse-Miller A**, **Porat A**, **Elazar Z**. GATE-16, a membrane transport modulator, interacts with NSF and the Golgi v-SNARE GOS-28. *EMBO J* 19: 1494–1504, 2000.
372. **Sakellariou GK**, **Pearson T**, **Lightfoot AP**, **Nye GA**, **Wells N**, **Giakoumaki II**, **Griffiths RD**, **McArdle A**, **Jackson MJ**. Long-term administration of the mitochondria-targeted antioxidant mitoquinone mesylate fails to attenuate age-related oxidative damage or rescue the loss of muscle mass and function associated with aging of skeletal muscle. *FASEB J* 30: 3771–3785, 2016.
373. **Sakellariou GK**, **Pearson T**, **Lightfoot AP**, **Nye GA**, **Wells N**, **Giakoumaki II**, **Vasilaki A**, **Griffiths RD**, **Jackson MJ**, **McArdle A**. Mitochondrial ROS regulate oxidative damage and mitophagy but not age-related muscle fiber atrophy. *Sci Rep* 6: 33944, 2016.
374. **Sallis RE**. Exercise is medicine and physicians need to prescribe it! *Br J Sports Med* 43: 3–4, 2008.
375. **Salminen A**, **Vihko V**. Autophagic response to strenuous exercise in mouse skeletal muscle fibers. *Virchows Arch B Cell Pathol Incl Mol Pathol* 45: 97–106, 1984.
376. **Sandoval H**, **Thiagarajan P**, **Dasgupta SK**, **Schumacher A**, **Prchal JT**, **Chen M**, **Wang J**. Essential role for Nix in autophagic maturation of erythroid cells. *Nature* 454: 232–235, 2008.
377. **Sandri M**, **Barberi L**, **Bijlsma AY**, **Blaauw B**, **Dyar KA**, **Milan G**, **Mammucari C**, **Meskers CGM**, **Pallafacchina G**, **Paoli A**, **Pion D**, **Roceri M**, **Romanello V**, **Serrano AL**, **Toniolo L**, **Larsson L**, **Maier**

AB, **Muñoz-Cánoves P**, **Musarò A**, **Pende M**, **Reggiani C**, **Rizzuto R**, **Schiaffino S**. Signalling pathways regulating muscle mass in ageing skeletal muscle. The role of the IGF1-Akt-mTOR-FoxO pathway. *Biogerontology* 14: 303–323, 2013.
378. **Santel A**, **Fuller MT**. Control of mitochondrial morphology by a human mitofusin. *J Cell Sci* 114: 867–74, 2001.
379. **Sardiello M**, **Palmieri M**, **di Ronza A**, **Medina DL**, **Valenza M**, **Gennarino VA**, **Di Malta C**, **Donaudy F**, **Embrione V**, **Polishchuk RS**, **Banfi S**, **Parenti G**, **Cattaneo E**, **Ballabio A**. A Gene Network Regulating Lysosomal Biogenesis and Function. *Science (80-)* 325: 473–7, 2009.
380. **Sarraf SA**, **Raman M**, **Guarani-Pereira V**, **Sowa ME**, **Huttlin EL**, **Gygi SP**, **Harper JW**. Landscape of the PARKIN-dependent ubiquitylome in response to mitochondrial depolarization. *Nature* 496: 372–6, 2013.
381. **Sauer H**, **Wartenberg M**, **Hescheler J**. Reactive oxygen species as intracellular messengers during cell growth and differentiation. *Cell Physiol Biochem* 11: 173–86, 2001.
382. **Scarpulla RC**. Transcriptional paradigms in mammalian mitochondrial biogenesis and function. *Physiol Rev* 88: 611–38, 2008.
383. **Scherz-Shouval R**, **Elazar Z**. ROS, mitochondria and the regulation of autophagy. *Trends Cell Biol* 17: 422–427, 2007.
384. **Scherz-Shouval R**, **Shvets E**, **Fass E**, **Shorer H**, **Gil L**, **Elazar Z**. Reactive oxygen species are essential for autophagy and specifically regulate the activity of Atg4. *EMBO J* 26: 1749–1760, 2007.
385. **Schiavi A**, **Maglioni S**, **Palikaras K**, **Shaik A**, **Strappazzon F**, **Brinkmann V**, **Torgovnick A**, **Castelein N**, **De Henau S**, **Braeckman BP**, **Cecconi F**, **Tavernarakis N**, **Ventura N**. Iron-Starvation-Induced Mitophagy Mediates Lifespan Extension upon Mitochondrial Stress in C. elegans. *Curr Biol* 25: 1810–1822, 2015.
386. **Schreiber SN**, **Knutti D**, **Brogli K**, **Uhlmann T**, **Kralli A**. The Transcriptional Coactivator PGC-1 Regulates the Expression and Activity of the Orphan Nuclear Receptor Estrogen-Related Receptor α (ERRα). *J Biol Chem* 278: 9013–9018, 2003.
387. **Schrepfer E**, **Scorrano L**. Mitofusins, from Mitochondria to Metabolism. *Mol Cell* 61: 683–694, 2016.
388. **Schwalm C**, **Jamart C**, **Benoit N**, **Naslain D**, **Prémont C**, **Prevet J**, **Van Thienen R**, **Deldicque L**, **Francaux M**. Activation of autophagy in human skeletal muscle is dependent on exercise intensity and AMPK activation. *FASEB J* 29: 3515–3526, 2015.
389. **Schwarten M**, **Mohrlüder J**, **Ma P**, **Stoldt M**, **Thielmann Y**, **Stangler T**, **Hersch N**, **Hoffmann B**, **Merkel R**, **Willbold D**. Nix directly binds to GABARAP: a possible crosstalk between apoptosis and autophagy. *Autophagy* 5: 690–8, 2009.
390. **Schweers RL**, **Zhang J**, **Randall MS**, **Loyd MR**, **Li W**, **Dorsey FC**, **Kundu M**, **Opferman JT**, **Cleveland JL**, **Miller JL**, **Ney PA**. NIX is required for programmed mitochondrial clearance during reticulocyte maturation. *Proc Natl Acad Sci* 104: 19500–19505, 2007.
391. **Scott I**, **Webster BR**, **Chan CK**, **Okonkwo JU**, **Han K**, **Sack MN**. GCN5-like Protein 1 (GCN5L1) Controls Mitochondrial Content through Coordinated Regulation of Mitochondrial Biogenesis and Mitophagy. *J Biol Chem* 289: 2864–2872, 2014.
392. **Scott S V**, **Hefner-Gravink A**, **Morano KA**, **Noda T**, **Ohsumi Y**, **Klionsky DJ**. Cytoplasm-to-vacuole targeting and autophagy employ the same machinery to deliver proteins to the yeast vacuole. *Proc Natl Acad Sci U S A* 93: 12304–8, 1996.
393. **Sebastián D**, **Sorianello E**, **Segalés J**, **Irazoki A**, **Ruiz-Bonilla V**, **Sala D**, **Planet E**, **Berenguer-Llergo A**, **Muñoz JP**, **Sánchez-Feutrie M**, **Plana N**, **Hernández-Álvarez MI**, **Serrano AL**, **Palacín M**, **Zorzano A**. Mfn2 deficiency links age-related sarcopenia and impaired autophagy to activation of an adaptive mitophagy pathway. *EMBO J* 35: 1677–93, 2016.
394. **Seirafi M**, **Kozlov G**, **Gehring K**. Parkin structure and function. *FEBS J* 282: 2076–2088, 2015.
395. **Settembre C**, **De Cegli R**, **Mansueto G**, **Saha PK**, **Vetrini F**, **Visvikis O**, **Huynh T**, **Carissimo A**, **Palmer D**, **Jürgen Klisch T**, **Wollenberg AC**, **Di Bernardo D**, **Chan L**, **Irazoqui JE**, **Ballabio A**. TFEB controls cellular lipid metabolism through a starvation-induced autoregulatory loop. *Nat Cell Biol* 15: 647–658, 2013.
396. **Settembre C**, **Di Malta C**, **Polito VA**, **Garcia Arencibia M**, **Vetrini F**, **Erdin SUSU**, **Erdin SUSU**, **Huynh T**, **Medina D**, **Colella P**, **Sardiello M**, **Rubinsztein DC**, **Ballabio A**, **Arencibia MG**, **Vetrini F**, **Erdin SUSU**, **Erdin SUSU**, **Huynh T**, **Medina D**, **Colella P**, **Sardiello M**, **Rubinsztein DC**, **Ballabio A**. TFEB links autophagy to lysosomal biogenesis. *Science* 332: 1429–33, 2011.
397. **Shen W-C**, **Li H-Y**, **Chen G-C**, **Chern Y**, **Tu P**. Mutations in the ubiquitin-binding domain of

OPTN/optineurin interfere with autophagy-mediated degradation of misfolded proteins by a dominant-negative mechanism. *Autophagy* 11: 685–700, 2015.
398. **Shimizu N**, **Kitada T**, **Asakawa S**, **Hattori N**, **Matsumine H**, **Yamamura Y**, **Minoshima S**, **Yokochi M**, **Mizuno Y**, **Shimizu N**. Mutations in the parkin gene cause autosomal recessive juvenile parkinsonism. *Nature* 392, 1998.
399. **Shimizu S**, **Tsujimoto Y**. Proapoptotic BH3-only Bcl-2 family members induce cytochrome c release, but not mitochondrial membrane potential loss, and do not directly modulate voltage-dependent anion channel activity. *Proc Natl Acad Sci U S A* 97: 577–82, 2000.
400. **Shin H-W**, **Shinotsuka C**, **Torii S**, **Murakami K**, **Nakayama K**. Identification and Subcellular Localization of a Novel Mammalian Dynamin-Related Protein Homologous to Yeast Vps1p and Dnm1p. *J Biochem* 122: 525–530, 1997.
401. **Shin J-H**, **Ko HS**, **Kang H**, **Lee Y**, **Lee Y-I**, **Pletinkova O**, **Troconso JC**, **Dawson VL**, **Dawson TM**. PARIS (ZNF746) repression of PGC-1α contributes to neurodegeneration in Parkinson's disease. *Cell* 144: 689–702, 2011.
402. **Shintani T**, **Klionsky DJ**. Autophagy in health and disease: a double-edged sword. *Science* 306: 990–5, 2004.
403. **Short KR**, **Vittone JL**, **Bigelow ML**, **Proctor DN**, **Rizza RA**, **Coenen-Schimke JM**, **Nair KS**. Impact of aerobic exercise training on age-related changes in insulin sensitivity and muscle oxidative capacity. *Diabetes* 52: 1888–96, 2003.
404. **Skorjanc D**, **Traub I**, **Pette D**. Identical responses of fast muscle to sustained activity by low-frequency stimulation in young and aging rats. *J Appl Physiol* 85: 437–41, 1998.
405. **Smith BK**, **Mukai K**, **Lally JS**, **Maher AC**, **Gurd BJ**, **Heigenhauser GJF**, **Spriet LL**, **Holloway GP**. AMP-activated protein kinase is required for exercise-induced peroxisome proliferator-activated receptor γ co-activator 1α translocation to subsarcolemmal mitochondria in skeletal muscle. *J Physiol* 591: 1551–1561, 2013.
406. **Soubannier V**, **McLelland G-L**, **Zunino R**, **Braschi E**, **Rippstein P**, **Fon E**, **McBride H**. A Vesicular Transport Pathway Shuttles Cargo from Mitochondria to Lysosomes. *Curr Biol* 22: 135–141, 2012.
407. **Soubannier V**, **Rippstein P**, **Kaufman BA**, **Shoubridge EA**, **McBride HM**. Reconstitution of mitochondria derived vesicle formation demonstrates selective enrichment of oxidized cargo. *PLoS One* 7: e52830, 2012.
408. **Stanfel MN**, **Shamieh LS**, **Kaeberlein M**, **Kennedy BK**. The TOR pathway comes of age. *Biochim Biophys Acta - Gen Subj* 1790: 1067–1074, 2009.
409. **Stevens DA**, **Lee Y**, **Kang HC**, **Lee BD**, **Lee Y-I**, **Bower A**, **Jiang H**, **Kang S-U**, **Andrabi SA**, **Dawson VL**, **Shin J-H**, **Dawson TM**. Parkin loss leads to PARIS-dependent declines in mitochondrial mass and respiration. *Proc Natl Acad Sci U S A* 112: 11696–701, 2015.
410. **Strappazzon F**, **Nazio F**, **Corrado M**, **Cianfanelli V**, **Romagnoli A**, **Fimia GM**, **Campello S**, **Nardacci R**, **Piacentini M**, **Campanella M**, **Cecconi F**. AMBRA1 is able to induce mitophagy via LC3 binding, regardless of PARKIN and p62/SQSTM1. *Cell Death Differ* 22: 419–432, 2015.
411. **Stump CS**, **Short KR**, **Bigelow ML**, **Schimke JM**, **Nair KS**. Effect of insulin on human skeletal muscle mitochondrial ATP production, protein synthesis, and mRNA transcripts. *Proc Natl Acad Sci U S A* 100: 7996–8001, 2003.
412. **Suen D-F**, **Narendra DP**, **Tanaka A**, **Manfredi G**, **Youle RJ**. Parkin overexpression selects against a deleterious mtDNA mutation in heteroplasmic cybrid cells. *Proc Natl Acad Sci U S A* 107: 11835–40, 2010.
413. **Sugiura A**, **McLelland G-L**, **Fon EA**, **McBride HM**. A new pathway for mitochondrial quality control: mitochondrial-derived vesicles. *EMBO J* 33: 2142–2156, 2014.
414. **Sullivan-Gunn MJ**, **Lewandowski PA**. Elevated hydrogen peroxide and decreased catalase and glutathione peroxidase protection are associated with aging sarcopenia. *BMC Geriatr* 13: 104, 2013.
415. **Sun N**, **Yun J**, **Liu J**, **Malide D**, **Liu C**, **Rovira II**, **Holmström KM**, **Fergusson MM**, **Yoo YH**, **Combs CA**, **Finkel T**. Measuring In Vivo Mitophagy. *Mol Cell* 60: 685–696, 2015.
416. **Sveinbjornsdottir S**. The clinical symptoms of Parkinson's disease. *J Neurochem* 139: 318–324, 2016.
417. **Takahashi M**, **Chesley A**, **Freyssenet D**, **Hood DA**. Contractile activity-induced adaptations in the mitochondrial protein import system. *Am J Physiol* 274: C1380-7, 1998.
418. **Takahashi M**, **Hood DA**. Chronic stimulation-induced changes in mitochondria and performance in rat skeletal muscle. *J Appl Physiol* 74: 934–41, 1993.
419. **Takahashi M**, **Hood DA**. Protein import into subsarcolemmal and intermyofibrillar skeletal muscle mitochondria. Differential import regulation in distinct subcellular regions. *J Biol Chem* 271: 27285–91,

1996.
420. **Takeshige K**, **Baba M**, **Tsuboi S**, **Noda T**, **Ohsumi Y**. Autophagy in yeast demonstrated with proteinase-deficient mutants and conditions for its induction. *J Cell Biol* 119: 301–11, 1992.
421. **Talanian JL**, **Holloway GP**, **Snook LA**, **Heigenhauser GJF**, **Bonen A**, **Spriet LL**. EXERCISE TRAINING INCREASES SARCOLEMMAL AND MITOCHONDRIAL FATTY ACID TRANSPORT PROTEINS IN HUMAN SKELETAL MUSCLE. *AJP Endocrinol Metab* 299: E180-8, 2010.
422. **Tam ZY**, **Gruber J**, **Ng LF**, **Halliwell B**, **Gunawan R**. Effects of Lithium on Age-related Decline in Mitochondrial Turnover and Function in Caenorhabditis elegans. *Journals Gerontol Ser A Biol Sci Med Sci* 69: 810–820, 2014.
423. **Tanaka A**, **Cleland MM**, **Xu S**, **Narendra DP**, **Suen D-F**, **Karbowski M**, **Youle RJ**. Proteasome and p97 mediate mitophagy and degradation of mitofusins induced by Parkin. *J Cell Biol* 191: 1367–1380, 2010.
424. **Tanida I**, **Sou Y**, **Minematsu-Ikeguchi N**, **Ueno T**, **Kominami E**. Atg8L/Apg8L is the fourth mammalian modifier of mammalian Atg8 conjugation mediated by human Atg4B, Atg7 and Atg3. *FEBS J* 273: 2553–2562, 2006.
425. **Tanida I**, **Tanida-Miyake E**, **Komatsu M**, **Ueno T**, **Kominami E**. Human Apg3p/Aut1p Homologue Is an Authentic E2 Enzyme for Multiple Substrates, GATE-16, GABARAP, and MAP-LC3, and Facilitates the Conjugation of hApg12p to hApg5p. *J Biol Chem* 277: 13739–13744, 2002.
426. **Tanida I**, **Tanida-Miyake E**, **Ueno T**, **Kominami E**. The Human Homolog of *Saccharomyces cerevisiae* Apg7p Is a Protein-activating Enzyme for Multiple Substrates Including Human Apg12p, GATE-16, GABARAP, and MAP-LC3. *J Biol Chem* 276: 1701–1706, 2001.
427. **Tassa A**, **Roux MP**, **Attaix D**, **Bechet DM**. Class III phosphoinositide 3-kinase--Beclin1 complex mediates the amino acid-dependent regulation of autophagy in C2C12 myotubes. *Biochem J* 376: 577–86, 2003.
428. **Terjung RL**. The turnover of cytochrome c in different skeletal-muscle fibre types of the rat. *Biochem J* 178: 569–74, 1979.
429. **Terman A**. The effect of age on formation and elimination of autophagic vacuoles in mouse hepatocytes. *Gerontology* 41 Suppl 2: 319–26, 1995.
430. **Terman A**, **Brunk UT**. Lipofuscin: mechanisms of formation and increase with age. *APMIS* 106: 265–76, 1998.
431. **Terskikh A**. "Fluorescent Timer": Protein That Changes Color with Time. *Science (80-)* 290: 1585–1588, 2000.
432. **Thomas RE**, **Andrews LA**, **Burman JL**, **Lin W-Y**, **Pallanck LJ**. PINK1-Parkin Pathway Activity Is Regulated by Degradation of PINK1 in the Mitochondrial Matrix. *PLoS Genet* 10: e1004279, 2014.
433. **Tian W**, **Li W**, **Chen Y**, **Yan Z**, **Huang X**, **Zhuang H**, **Zhong W**, **Chen Y**, **Wu W**, **Lin C**, **Chen H**, **Hou X**, **Zhang L**, **Sui S**, **Zhao B**, **Hu Z**, **Li L**, **Feng D**. Phosphorylation of ULK1 by AMPK regulates translocation of ULK1 to mitochondria and mitophagy. *FEBS Lett* 589: 1847–1854, 2015.
434. **Tohyama D**, **Yamaguchi A**. A critical role of SNF1A/dAMPKα (Drosophila AMP-activated protein kinase α) in muscle on longevity and stress resistance in Drosophila melanogaster. *Biochem Biophys Res Commun* 394: 112–118, 2010.
435. **Trempe J-F**, **Sauve V**, **Grenier K**, **Seirafi M**, **Tang MY**, **Menade M**, **Al-Abdul-Wahid S**, **Krett J**, **Wong K**, **Kozlov G**, **Nagar B**, **Fon EA**, **Gehring K**. Structure of Parkin Reveals Mechanisms for Ubiquitin Ligase Activation. *Science (80-)* 340: 1451–1455, 2013.
436. **Trifunovic A**, **Wredenberg A**, **Falkenberg M**, **Spelbrink JN**, **Rovio AT**, **Bruder CE**, **Bohlooly-Y M**, **Gidlöf S**, **Oldfors A**, **Wibom R**, **Törnell J**, **Jacobs HT**, **Larsson N-G**. Premature ageing in mice expressing defective mitochondrial DNA polymerase. *Nature* 429: 417–23, 2004.
437. **Tsukada M**, **Ohsumi Y**. Isolation and characterization of autophagy-defective mutants of Saccharomyces cerevisiae. *FEBS Lett* 333: 169–74, 1993.
438. **Tullson P**, **Terjung R**. Adenine Nucleotide Degradation in Striated Muscle. *Int J Sports Med* 11: S47–S55, 1990.
439. **Tumbarello DA**, **Manna PT**, **Allen M**, **Bycroft M**, **Arden SD**, **Kendrick-Jones J**, **Buss F**. The Autophagy Receptor TAX1BP1 and the Molecular Motor Myosin VI Are Required for Clearance of Salmonella Typhimurium by Autophagy. *PLOS Pathog* 11: e1005174, 2015.
440. **Turrens JF**. Mitochondrial formation of reactive oxygen species. *J Physiol* 552: 335–44, 2003.
441. **Twig G**, **Elorza A**, **Molina AJA**, **Mohamed H**, **Wikstrom JD**, **Walzer G**, **Stiles L**, **Haigh SE**, **Katz S**, **Las G**, **Alroy J**, **Wu M**, **Py BF**, **Yuan J**, **Deeney JT**, **Corkey BE**, **Shirihai OS**. Fission and selective fusion govern mitochondrial segregation and elimination by autophagy. *EMBO J* 27: 433–446, 2008.
442. **Twig G**, **Hyde B**, **Shirihai OS**. Mitochondrial fusion, fission and autophagy as a quality control axis: The

bioenergetic view. *Biochim Biophys Acta - Bioenerg* 1777: 1092–1097, 2008.
443. **Uguccioni G**, **Hood DA**. The importance of PGC-1 in contractile activity-induced mitochondrial adaptations. *AJP Endocrinol Metab* 300: E361–E371, 2011.
444. **Ulgherait M**, **Rana A**, **Rera M**, **Graniel J**, **Walker DW**. AMPK Modulates Tissue and Organismal Aging in a Non-Cell-Autonomous Manner. *Cell Rep* 8: 1767–1780, 2014.
445. **Umanskaya A**, **Santulli G**, **Xie W**, **Andersson DC**, **Reiken SR**, **Marks AR**. Genetically enhancing mitochondrial antioxidant activity improves muscle function in aging. *Proc Natl Acad Sci U S A* 111: 15250–5, 2014.
446. **Vainshtein A**, **Tryon LD**, **Pauly M**, **Hood DA**. Role of PGC-1α during acute exercise-induced autophagy and mitophagy in skeletal muscle. *Am J Physiol Cell Physiol* 308: C710-9, 2015.
447. **Valente EM**, **Abou-Sleiman PM**, **Caputo V**, **Muqit MMK**, **Harvey K**, **Gispert S**, **Ali Z**, **Del Turco D**, **Bentivoglio AR**, **Healy DG**, **Albanese A**, **Nussbaum R**, **González-Maldonado R**, **Deller T**, **Salvi S**, **Cortelli P**, **Gilks WP**, **Latchman DS**, **Harvey RJ**, **Dallapiccola B**, **Auburger G**, **Wood NW**. Hereditary early-onset Parkinson's disease caused by mutations in PINK1. *Science* 304: 1158–60, 2004.
448. **Valente EM**, **Brancati F**, **Caputo V**, **Graham EA**, **Davis MB**, **Ferraris A**, **Breteler MMB**, **Gasser T**, **Bonifati V**, **Bentivoglio AR**, **De Michele G**, **D�rr A**, **Cortelli P**, **Filla A**, **Meco G**, **Oostra BA**, **Brice A**, **Albanese A**, **Dallapiccola B**, **Wood NW**, **European Consortium on Genetic Susceptibility in Parkinson's Disease**. PARK6 is a common cause of familial parkinsonism. *Neurol Sci* 23: s117–s118, 2002.
449. **Valente EM**, **Brancati F**, **Ferraris A**, **Graham EA**, **Davis MB**, **Breteler MMB**, **Gasser T**, **Bonifati V**, **Bentivoglio AR**, **De Michele G**, **Dürr A**, **Cortelli P**, **Wassilowsky D**, **Harhangi BS**, **Rawal N**, **Caputo V**, **Filla A**, **Meco G**, **Oostra BA**, **Brice A**, **Albanese A**, **Dallapiccola B**, **Wood NW**, **European Consortium on Genetic Susceptibility in Parkinson's Disease**. PARK6-linked parkinsonism occurs in several European families. *Ann Neurol* 51: 14–8, 2002.
450. **Vellai T**, **Takacs-Vellai K**, **Zhang Y**, **Kovacs AL**, **Orosz L**, **Müller F**. Genetics: Influence of TOR kinase on lifespan in C. elegans. *Nature* 426: 620–620, 2003.
451. **Lo Verso F**, **Carnio S**, **Vainshtein A**, **Sandri M**. Autophagy is not required to sustain exercise and PRKAA1/AMPK activity but is important to prevent mitochondrial damage during physical activity. *Autophagy* 10: 1883–94, 2014.
452. **Vicencio JM**, **Ortiz C**, **Criollo A**, **Jones AWE**, **Kepp O**, **Galluzzi L**, **Joza N**, **Vitale I**, **Morselli E**, **Tailler M**, **Castedo M**, **Maiuri MC**, **Molgó J**, **Szabadkai G**, **Lavandero S**, **Kroemer G**. The inositol 1,4,5-trisphosphate receptor regulates autophagy through its interaction with Beclin 1. *Cell Death Differ* 16: 1006–1017, 2009.
453. **Vincow ES**, **Merrihew G**, **Thomas RE**, **Shulman NJ**, **Beyer RP**, **MacCoss MJ**, **Pallanck LJ**. The PINK1-Parkin pathway promotes both mitophagy and selective respiratory chain turnover in vivo. *Proc Natl Acad Sci* 110: 6400–6405, 2013.
454. **Vives-Bauza C**, **Zhou C**, **Huang Y**, **Cui M**, **de Vries RLA**, **Kim J**, **May J**, **Tocilescu MA**, **Liu W**, **Ko HS**, **Magrané J**, **Moore DJ**, **Dawson VL**, **Grailhe R**, **Dawson TM**, **Li C**, **Tieu K**, **Przedborski S**. PINK1-dependent recruitment of Parkin to mitochondria in mitophagy. *Proc Natl Acad Sci U S A* 107: 378–83, 2010.
455. **Volpi E**, **Mittendorfer B**, **Rasmussen BB**, **Wolfe RR**. The response of muscle protein anabolism to combined hyperaminoacidemia and glucose-induced hyperinsulinemia is impaired in the elderly. *J Clin Endocrinol Metab* 85: 4481–90, 2000.
456. **von Muhlinen N**, **Akutsu M**, **Ravenhill BJ**, **Foeglein Á**, **Bloor S**, **Rutherford TJ**, **Freund SMV**, **Komander D**, **Randow F**. LC3C, Bound Selectively by a Noncanonical LIR Motif in NDP52, Is Required for Antibacterial Autophagy. *Mol Cell* 48: 329–342, 2012.
457. **Walters TJ**, **Sweeney HL**, **Farrar RP**. Influence of electrical stimulation on a fast-twitch muscle in aging rats. *J Appl Physiol* 71: 1921–8, 1991.
458. **Wanagat J**, **Cao Z**, **Pathare P**, **Aiken JM**. Mitochondrial DNA deletion mutations colocalize with segmental electron transport system abnormalities, muscle fiber atrophy, fiber splitting, and oxidative damage in sarcopenia. *FASEB J* 15: 322–32, 2001.
459. **Wang H**, **Bedford FK**, **Brandon NJ**, **Moss SJ**, **Olsen RW**. GABAA-receptor-associated protein links GABAA receptors and the cytoskeleton. *Nature* 397: 69–72, 1999.
460. **Wang H**, **Song P**, **Du L**, **Tian W**, **Yue W**, **Liu M**, **Li D**, **Wang B**, **Zhu Y**, **Cao C**, **Zhou J**, **Chen Q**. Parkin Ubiquitinates Drp1 for Proteasome-dependent Degradation. *J Biol Chem* 286: 11649–11658, 2011.
461. **Wang X**, **Winter D**, **Ashrafi G**, **Schlehe J**, **Wong YL**, **Selkoe D**, **Rice S**, **Steen J**, **LaVoie MJ**, **Schwarz**

TL. PINK1 and Parkin Target Miro for Phosphorylation and Degradation to Arrest Mitochondrial Motility. *Cell* 147: 893–906, 2011.
462. **Wang Y**, **Michikawa Y**, **Mallidis C**, **Bai Y**, **Woodhouse L**, **Yarasheski KE**, **Miller CA**, **Askanas V**, **Engel WK**, **Bhasin S**, **Attardi G**. Muscle-specific mutations accumulate with aging in critical human mtDNA control sites for replication. *Proc Natl Acad Sci U S A* 98: 4022–7, 2001.
463. **Wauer T**, **Komander D**. Structure of the human Parkin ligase domain in an autoinhibited state. *EMBO J* 32: 2099–2112, 2013.
464. **Wende AR**, **Schaeffer PJ**, **Parker GJ**, **Zechner C**, **Han DH**, **Chen MM**, **Hancock CR**, **Lehman JJ**, **Huss JM**, **McClain DA**, **Holloszy JO**, **Kelly DP**. A role for the transcriptional coactivator PGC-1α in muscle refueling. *J Biol Chem* 282: 36642–36651, 2007.
465. **Wenzel DM**, **Lissounov A**, **Brzovic PS**, **Klevit RE**. UBCH7 reactivity profile reveals parkin and HHARI to be RING/HECT hybrids. *Nature* 474: 105–108, 2011.
466. **Wiedemann N**, **Frazier AE**, **Pfanner N**. The protein import machinery of mitochondria. *J Biol Chem* 279: 14473–6, 2004.
467. **Wojtaszewski JF**, **Nielsen P**, **Hansen BF**, **Richter EA**, **Kiens B**. Isoform-specific and exercise intensity-dependent activation of 5'-AMP-activated protein kinase in human skeletal muscle. *J Physiol* 528 Pt 1: 221–6, 2000.
468. **Wong YC**, **Holzbaur ELF**. Optineurin is an autophagy receptor for damaged mitochondria in parkin-mediated mitophagy that is disrupted by an ALS-linked mutation. *Proc Natl Acad Sci* 111: E4439–E4448, 2014.
469. **Woods A**, **Dickerson K**, **Heath R**, **Hong S-P**, **Momcilovic M**, **Johnstone SR**, **Carlson M**, **Carling D**. Ca2+/calmodulin-dependent protein kinase kinase-β acts upstream of AMP-activated protein kinase in mammalian cells. *Cell Metab* 2: 21–33, 2005.
470. **Wredenberg A**, **Wibom R**, **Wilhelmsson H**, **Graff C**, **Wiener HH**, **Burden SJ**, **Oldfors A**, **Westerblad H**, **Larsson N-G**. Increased mitochondrial mass in mitochondrial myopathy mice. *Proc Natl Acad Sci* 99: 15066–15071, 2002.
471. **Wright DC**, **Geiger PC**, **Han D-H**, **Jones TE**, **Holloszy JO**. Calcium Induces Increases in Peroxisome Proliferator-activated Receptor γ Coactivator-1α and Mitochondrial Biogenesis by a Pathway Leading to p38 Mitogen-activated Protein Kinase Activation. *J Biol Chem* 282: 18793–18799, 2007.
472. **Wu JJ**, **Liu J**, **Chen EB**, **Wang JJ**, **Cao L**, **Narayan N**, **Fergusson MM**, **Rovira II**, **Allen M**, **Springer DA**, **Lago CU**, **Zhang S**, **DuBois W**, **Ward T**, **deCabo R**, **Gavrilova O**, **Mock B**, **Finkel T**. Increased Mammalian Lifespan and a Segmental and Tissue-Specific Slowing of Aging after Genetic Reduction of mTOR Expression. *Cell Rep* 4: 913–920, 2013.
473. **Wu Z**, **Puigserver P**, **Andersson U**, **Zhang C**, **Adelmant G**, **Mootha V**, **Troy A**, **Cinti S**, **Lowell B**, **Scarpulla RC**, **Spiegelman BM**. Mechanisms Controlling Mitochondrial Biogenesis and Respiration through the Thermogenic Coactivator PGC-1. *Cell* 98: 115–124, 1999.
474. **Xu L**, **Eu JP**, **Meissner G**, **Stamler JS**. Activation of the cardiac calcium release channel (ryanodine receptor) by poly-S-nitrosylation. *Science* 279: 234–7, 1998.
475. **Xu S**, **Peng G**, **Wang Y**, **Fang S**, **Karbowski M**. The AAA-ATPase p97 is essential for outer mitochondrial membrane protein turnover. *Mol Biol Cell* 22: 291–300, 2011.
476. **Yach D**, **Stuckler D**, **Brownell KD**. Epidemiologic and economic consequences of the global epidemics of obesity and diabetes. *Nat Med* 12: 62–66, 2006.
477. **Yamano K**, **Youle RJ**. PINK1 is degraded through the N-end rule pathway. *Autophagy* 9: 1758–1769, 2013.
478. **Yoneda T**, **Benedetti C**, **Urano F**, **Clark SG**, **Harding HP**, **Ron D**. Compartment-specific perturbation of protein handling activates genes encoding mitochondrial chaperones. *J Cell Sci* 117: 4055–4066, 2004.
479. **Youle RJ**, **van der Bliek AM**. Mitochondrial Fission, Fusion, and Stress. *Science (80-)* 337: 1062–1065, 2012.
480. **Young JC**, **Hoogenraad NJ**, **Hartl FU**. Molecular chaperones Hsp90 and Hsp70 deliver preproteins to the mitochondrial import receptor Tom70. *Cell* 112: 41–50, 2003.
481. **Yu M**, **Stepto NK**, **Chibalin A V**, **Fryer LGD**, **Carling D**, **Krook A**, **Hawley JA**, **Zierath JR**. Metabolic and mitogenic signal transduction in human skeletal muscle after intense cycling exercise. *J Physiol* 546: 327–35, 2003.
482. **Yun J**, **Puri R**, **Yang H**, **Lizzio MA**, **Wu C**, **Sheng Z-H**, **Guo M**. MUL1 acts in parallel to the PINK1/parkin pathway in regulating mitofusin and compensates for loss of PINK1/parkin. *Elife* 3: e01958, 2014.

483. **Zechner C**, **Lai L**, **Zechner JF**, **Geng T**, **Yan Z**, **Rumsey JW**, **Collia D**, **Chen Z**, **Wozniak DF**, **Leone TC**, **Kelly DP**. Total Skeletal Muscle PGC-1 Deficiency Uncouples Mitochondrial Derangements from Fiber Type Determination and Insulin Sensitivity. *Cell Metab* 12: 633–642, 2010.
484. **Zesiewicz TA**, **Strom JA**, **Borenstein AR**, **Hauser RA**, **Cimino CR**, **Fontanet HL**, **Cintron GB**, **Staffetti JF**, **Dunne PB**, **Sullivan KL**. Heart failure in Parkinson's disease: analysis of the United States medicare current beneficiary survey. *Parkinsonism Relat Disord* 10: 417–420, 2004.
485. **Zhang H**, **Bosch-Marce M**, **Shimoda LA**, **Tan YS**, **Baek JH**, **Wesley JB**, **Gonzalez FJ**, **Semenza GL**. Mitochondrial Autophagy Is an HIF-1-dependent Adaptive Metabolic Response to Hypoxia. *J Biol Chem* 283: 10892–10903, 2008.
486. **Zhang J**, **Ney PA**. NIX induces mitochondrial autophagy in reticulocytes. *Autophagy* 4: 354–6, 2008.
487. **Zhang J**, **Ney PA**. Role of BNIP3 and NIX in cell death, autophagy, and mitophagy. *Cell Death Differ* 16: 939–946, 2009.
488. **Zhang Y**, **Uguccioni G**, **Ljubicic V**, **Irrcher I**, **Iqbal S**, **Singh K**, **Ding S**, **Hood DA**. Multiple signaling pathways regulate contractile activity-mediated PGC-1α gene expression and activity in skeletal muscle cells. *Physiol Rep* 2: e12008–e12008, 2014.
489. **Zhao M**, **New L**, **Kravchenko V V**, **Kato Y**, **Gram H**, **di Padova F**, **Olson EN**, **Ulevitch RJ**, **Han J**. Regulation of the MEF2 family of transcription factors by p38. *Mol Cell Biol* 19: 21–30, 1999.
490. **Zhao Q**, **Wang J**, **Levichkin I V**, **Stasinopoulos S**, **Ryan MT**, **Hoogenraad NJ**. A mitochondrial specific stress response in mammalian cells. *EMBO J* 21: 4411–9, 2002.
491. **Zid BM**, **Rogers AN**, **Katewa SD**, **Vargas MA**, **Kolipinski MC**, **Lu TA**, **Benzer S**, **Kapahi P**. 4E-BP Extends Lifespan upon Dietary Restriction by Enhancing Mitochondrial Activity in Drosophila. *Cell* 139: 149–160, 2009.
492. **Zmijewski JW**, **Banerjee S**, **Bae H**, **Friggeri A**, **Lazarowski ER**, **Abraham E**. Exposure to Hydrogen Peroxide Induces Oxidation and Activation of AMP-activated Protein Kinase. *J Biol Chem* 285: 33154–33164, 2010.
493. **Züchner S**, **Mersiyanova I V**, **Muglia M**, **Bissar-Tadmouri N**, **Rochelle J**, **Dadali EL**, **Zappia M**, **Nelis E**, **Patitucci A**, **Senderek J**, **Parman Y**, **Evgrafov O**, **Jonghe P De**, **Takahashi Y**, **Tsuji S**, **Pericak-Vance MA**, **Quattrone A**, **Battologlu E**, **Polyakov A V**, **Timmerman V**, **Schröder JM**, **Vance JM**. Mutations in the mitochondrial GTPase mitofusin 2 cause Charcot-Marie-Tooth neuropathy type 2A. *Nat Genet* 36: 449–451, 2004.

APPENDIX A:

SUPPLEMENTARY TABLES AND FIGURES

Supplementary Table 1.

Table 1. Exhaustive Exercise Protocol						
Duration (min)	5	5	10	15	20	+ 1 min
Speed (m/s)	0	0.08	0.17	0.25	0.33	+ 0.2

***Note:** Young animals were acclimatized to the treadmill for two days prior to exhaustive exercise on Day 3. Aged animals ran a similar protocol but began incremental exercise after 10 m/min for 10 minutes.

Supp. Fig. 1.

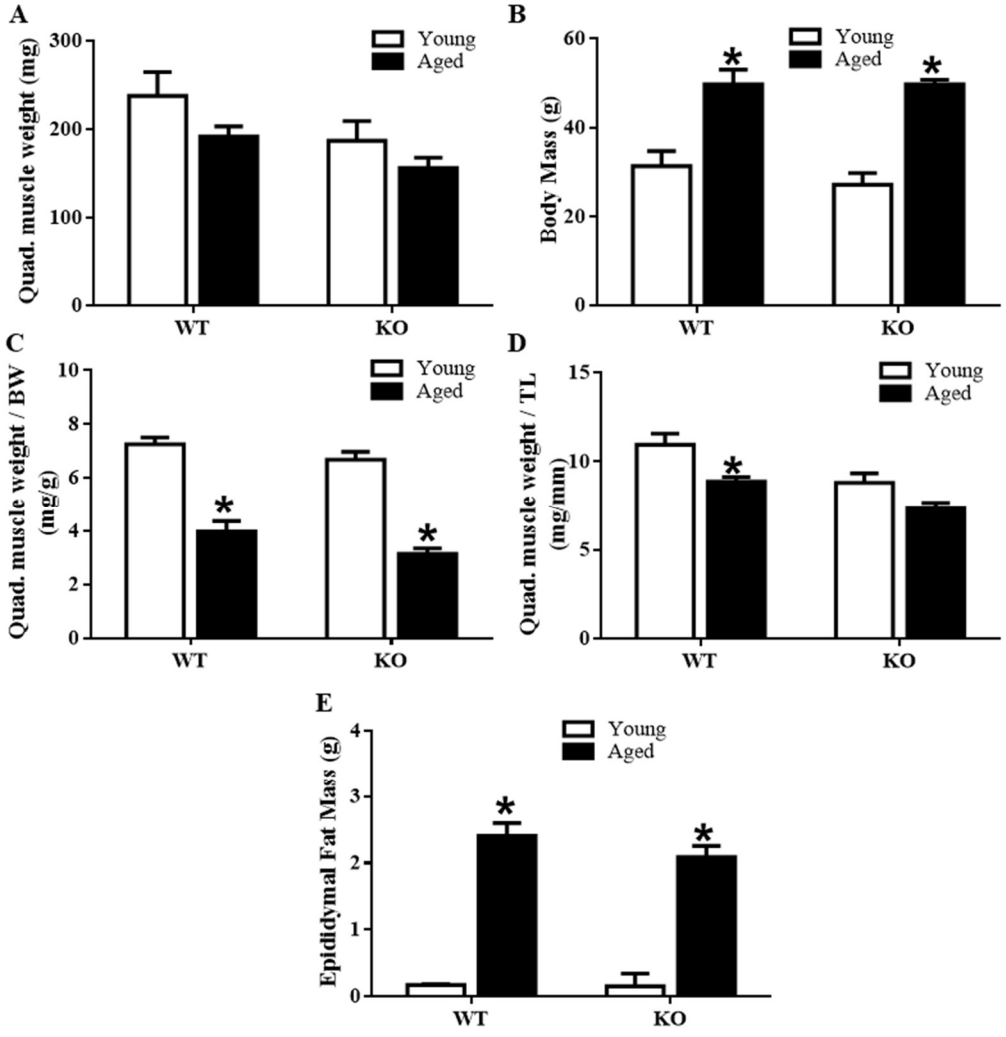

Supplementary Figure 1. A graphical representation of animal characteristics of WT and Parkin KO mice from Manuscript #1. Values are reported as means ± SEM, n = 6. * $P < 0.05$ vs. Young counterpart. Wild-type, WT; KO, Parkin KO; TL, tibia length.

Supp. Fig. 2.

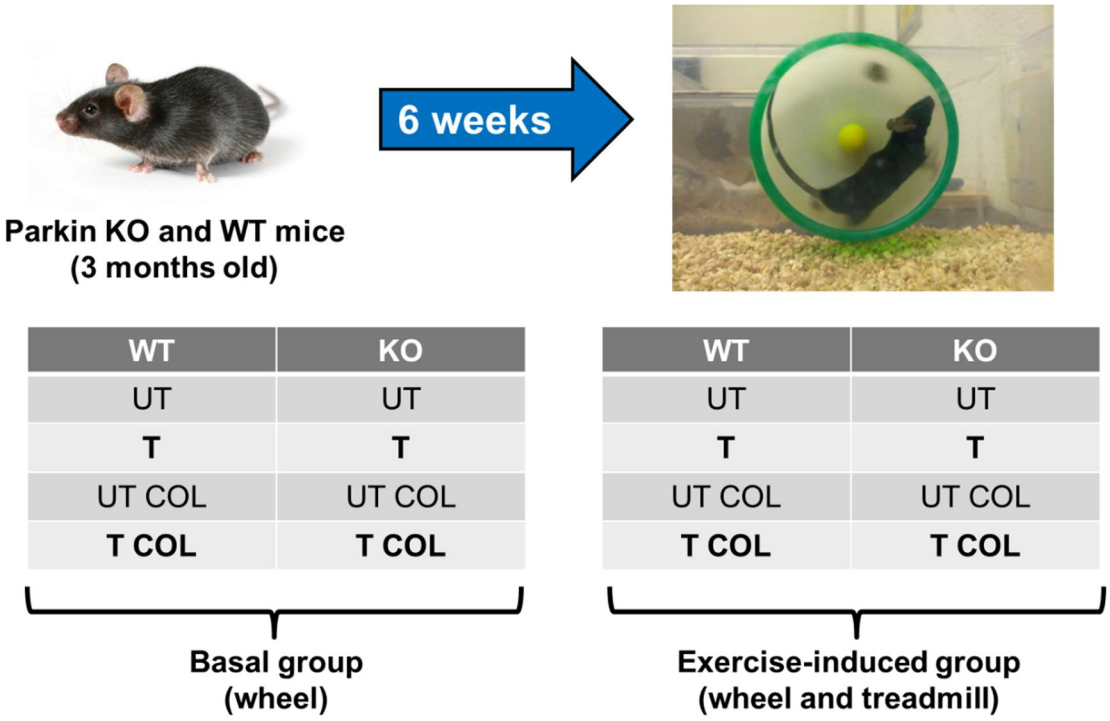

Supplementary Figure 2. A visual representation of voluntary wheel running protocol and animal group conditions. Following 6 weeks of endurance training, a subset of animals was subjected to acute exercise as illustrated in Supplementary Table 1. Wild-type, WT; Parkin knock-out, KO; untrained, UT; trained, T; colchicine, COL.

APPENDIX B:

ADDITIONAL DATA

STUDY 1: The role of Parkin in cardiac autophagy and mitophagy

Rationale

In this PhD dissertation, I established a role for Parkin-mediated mitophagy in skeletal muscle following acute exercise. However, the functional importance of Parkin in the heart with exercise and age remains unknown. Recent evidence suggests that mitochondrial turnover in cardiac muscle is mediated by Parkin under stress-induced conditions. A central function of the heart during exercise is to provide oxygenated blood to working muscles. Thus, cardiac function must increase to match the demands of the muscles and lungs. Because of this energy demand, the heart heavily relies on its own abundance of mitochondria for energy. Organelles that are unable to meet these demands are targeted for degradation. We sought to investigate whether autophagy and mitophagy flux were altered because of age and exercise within whole muscle samples and mitochondrial sub-fractions.

Results

Cardiac autophagy flux is enhanced in aged Parkin KO animals. To investigate the role of Parkin on autophagy flux in the heart, we utilized young and old groups of WT and Parkin KO animals. Western blot analyses on whole heart samples revealed that basal autophagy flux did not differ between young and aged WT animals (Fig. 1A–E). Aged Parkin KO animals displayed higher basal LC3II flux in cardiac tissue, compared to young (Fig. 2E, $P < 0.05$). Surprisingly, we detected enhanced p62 flux with age irrespective of genotype (Fig. 3D and 3F, $P < 0.05$).

Endurance training attenuates Parkin-mediated mitophagy flux. To assess the involvement of Parkin on mitophagy in cardiac muscle during training, mitochondria were isolated from the heart of trained WT and Parkin KO animals following 6 weeks of voluntary wheel running. Endurance training resulted in a significant increase in LC3-II localization to the mitochondria (Fig. 4B and 5B, $P < 0.05$), and did not increase additionally with a subsequent bout of acute exercise. We found that acute exercise significantly attenuated mitophagic LC3II and p62 flux following training in WT animals (Fig. 4C and 4E, $P < 0.05$), and this relationship did not occur in the absence of Parkin.

Conclusions

There is emerging evidence on mitochondrial dysfunction and its role in heart failure. It is relatively unknown if mitochondrial turnover in the heart is influenced by other physiological metabolic states, such as exercise and aging. Our results indicate that Parkin may be involved in this process. Interestingly, we noted that autophagy LC3-II and p62 flux were enhanced in Parkin KO mice with age. The absence of Parkin can impair mitophagy and evoke an accumulation of dysfunctional mitochondria in the heart that can execrate with age. The enhancement of autophagy flux observed in aged KO animals may function as a compensatory response to the impairment of mitophagy. Future work will need to investigate this possibility by directly measuring mitophagy flux. Nonetheless, these data indicate that Parkin may play a role in maintaining mitochondrial quality in the aging heart.

Exercise training commonly leads to a physiological, adaptive hypertrophy of the left ventricle. This may be accompanied by a proliferation of mitochondria as a response to upregulate cardiac energy production and increase cardiac workload. To examine this, we isolated

mitochondria from untrained and trained hearts of WT and Parkin KO mice. For WT animals, 6 weeks of endurance exercise was sufficient to increase the expression and localization of autophagosomal marker LC3-II to mitochondria; and with a subsequent bout of acute exercise was able to reduce mitophagic flux of LC3-II and p62. These data support our findings from manuscript #2 that the occurrence of Parkin-mediated mitophagy is attenuated with successive exercise bouts to attain training-induced mitochondrial adaptations.

Fig. 1

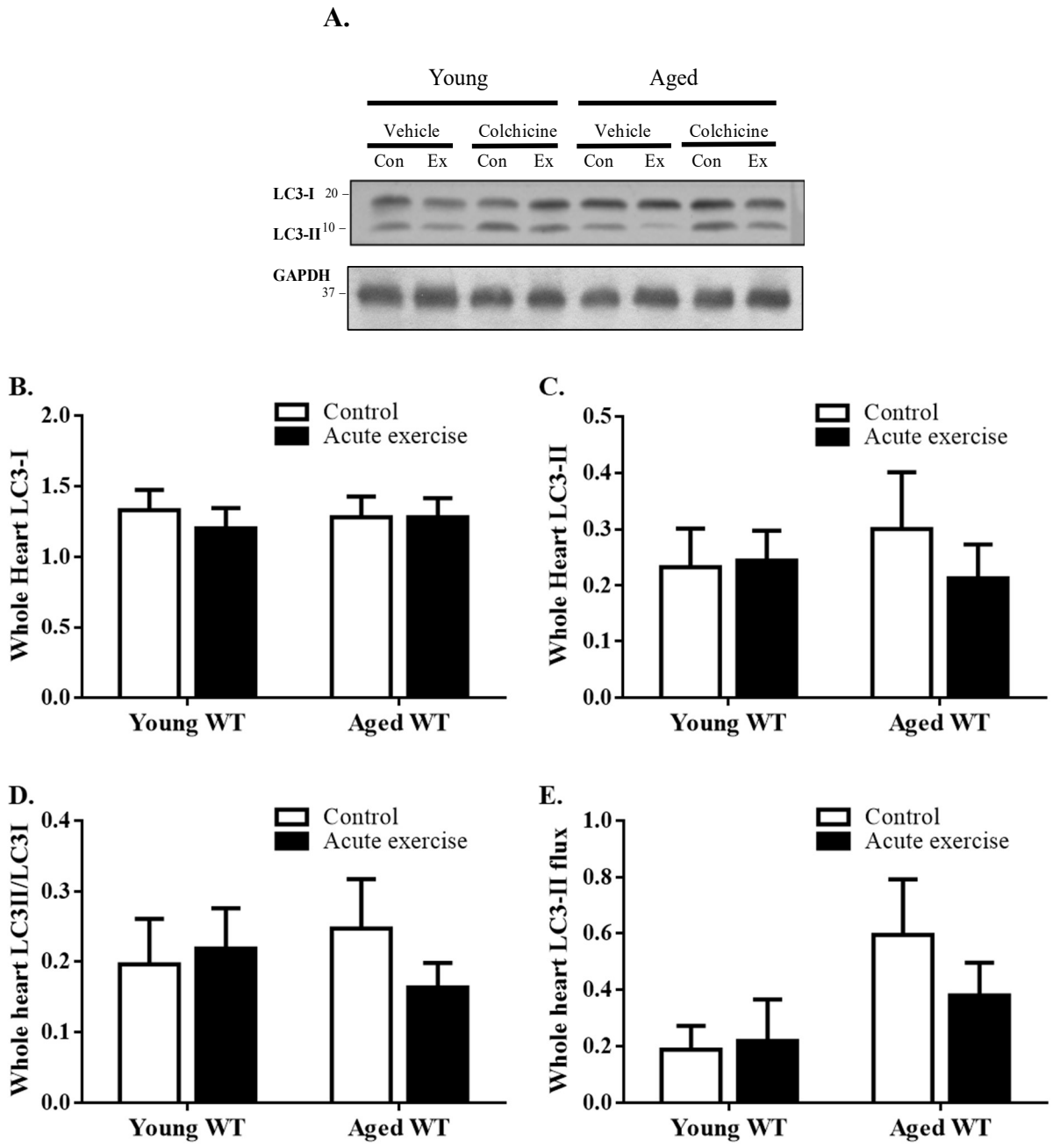

Figure 1. Expression of autophagosomal protein LC3 in cardiac muscle of young and aged WT animals. A) Representative blot of LC3. Quantification of whole heart B) LC3I, C) LC3II, D) ratio of LC3II over LC3I, and E) LC3II flux. GAPDH was used as a loading control. Values are represented in arbitrary units. (n=6 for all groups).

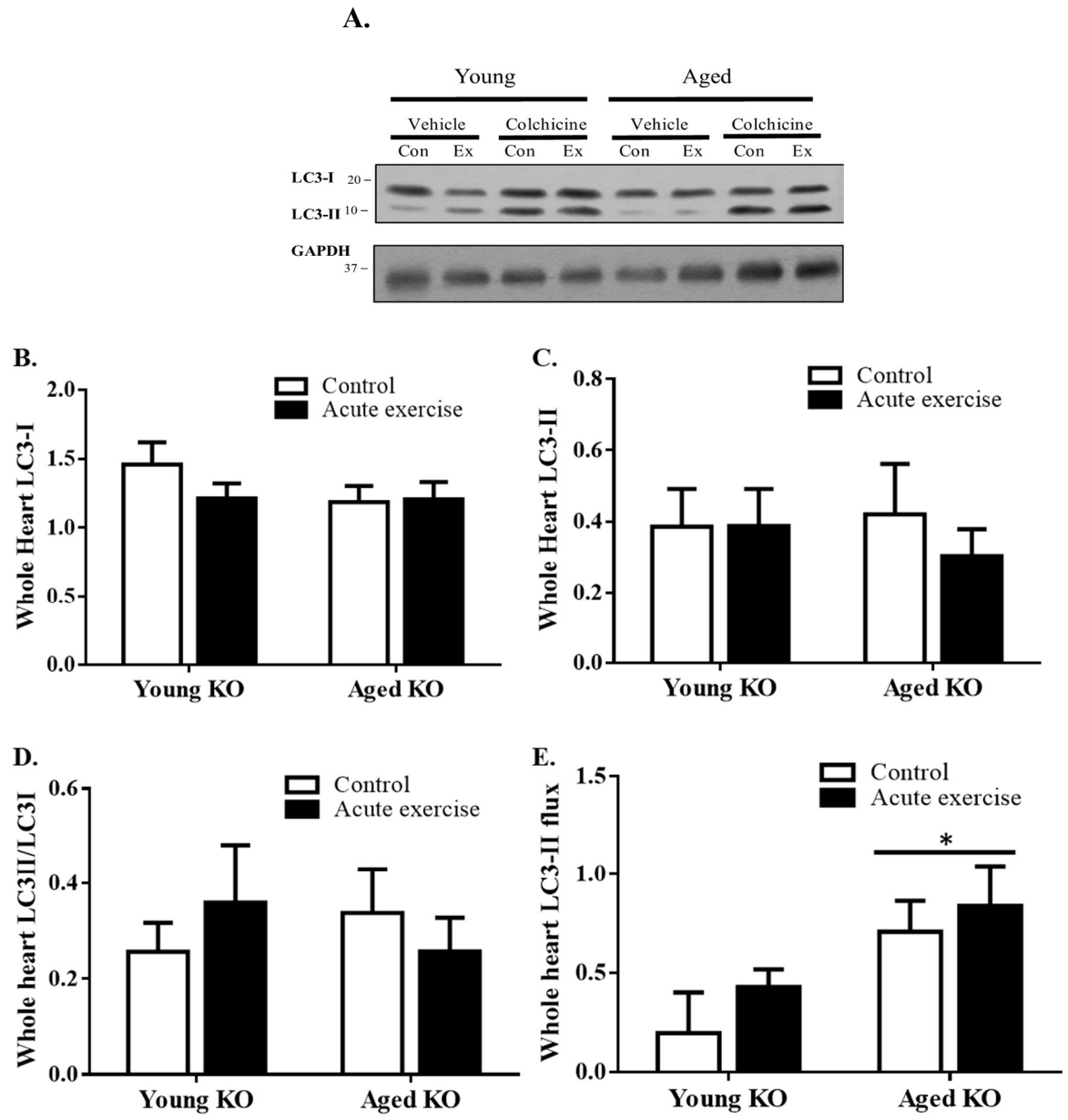

Figure 2. Expression of autophagosomal protein LC3 in cardiac muscle of young and aged KO animals. A) Representative blot of LC3. Quantification of whole heart B) LC3I, C) LC3II, D) ratio of LC3II over LC3I, and E) LC3II flux. *P<0.05, main effect of age. GAPDH was used as a loading control. Values are represented in arbitrary units. (n=6 for all groups).

Fig. 3

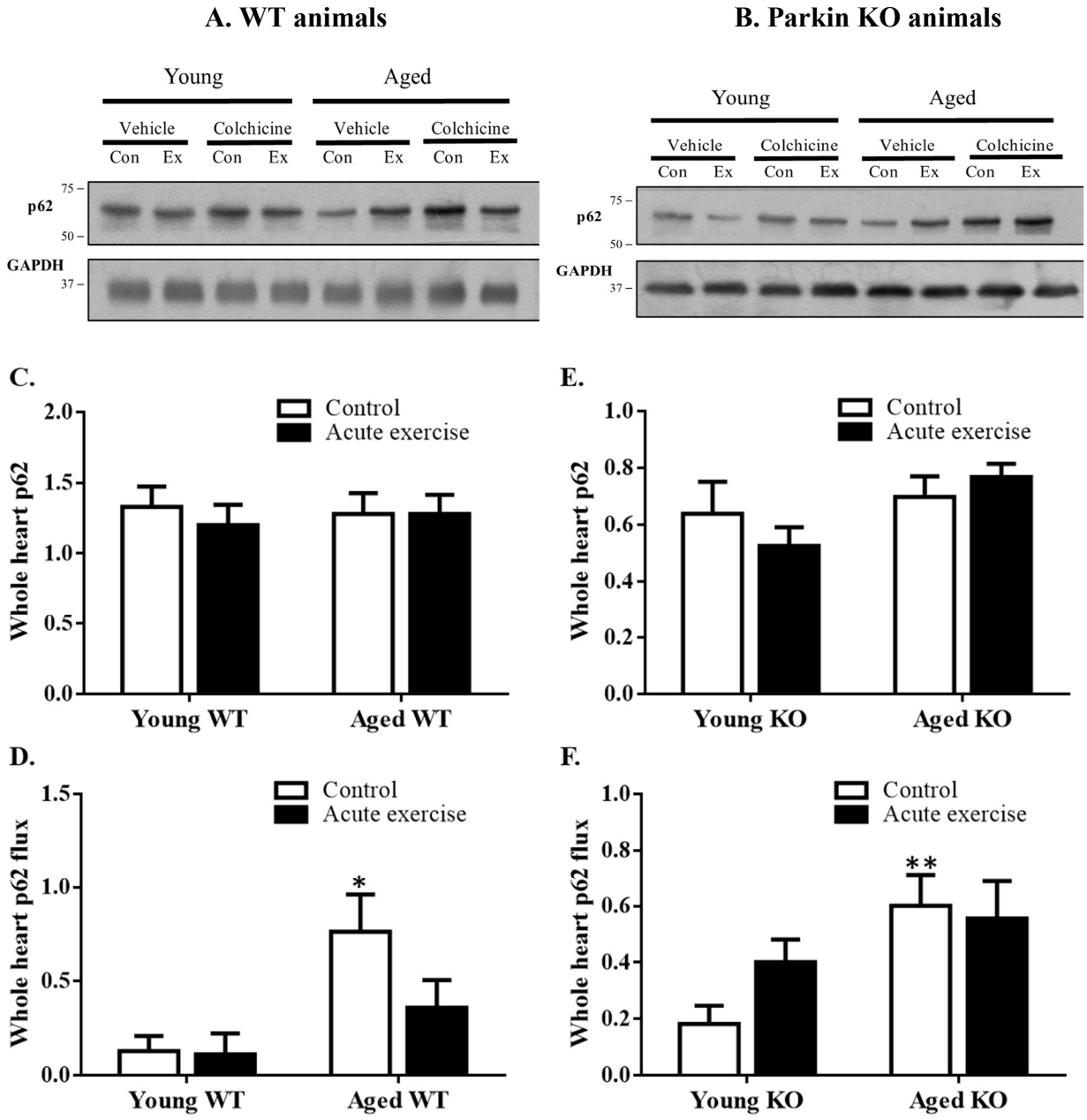

Figure 3. Expression of autophagy adaptor p62 in cardiac muscle of WT and Parkin KO animals. Representative blots of whole heart p62 in A) WT and B) Parkin KO mice. Quantification of p62 content between young and aged C) WT and E) Parkin KO mice. Evaluation of p62 flux in the heart between young and aged D) WT and F) Parkin KO mice. *P<0.05, vs young WT. *P<0.05, vs young KO control. GAPDH was used as a loading control. Values are represented in arbitrary units. (n=6 for all groups).

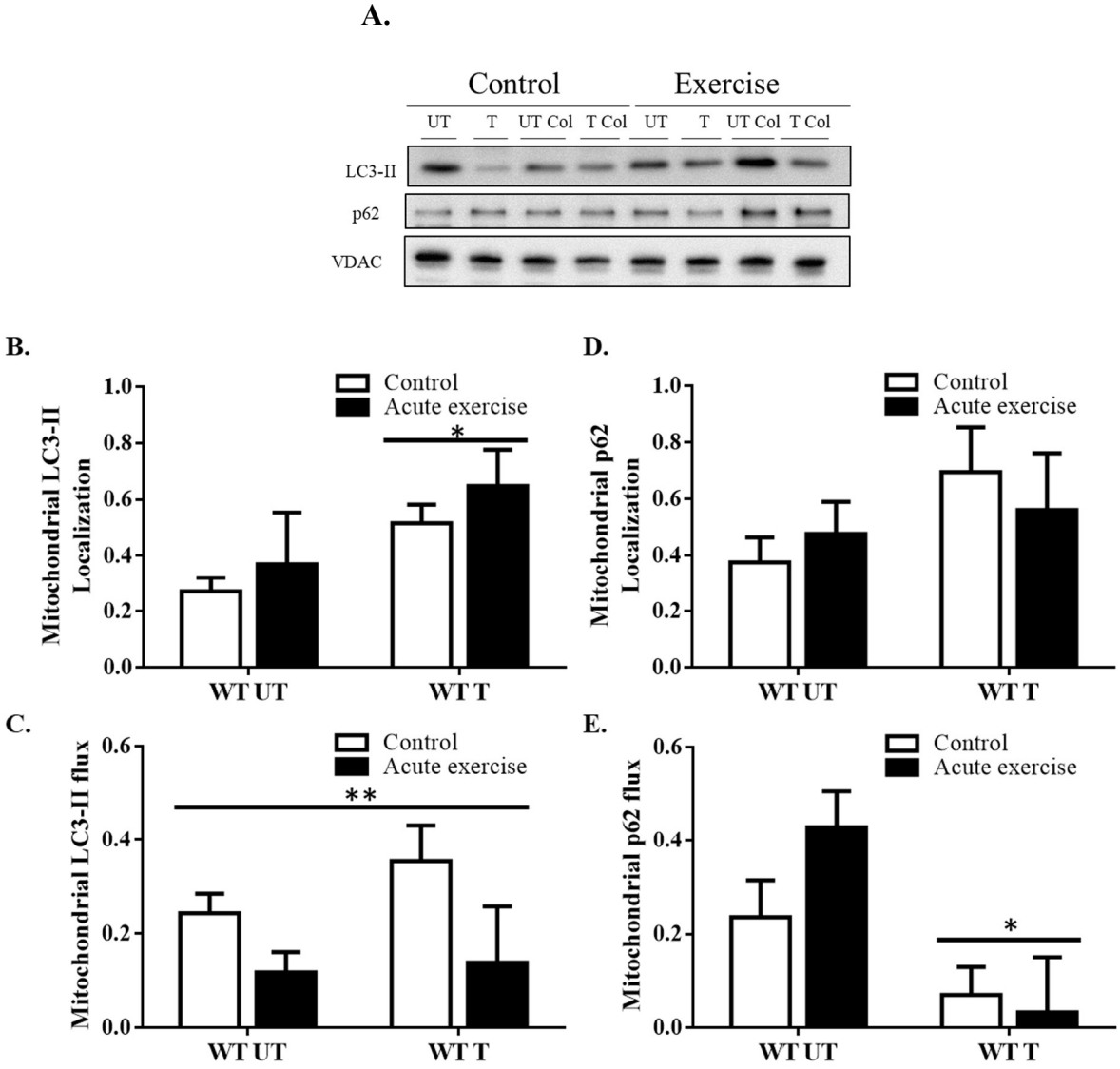

Figure 4. Mitochondrial localization of autophagy proteins LC3-II and p62 from WT animals. Representative blots of LC3-II and p62 on isolated cardiac mitochondria from WT mice. Quantification of B) LC3-II and D) p62 localization on mitochondria between untrained and untrained animals. Evaluation of C) LC3-II flux and E) p62 flux on cardiac mitochondria following exercise and training. *P<0.05, main effect of training. **P<0.05, main effect of acute exercise. VDAC was used as a mitochondrial loading control. Values are represented in arbitrary units. (n=4 for all groups).

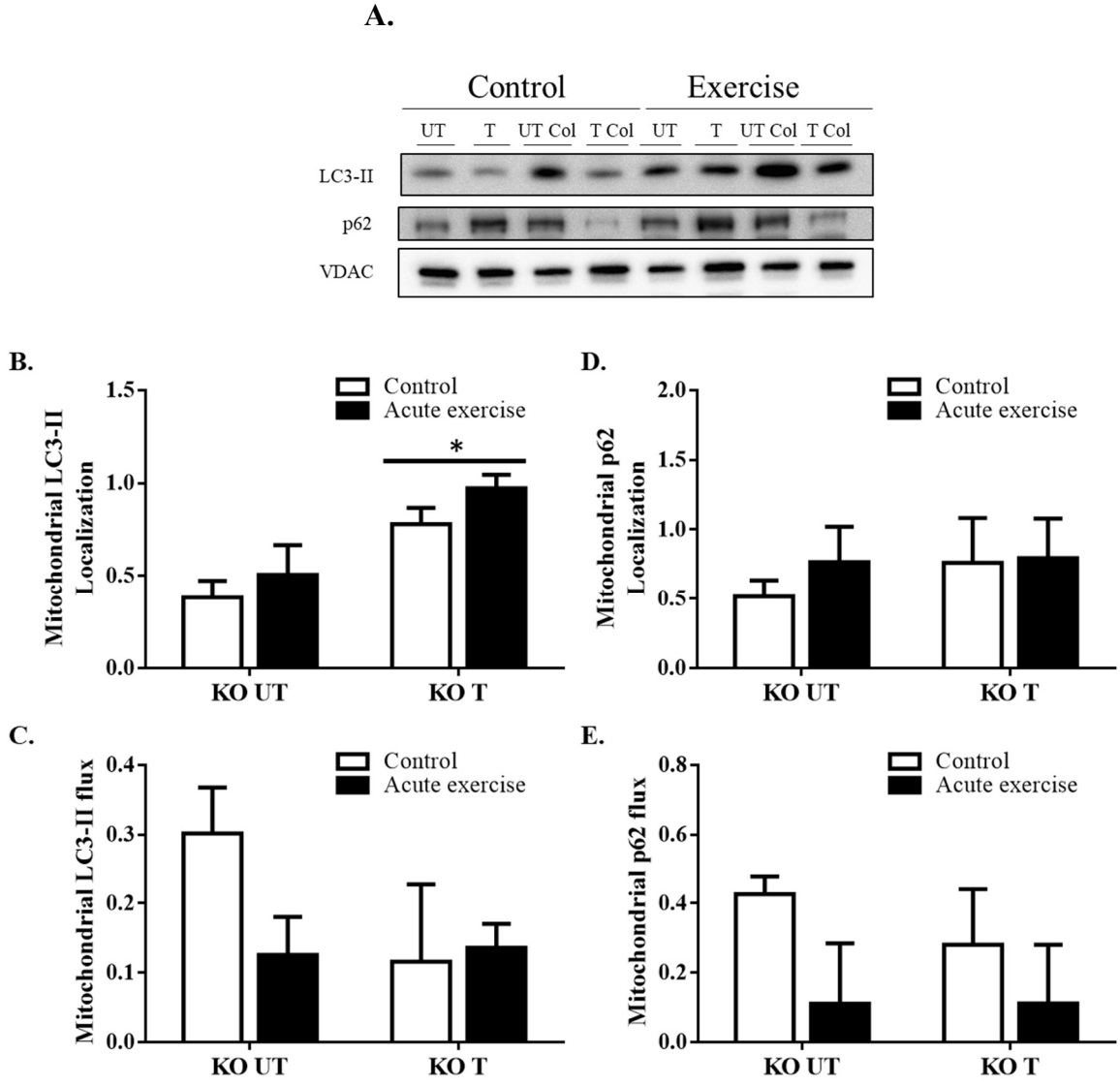

Figure 5. Mitochondrial localization of autophagy proteins LC3-II and p62 from KO animals. Representative blots of LC3-II and p62 on isolated cardiac mitochondria from KO mice. Quantification of B) LC3-II and D) p62 localization on mitochondria between untrained and untrained animals. Evaluation of C) LC3-II flux and E) p62 flux on cardiac mitochondria following exercise and training. *P<0.05, main effect of training. VDAC was used as a mitochondrial loading control. Values are represented in arbitrary units. (n=4 for all groups).

STUDY 2: Skeletal muscle autophagy proteins in endurance trained, obese and obese diabetic individuals (Laval University collaborators: Claire Huth and Dr. Denis Joanisse)

Rationale

Emerging evidence points to autophagic dysregulation in obesity and in diabetes. The sustained energy surplus of intracellular substrates, such as lipids, can impair autophagy and reduce the responsiveness of cells to changes in nutrient status. This close regulation of energetic status and metabolism is particularly important in organs like skeletal muscle and liver that are insulin-sensitive and responsible for maintaining glucose homeostasis. The energy requirements of these organs correspond to the high abundance and turnover of mitochondria. As such, proper preservation of mitochondrial function and content in these organs is critical for substrate utilization and metabolism.

It is now recognized that several metabolic pathologies, including insulin resistance, are induced by mitochondrial dysfunction. Physical inactivity and muscle atrophy are also often accompanied in individuals with these metabolic pathologies. Furthermore, impairments of mitochondrial dynamics and mitophagic clearance are evident. Consequent reductions in muscle mass and mitochondrial integrity can, in turn, reduce the aerobic capacity of obese and diabetic individuals.

However, what remains unanswered is whether autophagy contributes to the decline in mitochondrial content seen in individuals with obesity and insulin resistance. Furthermore, the effect of regular exercise training on autophagy is not fully established. Exercise training is a possible non-pharmacological treatment for obesity and diabetes which is known to increase mitochondrial content. To assess this, autophagic flux should be measured. However, this is not technically feasible in human subjects currently. Thus, we have investigated well established

markers of autophagy in human skeletal muscle. We hypothesized that because of autophagy upregulation, mitochondrial content and function would be reduced in muscle of obese and insulin resistant individuals. This autophagy upregulation would serve to normalize the metabolic "load" of having greater dysfunctional mitochondria. In athletic individuals, the preservation of autophagy would also assist in the maintenance of healthy mitochondrial turnover in skeletal muscle. In this study, we investigated the influence of endurance training, obesity and obesity accompanied by Type 2 diabetes on human skeletal muscle autophagy markers and mitochondrial dynamic proteins. Muscle biopsies were performed on the Vastus Lateralis muscle from individuals that were: sedentary (S), endurance-trained (A), obese (O) or obese with type 2 diabetes (I).

Results

Mitochondrial morphology

Past research has implicated organelle morphology as an important regulator of skeletal muscle metabolism in both rodent and human models. Thus, we sought to examine the expression of mitochondrial regulatory fusion (Mfn2 and Opa1) and fission (Drp1 and Fis1) proteins in whole muscle. An overall significant 40% decrease in fusion protein Opa1 was present in both obese and obese glucose-intolerant subjects, when compared to endurance trained athletes ($P < 0.05$; Fig. 1B). However, no group differences were detected in Mfn2, Drp1 or Fis1.

Autophagy protein expression

Whole muscle autophagy protein expression was examined for ATG7, p62, Parkin and PARL. Expression of ATG7 and adaptor protein p62 did not significantly differ between conditions. In endurance trained athletes, the mitochondrial protease PARL exhibited a significant

2.1-fold increase in expression compared to obese individuals ($P < 0.05$; Fig. 2B). In contrast, athletic participants displayed a ~50% significant decrement in E3 ubiquitin ligase Parkin when compared to obese glucose-intolerant subjects ($P < 0.05$; Fig. 2A). Following the dietary intervention, obese glucose-intolerant subjects presented a significant 42% reduction in PARL levels ($P < 0.05$; Table 2B).

Endoplasmic reticulum stress

To assess a role for endoplasmic reticulum stress in chronic metabolic diseases, whole muscle expression of CHOP and BIP, two proteins involved in the unfolded protein response, were also examined. Our analyses revealed an overall significant main effect of conditions on CHOP expression ($P < 0.05$; Fig. 3A), but BIP remained unaffected.

Conclusions

The purpose of our investigation was to examine the influence of endurance training, obesity and insulin resistance accompanied by glucose intolerance on human skeletal muscle autophagy markers, as well as proteins related to the maintenance of mitochondrial morphology. ET athletes displayed 50% higher levels of Opa1 fusion protein. No differences were observed in the fission proteins Fis1 and Drp1, suggesting a cellular environment which promotes mitochondrial fusion and an expansion of the mitochondrial reticulum with endurance training. OBD subjects also exhibited a 50% decrement in PARL and a 100% increase in Parkin levels, which are indicators of dysfunctional mitochondria and increased mitophagy. Furthermore, OB individuals expressed elevated levels of CHOP, an endoplasmic reticulum (ER) stress-related protein, while CHOP levels were significantly lower in ET athletes. Our findings suggest that

upregulation of autophagy and the ER-stress response in skeletal muscle appears to be associated with impaired insulin sensitivity in obesity. Endurance training may serve to ameliorate the relationship between autophagy and insulin resistance and obesity.

Fig. 1

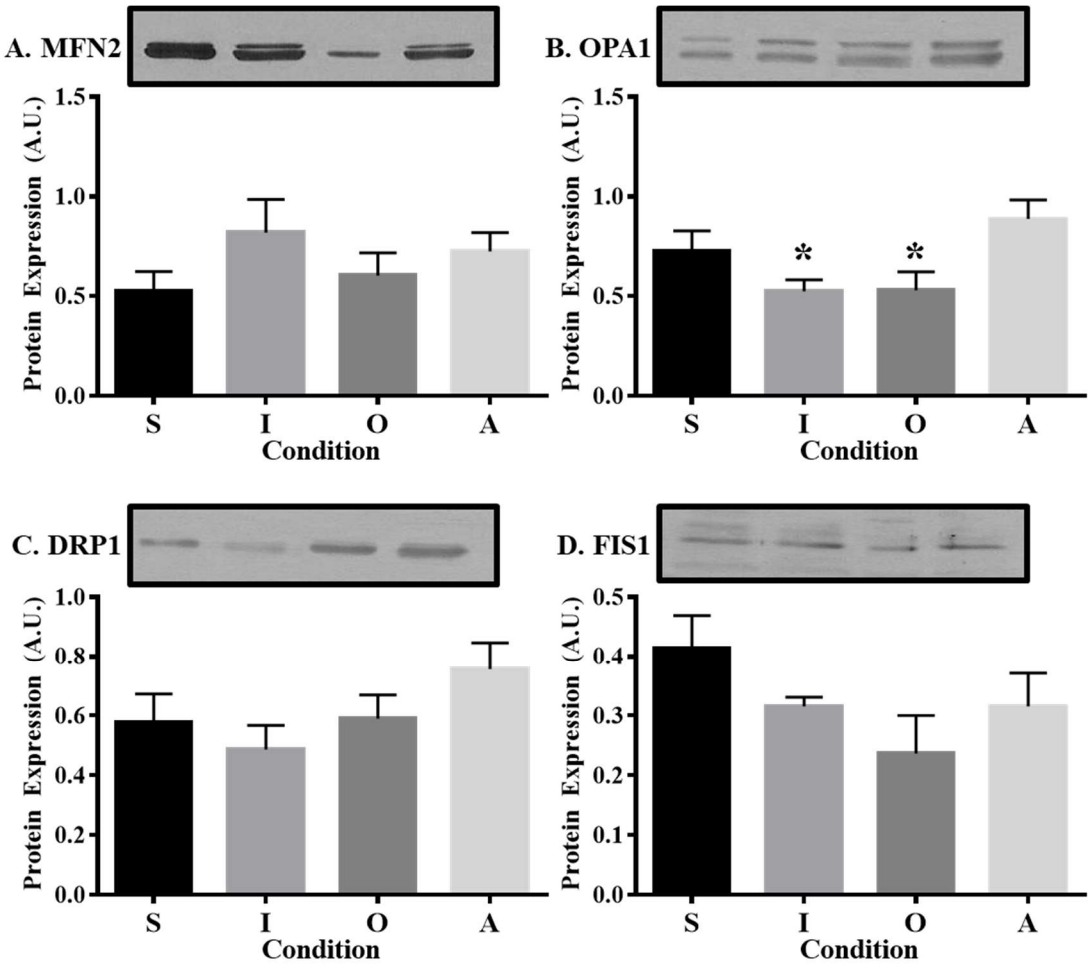

Figure 1. Mitochondrial fusion and fission protein expression in sedentary (S), endurance-trained (A), obese (O) or obese with type 2 diabetes (I) individuals. A to D blots and quantification of mitochondrial fusion and fission proteins in Vastus Lateralis muscle. Quantification of A) Mfn2, B) Opa1, C) Drp1, and D) Fis1. *P<0.05, main effect of condition. Values that share the same asterisk are not statistically different, using the Tukey HSD post-hoc test. (n=8-11 for all groups).

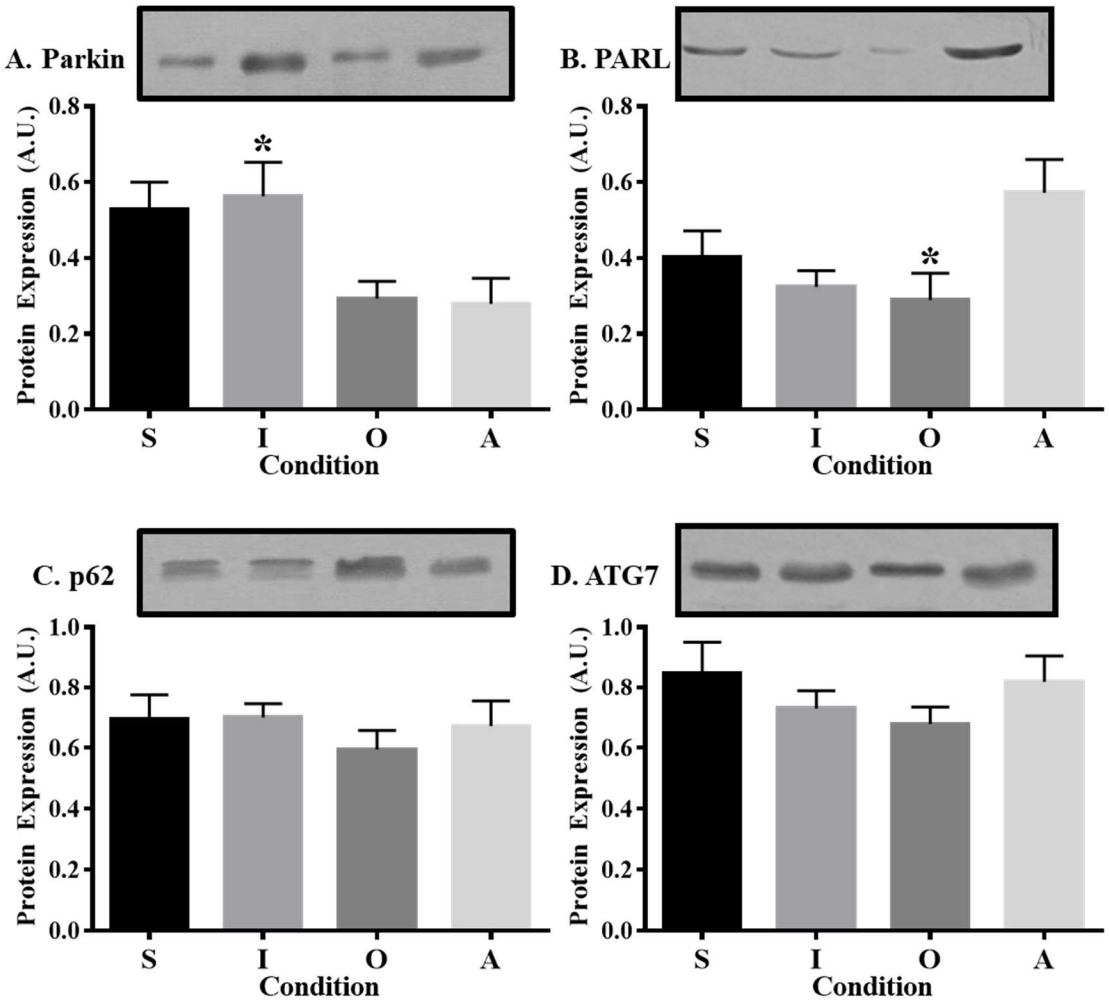

Figure 2. Expression of autophagy and mitophagy markers in sedentary (S), endurance-trained (A), obese (O) or obese with type 2 diabetes (I) individuals. A to D blots and quantification of autophagy and mitophagy proteins in Vastus Lateralis muscle. Quantification of A) Parkin, B) PARL, C) p62, and D) Atg7. *P<0.05, main effect of condition. Values that share the same asterisk are not statistically different, using the Tukey HSD post-hoc test. (n=8-11 for all groups).

Fig. 3

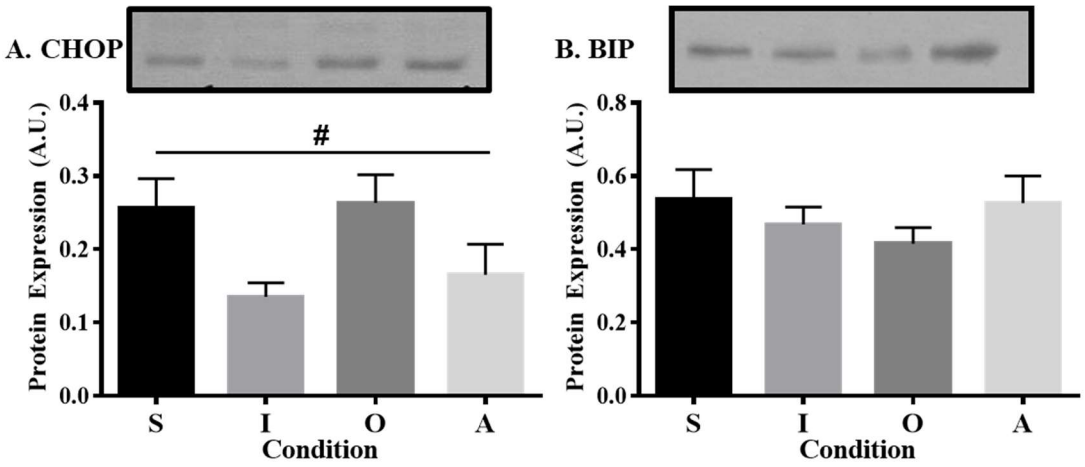

Figure 3. Expression of endoplasmic reticulum (ER) stress in sedentary (S), endurance-trained (A), obese (O) or obese with type 2 diabetes (I) individuals. A to B blots and quantification of ER stress proteins in Vastus Lateralis muscle. Quantification of A) CHOP and, B) BIP. #P<0.05, main effect of condition. (n=8-11 for all groups).

STUDY 3: PINK1 import in skeletal muscle mitochondria

Rationale

The selective degradation of dysfunctional mitochondria is termed mitophagy. Recently, key proteins such as PINK1 and Parkin have been implicated in regulating this process. Mutations arising from these genes are thought to contribute to the development and pathogenesis of human neurological disorders such as Parkinson's Disease. While an extensive amount of research has focused on the function of PINK1 and Parkin function in the brain, very little research has examined these proteins in muscle – an organ that relies heavily on mitochondria to meet its high energy requirements.

Under normal conditions, functional respiring mitochondria rapidly degrade PINK1 through the assistance of PARL. PARL is an enzyme found within the inner mitochondrial membrane that proteolytically cleaves PINK1. The half-life of PINK1 has been estimated to be less than 30 minutes. When a mitochondrion become dysfunctional, the loss of membrane prevents PINK1 from being subjected to PARL degradation, resulting in its accumulation on the outer membrane. Immediately after, PINK1 recruits and activates Parkin from the cytosol to the dysfunctional mitochondrion. Parkin then mobilizes a suite of mitophagy proteins that surround the mitochondrion, sequestering it for lysosomal degradation in the cell. Amino acid remnants are reused for the synthesis of new organelles and proteins in the cell. Currently, it is not known how PINK1 import is regulated in skeletal muscle. Static protein measurements of PINK1 import are not wholly accurate, and only provide a snapshot of the process like that of mitophagy flux.

The purpose of this study was to examine how PINK1 mitochondrial protein import is regulated in skeletal muscle and investigate how mitochondrial dysfunction affects PINK1 import.

Results

PINK1 is a protein kinase implicated in mitophagy as a sensor of mitochondrial dysfunction. Under healthy conditions, PINK1 is translocated into mitochondria by the protein import machinery (PIM) and proteolytically processed by the protease PARL. When mitochondria become dysfunctional, the dissipation of the membrane potential prevents the import and processing of PINK1 resulting in its accumulation on the outer membrane. Once on the outer membrane, PINK1 activates Parkin-mediated ubiquitination leading to the degradation of damaged mitochondria. However, the mechanisms of PINK1 import and its role in muscle remain unclear. In this study we examined PINK1 import into mitochondria isolated from mouse muscles (Fig. 1). A rapid increase in PINK1 insertion into the outer membrane (59 ± 6.9%) and processing (56 ± 7.3%) was observed by 15 minutes of incubation with mitochondria (Fig. 2B). When an uncoupler (CCCP) was supplemented, PINK1 import was reduced by 50%, confirming that complete PINK1 import is membrane potential-dependent (Fig. 2B).

Skeletal muscle contains two distinct mitochondrial populations that differ biochemically. To investigate this comparison, we examined PINK1 protein import into SS and IMF mitochondria. Surprisingly, our preliminary data indicated that SS mitochondria exhibited greater PINK1 import (Fig. 3). SS mitochondria are considered more labile than IMF mitochondria, and may indicate that SS mitochondria are more susceptible to mitophagy.

This work presents the PINK1 protein import assay as a viable method to study mitochondrial function and mitophagy activation in skeletal muscle.

Fig. 1

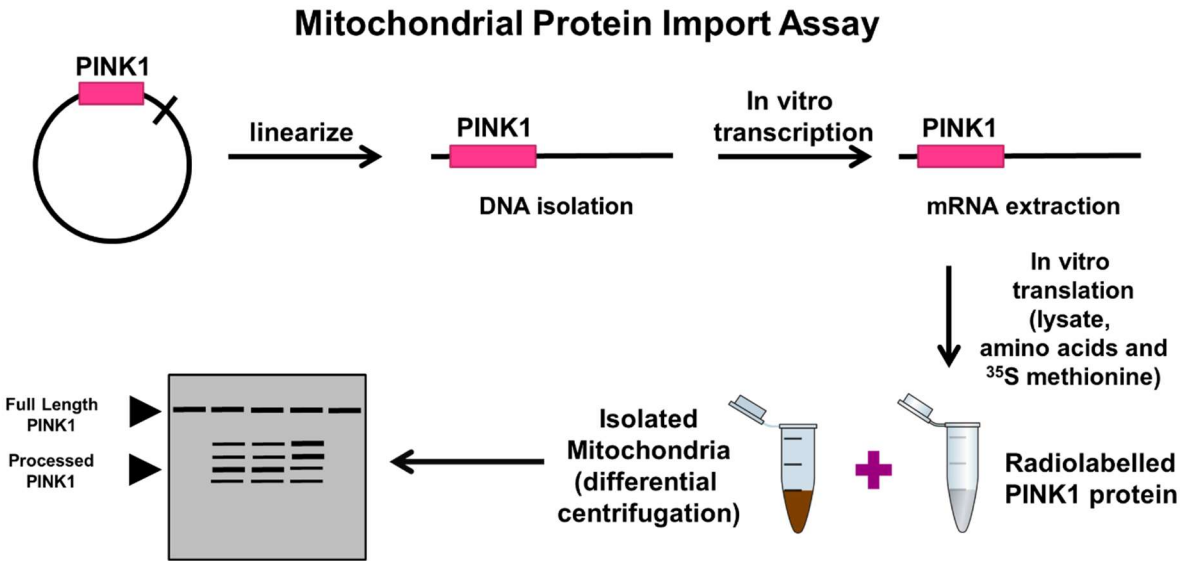

Figure 1. Schematic outline of PINK1 import into isolated mitochondria. Full length cDNA encoding PTEN-induced putative kinase 1 (PINK1, from Dr. Richard J. Youle, National Institutes of Health, Maryland, USA) was linearized and transcribed. In vitro translation was performed using cell free rabbit reticulocyte lysate (Promega, Fisher Canada) in the presence of [35S]-methionine (Perkin Elmer, Canada). Afterwards, isolated mitochondria and reticulocyte lysate containing the translated radiolabeled precursor PINK1 were initially allowed to equilibrate separately at 30 °C for 25 minutes. To examine the dissipation of membrane potential, isolated mitochondria were pre-treated with carbonyl cyanide m-chlorophenyl hydrazone (CCCP). The two samples were combined and further incubated at 30 °C for 25 minutes. To standardize import reactions using SDS-PAGE, 75 µg of mitochondria and 18 µl of reticulocyte lysate were used. Mitochondria were recovered by centrifugation (16,000 x g) through 600 µl of 20% sucrose in 0.1 M potassium chloride, 2 mM magnesium chloride, and 20 mM HEPES (pH 7.4) at 4 °C for 15 minutes. For outer membrane proteins, such as PINK1, the mitochondrial pellet after the sucrose gradient spin was re-suspended in freshly prepared 0.1 M sodium carbonate (Na2CO3). The samples were left on ice for 30 minutes to eliminate any bound, peripheral PINK1 to the outer mitochondrial membrane that was not imported. Mitochondria were recovered after centrifugation (16,000 x g) at 4 °C for 15 minutes. Samples were denatured at 95 °C for 5 minutes and electrophoresed through a 12% SDS-polyacrylamide gel. Following electrophoresis, gels were treated for 5 minutes in boiling 5% trichloroacetic acid, followed by a 1-minute wash in distilled water, 5 minutes in 10 mM Tris base (pH 9.0), and 30 minutes in 1 M sodium salicylate. Gels were subsequently dried with a vacuum gel dryer (Model 583; Bio-Rad). Radiolabeled precursor proteins were detected using storage phosphor imaging (Typhoon Trio; GE Healthcare Life Sciences) and quantified using ImageJ software.

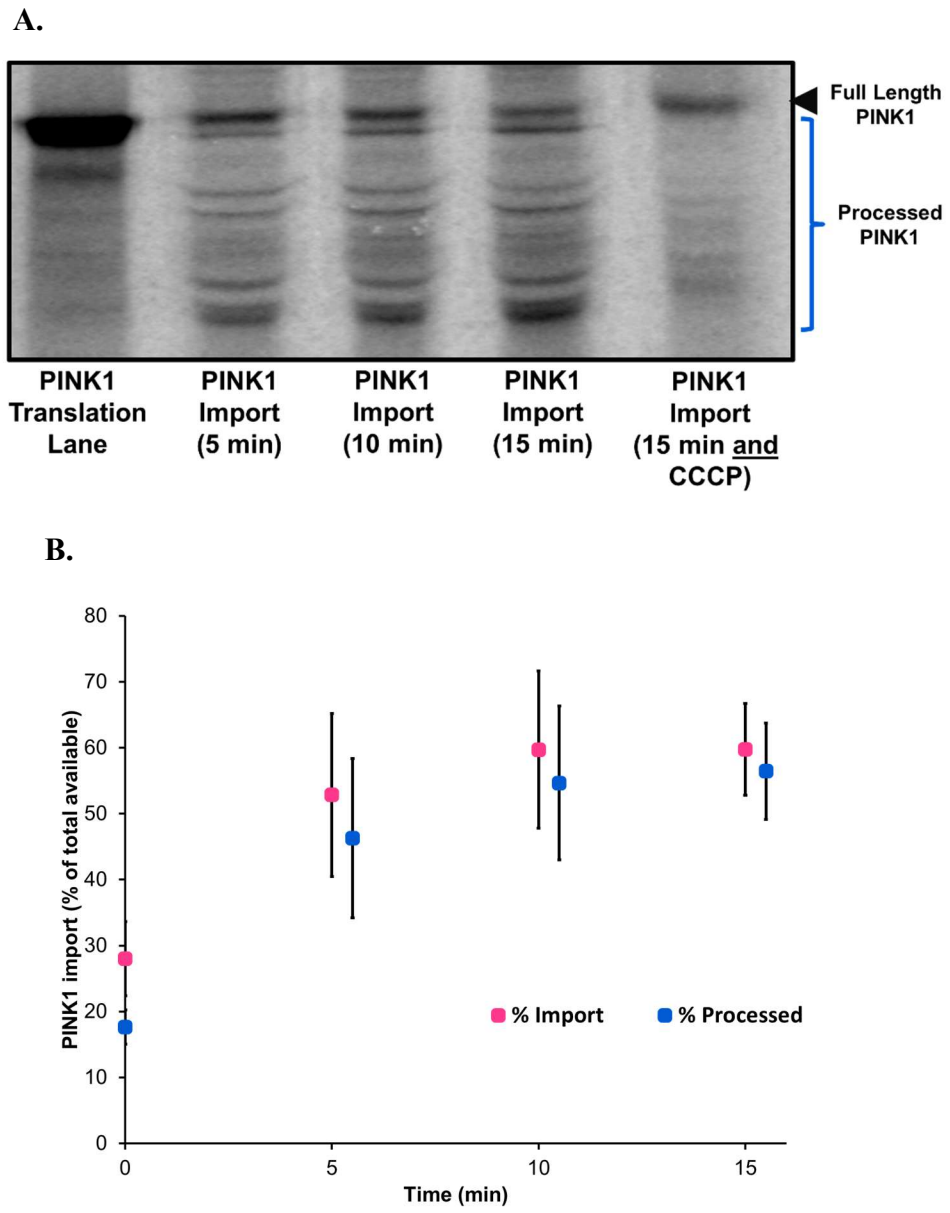

Figure 2. PINK1 protein import and processing in IMF mitochondria. A) Import blot of translated radiolabeled PINK1 protein into IMF mitochondria over 15 minutes. For time "zero", CCCP was added to isolated mitochondria to dissipate the membrane potential. **B)** Graphical representation of PINK1 protein import and processing over 15 minutes represented as percentage of total available protein (N = 7). For each 5-minute period, the quantification of all bands was represented as "% Import". The quantification of all bands except the full length PINK1 band was calculated as "% Processed".

Fig. 3

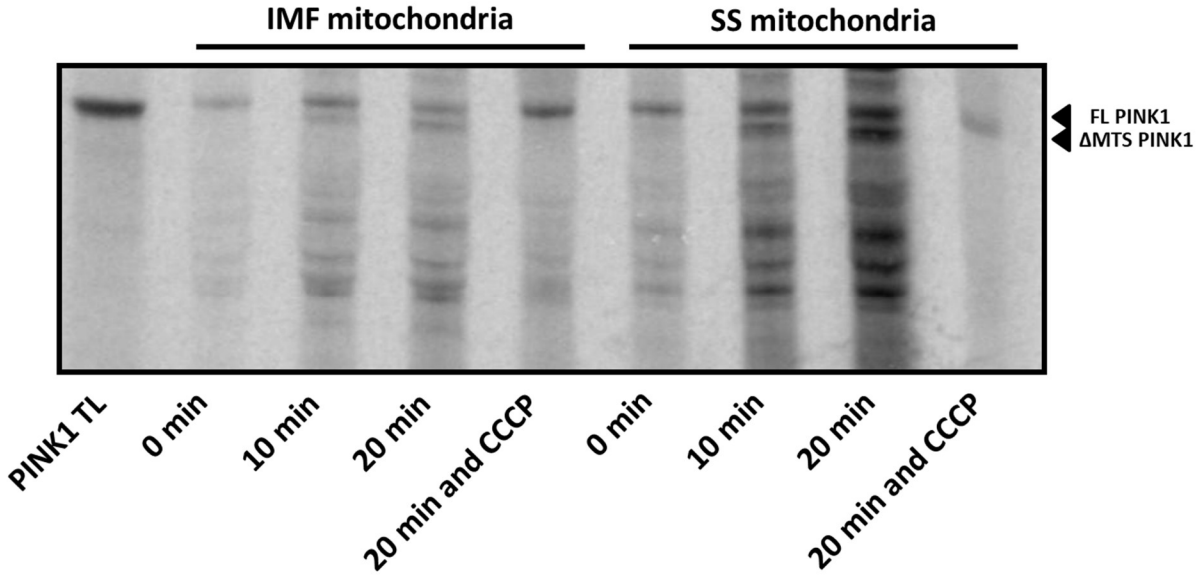

Figure 3. PINK1 protein import and processing in IMF and SS mitochondria. Import blot of translated radiolabeled PINK1 protein into IMF and SS mitochondria over 20 minutes. Following 20 minutes, CCCP was added to isolated mitochondria to dissipate the membrane potential. Full length, FL; MTS, mitochondrial targeting sequence.

APPENDIX C:

LABORATORY METHODS

MITOCHONDRIAL ISOLATIONS FROM MUSCLE

References: Cogswell et al. Am J Physiol, 1993, 264: C388-C389
Krieger et al. J Appl Physiol, 1980, 48: 23-28

Reagents:

All buffers are set to pH 7.4 and stored at 4 °C

- Buffer 1
  - 100 mM KCl
  - 5 mM MgSO4
  - 5 mM EDTA
  - 50 mM Tris base
- Buffer 2
  - 100 mM KCl
  - 5 mM MgSO4
  - 5 mM EGTA
  - 50 mM Tris base
  - 1 mM ATP
- Nagarse protease (Sigma, P-4789)
  - 10 mg/ml in Buffer 2
  - Make fresh for each isolation, keep on ice
- Buffer 1 + ATP
  - Add 1 mM ATP to Buffer 1
- Resuspension medium
  - 100 mM KCl
  - 10 mM MOPS
  - 0.2% BSA

Procedure:

1. Remove various muscles from mouse and place in a scintillation vial containing ice cold buffer 1.
2. Place muscles on a watch glass that is also on ice and trim away fat and connective tissue. Proceed to thoroughly mince the muscle sample with forceps and scissors, until no large pieces are remaining.
3. Place the minced tissue in a plastic centrifuge tube and record the exact weight of tissue.
4. Add a 10-fold dilution of Buffer 1 + ATP to the tube.
5. Homogenize the samples using the Ultra-Turrax polytron with 40% power output (9.8 Hz) and 10 sec exposure time.
6. Using a Beckman JA 25.50 rotor, centrifuge the homogenate at a setting of 800 g for 10 min. This step divides the IMF and SS mitochondrial subfractions. The supernate will contain the SS mitochondria and the pellet will contain the IMF mitochondria.

SS mitochondrial isolation:

7. Filter the supernate through a single layer of cheesecloth into a second set of 50 ml plastic centrifuge tubes.
8. Centrifuge tubes at 9000 g for 10 min. Upon completion of the spin discard the supernate and gently resuspend the pellet in 3.5 ml of Buffer 1 + ATP. Since the mitochondria are easily damaged, it is important that the resuspension of the pellet is done carefully.
9. Repeat the centifugation of the previous step (9000 g for 10 min) and discard the supernate.
10. Resuspend the pellet in 100 µl of Resuspension medium, being gentle so as to prevent damage to the SS mitochondria. Some extra time is needed during this final resuspension to ensure the SS pellet is completely resuspended.
11. Keep the SS samples on ice while proceeding to islolate the IMF subfraction.

IMF mitochondrial isolation:

7. Gently resuspend the pellet (from step 6) in a 10-fold dilution of Buffer 1 + ATP using a teflon pestle.
8. Using the Ultra-Turrax polytron set at 40% power output, polytron the resuspended pellet for 10 s. Rinse the shaft with 0.5 ml of Buffer 1 + ATP.
9. Centrifuge at 800 g for 10 min and discard the resulting supernate.
10. Resuspend the pellet in a 10-fold dilution of Buffer 2 using a teflon pestle.
11. Add the appropriate amount of nagarse. The calculation for the appropriate volume is 0.025 ml/g of tissue. Mix gently and let stand exactly 5 min.
12. Dilute the nagarse by adding 20 ml of Buffer 2.
13. Centrifuge the diluted samples at 5000 g for 5 min and discard the resulting supernate.
14. Resuspend the pellet in a 10-fold dilution of Buffer 2. Gentle resuspension is with a teflon pestle.
15. Centrifuge the samples at 800 g for 10 min. Upon the completion of the spin, the supernate is poured into another set of 50 ml plastic tubes (on ice), and the pellet is discarded.
16. Centrifuge the supernate at 9000 g for 10 min. The supernate is discarded and the pellet is resuspended in 3.5 ml of Buffer 2.
17. Centrifuge samples at 9000 g for 10 min and discard the supernate.
18. Gently resuspend the pellet in 200 µl of Resuspension medium.

MITOCHONDRIAL RESPIRATION

Reference: Estabrook, R.W., Meth. Enzymol., 10: 41-47 (1967)

The rate of mitochondrial respiration is an important consideration in the biochemical analysis of mitochondria. There are three phases of interest in analyzing the respiratory ability of mitochondria. Mitochondria produce ATP in the presence of oxygen. The respiratory ability of the freshly isolated IMF and SS mitochondrial fractions and the homogenates can be illustrated by measuring the rate of oxygen consumption using a Clark oxygen electrode in the presence of a) the substrate alone (e.g. glutamate for state 4 or resting respiration); b) ADP, (state 3 or active respiration); and c) $NADH^+$, which is used to measure the amount of damage that has occurred to the mitochondria, since the inner membrane is impermeable to $NADH^+$.

Reagents:

1. VO_2 Buffer for **muscle** mitochondria:

   250 mM **Sucrose** 42.8 g/500 ml
   50 mM **KCl** 1.86 g/500ml
   25 mM **Tris-HCl *** 1.97 g/500ml
   10 mM **K_2HPO_4** 0.871 g/500ml
   pH to 7.4

   * In place of 25mM Tris-HCl you can use 25 mM Tris (aka Tris (hydroxymethyl) methylamine). This works out to 1.5125 g/500ml (FW=121.4). Using Tris in place of Tris-HCl means that you will have to add more HCl to get the pH down to 7.4
2. **Glutamate** - final conc. of 11.1 mM.....**2.0 M initial conc**. (406.4 mg/ml)
3. **ADP** - Final conc of 0.44 mM ..... **20 mM initial conc.** (8.54 mg/ml)
4. **NADH** - Final conc.: 2.8 mM.....**0.5 M initial conc.** (354.7 mg/ml)

Procedure:

1. Set water bath at 30ºC -- clean out chambers (Clark oxygen electrode; Yellow Springs Inst. Co., Yellow Springs, OH) and stir bars.
2. Add 250uL of VO_2 Buffer to each chamber.
3. Insert electrode # 2 into the chamber.
4. Remove all bubbles in the chamber and allow it to reach equilibrium temperature (30ºC) while spinning.
5. Set recorder for chamber # 2 and paper speed for 3 cm/min.
6. Set monitor and recorder to 100 %.
7. Remove electrode. Add 50 µl of mitochondria into the chamber.
8. Allow a steady state to be reached.
9. Add 12.5 µl of pyruvate and 12.5 µl of malate (heart) or 12.5 µl glutamate (muscle).
10. Wait approximately 3 minutes then add ADP: 50 µl for muscle, 100 µl for heart.
11. Wait (about 2-3 minutes) for a steady rate of state 3 respiration before adding 12.5 µl of NADH. Prepare the next chamber while the respiration recordings are being made.
12. Clean out the chamber in the following manner: Remove the electrode and aspirate, remove the magnetic stir bar and aspirate, and finally, clean the electrode by rinsing with distilled water and pat dry.
13. Put electrode in the next chamber (which should already have the buffer and sample in it).
14. Prepare the next chamber while measuring the respiration of the current chamber (ie. add 2 ml of VO_2 Buffer and allow to equilibrate).
15. Calculate the state 4, state 3 and $NADH^+$ rates for each sample. Remember that the chart speed is 3 cm/sec and full scale is 100 %. (slope=rate=blocks/min)
16. Calculate the rates of state 3 and state 4 respiration per mg of mitochondrial protein by dividing the state 3 and 4 rates by the amount of protein (mg) added to the VO_2 Buffer.

ROS EMISSION

Background: Mitochondria are the primary source of reactive oxygen species (ROS) to the cell. It is estimated that about 2% of total cellular oxygen is converted to ROS by the inappropriate reduction of molecular oxygen by intermediate members of the electron transport chain (ETC). ROS are damaging molecules that can compromise the integrity of macromolecules within the mitochondria and may lead to overall organelle dysfunction. MtDNA may be prone to attack by ROS because 1) mtDNA is near the ETC, 2) mtDNA lacks the protective sheath of histones compared to nuclear DNA and, 3) mitochondria have an insufficient repair system for mtDNA mutations. ROS can exist in a variety of molecular permutations such as superoxide (O_2^-), hydroxyl radical (OH^-) and hydrogen peroxide (H_2O_2).

DCF (2,7, -dichloro-fluorescein; Fig.1) is a reagent that is non-fluorescent until the acetate groups are removed by intracellular esterases and oxidation occurs within the mitochondria (Figure 1). DCF is oxidized by all the different forms of ROS and this can be detected by monitoring the increase in fluorescence with a fluorometric plate reader. The appropriate plate reader filter settings for fluorescein are the following: **Excitation 485/20 and Emission 528/20** (Figure 2).

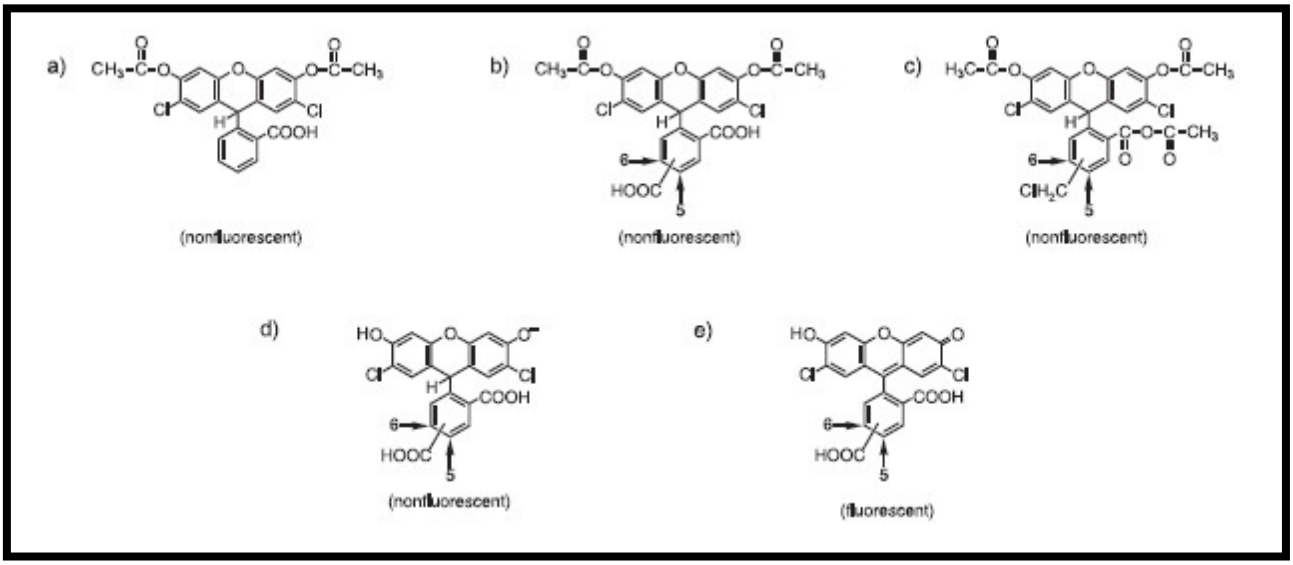

Figure 1. DCF molecule and oxidation of DCF resulting in fluorescence

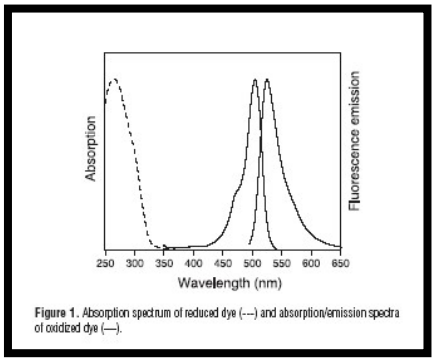

Figure 2. Absorption and Emission Spectra of oxidized dye

KC4 Software Settings: The Settings icon in the upper left corner allows the alteration of various parameters. Once clicked, another window appears, click on the Wizard Icon. In this window there will be a variety of components that can be altered. The following are the parameters that need to be changed to utilize the DCF and measure time-dependent ROS production from isolated mitochondria:

1) Top Middle Panel- Absorbance, Fluorescence, Luminescence- choose **Fluorescence**

2) Top Left Panel- End Point, Kinetic, Spectrum- choose **Kinetic**

3) Top Middle Panel- Click on larger box labeled Kinetic to set parameters- **Run Time 1:20:00, Interval 5:00 (takes a measure every 5 minutes),** click on box labeled **Allow Well Zoom during Read,** and click on box labeled **Individual Well Auto Scaling**- The Well Zoom and Auto scaling allows for monitoring each individual well during the experiment and scales it appropriately.

4) Middle Panel-***Filter Set***- Choose #1, then set the **excitation to 485/20**, and **emission to 528/20** as described above. The optics position should be set to the **TOP** (i.e. readings are taken from the top of the well) and the sensitivity is set at **50** (depending upon the amount and/or nature of the sample).

5) Plate-Type-choose **96-well plate**, choose which wells are to be read i.e. **A1-C12.**

6) Shaking-**Intensity** set at **1, Duration** set at **15s** and then click the box that is labeled **before every reading** (it shakes the samples for 15 s before every reading).

7) Temperature Control- Click on the box indicating **YES,** also click on box labeled pre-heating, and put 37°C into the temperature box.

Reagents:

DCF (2,7,-dichlorodihydrofluorescein diacetate) reagent MW=487.29 (Molecular Probes D-399/ 100mg)

1° STOCK- Make up **50mM** Stock Solution in EtOH- 24 mg/ml- only make about 500ul i.e. 12 mg per 500ul EtOH. Wrap stock solution in aluminum foil and limit exposure to light since DCF is light-sensitive.

Working Stock Solution-2° STOCK- Dilute 50mM by 100-fold by taking 10ul and adding 990 ul of EtOH to attain a **500uM DCF Stock Solution**. This will be the DCF concentration used to add to the reaction mixture.

VO_2 Buffer- refer to mitochondrial respiration protocol

Procedure:

1. SS and IMF mitochondria are isolated as described in the mitochondrial isolation protocol. Alternatively, frozen mitochondrial extracts can also be used.

2. Determine the volume necessary for 50ug of mitochondria. Typical volumes should range between 5-40ul depending upon concentration of mitochondrial extracts.

3. Final concentration of DCF is 50uM. The total volume of the reaction mixture is 250ul. Thus, 25ul of DCF is used in the reaction mixture since this represents a 10-fold dilution. Set up table and determine the amount of VO_2 buffer necessary to make each of the reaction mixtures equal to 250 ul. (Remember to include a ***control*** with only VO2 buffer and DCF reagent)

4. Once table is complete and volumes for all samples have been determined, place the frozen (already thawed) or fresh mitochondria, VO_2 buffer and DCF (500uM) into a 37°C circulating water bath for 5-10 min.

5. Pipette the volume of VO_2 buffer required for each of the samples followed by the mitochondrial samples into the appropriate wells of a 96-well plate. In addition, include a well (usually in the corner well) with only 250 ul of VO_2 buffer to monitor temperature (see below). Place the 96-well plate with the VO_2 buffer and mitochondria into a 37°C incubator. Using the YSI temperature probe, place the recording electrode into the well with buffer only and monitor the temperature until 37°C is reached. During this time, be sure that the KC4 software is set up and that the Biotek plate reader is pre-heating to 37°C.

6. Once mitochondria and buffer have reached temperature (37°C), take the DCF out of the circulating water bath (37°C) and quickly add the DCF to each of the reaction mixtures. Following addition of DCF, promptly place the plate into the Biotek plate reader for fluorescence measurement and start the KC4

program by pressing **READ** plate on the upper left portion of the computer screen. Kinetic program will operate for 1 h and 20 min.

WESTERN BLOTTING

Reagents:

1. Acrylamide/Bis-Acrylamide, 30% Solution 37.5:1 (BioShop 10.502)
    a. Store at 4°C
2. Under Tris Buffer
    a. 1M Tris-HCl, pH 8.8 (60.5g/500ml)
    b. Store at 4°C
3. Over Tris Buffer
    a. 1M Tris-HCl, pH 6.8 (12.1g/100ml)
    b. Bromophenol Blue (for colour)
    c. Store at 4°C
4. Ammonium Persulfate (APS)
    a. 10% (w/v) APS in ddH_20 (1g/10ml)
    b. Stored at 4°C
5. Sodium Dodecyl Sulfate (SDS)
    a. 10% (w/v) in ddH_20 (1g/10ml)
    b. Store at room temperature
6. TEMED (Sigma T-9281)
7. Electrophoresis Buffer, pH 8.3 (10L)
    a. 25mM Tris 30.34g, 192mM Glycine 144g, 0.1% SDS 10g
    b. Volume to 10L with ddH_20
    c. Store at room temperature
8. 6X SDS
    a. Warm 100% glycerol in water bath at 65°C for 30 minutes
    b. Combine 1.2g SDS, 0.06g Bromophenol Blue, 3mL of 1M Tris, pH 6.8 and 1ml of ddH_2O and stir at 4°C for 5 minutes
    c. Add 3mL of 100% glycerol, stir and aliquot mixture.
    d. Store at -20°C
    e. Add 5% (v/v) ß-mercaptoethanol (Sigma M6250) to 6X SDS <u>just prior</u> to use
9. *tetra*-Amyl alcohol ReagentPlus, 99% (Sigma 152463)

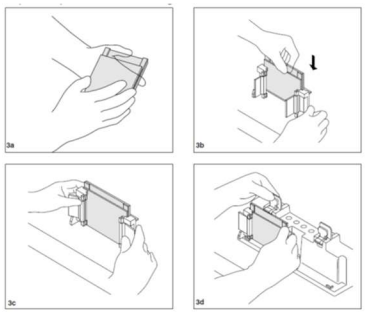

Procedure:

1. **Prepare electrophoresis rack:**
    a. Clean glass plates thoroughly with soap followed by 95% ethanol then ddH_2O.
    b. Dry carefully with a kimwipe.
    c. Assemble glass plates as shown below:
    d. Check the seal by adding a small volume of ddH_2O then pour off and let dry.
2. **Prepare separating gels:**
    a. Mini Protean 3 Bio-Rad System volumes:

	8%	10%	12%	15%	18%
Acrylamide	2.7 ml	3.3 ml	4.0 ml	5.0 ml	6.0 ml
ddH_20	4.1 ml	3.5 ml	2.8 ml	1.8 ml	0.8 ml
Under Tris	3.0 ml	3.0 ml	3.0 ml	3.0 ml	3.0 ml
SDS	100µl	100µl	100µl	100µl	100µl
APS	100µl	100µl	100µl	100µl	100µl
TEMED	10µl	10µl	10µl	10µl	10µl

b. Mix the contents of the separating gel without adding APS or TEMED. Stir.
c. Add APS and TEMED. Stir.
d. Slowly pour the entire volume of the solution into the space between the two plates while keeping plates tilted to prevent bubble formation.
e. Add *tert*-Amyl alcohol to coat top surface of gel solution.
f. Allow 30 minutes for gel polymerization.
g. Remove *tert*-Amyl alcohol by pouring it off and remove any remainder with a kimwipe. Rinse with ddH_20.

3. Prepare stacking gel:

a. For a single mini gel use the following volumes:

Acrylamide	500 µl
Over Tris	625 µl
ddH_20	3.75 ml
SDS	50 µl
APS	50 µl
TEMED	7.5 µl

b. Mix the contents of the stacking gel without adding APS or TEMED. Stir.
c. Add APS and TEMED. Stir.
d. Using a Pasteur pipette slowly add the entire volume from the beaker in between the plates.
e. Add comb for desired number of wells.
f. Allow 30 minutes for gel polymerization.

4. Prepare samples:

a. Turn on the block heater to 95ºC.
b. Pipette required volume of sample into new Eppendorf tube with same amount of lysis buffer and 5 µl of sample dye. Keep samples on ice until all samples are prepared (use pipette plan).
c. Briefly centrifuge each sample to bring volume to the bottom of the Eppendorf tube.

d. Incubate each sample at 95 ºC for 5 minutes in the heating block to denature the proteins.
e. Briefly centrifuge again to return volume to the bottom of the Eppendorf tube.

5. **Assemble Mini-PROTEAN gel caster system:**
   a. See images below
   b. If you are only running one gel a plastic rectangular pseudo plate must be clamped on the other side of the caster.
   c. Fill with electrophoresis buffer between the plates and outside of the plates in the chamber.
   d. Slowly remove the comb using both hands (one on each side) by pulling the comb straight upwards.
   e. Fix any wells that are deformed using a small spatula.
   f. Clean out the wells using a syringe filled with electrophoresis buffer.
   g. Withdraw the entire volume of the sample using a Hamilton syringe. Inject volume slowly into the bottom of the well.

6. **Gel electrophoresis**
   a. Immediately after all samples are loaded place the lid on the gel chamber.
   b. Place positive and negative plugs into the power supply and turn on power supply.
   c. Set power supply to 120V. Gel will run for ~2 hours depending on percent gel made.
   d. When the bromophenol blue has run off the bottom of the gel (or when gel has separated the desire amount) turn off the power supply. Remove plugs from power supply and remove lid.
   e. Prepare for electrotransfer of proteins from the gel to nitrocellulose membrane.

<u>Western Blotting-Transfer and Immunodetection:</u>

Reagents:

1. Transfer Buffer
   a. 0.025M Tris-HCl pH 8.3 12.14g
   b. 0.15M Glycine 45.05g
   c. 20% Methanol 800ml
   d. make up to 4L with ddH_20
   e. store at 4°C
2. Ponceau S stain
   a. 0.1% (w/v) Ponceau S
   b. 0.5% (v/v) Acetic Acid
   c. Store at room temperature
3. Wash Buffer
   a. Tris-HCl pH 7.5 12g
   b. NaCl 58.5g
   c. 0.1% Tween 10ml
   d. Store at room temperature
4. Blocking Solution
   a. 5% (w/v) skim milk power in wash buffer OR
   b. 5% (w/v) BSA in wash buffer
5. Enhanced Chemiluminescence Fluid (ECL; Santa Cruz sc-2048)
6. Film/Developer/Fixer

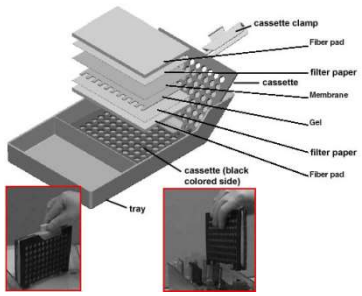

Procedure:

1. **Transfer Procedure**

a. Remove electrophoresis plates from chamber and separate the plates.
b. Cut away unnecessary parts of the gel using a spatula and measure remaining gel size.
c. Using a paper cutter cut 6 pieces of Whatman paper per gel to the same size as the gel. Wearing gloves cut nitrocellulose membrane (GE Healthcare RPN303D) to the dimensions of the gel.
d. Assemble Whatman paper, nitrocellulose memebrane and gel as shown above:
e. Close the cassette and place in the transfer chamber with the black side of the cassette facing the back side of the chamber.
f. Place ice pack in the chamber.
g. Place lid on the chamber and connect the leads to the power supply.
h. Turn on the power supply and run at 120V for 2 hours. This can vary depending on the size of the protein of interest.

2. Removal of transfer membrane:

a. Turn off the power supply and disconnect leads from the power supply then remove the lid from the chamber.
b. Remove the cassette from the chamber.
c. With gloves on, remove the Whatman paper and gel and place the nitrocellulose membrane in a plastic dish.
d. Add Ponceau S stain on the membrane and gently swirl.
e. Drain off the remaining Ponceau S and save for reuse.
f. Rinse the membrane with ddH_2O to reduce the red background. Wrap membrane in saran wrap and scan image.
g. Cut the membrane while protein bands are still visible at the desired molecular weight.
h. Rotate membrane at room temperature in wash buffer until remaining Ponceau S has been removed.
i. Incubate membrane for 1 hour with rotation in blocking solution.
j. Incubate membrane with desired antibody diluted in blocking solution overnight at 4ºC. Membrane is placed face up into the solution on a glass plate covered in parafilm. To maintain a moist environment overnight, wet a small kimwipe and form it into a ball and place in each corner of the dish. Cover the dish with saran wrap.

3. Immunodetection

a. Wash the blots in wash buffer with gentle rotation for 5 minutes 3X.
b. Incubate the blots for 1 hour in room temperature with the appropriate secondary antibody diluted in blocking solution.
c. Membrane is placed face up in solution on a glass plate covered with parafilm. Place moist kimwipes in each corner of the dish and cover the dish with saran wrap.
d. Following the incubation, wash the membrane 3X for 5 minutes with wash buffer.

4. Enhanced Chemiluminescence Detection

a. Mix ECL fluids “A” and “B” in a 1:1 ratio in a disposable Rohr tube.
b. Place blots on saran wrap face up and apply ECL solution for 2 minutes.
c. Dab off excess ECL on a kimwipe and place blots face down on a fresh piece of saran wrap and wrap tightly.
d. Expose blot to film (time will vary depending on protein and antibody).
e. Place film into developer (time will vary).
f. Once image appears place film into fixer for 2 minutes. Wash with fresh water when complete.

CYTOCHROME C OXIDASE ASSAY FOR MICROPLATE READER

References: J. Biol. Chem. 189:665, 1951,
Meth. Biochem. Anal. 2:427, 1955,
Meth. Enzymol. 10:245, 1967.

THEORY:

Tissue extract containing cytochrome c oxidase is added to the test solution containing fully reduced cytochrome c. The rate of cytochrome c oxidation is measured over time as a reduction in absorbance at 550 nm. The reaction is carried out at 30° C.

REAGENTS:

1. 20 mM KCN; MW= 65.12, 13.02 mg/10 ml dH_2O
2. 100 mM K-Phosphate Buffer

   - make up 0.1 M KH_2PO_4; MW= 136.09
     = 13.6 g/1000 ml
     (pH approx. 5)
     (rm. temp)
   - make up 0.1 M $K_2HPO_4.3H_2O$; MW= 174.18
     = 17.4 g/1000 ml
     (pH approx. 8)
     (rm. temp)
   - mix in equal proportions, pH to 7.0

3. 10 mM K-Phosphate Buffer
   - dilute 0.1 M KPO_4 Buffer prepared above 1:10 with ddH_2O (eg. 10 ml buffer + 90 ml ddH_2O)
4. Extraction Buffer (100 mM Na-K-Phosphate, 2 mM EDTA; pH 7.2)
   - 500 ml 0.1 M Na_2HPO_4. $2H_2O$;
     Combine 8.9 g sodium phosphate with 0.372 g EDTA up to 500 ml.
   - 200 ml 0.1 M KH_2PO_4;
     Combine 2.7 g potassium phosphate with 0.149 g EDTA up to 200 ml.
   - combine both solutions and pH to 7.2
5. Test Solution (reduced cytochrome c, 2 mg/ml), for 10 ml (enough for 36 microplate wells);
   - weigh out 20 mg of horse heart cytochrome c (Sigma, C-2506) in a scintillation vial
   - add 1 ml of 10 mM KPO_4 buffer and dissolve cytochrome c
   - make up a small volume of 10 mg/ml sodium dithionite-10 mM KPO_4 stock solution (make fresh each experiment and use within twenty minutes)
   - add 40 μl of the dithionite stock solution to the test solution and observe red-orange colour change
   - add 8 ml of ddH_2O
   - add 1 ml of 100 mM KPO_4 buffer.

PROCEDURE:

1. Place powdered muscle samples in liquid N_2.
2. Add 50 μl of extraction Buffer to 1.5 ml Eppendorf tubes in the aluminum block on ice. (One Eppendorf per sample).
3. Add 5-7.5 mg tissue to each tube, recording exact tissue mass. Mix by tapping.
4. Add the volume of Extraction Buffer required to obtain a 20-fold dilution.
5. Add a stir bar and mix for 15 min. Make up Test Solution during this time and wrap in foil.
6. Sonicate each tube 3 x 3 seconds, cleaning the probe between samples.

7. Pipette some of 20-fold sample extract into new Eppendorf tube and add volume of Extraction Buffer required to obtain an 80-fold dilution. (eg. 50 μl of 20-fold extract + 150 μl Ext. Buffer = 200 μl of 80-fold sample extract). Keep 80-fold sample extract tube on ice for duration of experiment
8. Add 270 μl of Test Solution into 4-8 wells of 96-well microplate and incubate at 30°C for 10 minutes to stabilize the temperature and absorbance.
9. Open KC4 plate reader program (on Triton). Select CONTROL icon, then PRE-HEATING tab, enter 30°C and select ON. (Do not run assay until KC4 temperature has reached 30°C.)
10. Select WIZARD icon, then READING PARAMETERS icon.
    - Select Kinetic for Reading Type.
    - Select Absorbance for Reader and 550 nm for wavelength (drop-down menu).
    - Select Sweep for Read Mode.
    - Select 96 Well Plate (default) for Plate Type.
    - Enter first and last well to be read (eg. A1 and A4 if reading 4 samples simultaneously).
    - Select Yes and Pre-heating and enter 30 for Temperature Control.
    - For Shaking enter 0 for both intensity and duration (shaking is not necessary and it will delay the first reading).
    - Do not select either of the two options for Pre-reading.
    - Click on the KINETIC… rectangular tile to open the Kinetic window.
    - Enter run time (1 minute is recommended) and select MINIMUM for Interval time (under these conditions the minimum Interval time should be 3 seconds).
    - Select Allow Well Zoom During Read to see data in real time (optional).
    - Under Scales, checkmarks should appear for both Auto check boxes. Do not select Individual Well Auto Scaling.
    - Press OK to return to Reading Parameters window. Press OK to return to Wizard window. Press OK. Do not save the protocol.

11. Set the multipipette to 250 μl and secure 4-8 yellow tips on the white projections (make sure they are on tight and all at the same height).
12. In a second, clean 96 well plate, pipette samples into 4-8 empty wells (start with A1). Recommended volumes: 30 μl of 80-fold extract for Mixed Gastroc, 10 μl for Heart. Adjust volumes according to oxidative capacity of the tissue. (eg. 25 μl for Red Gastrocnemius and 35 μl for White Gastrocnemius).
13. Remove microplate with Test Solution in 4-8 wells from the incubator (if it has been incubating for 10 minutes). Place this plate beside the plate with the sample extracts in it.
14. On KC4 program, select the READ icon and press the START READING icon, then press the READ PLATE button. A box will appear that says, “Insert plate and start reading”. Do not press OK yet, but move the mouse so that the cursor hovers over the OK button.
15. Using the multipipette (set to 250 μl) carefully draw up the Test Solution. Make sure the volume is equal in all the pipette tips, and that no significant air bubbles have entered any of the tips.
16. Pipette the Test Solution into the wells with the sample extracts (the second plate). As soon as all the Test Solution has been expelled from the tips (do not wait for the second push from the multipipette), place the plate onto the tray of the plate reader and with the other hand on the mouse, press the OK button. (Speed at this point is paramount, as there is an unavoidable latency period between the time of pressing the OK button and the time of the first reading.)
17. If desired, add 5 μl KCN to one of the wells to measure any absorbance changes in the presence of the CYTOX inhibitor.
18. Once reading is complete, hold the CTRL key on the keyboard, and use the mouse to click once on each of the squares corresponding to a well that had sample in it. Once all the desired wells have been highlighted by a black square (up to a maximum of 8 wells), let go of the CTRL key and a large graph will appear with lines on it representing each sample.

19. To obtain the rate of change of absorbance over different time periods, select Options and enter the amount of time for which you would like a rate of change of absorbance to be calculated. The graph, along with one rate (at whichever time interval is selected) for each sample can be printed on a single sheet of paper, and the results can be saved.
20. The delta absorbance will appear in units of mOD/min and the number given will be negative. Convert this to OD/min by dividing by 1000 and omit the negative sign in the calculation. (eg. if Mean V: -394.8 mOD/mn, then use 0.395 OD/min)

$$\text{CALCULATION: CYTOX activity } (\mu\text{mole/min/g tissue}) = \frac{\text{delta absorbance/min x total volume (ml) x 80 (dilution)}}{18.5\ (\mu\text{mol/ml extinction coeff.}) \text{ x sample vol (ml)}}$$

MITOCHONDRIAL PROTEIN IMMUNOPRECIPITATION

Mitochondrial Sample Solubilization

1. Take isolated mitochondria (Whole tissue 200–300 mg) and dilute with mitochondrial isolation buffer to give a final protein concentration of 1 mg/ml.
2. Add 1/10 volume of 10% Triton X-100 detergent (final detergent concentration 1%) and mix well with isolated mitochondria fraction.
3. Add protease inhibitor cocktail and incubate on ice for 30 minutes.
4. Centrifuge at 12,000g for 10 minutes at 4°C in ultracentrifuge and collect the supernatant. Keep the sample on ice until immunoprecipitation is performed.

Immunoprecipitation

1. Add desired amount of polyclonal or monoclonal antibody of interest to the solubilized mitochondrial supernatant. A pilot experiment should be completed beforehand with a fixed amount of protein and precipitated by an increasing amount of antibody. Alternatively, one can check the antibody datasheet for recommended antibody concentration. Allow this mixture to mix overnight at 4°C on a nutator mixer.
2. Add Protein A/G-coupled agarose beads (~100 mg, prewashed with PBS) to the mixture and incubate for 1 hour at 4°C on a nutator mixer. Collect the beads by centrifuging for 1 minute at 3,000g on a bench top microfuge. Remove the supernatant from the beads. This represents unbound proteins.
3. Carefully wash the beads to remove any non-specific bound proteins by adding 2 volumes of PBS containing detergent to the beads. Gently mix for 5 minutes by inverting, and collect the beads by centrifugation as performed in step 2.
4. Remove the PBS from the beads and discard. Wash the beads with PBS two additional times to remove non-specific binding. Repeat depending on the stringency.
5. Elute the complex by adding 50 ul of SDS-PAGE gel loading buffer. The purified complexes have now been released into the supernatant, which should be collected from above the beads. Repeat the elution twice to ensure that the entire captured complex has been released from the beads.
6. Run the samples on a Western blot to check the precipitation of proteins.

Table 1. Pipette plan for mitochondrial Mfn2 immunoprecipitation

Sample Condition	Mito Concentration (ug/uL)	Amount for IP (ug)	Vol of Mito Lysate (uL)	Vol of isolation buffer to dilute to 1 ug/uL	Vol required from 10% Triton X-100 stock to 1% (ul)	Vol of Mfn2 Ab added (uL)
WT CON	7.1122	200	28.12	171.88	22	10
WT EX	8.0305	200	24.91	175.09	22	10
KO CON	6.6709	200	29.98	170.02	22	10
KO EX	5.9911	200	33.38	166.62	22	10

BREEDING AND PCR GENOTYPING OF WT and PARKIN KO MICE

Breeding: Homozygous mice (~2 months of age) may be bred. A female KO mouse can breed with a male KO mouse, and generate viable homozygote KO offspring. There is no need to generate heterozygotes for this strain of animal.

WT: Stock No. 000664 (C57BL/6J, The Jackson Laboratory)
Parkin KO: Stock No. 006582 (B6.129S4-Park2tm1Shn/J, The Jackson Laboratory)

Background: This protocol is designed to detect sequences in the murine genome that differ between wild-type and null animals using polymerase chain reaction amplification. PCR is a rapid, inexpensive and straightforward way of copying specific DNA fragments from minute quantities of source DNA material. There are basically 3 procedural steps involved in PCR:

1) *Denaturation*: DNA is heated to hot temperature to separate the DNA double helix to single strands making them accessible to primers. During denaturation, the DNA strands separate to form single strands.
2) *Annealing*: The reaction mixture is cooled down. Primers anneal to the complementary regions in the DNA template strands, and double strands are formed again between primers and complementary sequences. During annealing one primer binds to one DNA strand and another bind to the complementary strand. The annealing sites of the primers are chosen so that they will prime DNA synthesis in the region of interest during extension.
3) *Extension*: The DNA polymerase synthesizes a complementary strand. The enzyme reads the opposing strand sequence and extends the primers by adding nucleotides in the order in which they can pair. During extension, DNA synthesis proceeds through the target region and for variable distances into the flanking region, giving rise to long fragments of variable lengths. The entire process is repeated over and over.

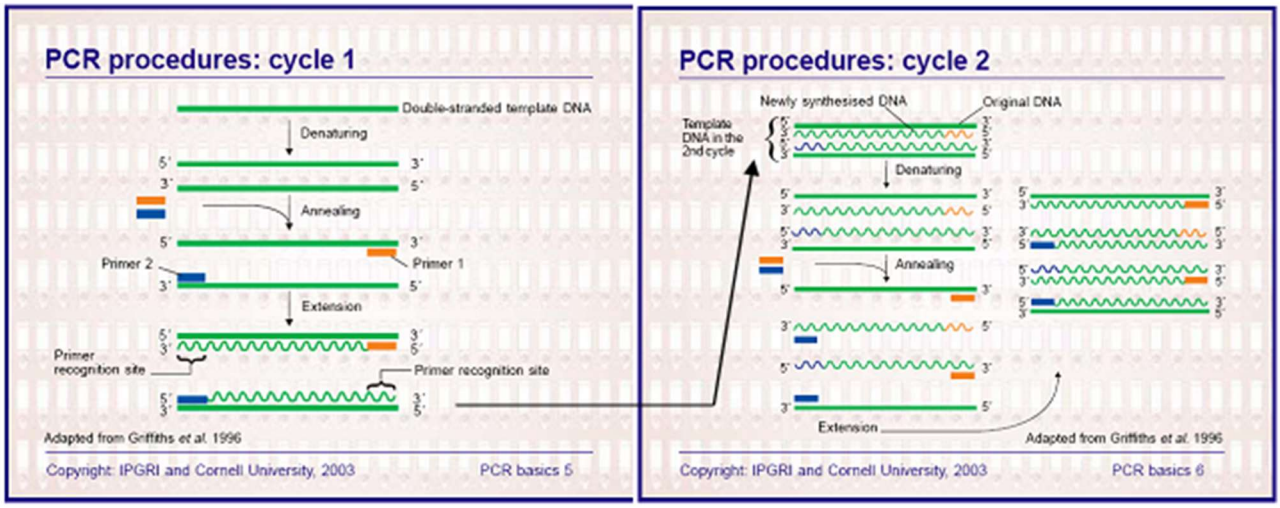

Figure 3. Schematic of basic PCR procedures.

The DNA polymerase, known as Taq polymerase, is named after the hot-spring bacterium *Thermus aquaticus* from which it was originally isolated. The enzyme can withstand the elevated temperature needed for DNA-strand separation. The cycle of heating and cooling is repeated over and over, stimulating the primers to bind to the original sequences and to newly synthesized sequences. The enzyme will continue to extend primer sequences. This cycling of temperatures results in copying and then copying of copies, leading to an exponential increase in the number of copies of specific sequences. Because the amount of DNA placed in the tube at the beginning is very small, almost all the DNA at the end of the reaction cycles

are copied sequences. The reaction products are then separated by gel electrophoresis and visualized with the use of ethidium bromide.

Reagents

Lysis Buffer (pH=8.0)
10 mM Tris HCl (0.121g/100ml)
150 mM NaCl (0.8766g/100ml)
20 mM EDTA (0.744g/100ml)
Autoclave for 30min and store at room temperature.

Supermix

Sigma Jumpstart REDtaq Ready Mix PCR Reaction Mix (P0982)
Product contains 20 mM Tris-HCl, pH 8.3, 100mM KCl, 4 mM MgCl2, 0.002% gelatin, 0.4 mM each dNTP (dATP, dCTP, dGTP, TTP), inert dye, stabilizers, 0.06 unit/µl Taq DNA polymerase, JumpStart Taq antibody.

Primers

Common and Reverse for WT and KO Stock Concentration 500 pmol/µl
Working Concentration of Primers (10X dilution): 50 pmol/ul
To make up 50 pmol/µl: use 5 µl of 500 pmol/µl stock and add 45µl of sterile water

Table 2. Protocol Primers

Primer	5' Label	Sequence 5' --> 3'	3' Label	Primer Type
oIMR7026		CCT ACA CAG AAC TGT GAC CTG G		Wild-type Reverse
oIMR7027		GCA GAA TTA CAG CAG TTA CCT GG		Wild-type Forward
oIMR7028		ATG TTG CCG TCC TCC TTG AAG TCG		KO Reverse

Proteinase K

ProK- concentration of 1mg/ml

Reagents for Agarose Gel Electrophoresis of PCR product

Agarose	50XTAE
50 X TAE	242 g TRIS
1X TAE (dilute 50X TAE with stH2O)	500ml dH2O
10mg/ml EtBr	100ml 0.5M EDTA (pH 8.0)
Sterile water	57.1ml Glacial Acetic Acid
	Make up to 1L and autoclave

DNA Extraction from ear clippings

1. Make (fresh) 10:1 mixture of lysis buffer to ProK (@concentration of 1mg/ml-fresh)
2. Add 20 µl of this mixture to a 1.5 ml sterile eppendorf tube.
3. Obtain ear clipping from animal, add to tube and vortex (ensure ear clipping is immersed in solution).
4. Incubate in a 55 °C water bath (no higher than 60 °C) for 30min, vortexing every 15 minutes.
5. Add 180 µl sterile distilled water.
6. Place in boiling water for 5 minutes (use hot plate) and then vortex.
7. Store at -20°C, or use immediately for PCR

PCR method

1. Make mastermix for each of the primers you will be using.

Mastermix contains: 25 µl of Supermix sample per sample
1 µl of WT Reverse Primer per sample
2 µl of WT Forward per sample
2 µl of KO Reverse per sample
Enough sterile distilled water for a volume per sample of 48 µl.

2. For each sample use 48 µl of mastermix and 2 µl of template DNA extracted from procedure described above. Add 1 drop of mineral oil to each PCR tube to prevent evaporation of sample during cycling.

3. Cycling times:	Initial Denaturation		94°C 3min
	35 cycles:	Denaturation	94°C 30sec
		Annealing	60°C 1min
		Extension	72°C 1min
	Final Extension		72°C 2min
	Hold		10°C

Electrophoresis of PCR products

1. Loading buffer is already included in Supermix.
2. Preparation of a 1.2% agarose gel. ***For large gel system***: 3.6g Agarose, 6 ml 50X TAE and volume up to 300 ml with sterile H_2O. Mix solution and note weight followed by boiling in microwave. Remove periodically to mix during boiling procedure in microwave. Upon complete dissolving of agarose and a homogenous and relatively clear agarose solution, weigh solution and replace lost amount of evaporated H_2O. Add 25µl of EtBr (10mg/ml), slightly cool solution at room temperature (5-10min), then pour into caster. ***For small gel system***: 1.92g Agarose, 3.2 ml 50X TAE, and 156.8ml st H_2O; follow same procedure as noted above. Only add 8 µl of EtBr (10mg/ml).
Electrophoresis Running Buffer: 1X TAE: 40 ml of 50X TAE made up to 2L with H_2O.
3. Electrophorese 40 µl of PCR product reaction on either a small or large 1.2% agarose gel for 1hr @ approximately 120V.
4. Visualize PCR products using UV lightbox. Parkin KO PCR product should be about 500bp whereas WT PCR product will be about 250bp.

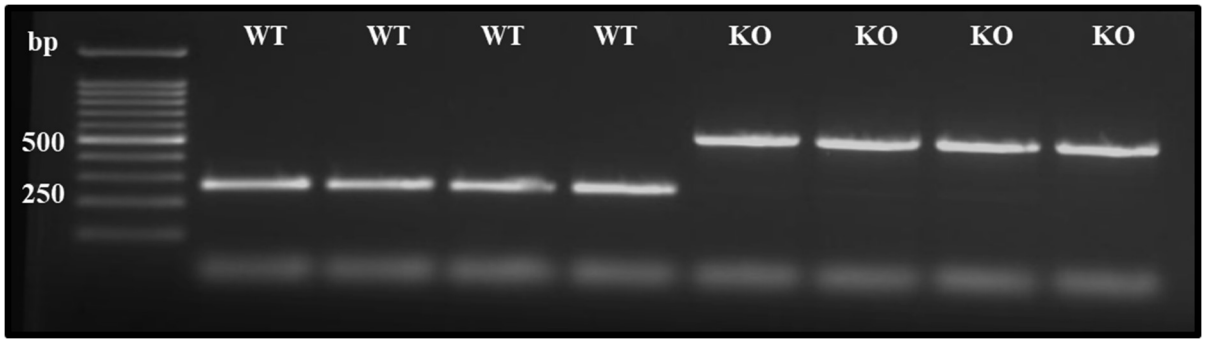

Figure 4. Typical agarose gel displaying PCR products and animal genotypes.

APPENDIX D:

OTHER CONTRIBUTIONS

During my doctoral studies, I made the following contributions to literature that are not included in my dissertation:

Refereed Publications

3. Hood, D.A., Tryon, L., Carter, H.N., Yuho, K., **Chen, C.CW**. Unraveling the mechanisms regulating muscle mitochondrial biogenesis. *Biochemical Journal*, 473(15): 2295 – 2314, 2016.

2. Carter, H.N., **Chen, C.C.W.** & Hood, D.A. Mitochondria, muscle health, and exercise with advancing age. *Physiology*, 30(3): 208 – 223, 2015.

1. Hood, D.A., Tryon, L., Vainshtein, A., Memme, J., **Chen, C.**, Pauly, M., Crilly, M., Carter, H. Exercise and the Regulation of Mitochondrial Turnover. *Progress in Molecular Biology and Translational Science*, 135: 99 – 127, 2015.

Published Abstracts

5. **Chen, C.C.W.** & Hood, D.A. Parkin-Mediated Mitophagy in Skeletal Muscle with Endurance Training. Experimental Biology (EB) 2017 Meeting, Chicago, Illinois. *The FASEB Journal*. 31 (Suppl 1): 839.18, 2017. (**poster**)

4. **Chen, C.C.W.** & Hood, D.A. Parkin-Mediated Mitophagy in Skeletal Muscle with Aging and Exercise. Experimental Biology (EB) 2016 Meeting, San Diego, California. *The FASEB Journal*. 30 (Suppl 1): 764.3, 2016. (**oral and poster**)

3. **Chen, C.C.W.** & Hood, D.A. The role of Parkin during acute exercise-induced mitophagy. Proceedings of the Canadian Society for Exercise Physiology (CSEP) Annual General Meeting − Where Science is the New Steel, Hamilton, Ontario. *Appl. Physiol. Nutr. Metab*. 40 (Suppl 1): S11-S12, 2015. (**oral**)

2. **Chen, C.C.W.** & Hood, D.A. Parkin and its Role in Skeletal Muscle Function. Experimental Biology (EB) 2015 Meeting, Boston, Massachusetts. The FASEB Journal. 29 (Suppl 1): 821.3, 2015. (**poster**)

1. **Chen, C.C.W.** & Hood, D.A. PINK1 import in skeletal muscle mitochondria. Proceedings of the Canadian Society for Exercise Physiology (CSEP) Annual General Meeting − Science on the Edge of the Continent, St. John's, Newfoundland. Appl. Physiol. Nutr. Metab. 39 (Suppl 1): S9, 2014. (**poster finalist**)

Conference Proceedings

6. **Chen, C.C.W.** & Hood, D.A. Mitochondrial degradation in skeletal muscle with aging and exercise. Multi-disciplinary Perspectives in Aging Research Symposium, York University, Ontario, 2016. (**oral**)

5. Joanisse, D.R., Huth, C., **Chen, C.C.W.**, Hood, D.A. Skeletal muscle mitochondrial quality control and mitophagy in obese and endurance trained men. 21st Annual Congress of the European College of Sport Science, Vienna, Austria, 2016.

4. Samoilov, L., **Chen, C.C.W.** and Hood, D.A. The effects of Parkin on mitophagy flux. NSERC Undergraduate Student Research Award Day, York University, Ontario, 2015.

3. Huth, C., **Chen, C.C.W.**, Hood, D.A. & Joanisse, D.R. La mitophagie est suractivée dans le muscle squelettique d'hommes obèses (mitophagy is hyperactive in skeletal muscle of obese individuals). The Quebec Association of Physical Activity Sciences Symposium, Laval University, Quebec, 2015.

2. **Chen, C.C.W.**, Huth, C., Joanisse, D.R. & Hood, D.A. Skeletal muscle autophagy proteins in endurance trained, obese and obese diabetic individuals. Obesity Symposium, York University, Ontario, 2014. (**poster**)

1. Hood, D.A., Vainshtein, A., Carter, H.N., **Chen, C.C.W.** & Tryon, L. Molecular mechanisms of mitochondrial biogenesis during chronic muscle use and disuse. Proceedings of the Symposium on Integrative Physiology, Busan, South Korea, 2014.